

UNCLASSIFIED

AD NUMBER	
AD020133	
CLASSIFICATION CHANGES	
TO:	unclassified
FROM:	confidential
LIMITATION CHANGES	
TO:	Approved for public release, distribution unlimited
FROM:	Distribution authorized to U.S. Gov't. agencies and their contractors; Administrative/Operational Use; DEC 1952. Other requests shall be referred to Office of Naval Research, One Liberty Center, 875 North Randolph Street, Arlington, VA 22203-1995.
AUTHORITY	
ONR ltr, 31 Jul 1958; ONR ltr, 15 Aug 1968	

THIS PAGE IS UNCLASSIFIED

Armed Services Technical Information Agency

AD

20133

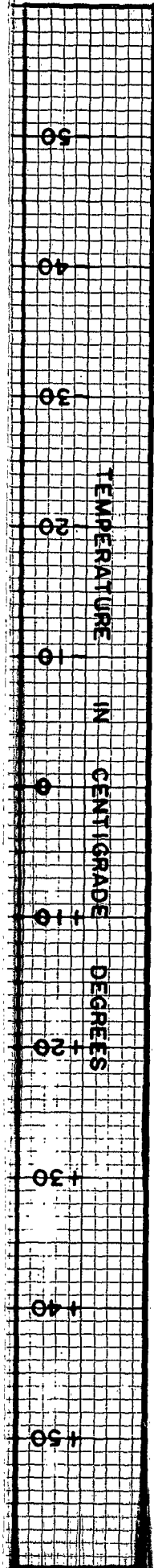
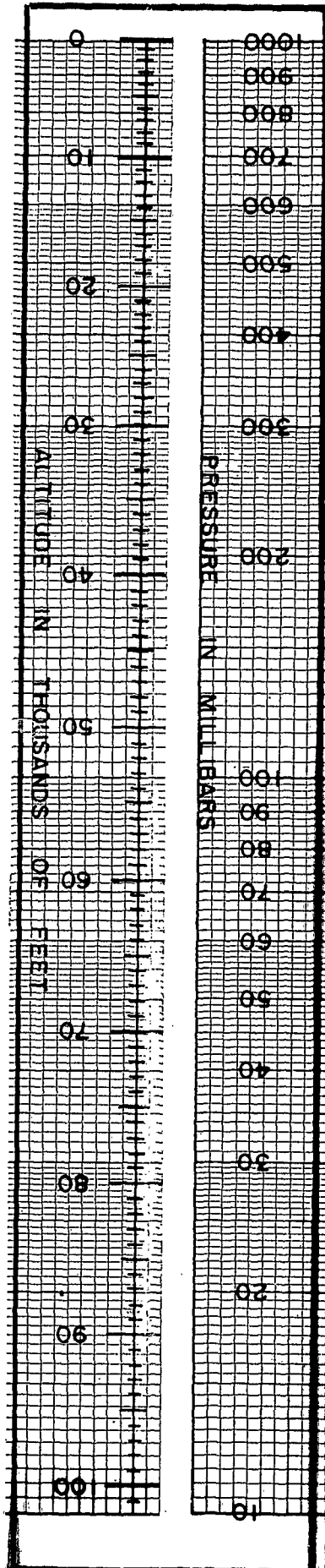
NOTICE: WHEN GOVERNMENT OR OTHER DRAWINGS, SPECIFICATIONS OR OTHER DATA ARE USED FOR ANY PURPOSE OTHER THAN IN CONNECTION WITH A DEFINITELY RELATED GOVERNMENT PROCUREMENT OPERATION, THE U. S. GOVERNMENT THEREBY INCURS NO RESPONSIBILITY, NOR ANY OBLIGATION WHATSOEVER; AND THE FACT THAT THE GOVERNMENT MAY HAVE FORMULATED, FURNISHED, OR IN ANY WAY SUPPLIED THE SAID DRAWINGS, SPECIFICATIONS, OR OTHER DATA IS NOT TO BE REGARDED BY IMPLICATION OR OTHERWISE AS IN ANY MANNER LICENSING THE HOLDER OR ANY OTHER PERSON OR CORPORATION, OR CONVEYING ANY RIGHTS OR PERMISSION TO MANUFACTURE, USE OR SELL ANY PATENTED INVENTION THAT MAY IN ANY WAY BE RELATED THERETO.

Reproduced by
DOCUMENT SERVICE CENTER
KNOTT BUILDING, DAYTON, 2, OHIO

CONFIDENTIAL

The following ESPIONAGE NOTICE can be disregarded unless this document is plainly marked RESTRICTED, CONFIDENTIAL, or SECRET.

NOTICE: THIS DOCUMENT CONTAINS INFORMATION AFFECTING THE NATIONAL DEFENSE OF THE UNITED STATES WITHIN THE MEANING OF THE ESPIONAGE LAWS, TITLE 18, U.S.C., SECTIONS 793 and 794. THE TRANSMISSION OR THE REVELATION OF ITS CONTENTS IN ANY MANNER TO AN UNAUTHORIZED PERSON IS PROHIBITED BY LAW.



PROGRESS REPORT ON
RESEARCH AND DEVELOPMENT
IN THE FIELD OF
HIGH ALTITUDE PLASTIC BALLOONS

This material contains information affecting the national defense of the United States within the meaning of the Espionage Laws, Title 18, U.S.C., Sections 793 and 794, the transmission or revelation of which in any manner to an unauthorized person is prohibited by law.

CONDUCTED UNDER
CONTRACT NONR-710(01), NR 211 002
FOR PERIOD JUNE 15, 1952 to DECEMBER 22, 1952
WITH THE
OFFICE OF NAVAL RESEARCH

AND SPONSORED JOINTLY
BY THE ARMY, NAVY AND AIR FORCE

This document has been reviewed in accordance with OPNAVINST 5510.17 paragraph 5. The security classification assigned to it is correct.

Date: oct 16/1953 J. D. Christian
By direction of
Chief of Naval Research (Code 461)

REPRODUCTION OF THIS DOCUMENT IN WHOLE OR IN PART IS PROHIBITED EXCEPT WITH PERMISSION OF CHIEF OF NAVAL RESEARCH (CODE 461)

PREPARED BY THE
DEPARTMENT OF PHYSICS
UNIVERSITY OF MINNESOTA
MINNEAPOLIS 14, MINNESOTA

PROGRESS REPORT ON CONTRACT # 710 (01)

From June 15, 1952 to December 22, 1952

VOLUME VII

CONFIDENTIAL SECURITY INFORMATION

Table of ContentsSection I - Rasonde Charts, Time-Altitude Charts,
Trajectories

Pages I-1 - I-98

Time-Temperature Charts

Pages I-99 - I-112

Section II - Theoretical Meteorological Analysis

Part A - Characteristics of Stratospheric Flow

Pages II-113 - II-138

Part B - Winds in the Upper Troposphere and
Lower Stratosphere

Pages II-139 - II-145

THEORETICAL
CEILING 34,800 FT.

TIME - PRESSURE - ALTITUDE

FLIGHT NO. 21

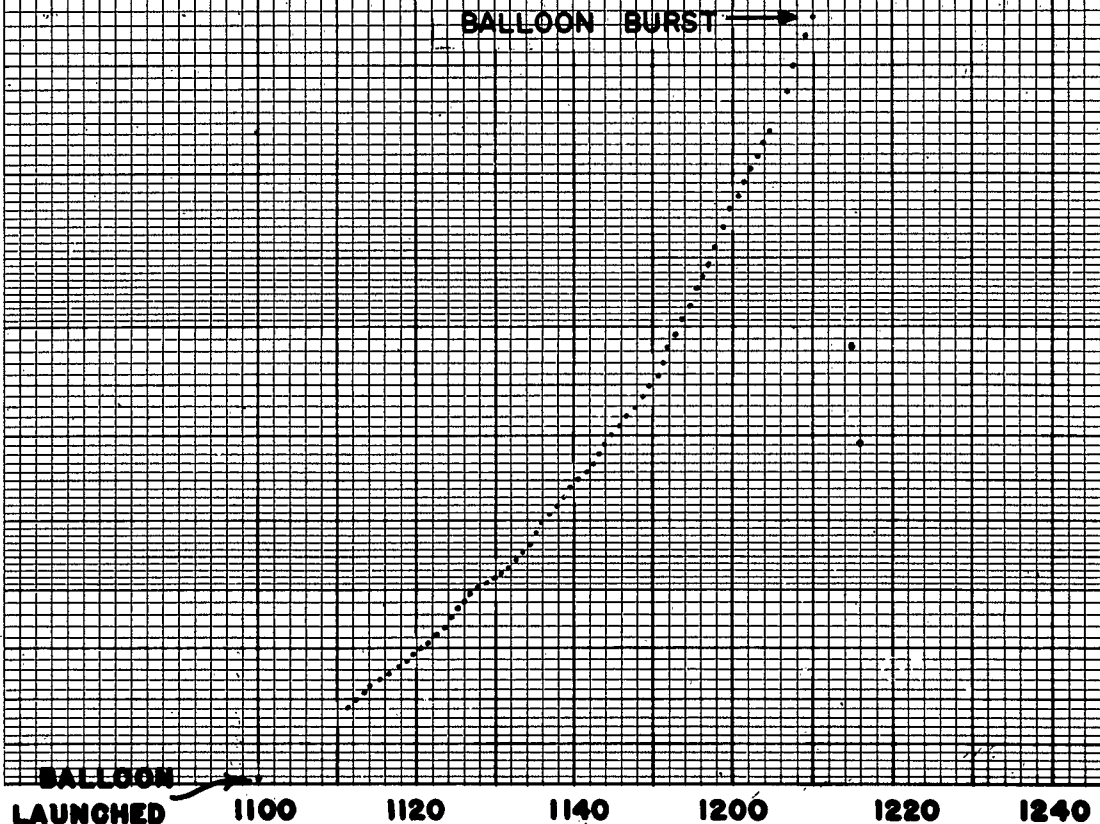
25 JUNE, 1952

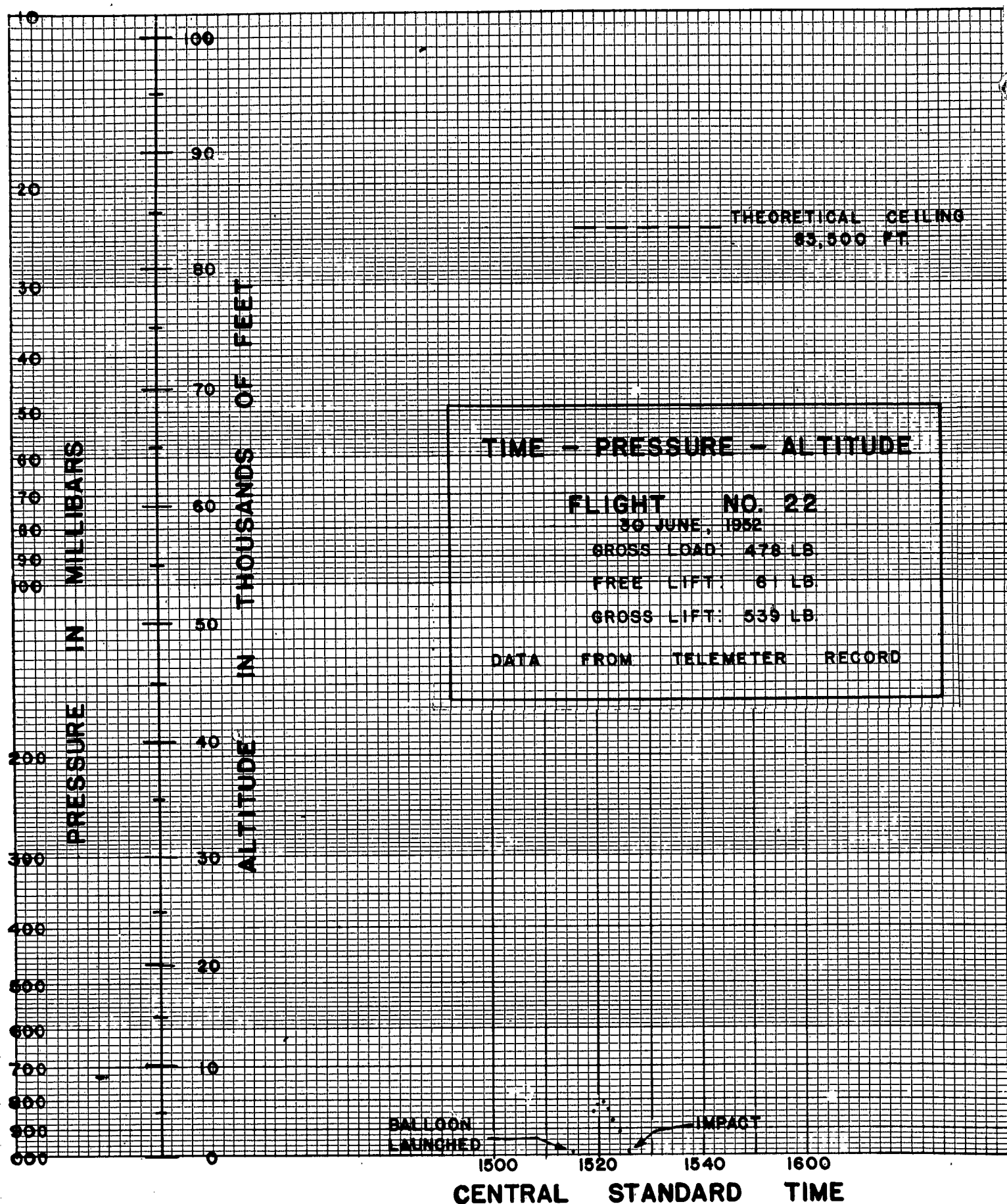
GROSS LOAD: 417 lbs.

FREE LIFT: 66 lbs.

GROSS LIFT: 483 lbs.

Altitude data from telemeter record

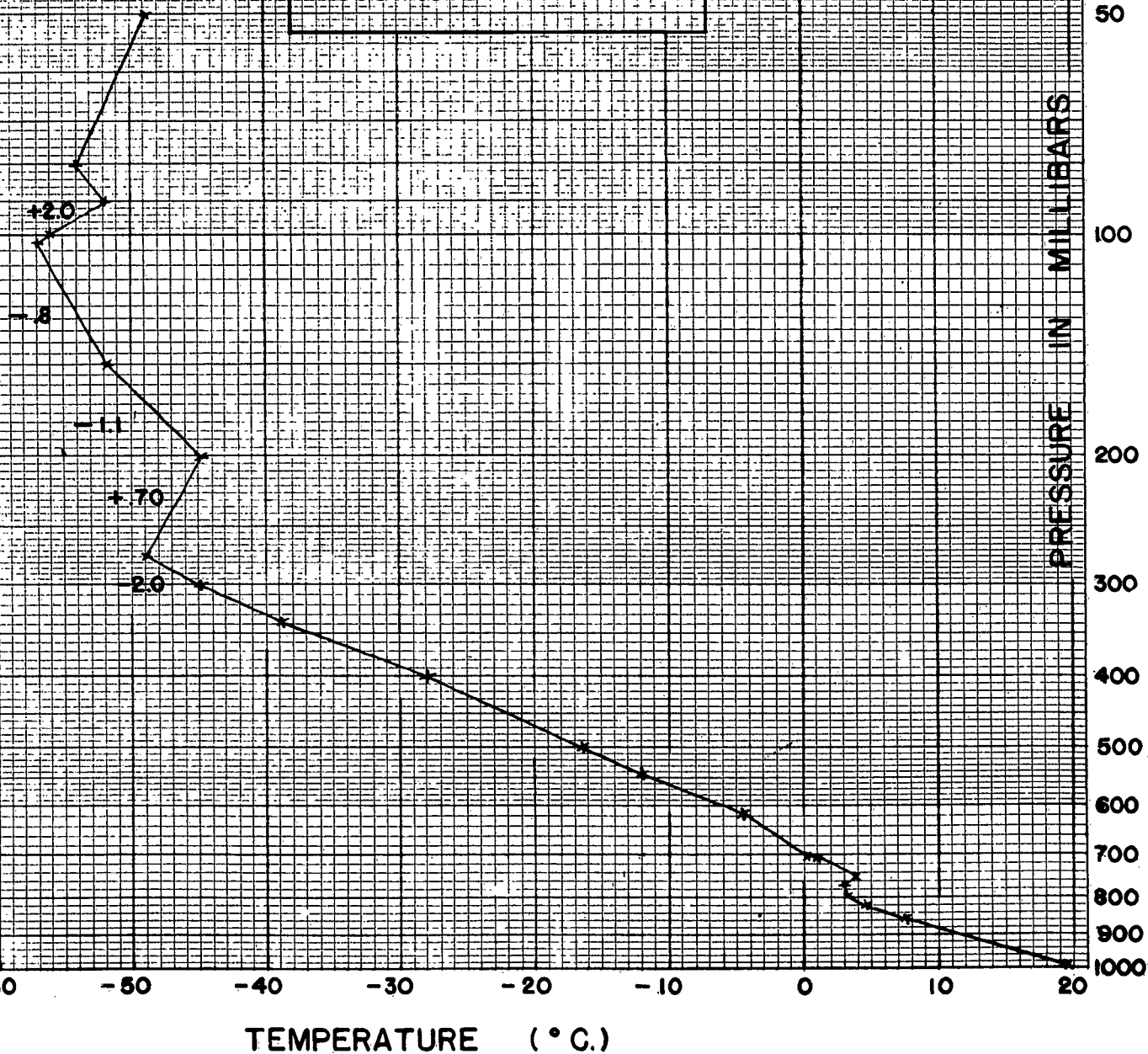


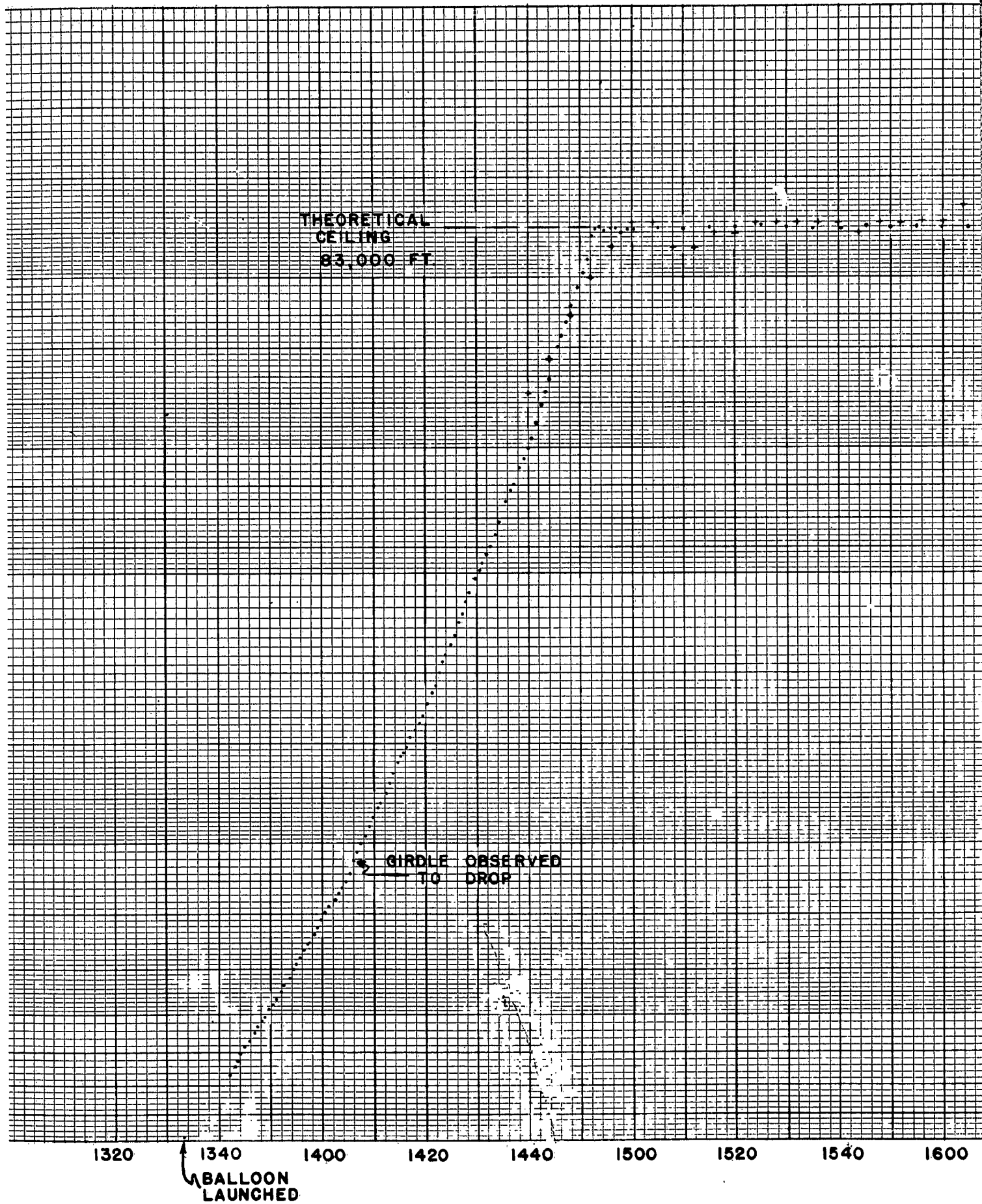


RASONDE DATA

FLIGHT NO. 24

8 JULY, 1952

Meteorological station
reporting:ST. CLOUD, MINN. 655
1500 ZNumbers along curve show
lapse rates in degrees per
1000 feet.



TIME - PRESSURE - ALTITUDE

FLIGHT NO. 24

8 JULY, 1952

GROSS LOAD: 432 LB.

FREE LIFT: 86 LB.

GROSS LIFT: 498 LB.

DATA OBTAINED

FROM:	TELEMETER	RECORD
	BAROGRAPH	RECORD

1600

1620

1640

1700

1720

1740

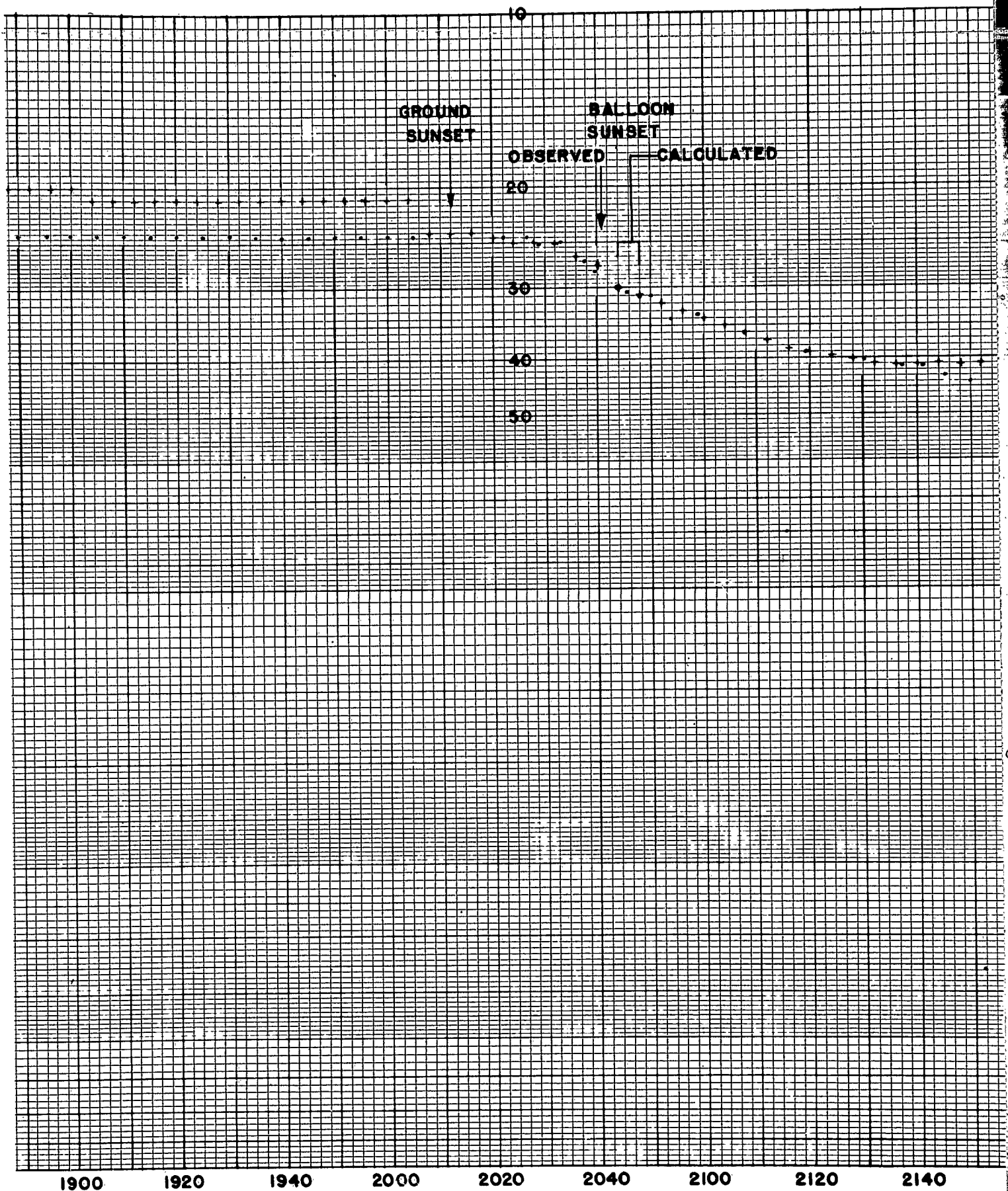
1800

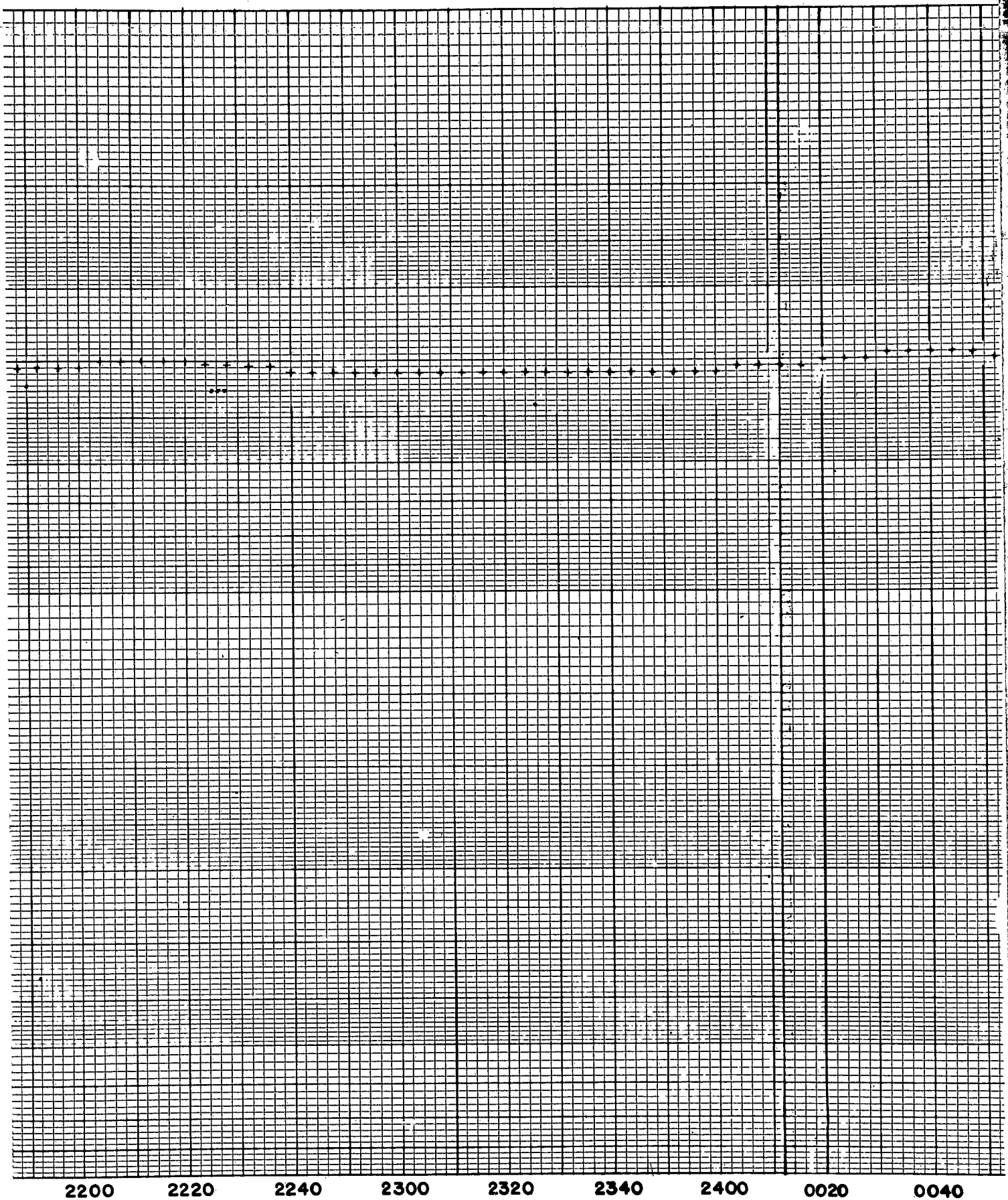
1820

1840

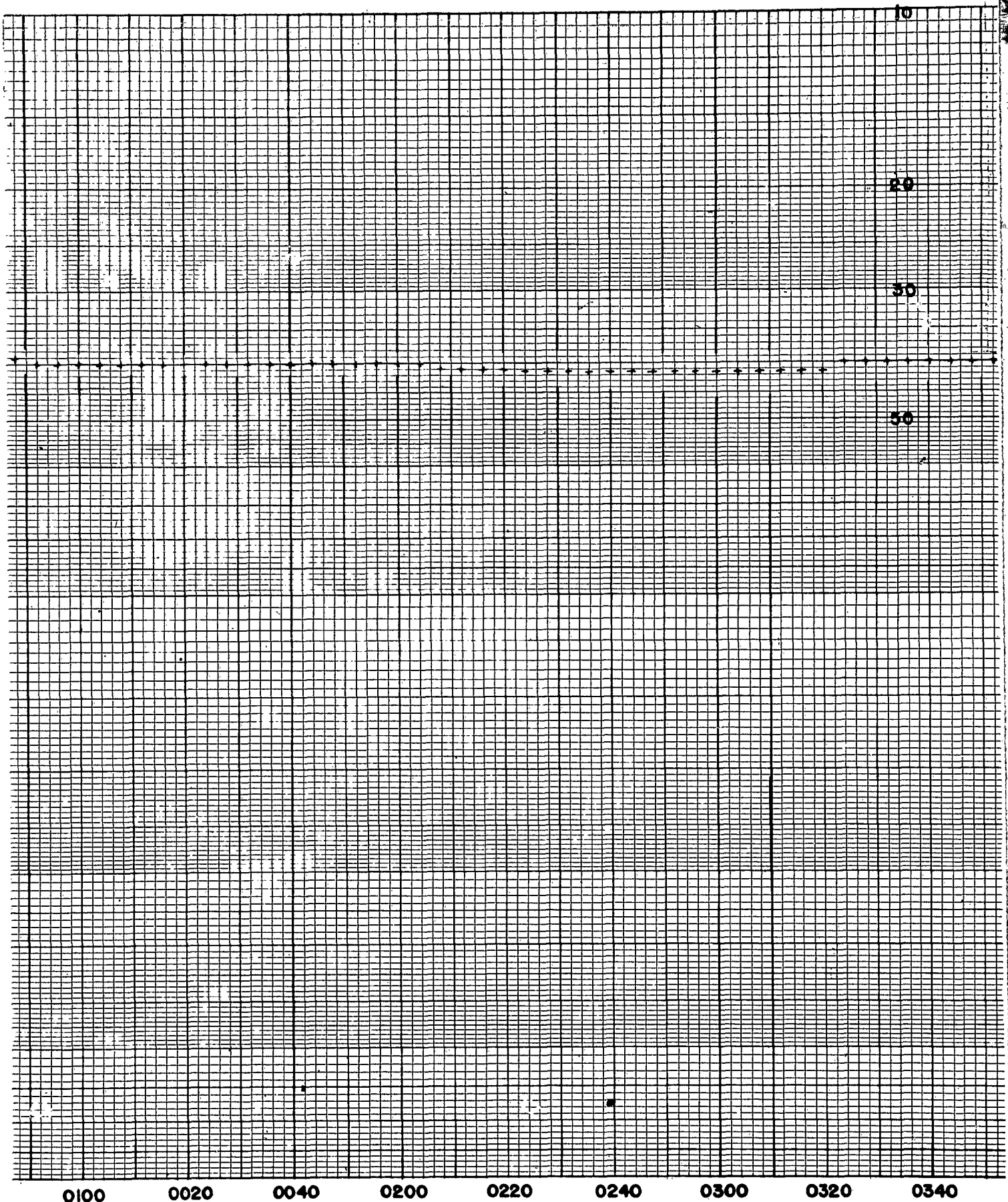
19

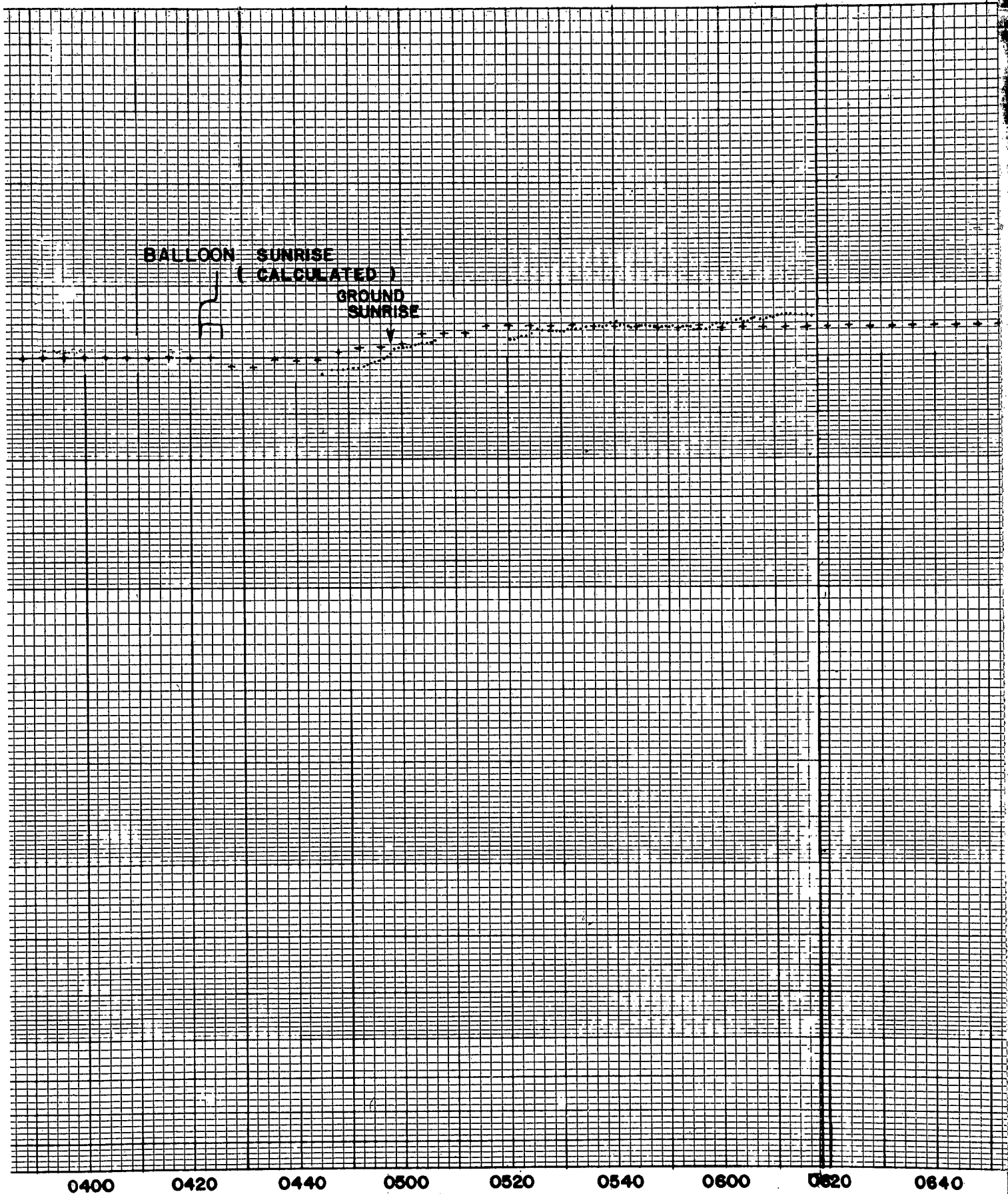
CENTRAL STANDARD TIME

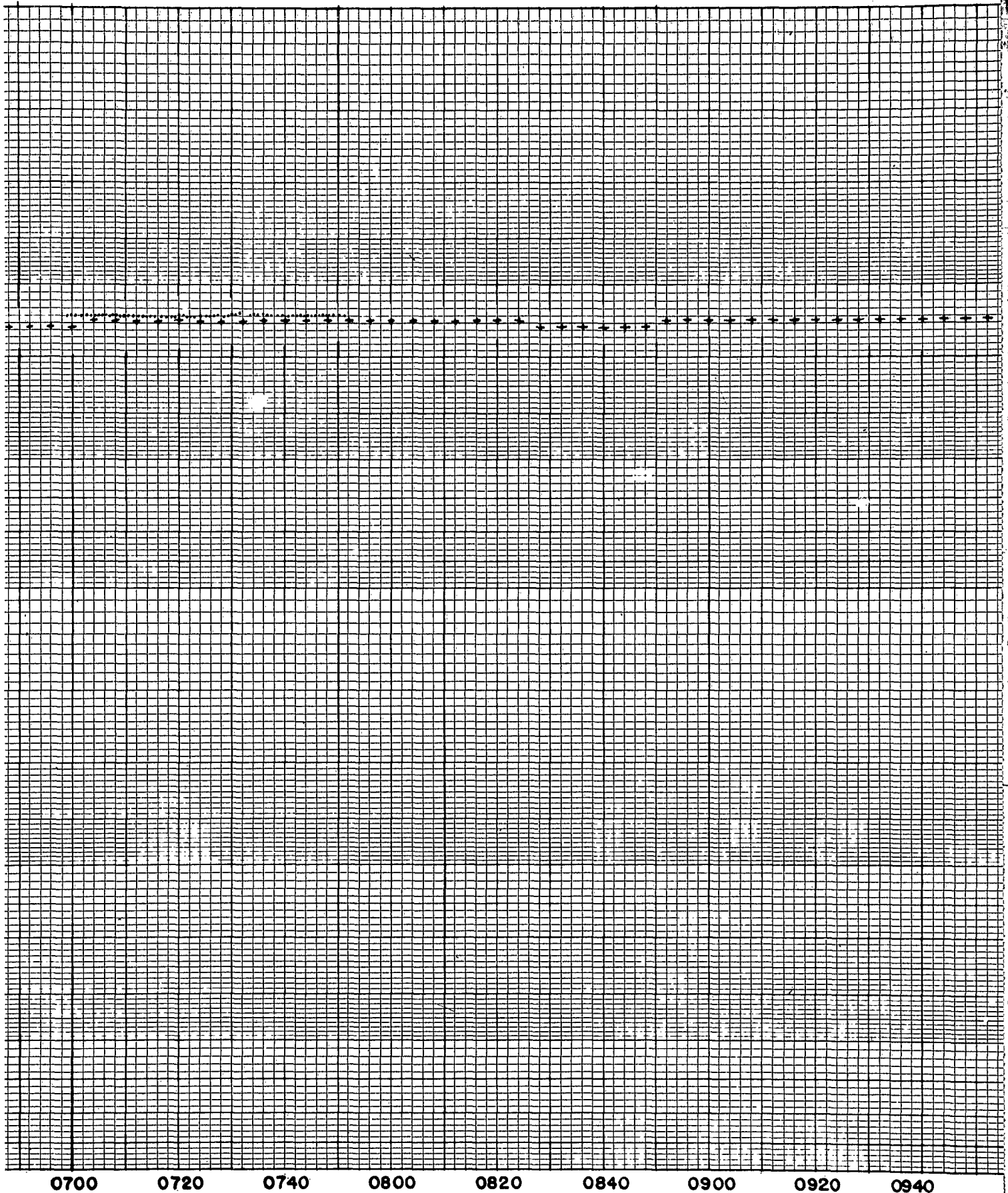


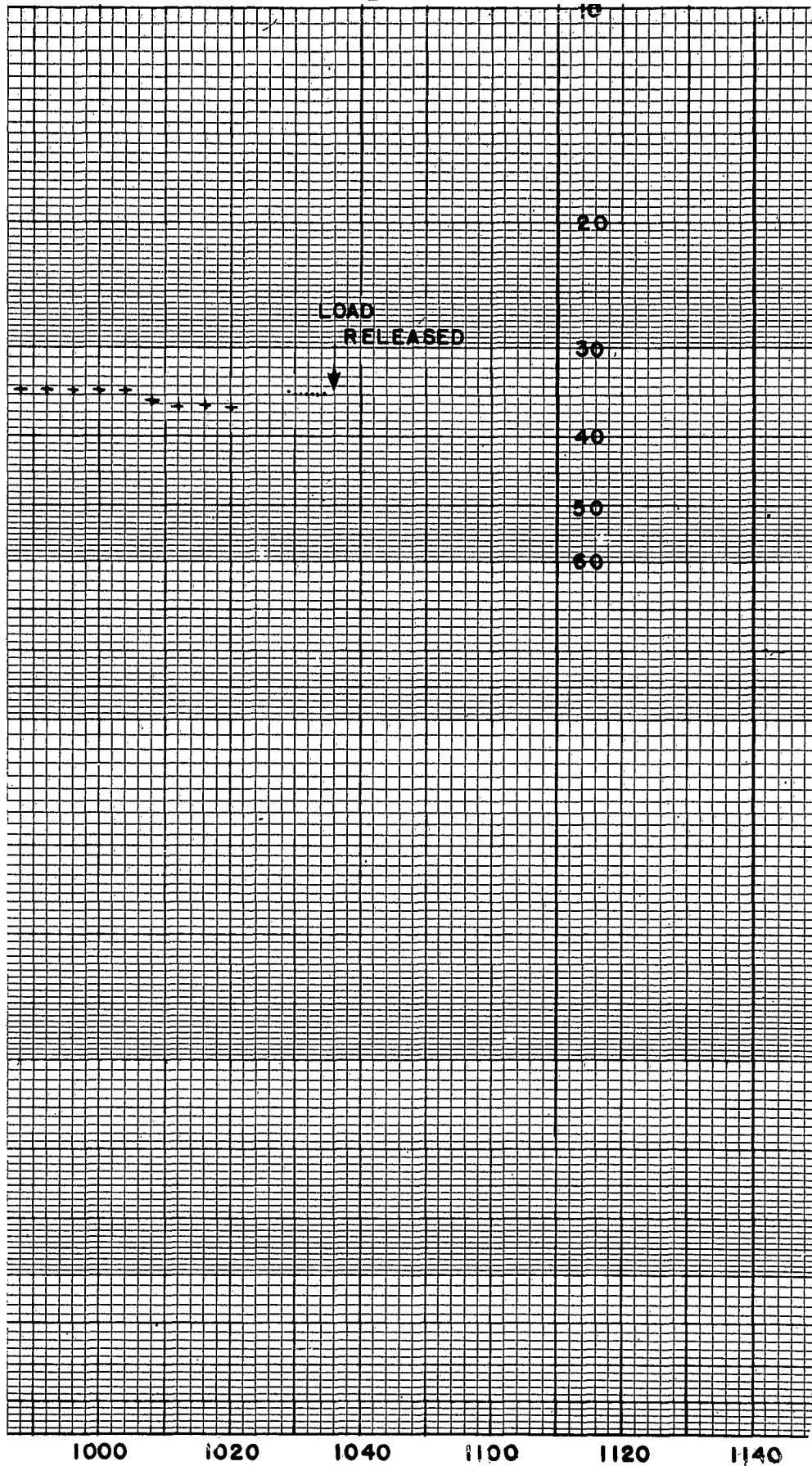


→ 9 JULY



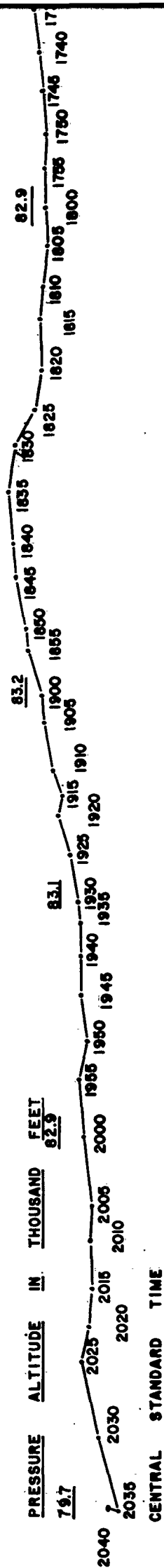






CONFIDENTIAL SECURITY INFORMATION

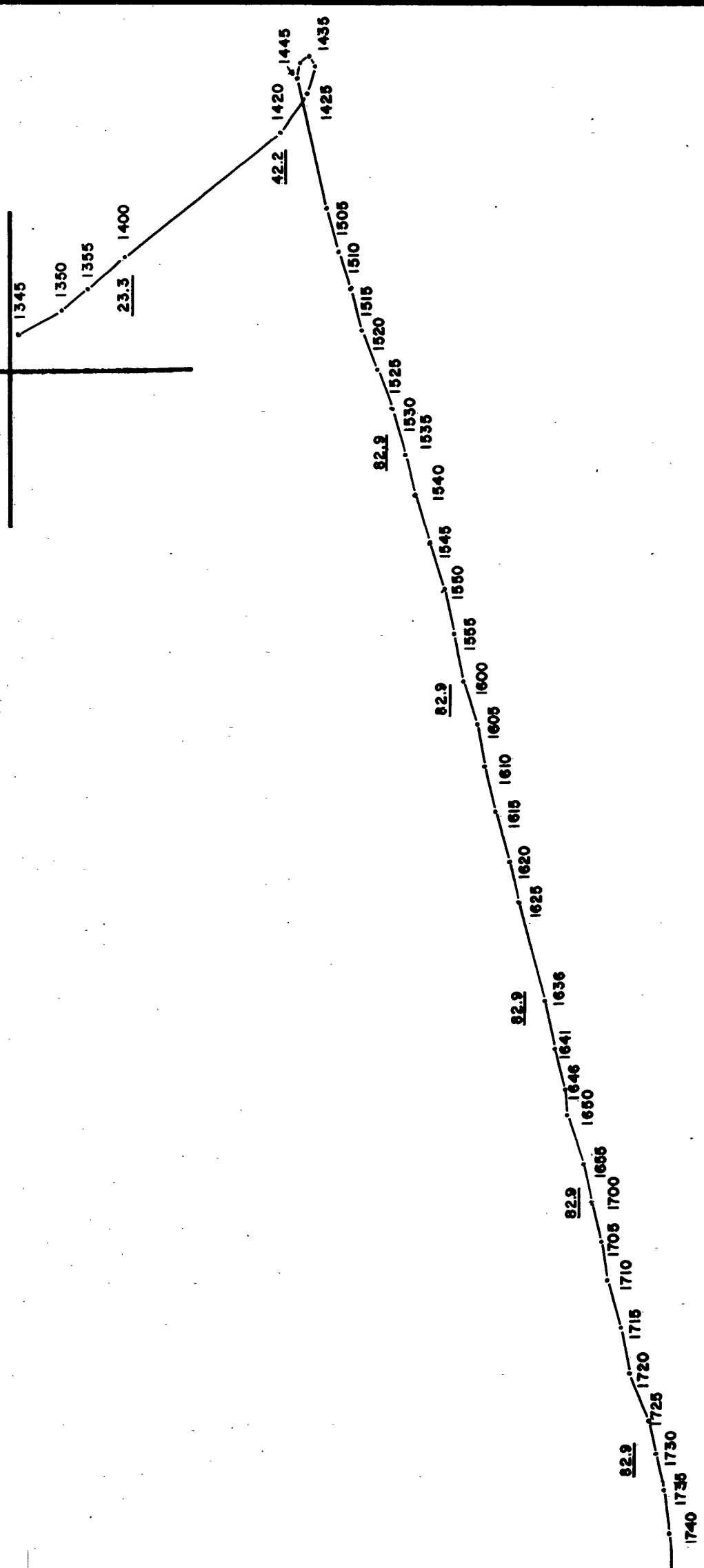
PRESSURE ALTITUDE IN 1000 FEET



CONFIDENTIAL SECURITY INFORMATION

N

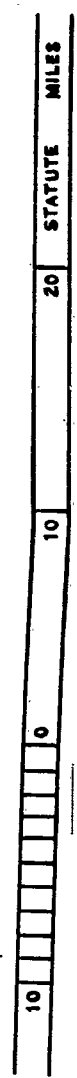
Launched at:
MINNEAPOLIS, MINN.



FLIGHT NO. 24
LAUNCHED 1333 CST
8 JULY, 1952

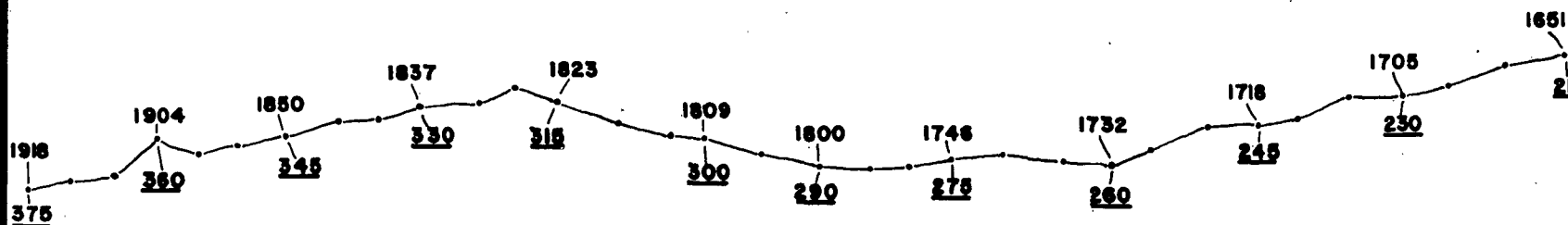
TRAJECTORY FROM THEODOLITE FIXES

CENTRAL STANDARD TIME



CONFIDENTIAL SECURITY INFORMATION

CENTRAL STANDARD TIME



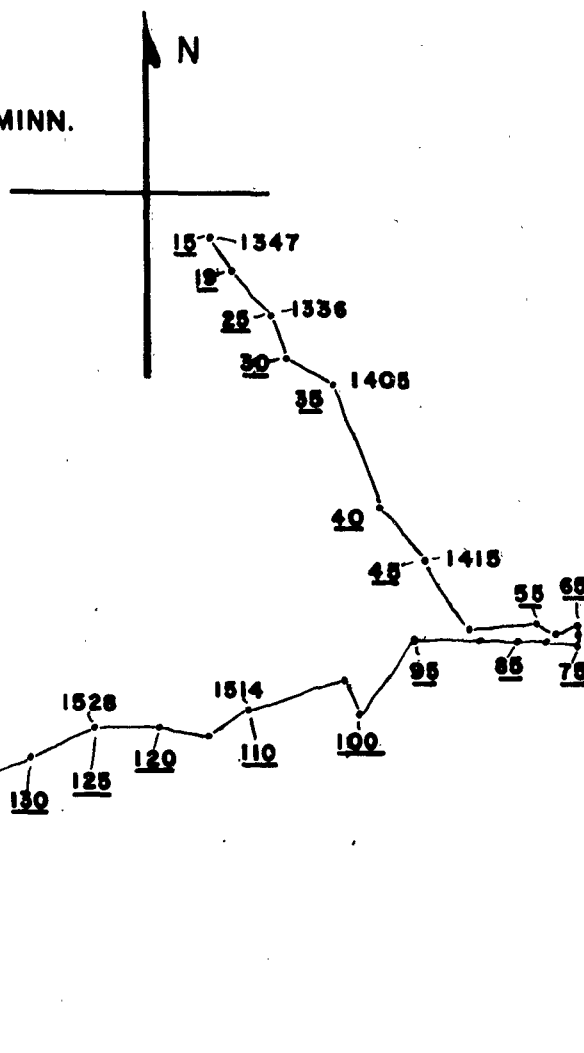
FILM FRAME NUMBER

1

10

CONFIDENTIAL

Launched at:
MINNEAPOLIS, MINN.



FLIGHT NO. 24

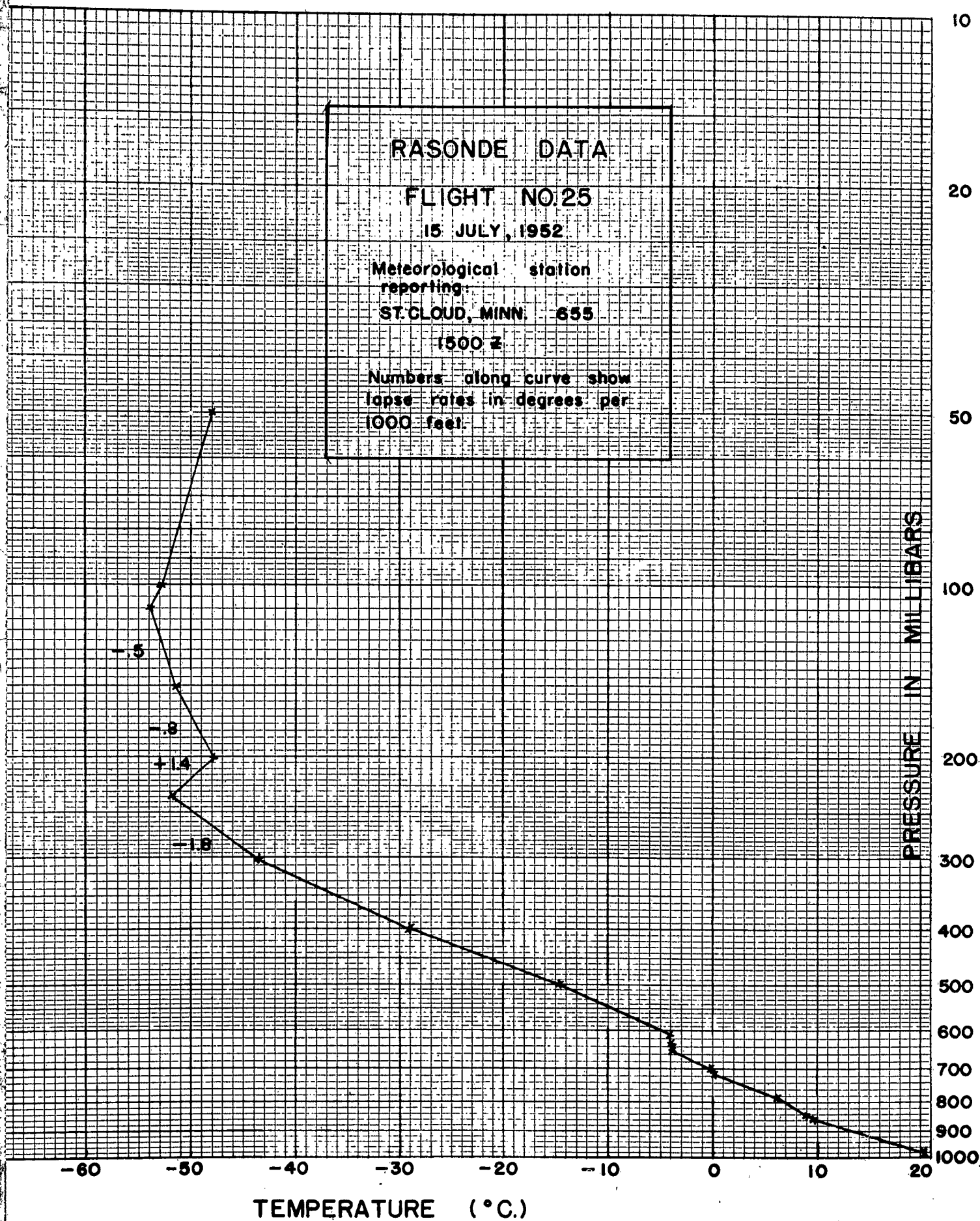
LAUNCHED 1333 CST

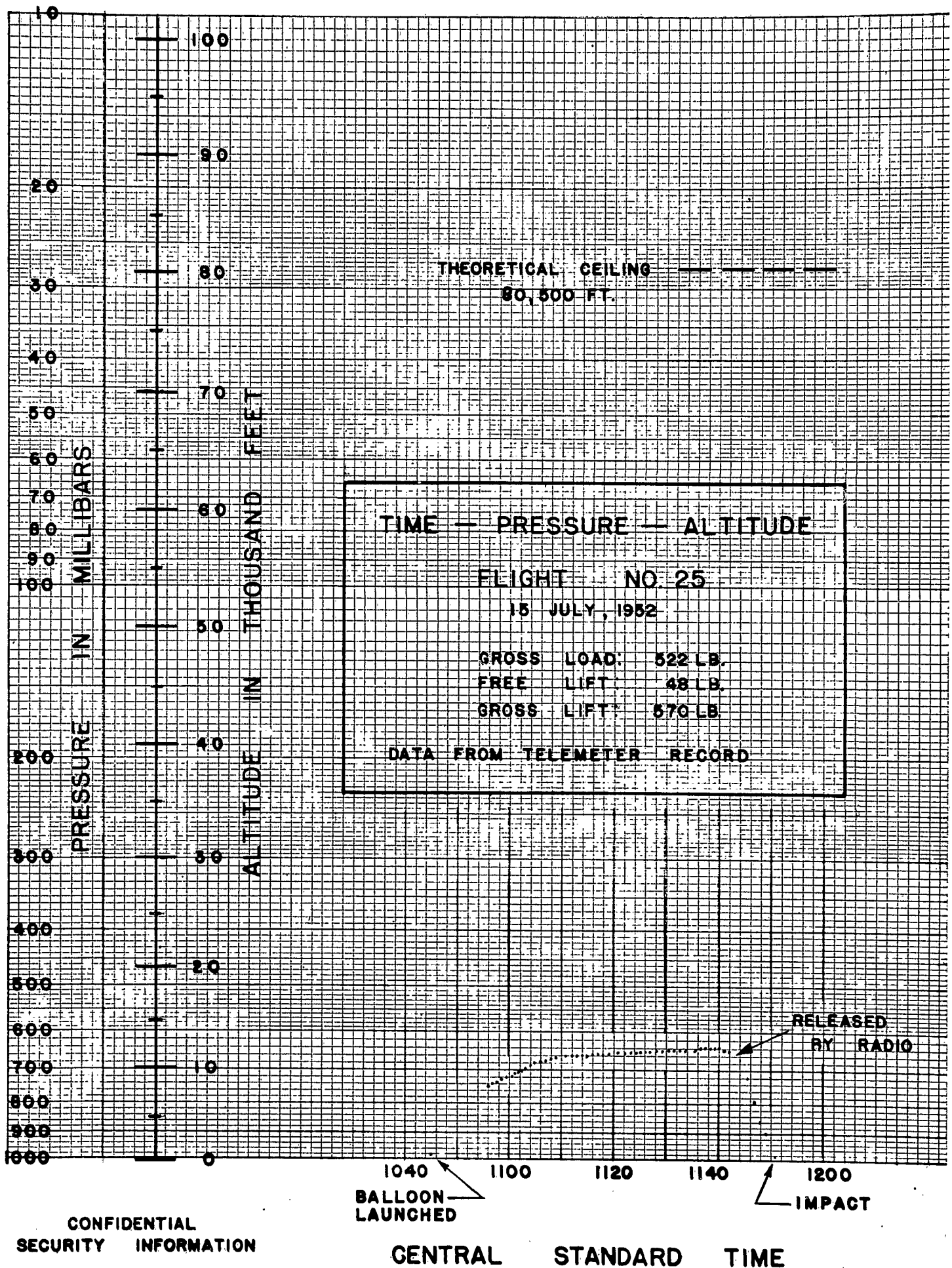
8 JULY, 1953

TRAJECTORY FROM DOWN PICTURES



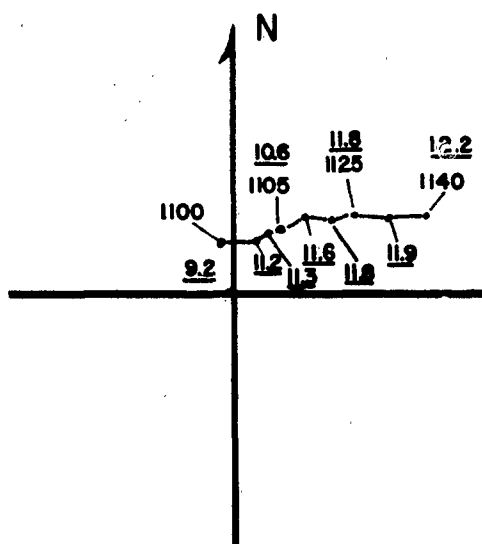
10 0 10 20 STATUTE MILES





CONFIDENTIAL

Launched at:
MINNEAPOLIS, MINN.



CENTRAL STANDARD TIME

PRESSURE ALTITUDE IN 1000 FT.

FLIGHT NO. 25

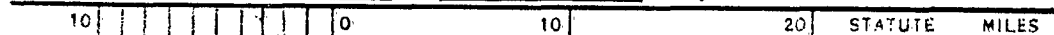
LAUNCHED 1045

15 JULY, 1952

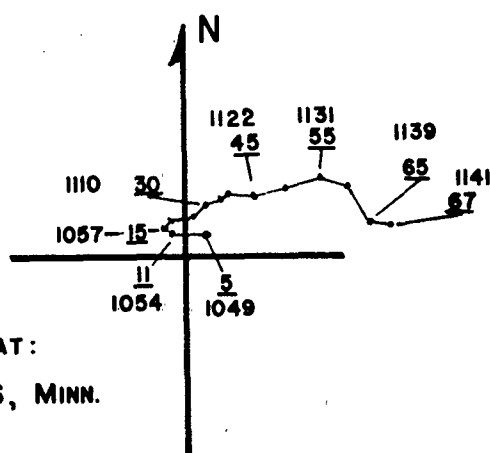
TRAJECTORY FROM THEODOLITE FIXES

SCALE $1:5 \times 10^5$

CONFIDENTIAL SECURITY INFORMATION



CONFIDENTIAL



CENTRAL STANDARD TIME

FILM FRAME NUMBER

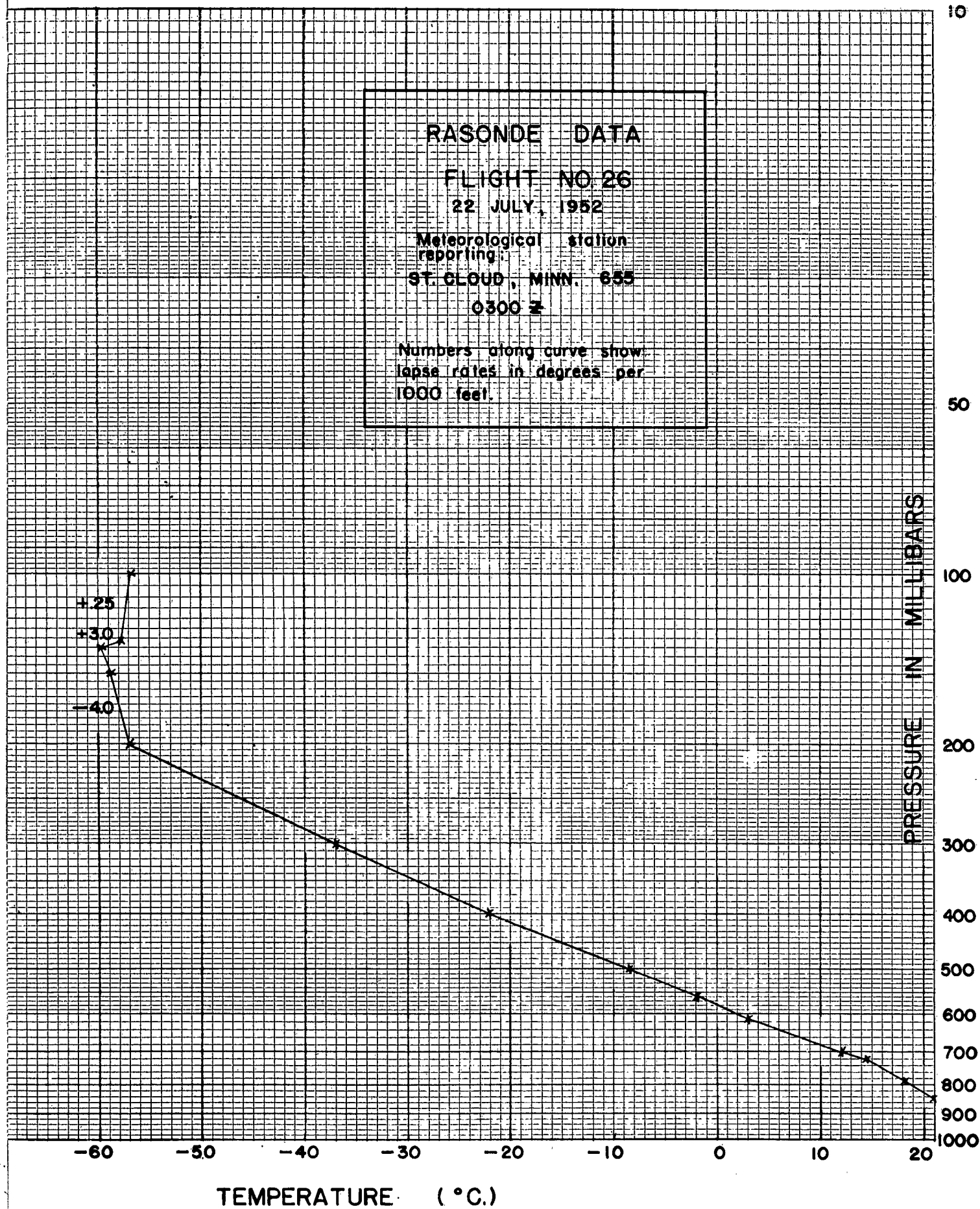
FLIGHT NO. 25

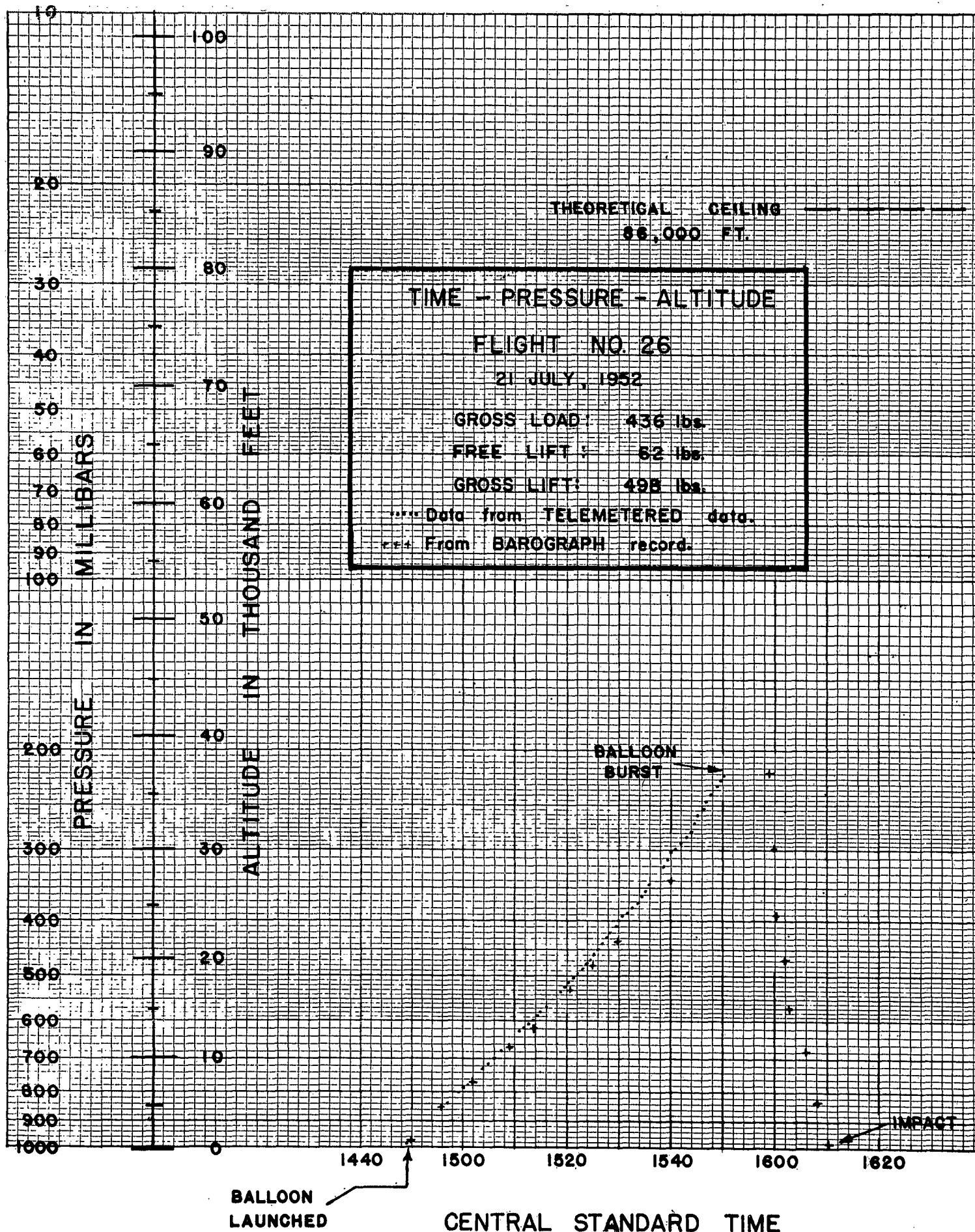
LAUNCHED 1045 CST
15 JULY, 1952

TRAJECTORY FROM DOWN PICTURES

SCALE $1:5 \times 10^5$ CONFIDENTIAL SECURITY INFORMATION

10										0	10	20	STATUTE MILES
----	--	--	--	--	--	--	--	--	--	---	----	----	---------------

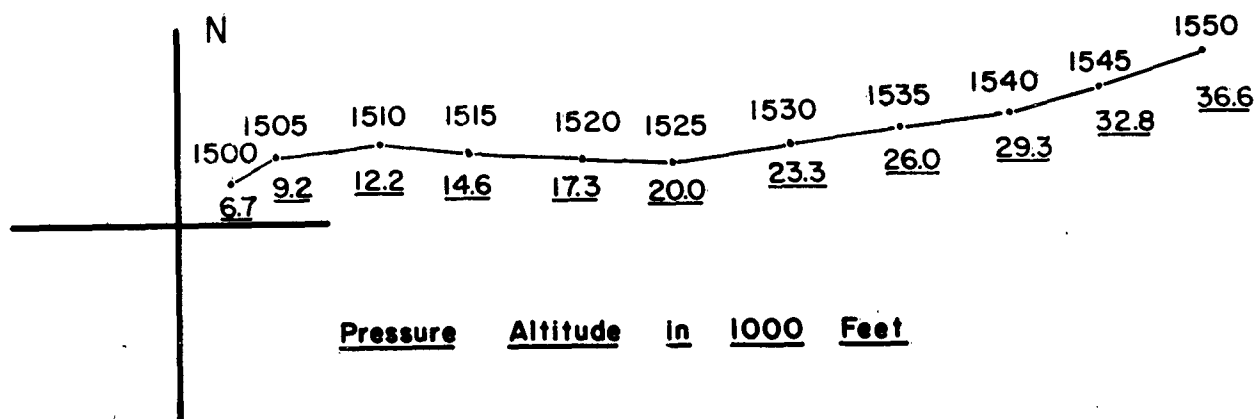




CONFIDENTIAL

Launched at:
MINNEAPOLIS, Minn.

Central Standard Time

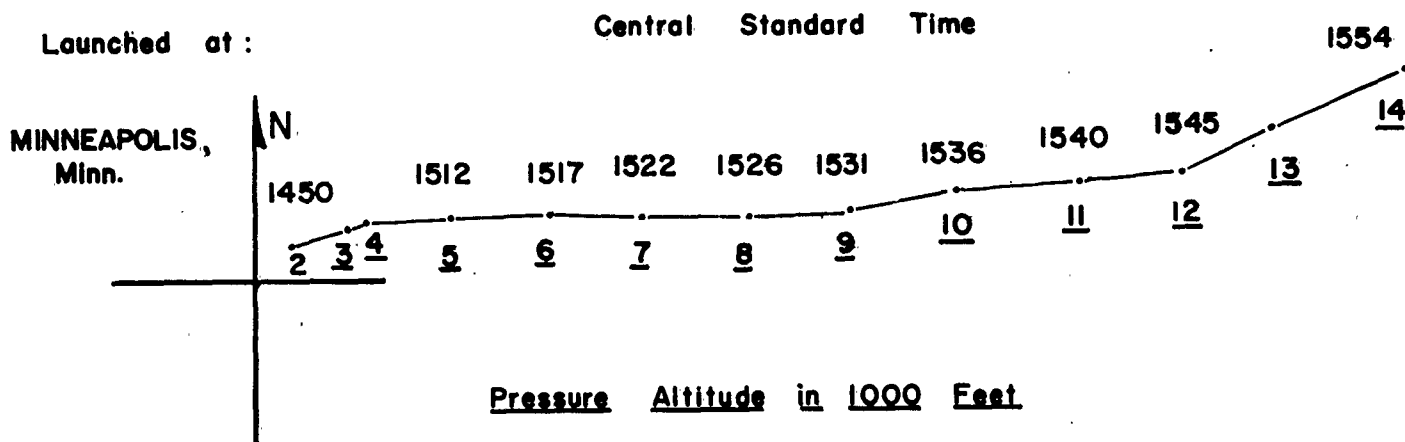


FLIGHT NO. 26
LAUNCHED 1449 CST
21 JULY, 1952
TRAJECTORY FROM THEODOLITE FIXES
SCALE $1:5 \times 10^6$

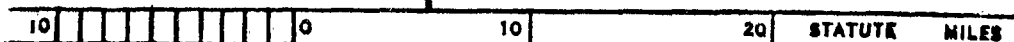
10 0 10 20 STATUTE MILES

CONFIDENTIAL SECURITY INFORMATION

CONFIDENTIAL



FLIGHT NO. 26
 LAUNCHED 1449 CST
 21 JULY, 1952
 TRAJECTORY FROM DOWN PICTURES
 SCALE $1:5 \times 10^5$



RASONDE DATA

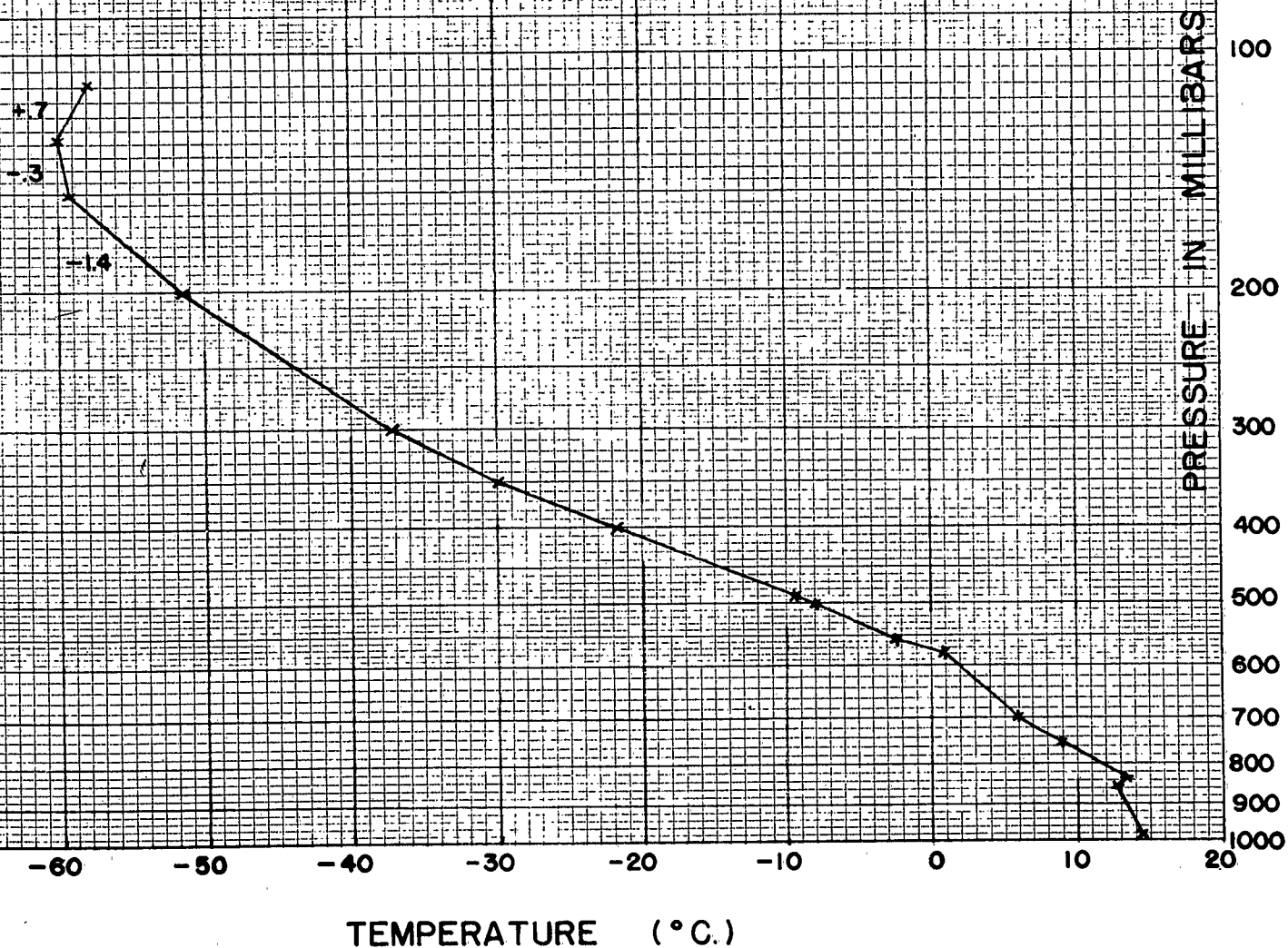
FLIGHT NO. 27

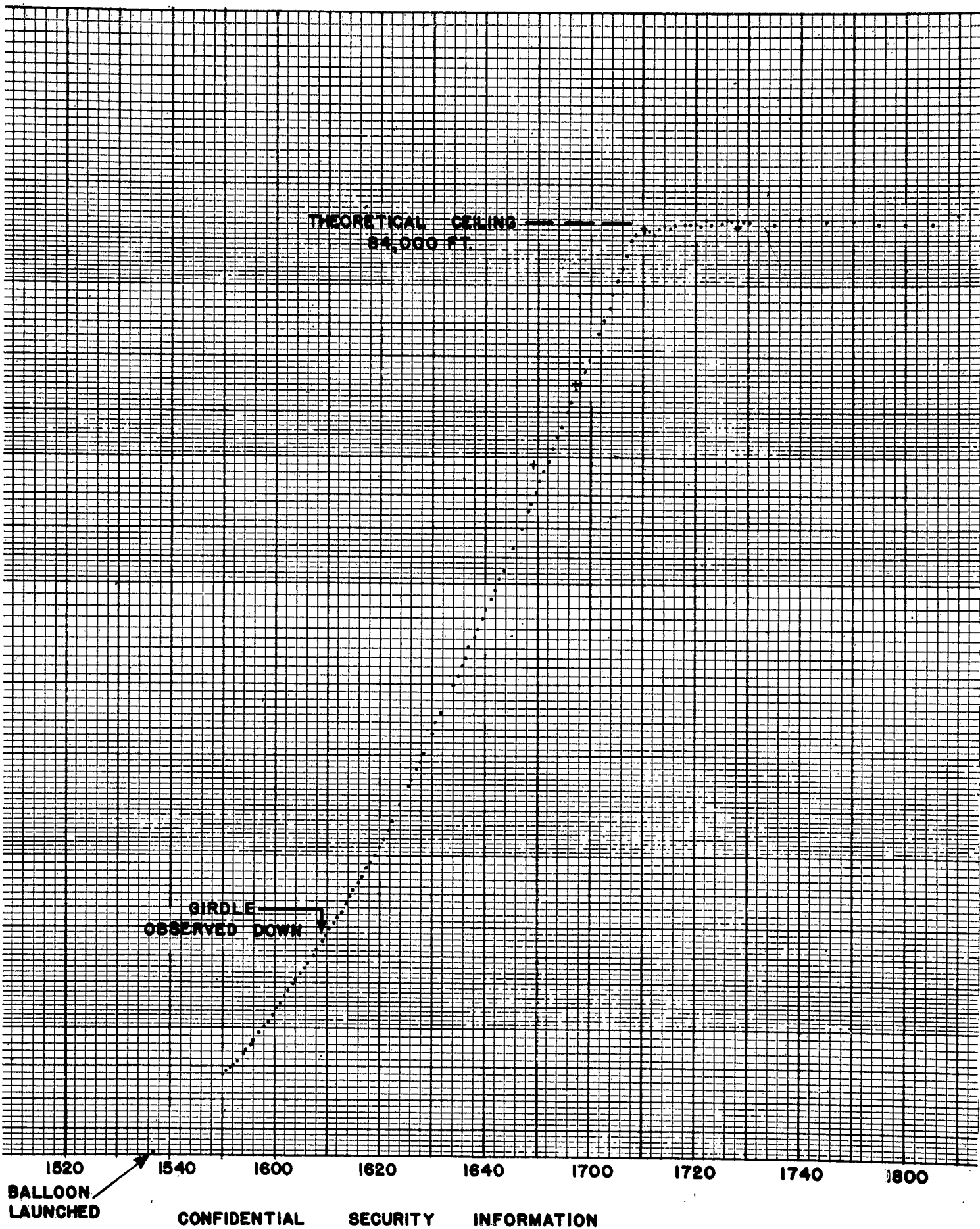
24 JULY, 1952

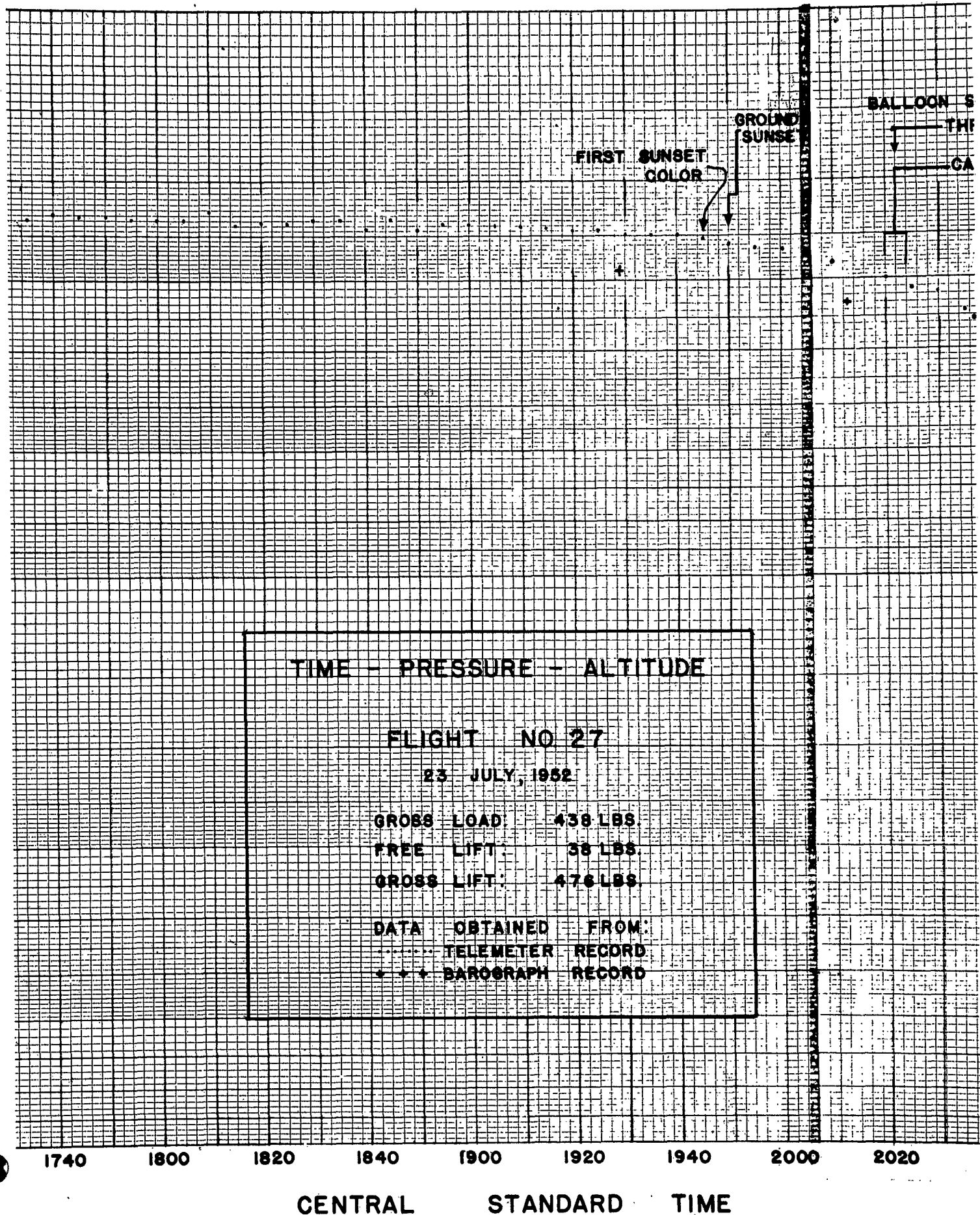
METEOROLOGICAL STATION
REPORTING:
ST. CLOUD, MINN. 655

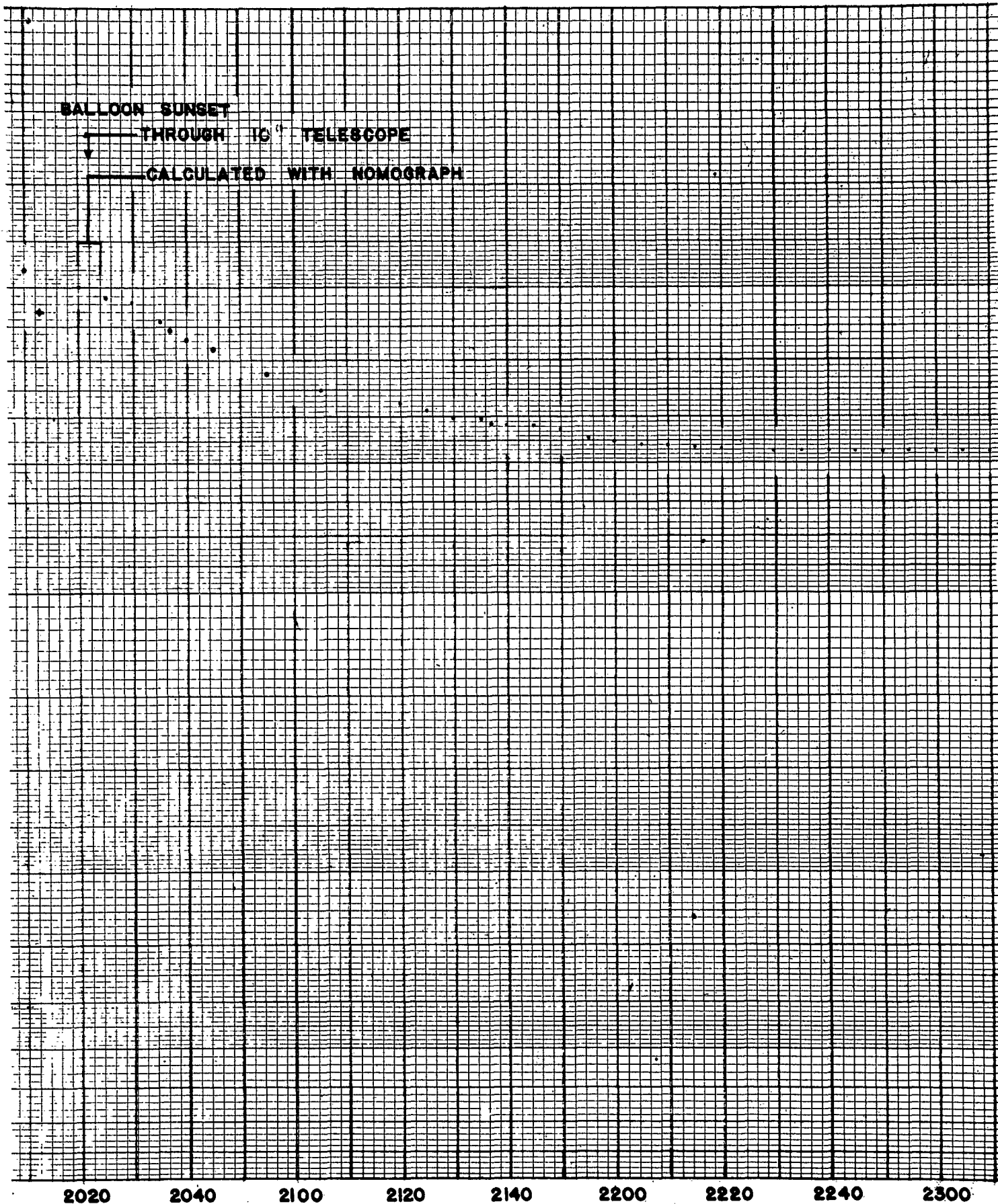
0300 Z

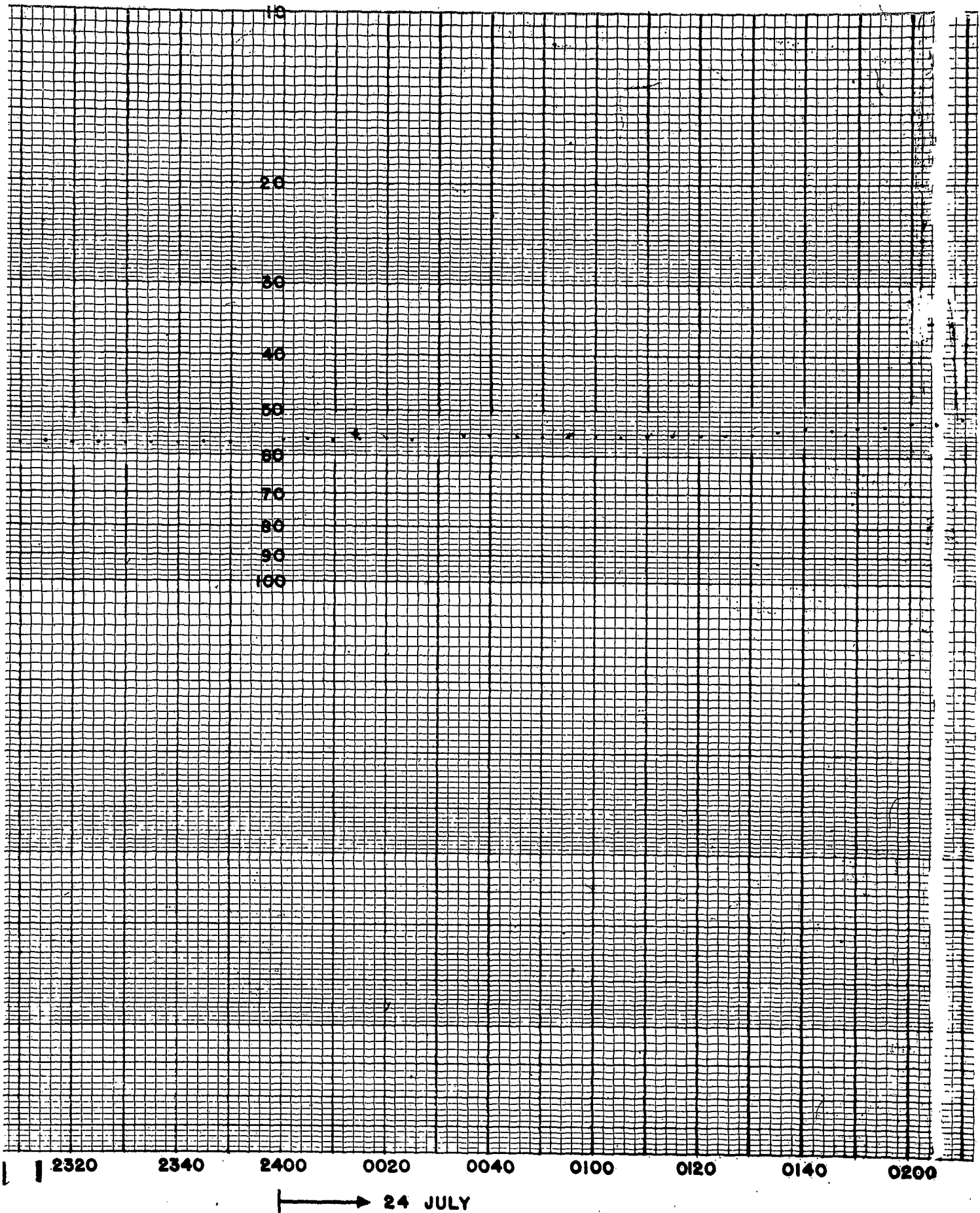
Numbers along curve show
lapse rates in degrees per
1000 feet.

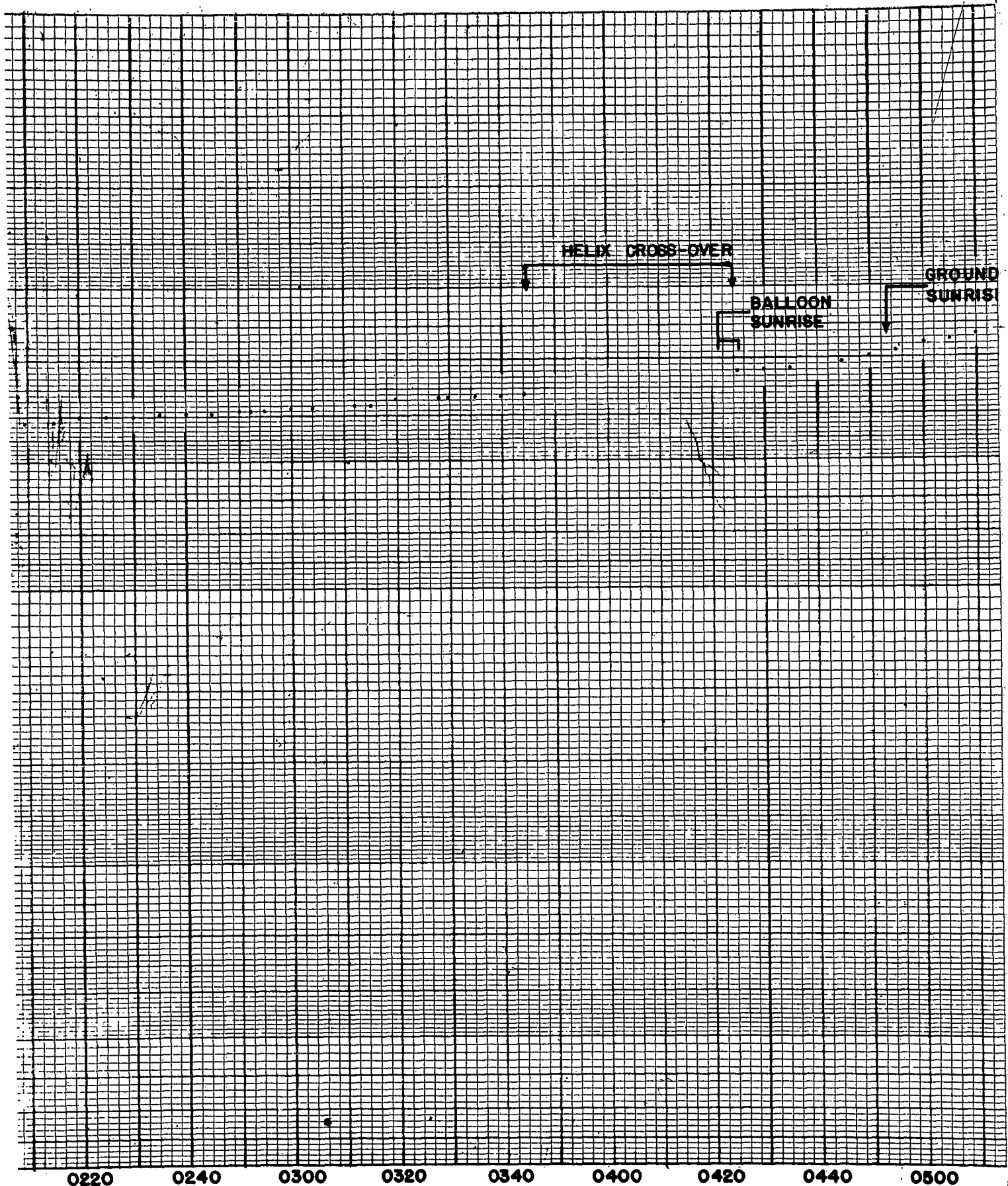


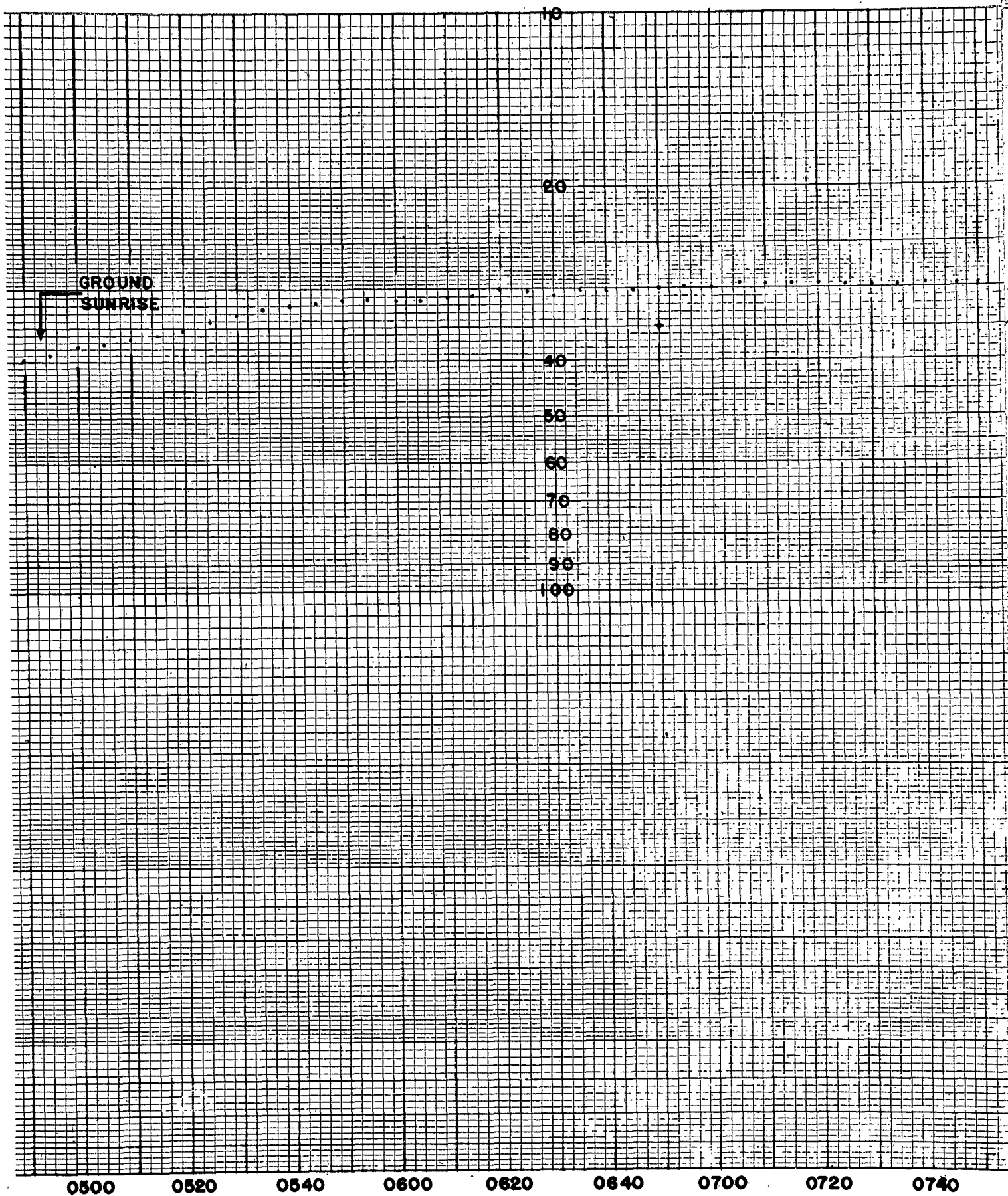


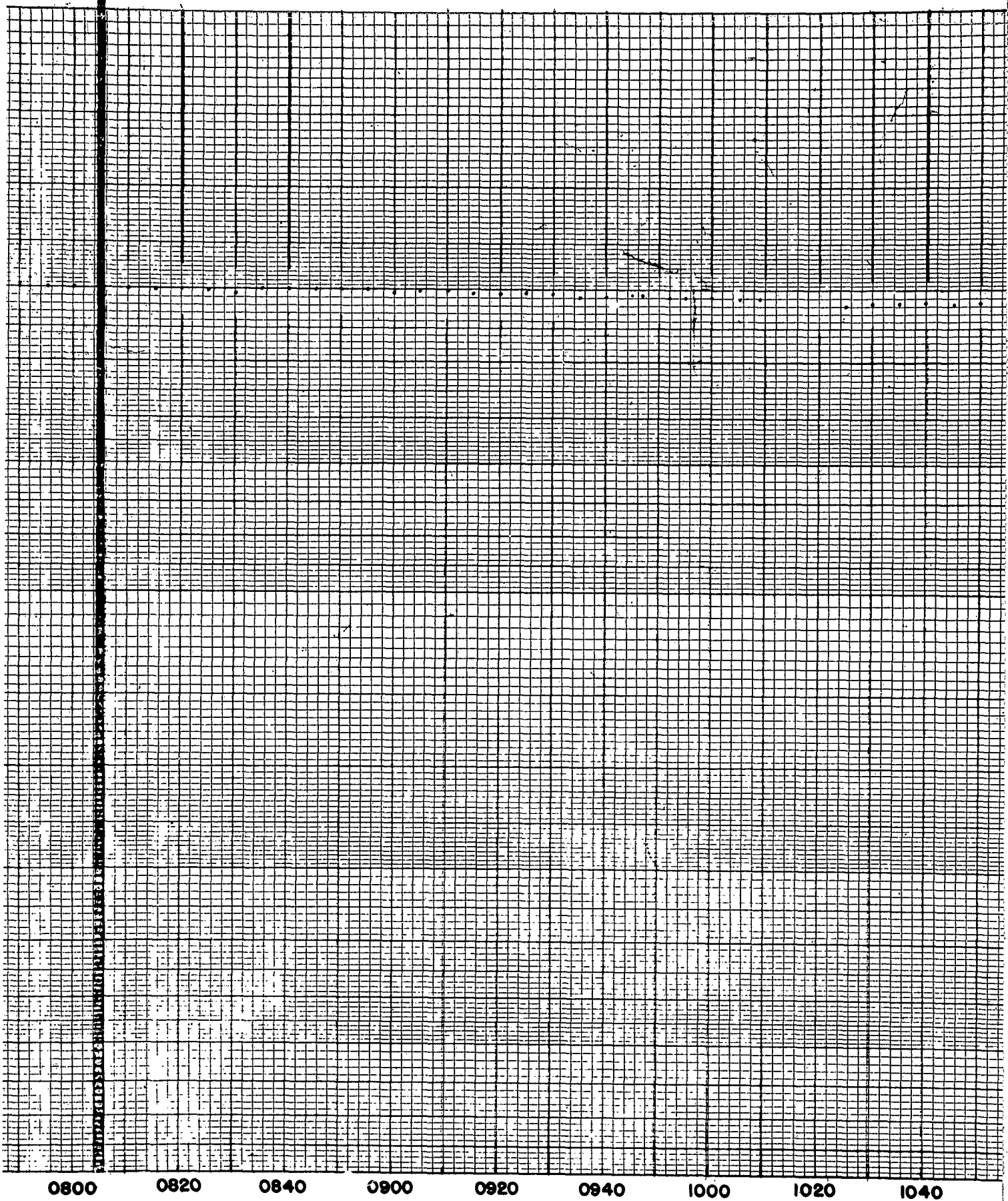


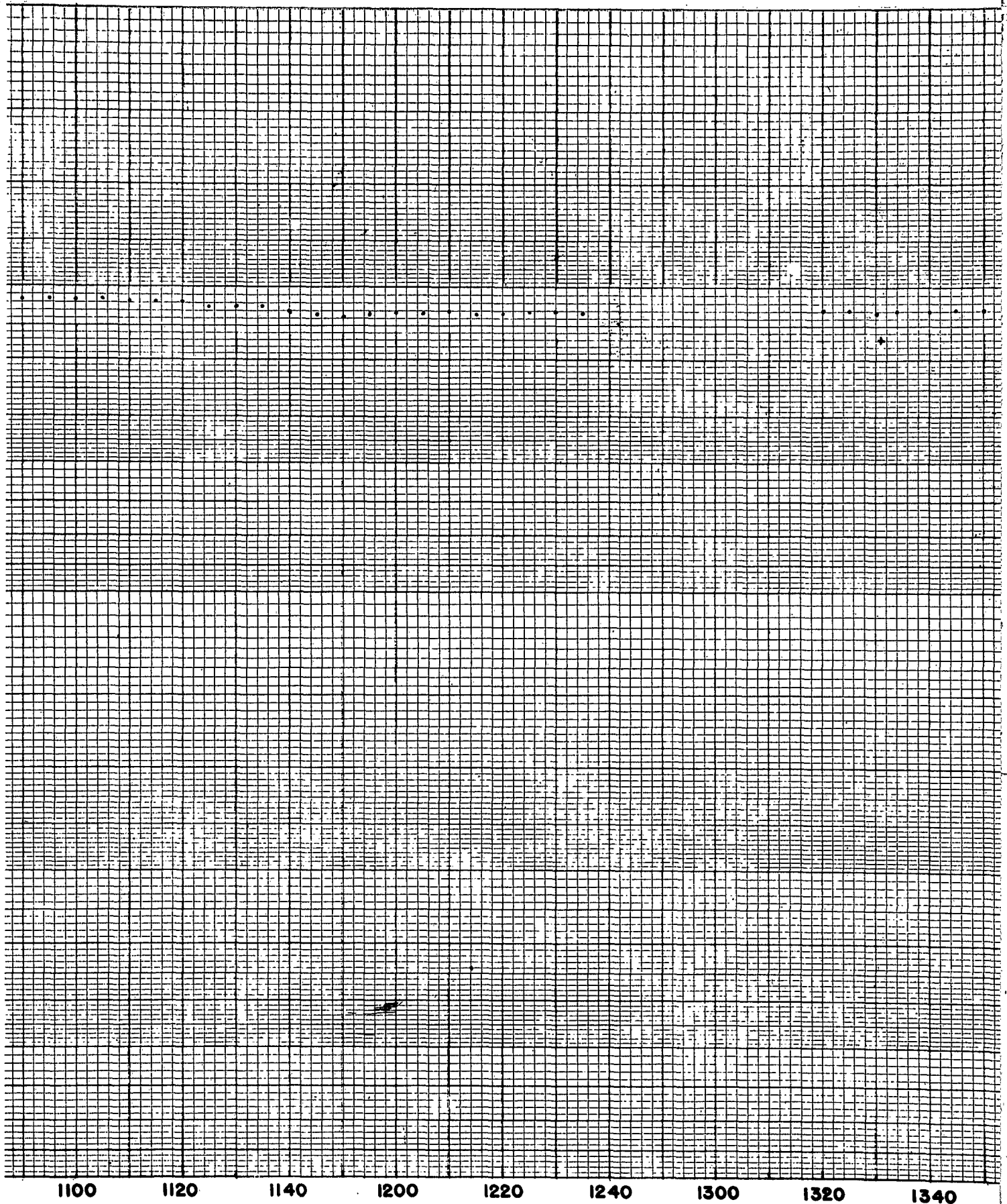




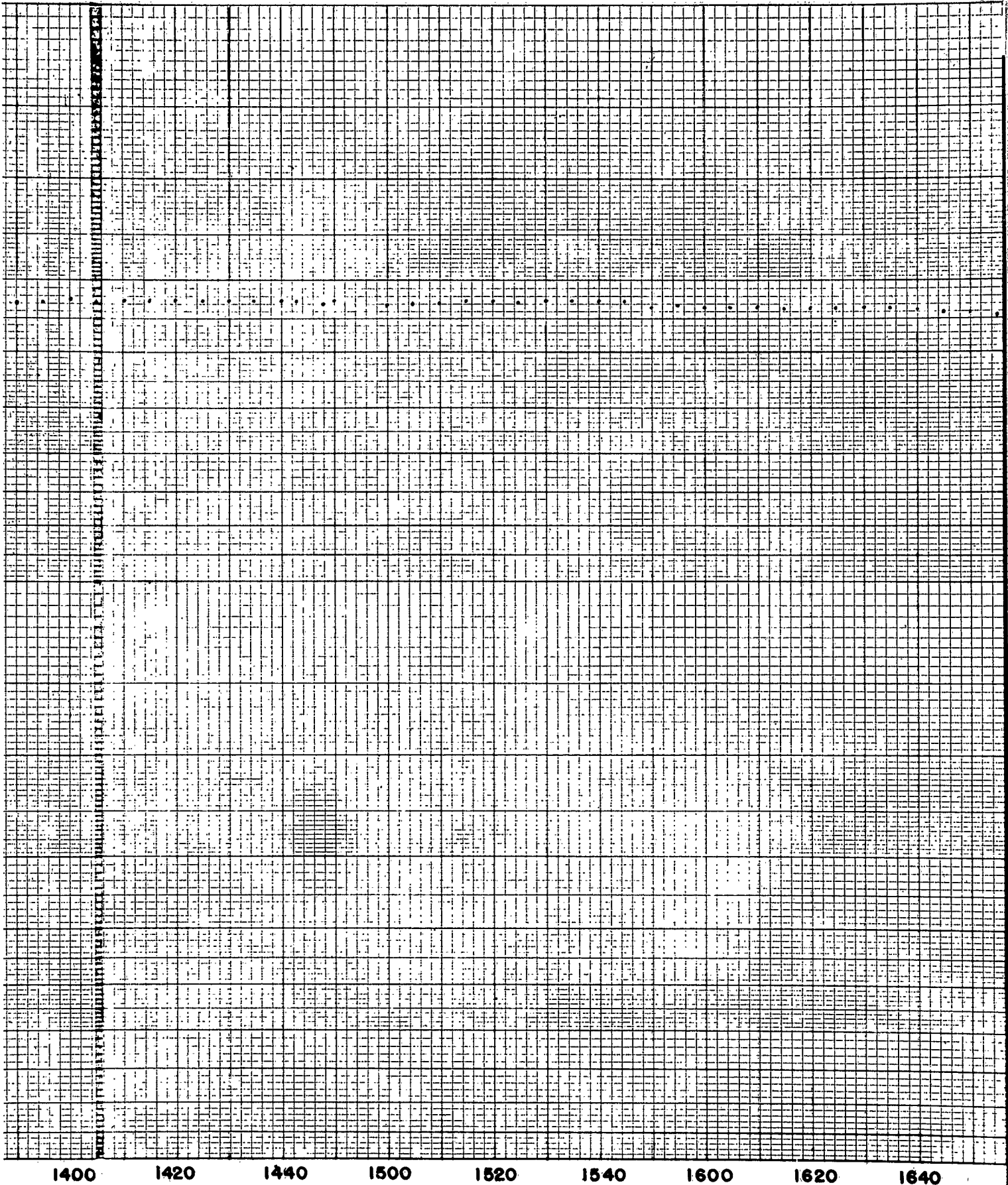


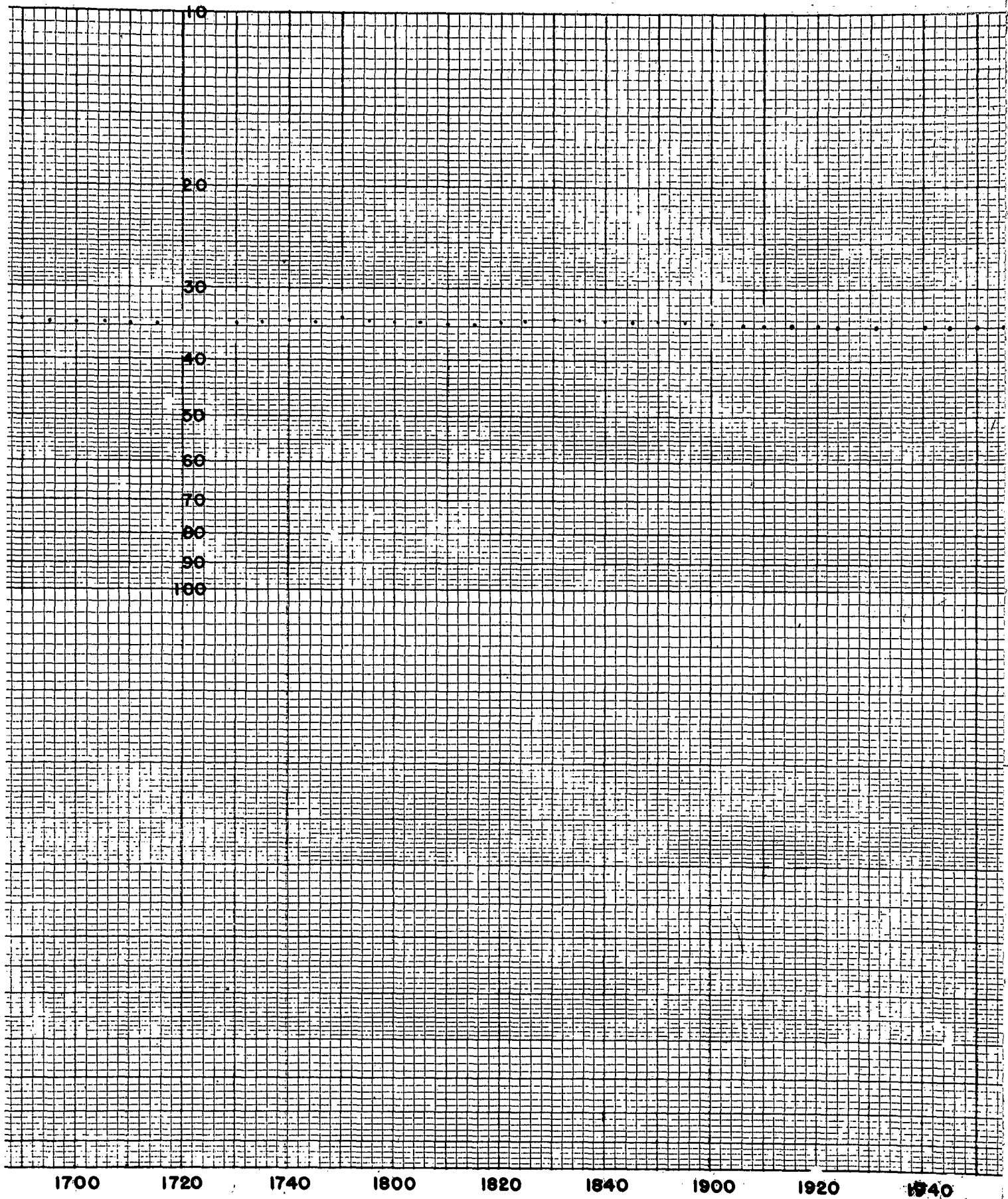


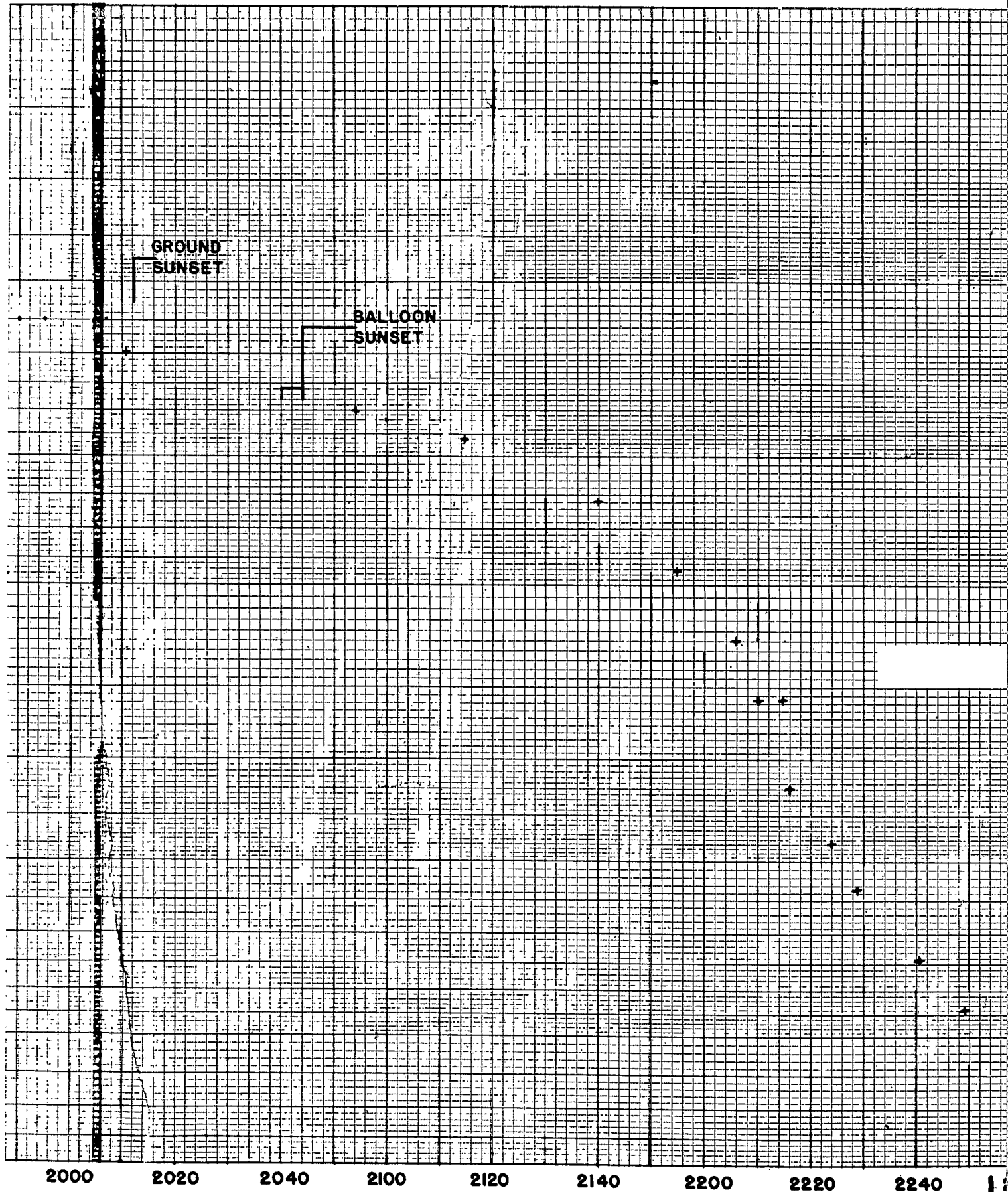


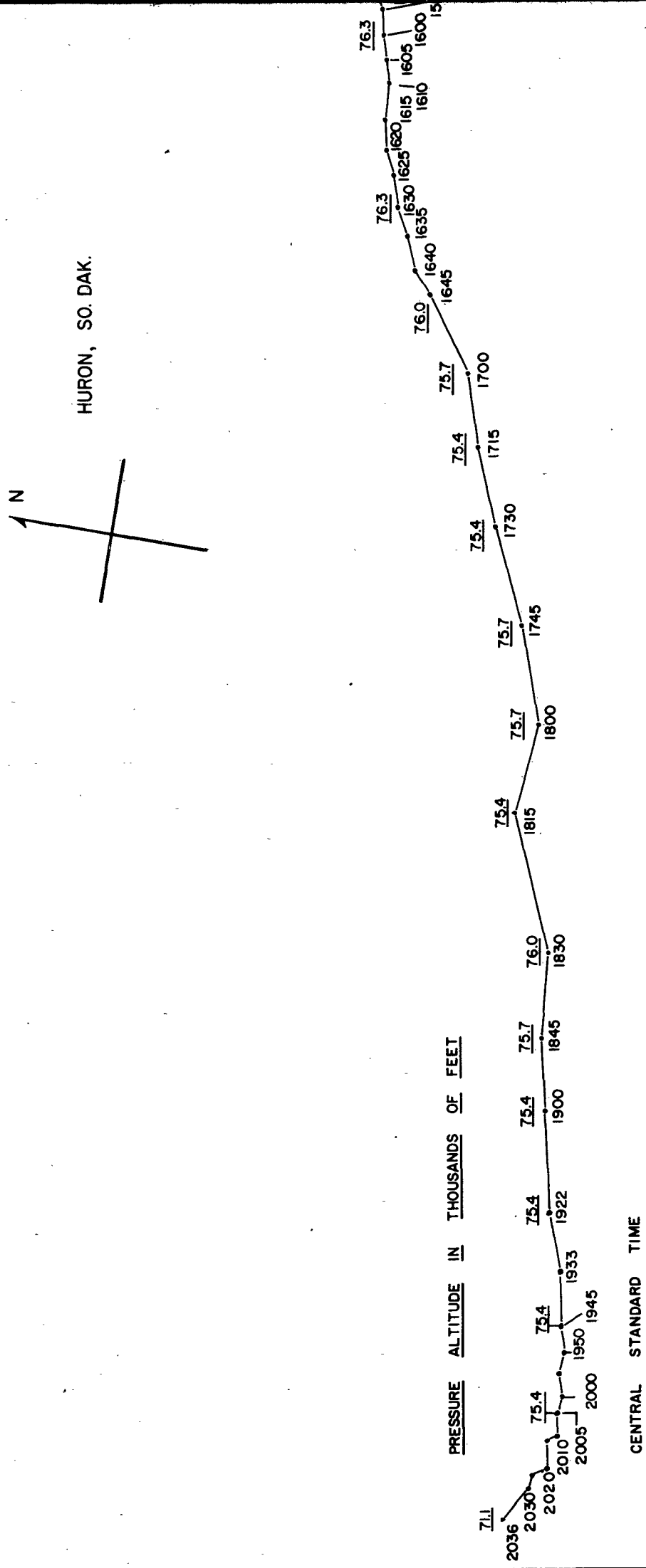


CENTRAL STANDARD TIME
24 JULY









FLIGHT NO. 27

LAUNCHED 1537

23 JULY, 1952

TRAJECTORY FROM THEODOLITE FIXES

CONFIDENTIAL **SECURITY** **INFORMATION**

SECURITY

CONFIDENTIAL

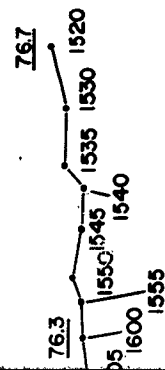
INFORMATION

201	STATUTE	MILES

01

C

12



77.0

1155

1140

1135

1125

1110

77.6

1055

1040

1030

1020

1015

1005

995

995

945

935

925

920

910

900

850

840

830

820

815

805

78.7

750

740

730

720

710

700

650

640

630

ALTITUDE IN THOUSANDS OF FEET

CENTRAL

CONFIDENTIAL

Launched at:
MINNEAPOLIS, Minn.

N

1844

10

15

1552

15

1557

20

25

1603

30

1613

35

40

1623

45

1628

50

55

1638

60

65

70

75

80

85

90

95

100

105

110

115

120

125

130

135

140

145

150

155

160

165

170

175

180

185

190

1911

1920

1930

1940

1950

1960

1970

1980

1990

2000

2010

2020

2030

2040

2050

2060

2070

2080

2090

2100

2110

2120

2130

2140

2150

2160

2170

2180

2190

2200

2210

2220

2230

2240

2250

2260

2270

2280

2290

2300

2310

2320

2330

2340

2350

2360

2370

2380

Central Standard Time

Film Frame Number

FLIGHT NO. 27

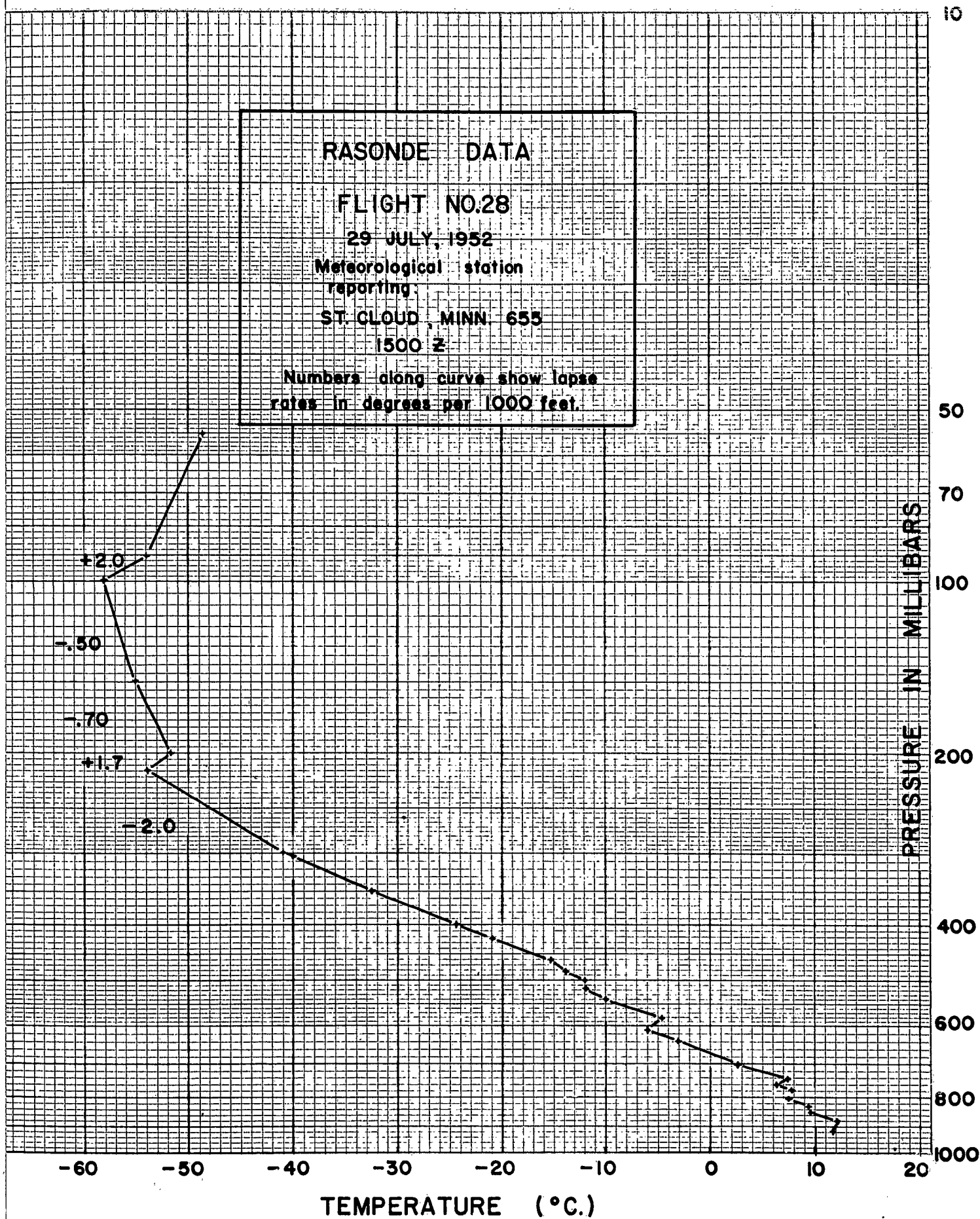
Launched 1537 CST

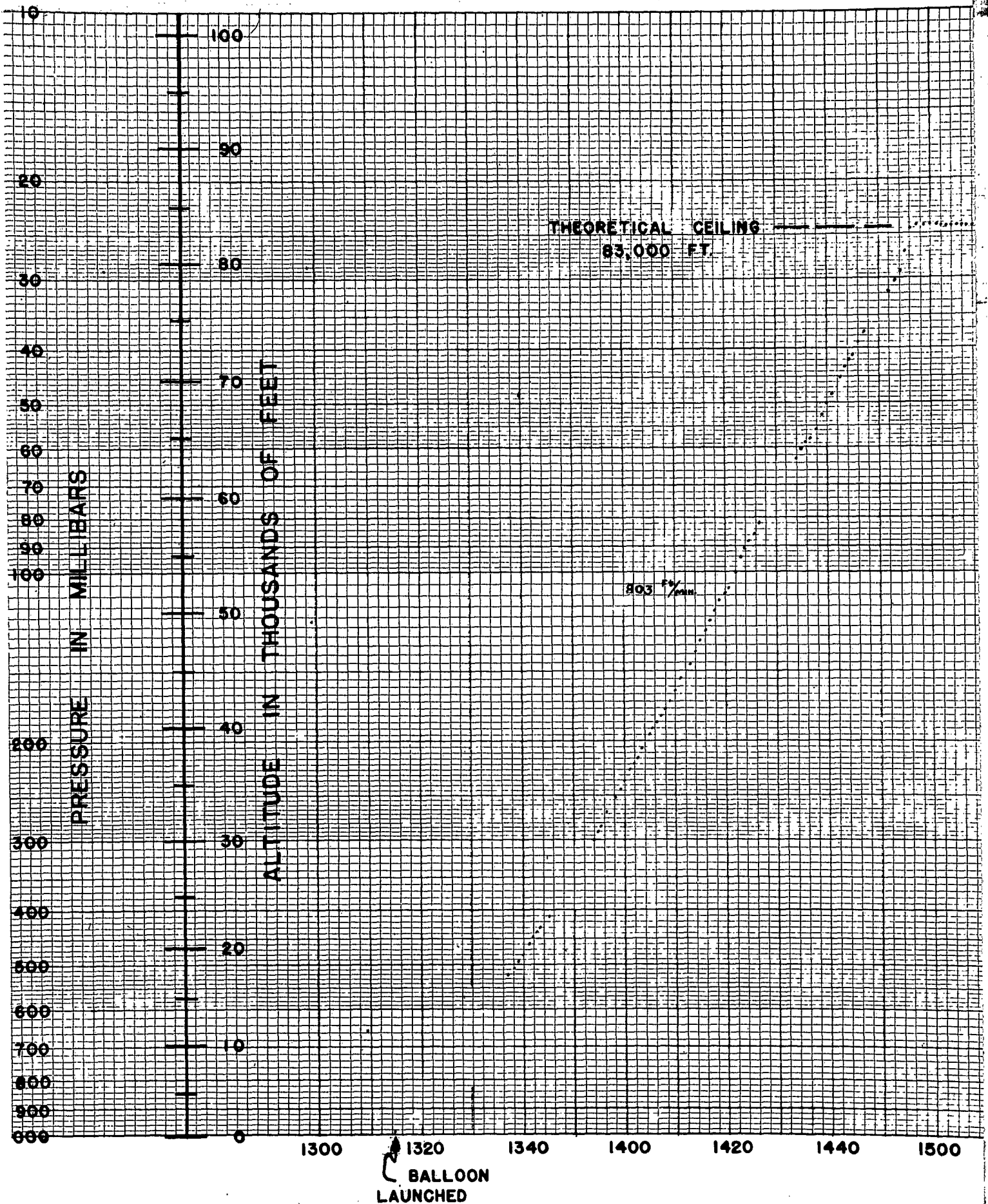
23 JULY, 1953

TRAJECTORY FROM DOWN PICTURES

SCALE 1:5 x 10⁵

10	0	10	20	STATUTE MILES





BALLOON
LAUNCHED

TIME - PRESSURE - ALTITUDE

FLIGHT NO. 28

29 JULY, 1952

GROSS LOAD: 456 LBS.

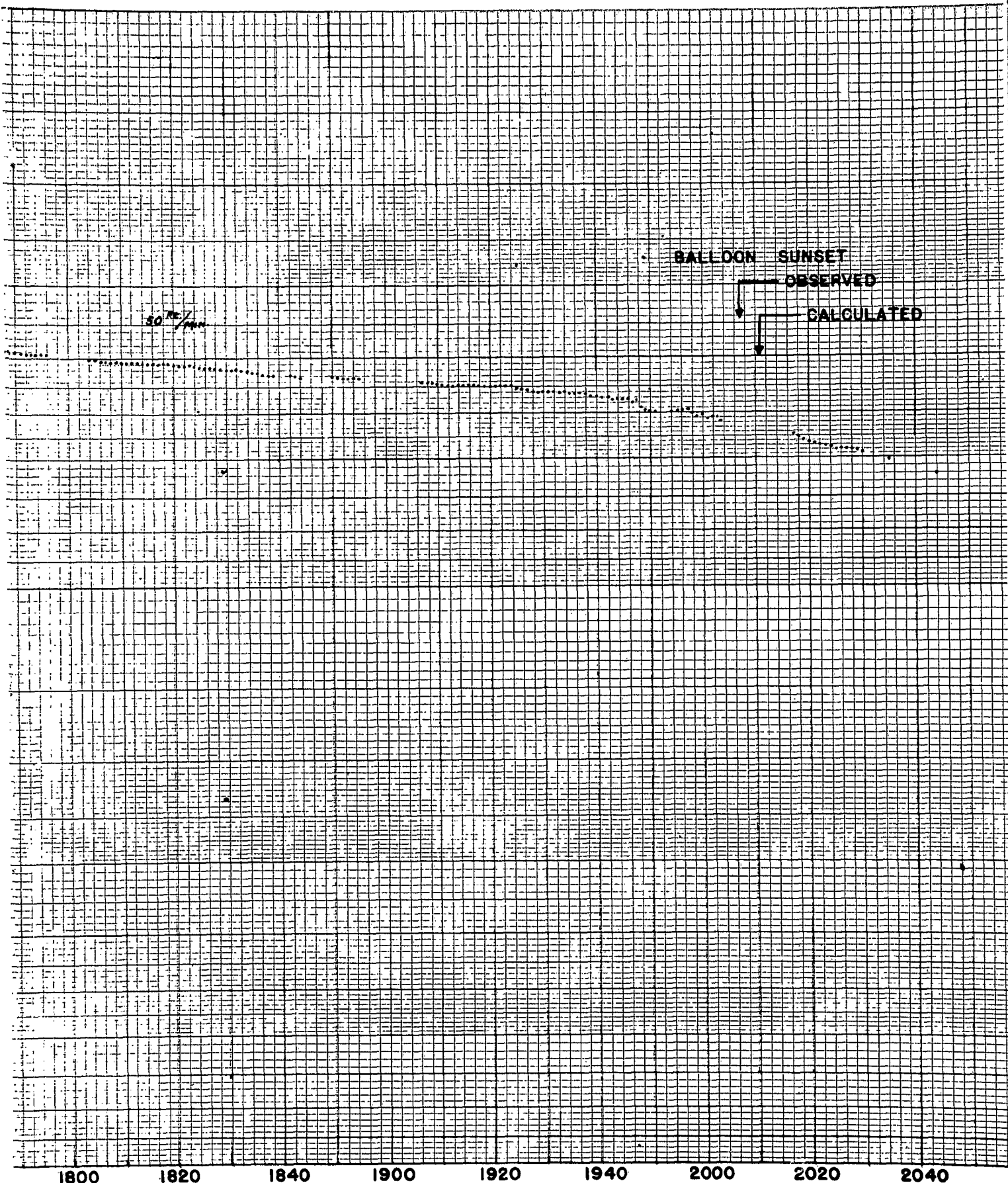
FREE LIFT: 80 LBS.

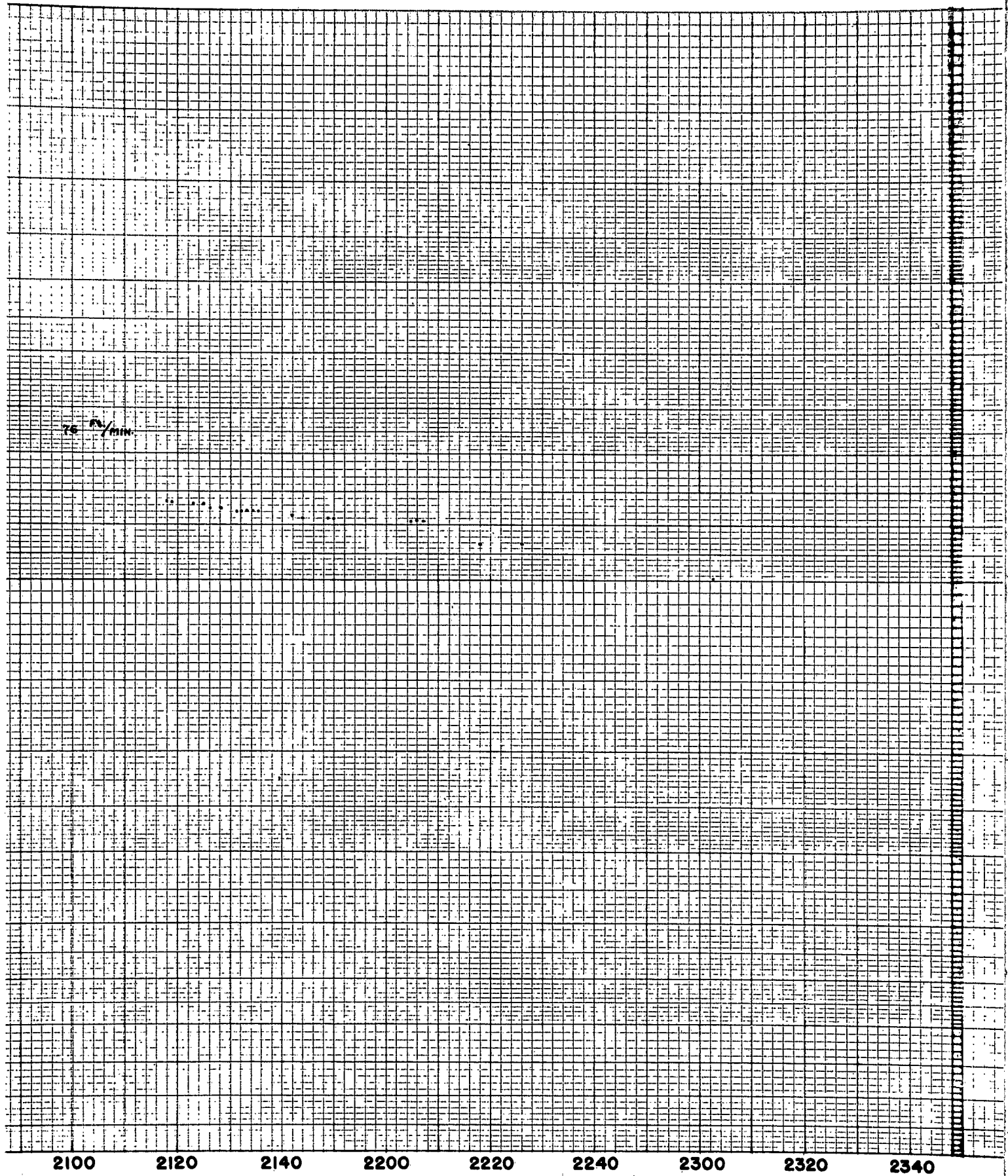
GROSS LIFT: 536 LBS.

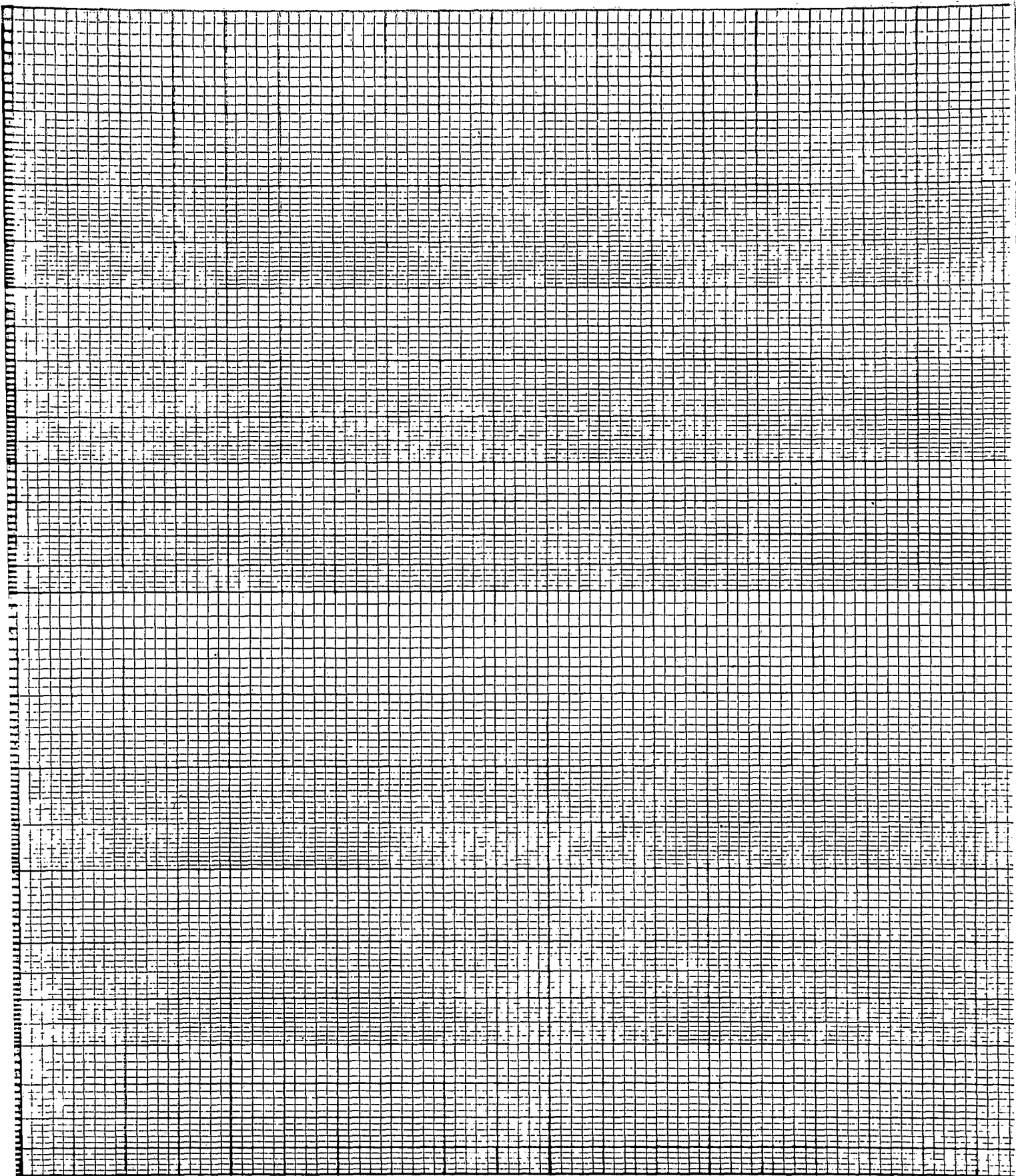
TELEMETER RECORD

1500 1520 1540 1600 1620 1640 1700 1720 1740 180

CENTRAL STANDARD TIME



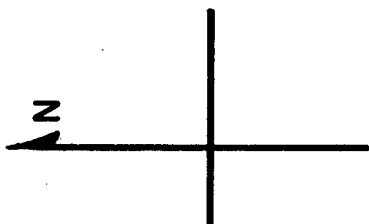




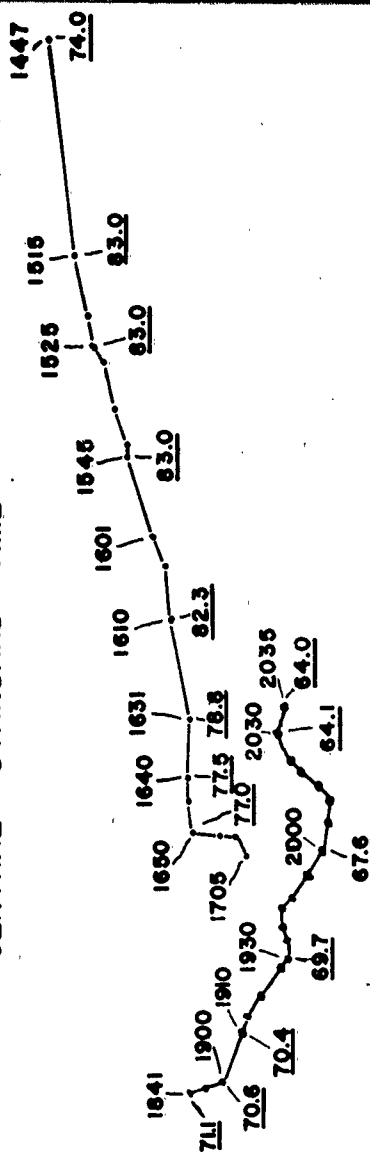
→ 30 JULY

CONFIDENTIAL

Launched at:
MINNEAPOLIS, Minn.



CENTRAL STANDARD TIME



PRESSURE ALTITUDE IN 1000 FT.

FLIGHT NO. 28

LAUNCHED 1315 CST

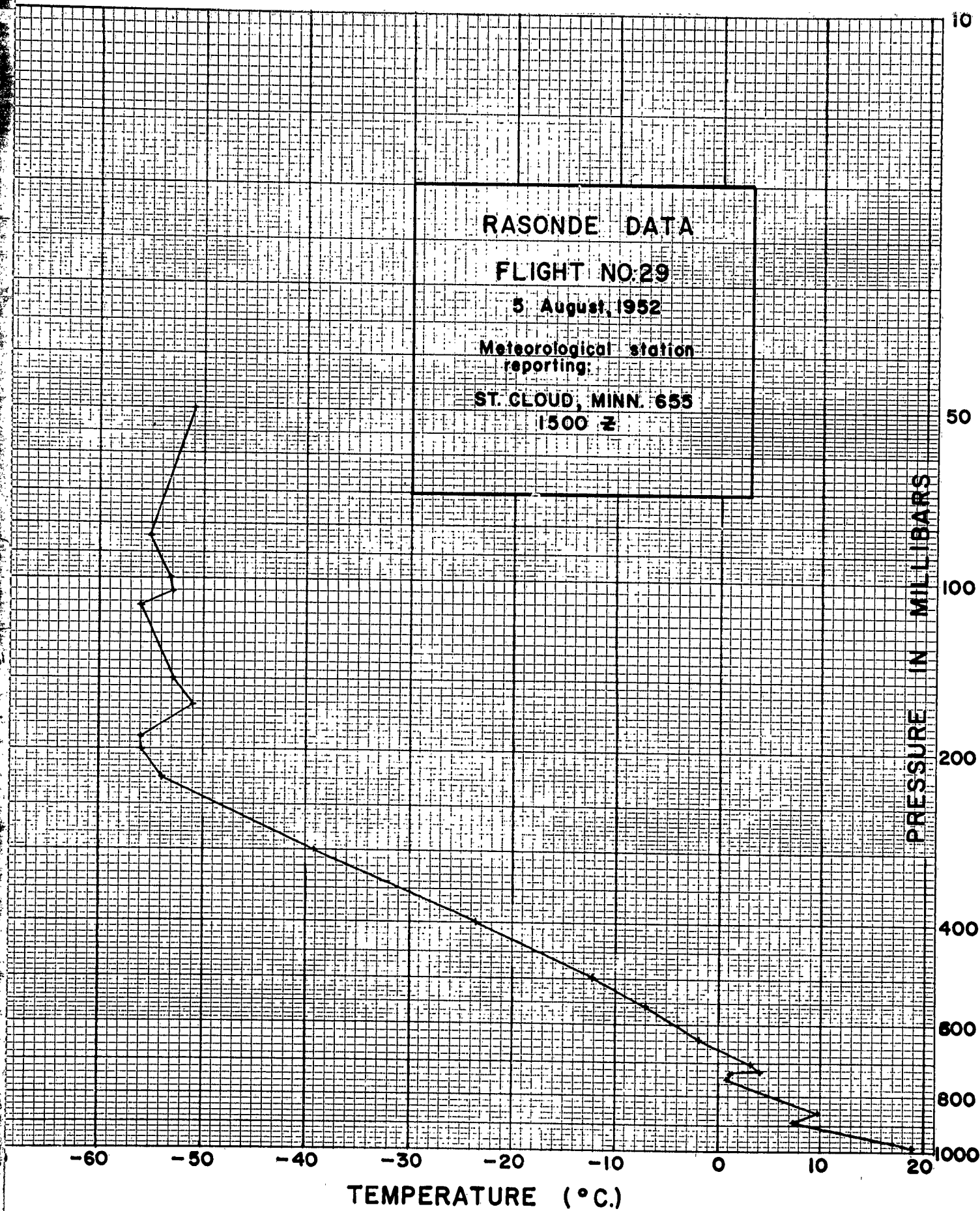
29 JULY, 1952

TRAJECTORY FROM THEODOLITE FIXES

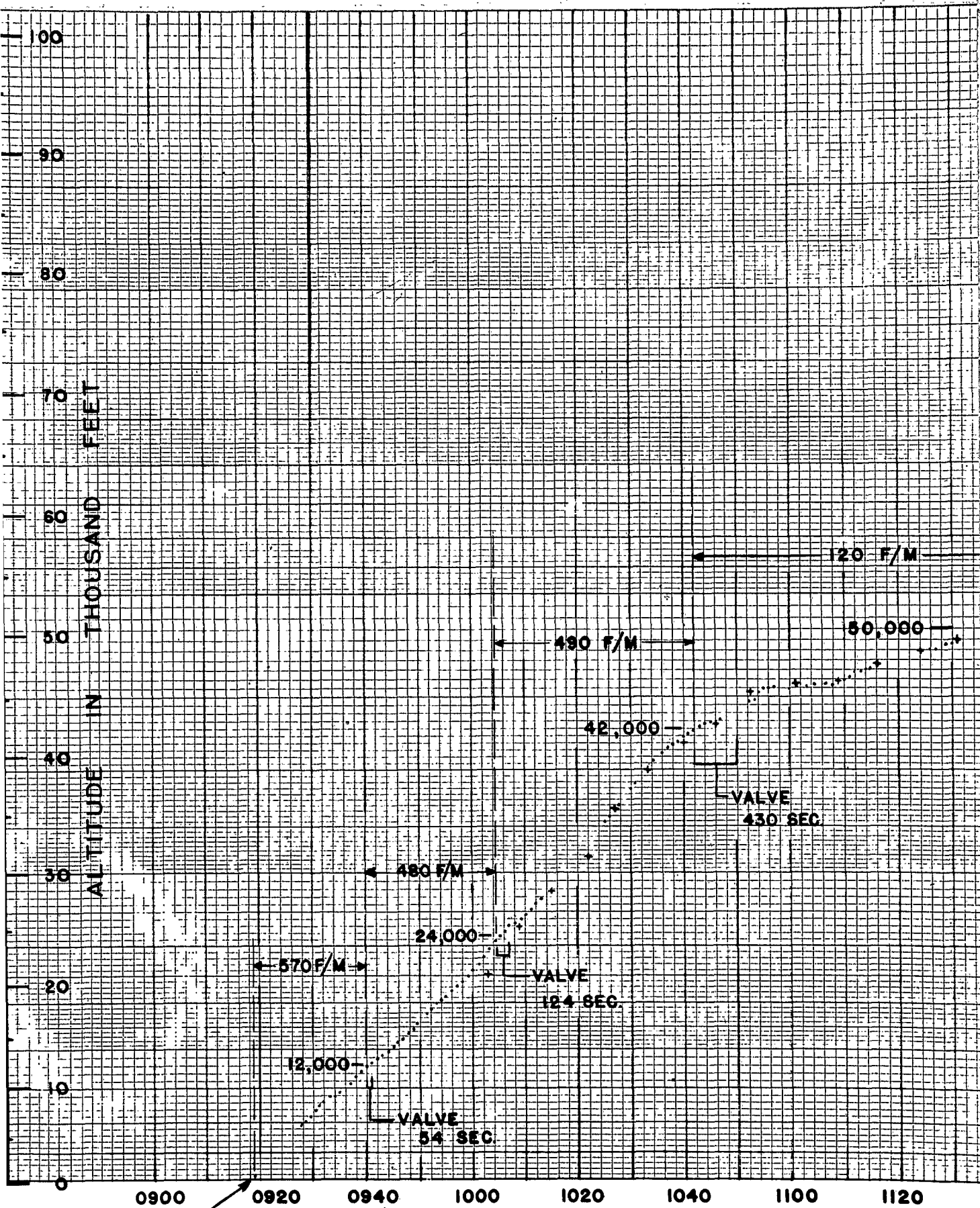
SCALE 1:5 x 10⁵

STATUTE MILES									
10									
	10								
		20							

Confidential

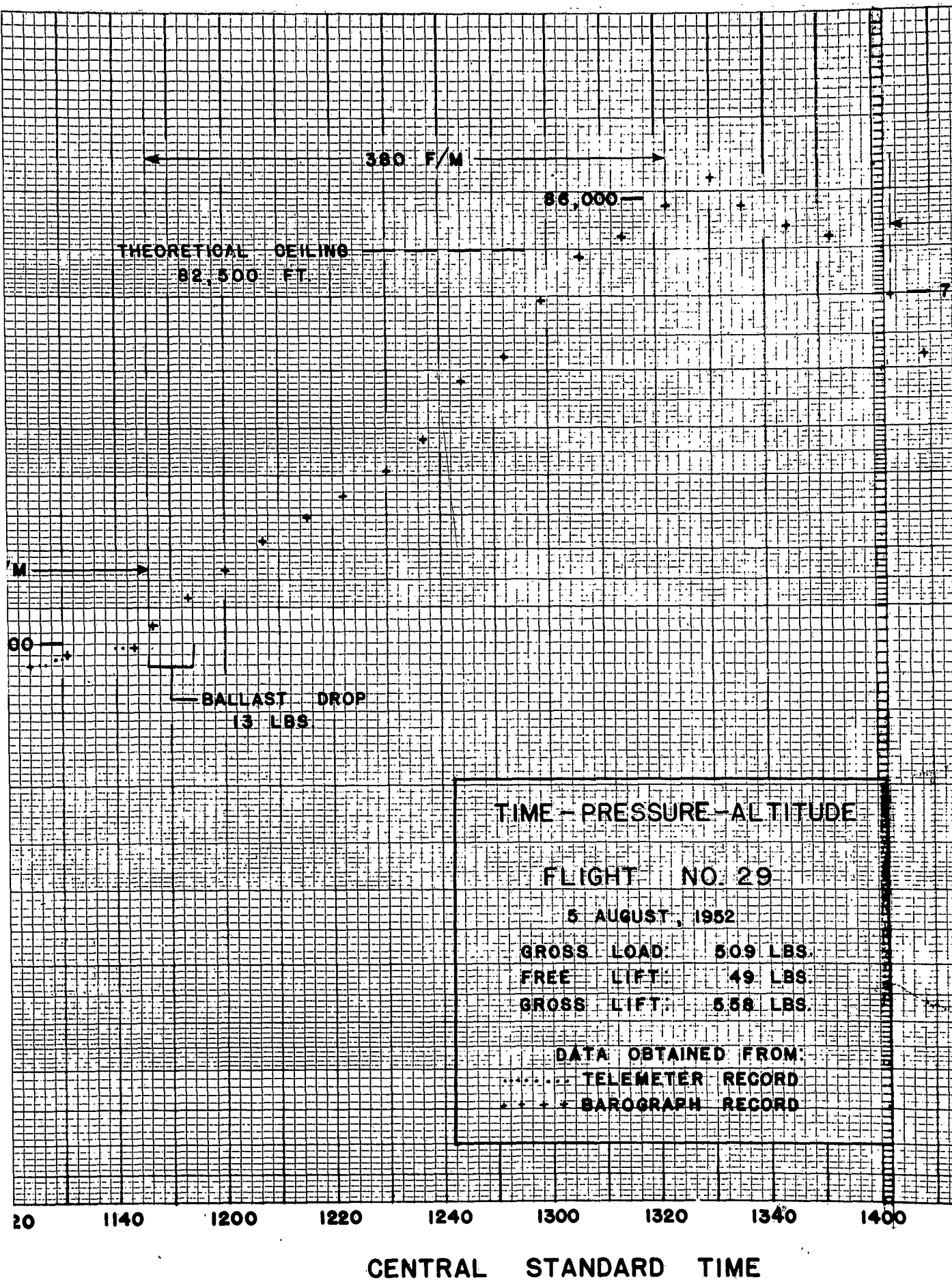


Confidential Security Information

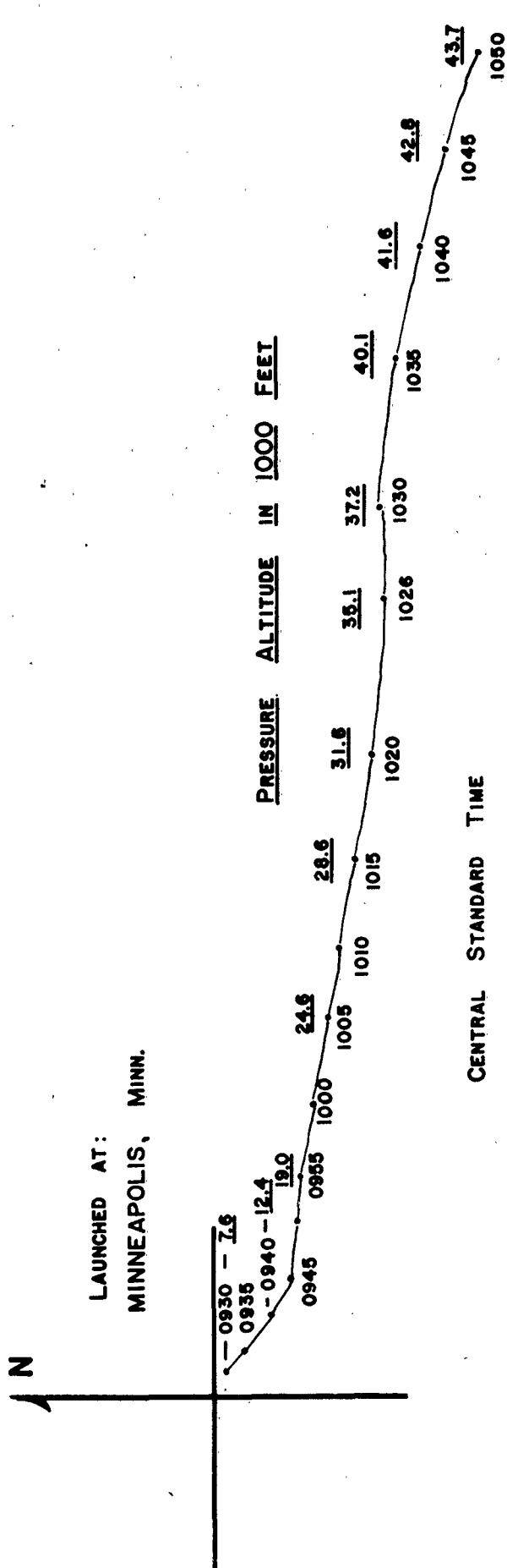


BALLOON
LAUNCHED

CONFIDENTIAL SECURITY INFORMATION



CONFIDENTIAL



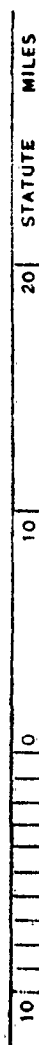
FLIGHT NO. 29

LAUNCHED 0919

5 AUGUST, 1952

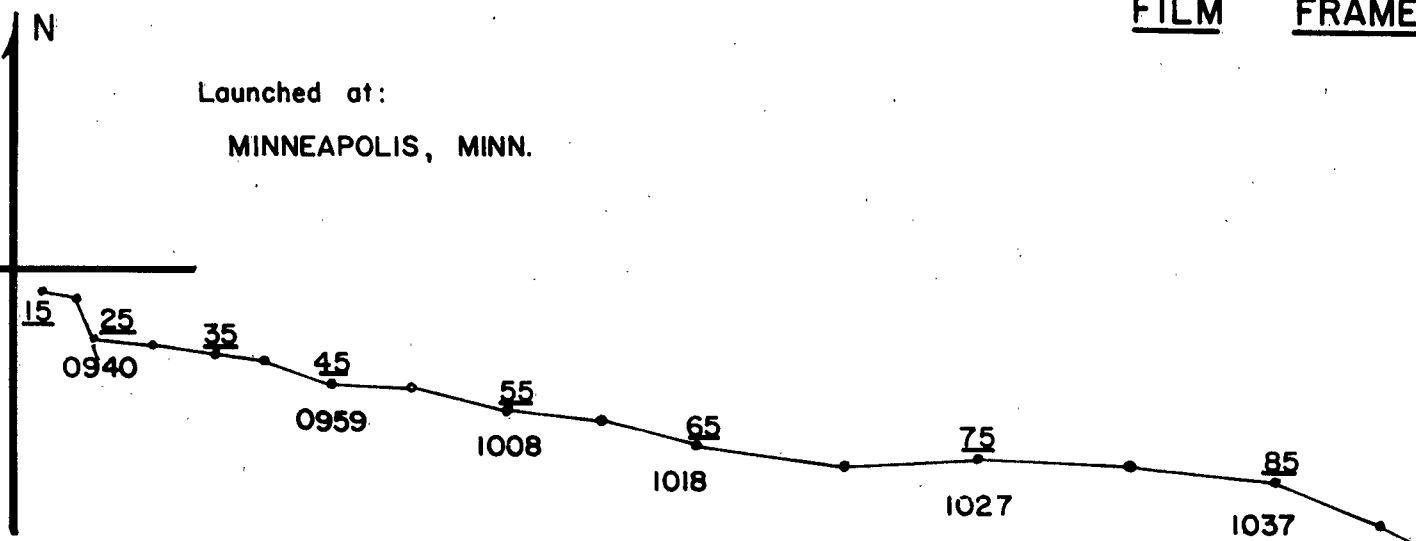
TRAJECTORY FROM THEODOLITE FIXES

SCALE: 1:5 x 10⁵



FILM FRAME

Launched at:
MINNEAPOLIS, MINN.



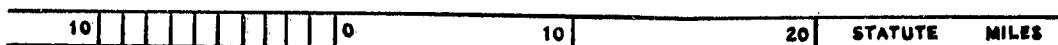
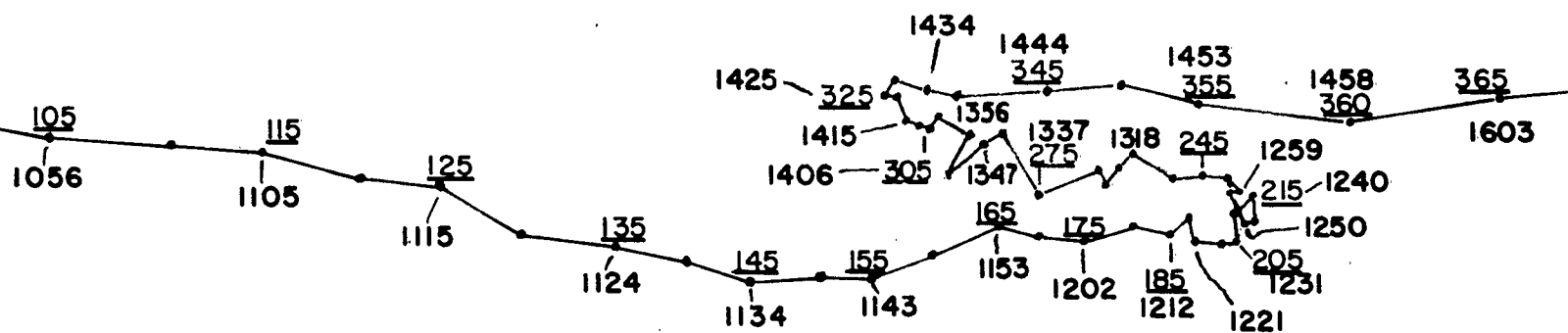
CENTRAL STANDARD TIME

CONFIDENTIAL
SECURITY
INFORMATION

1

CONFIDENTIAL SECURITY INFORMATION

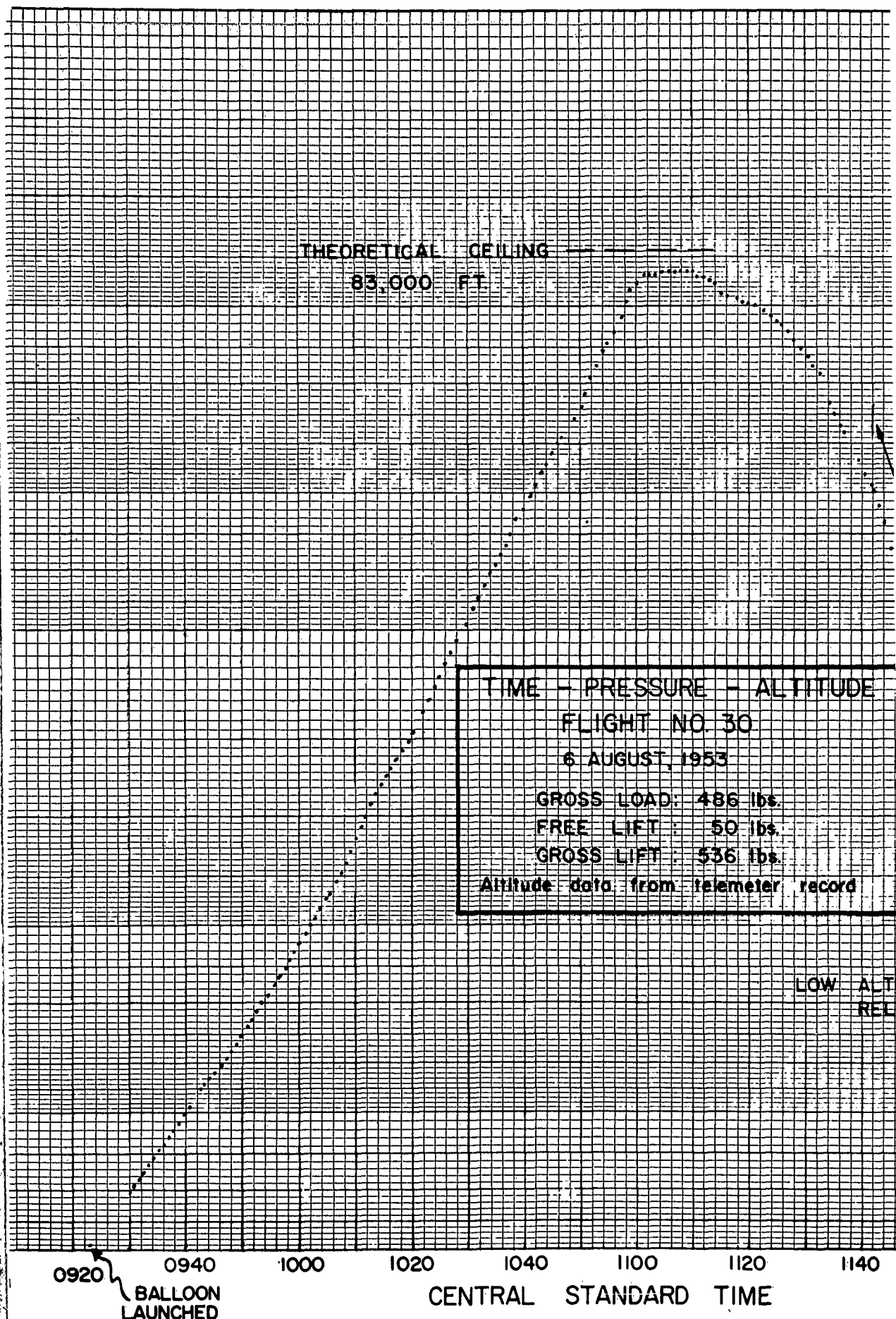
RS



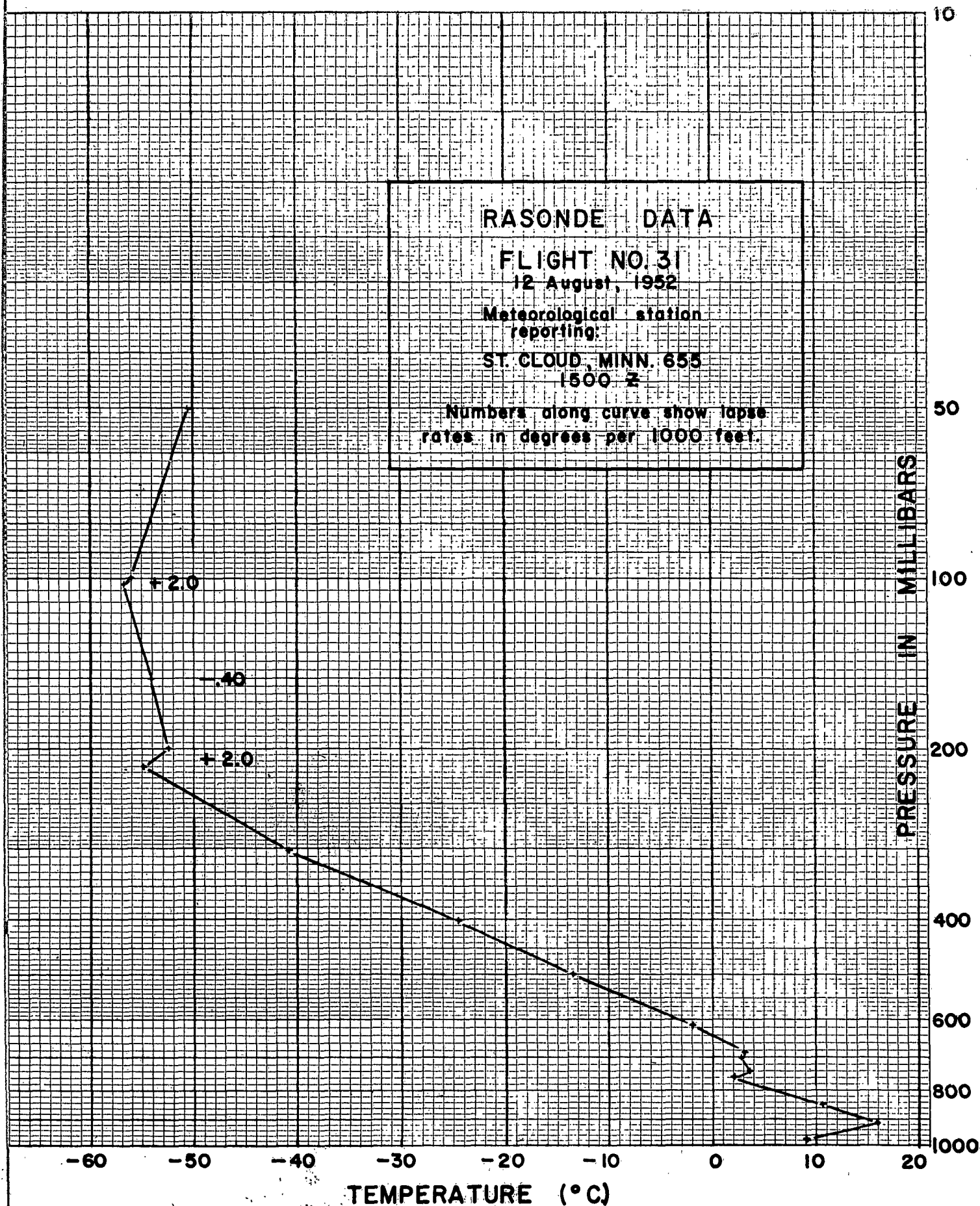
FLIGHT I
 LAUNCHED 09
 5 AUGUST,
 TRAJECTORY FROM I

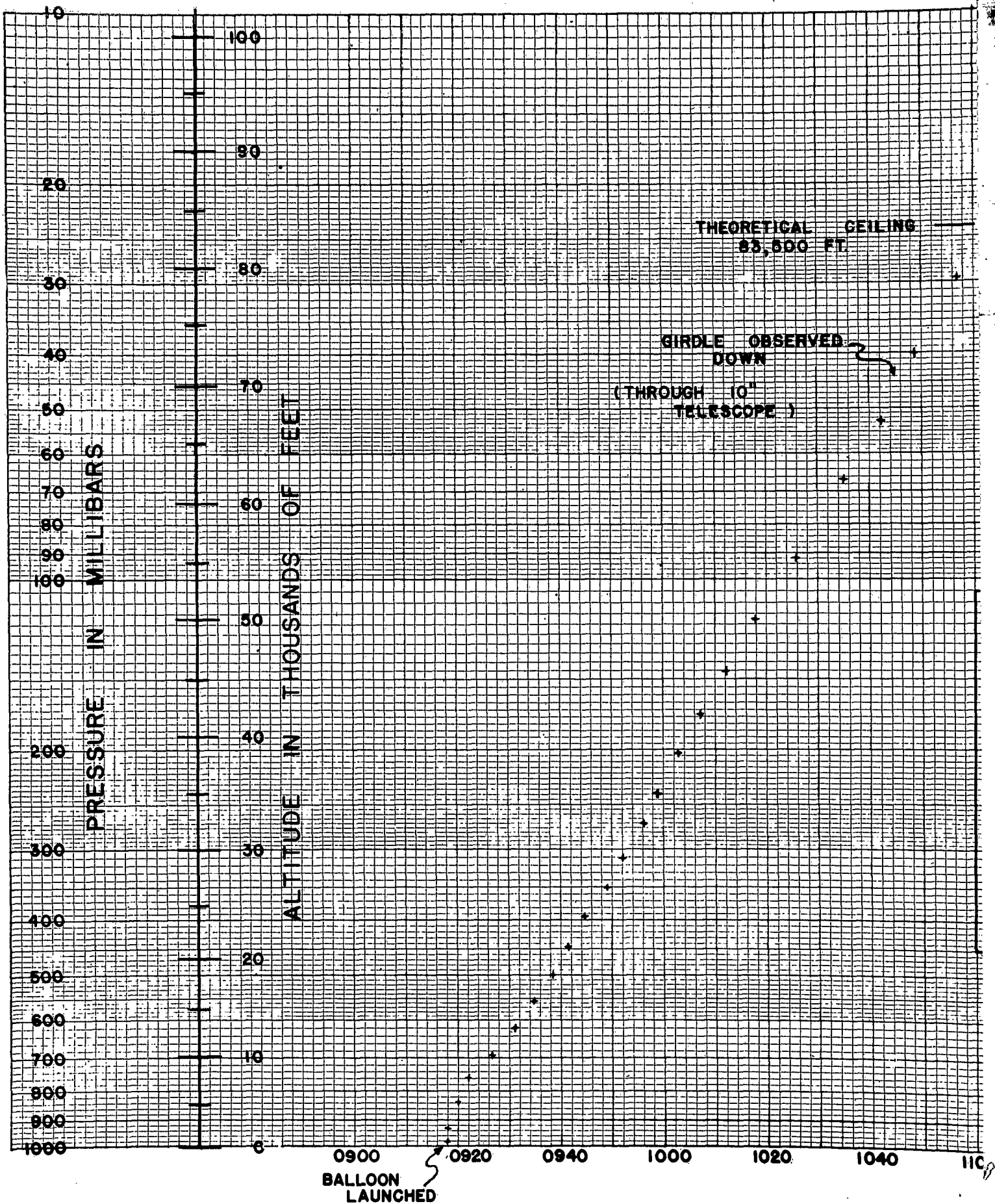
CONFIDENTIAL

CONFIDENTIAL



CONFIDENTIAL SECURITY INFORMATION





CONFIDENTIAL SECURITY INFORMATION

TIME - PRESSURE - ALTITUDE

FLIGHT NO 31

12 AUGUST, 1952

GROSS LOAD: 457 LBS.

FREE LIFT: 65 LBS.

GROSS LIFT: 522 LBS.

+++ BAROGRAPH RECORD

●●● DOUBLE THEODOLITE

1100

1120

1140

1200

1220

1240

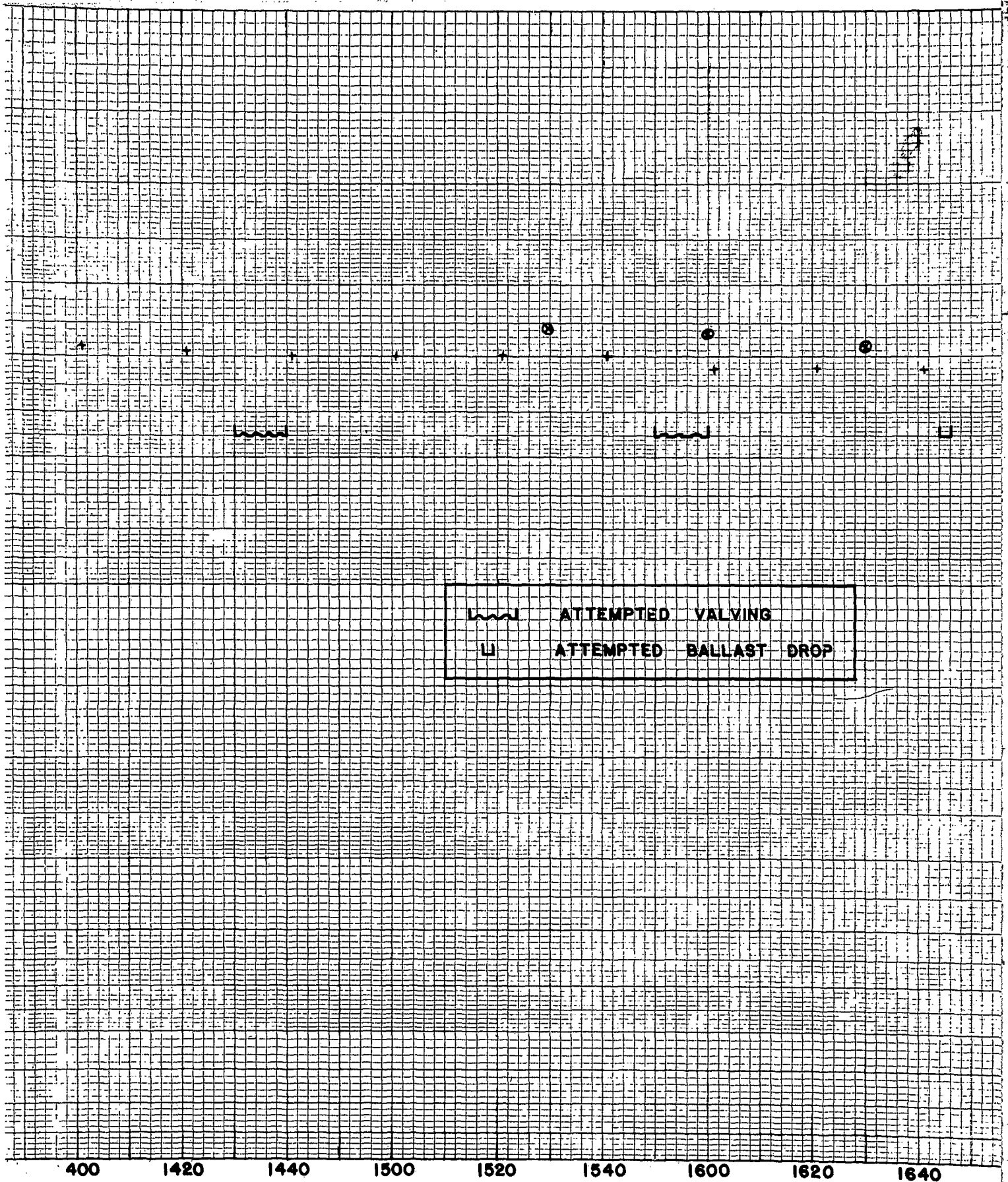
1300

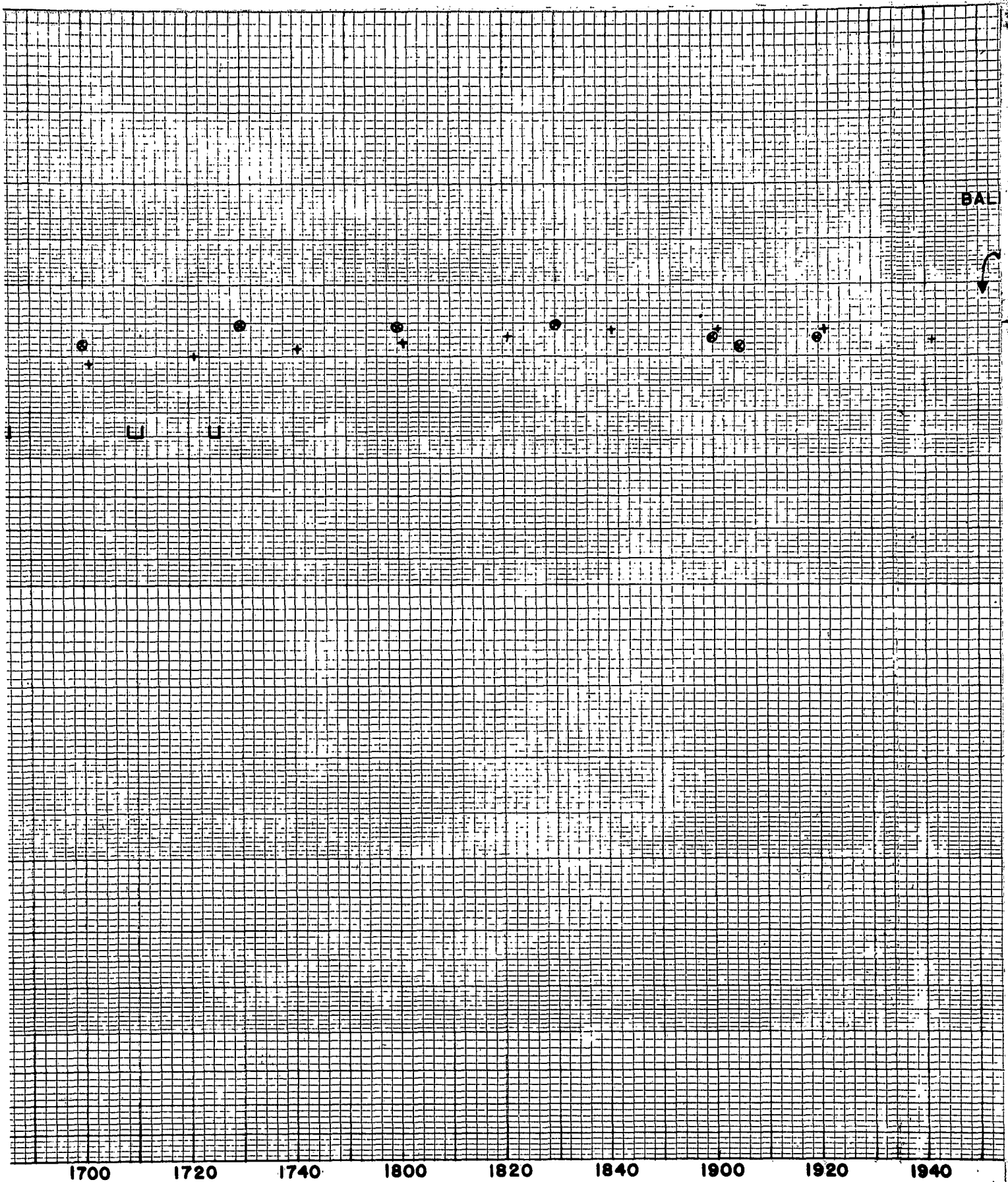
1320

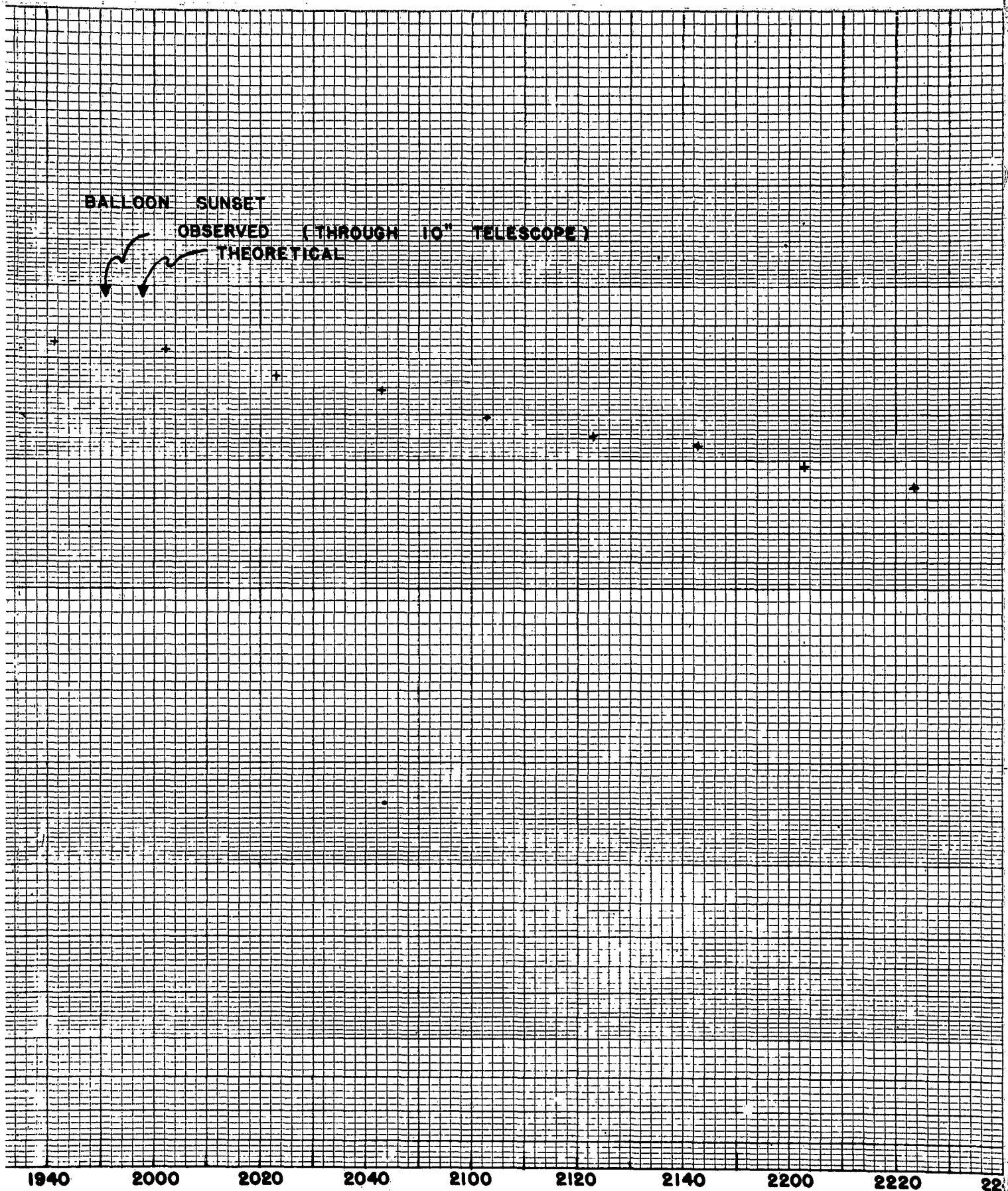
1340

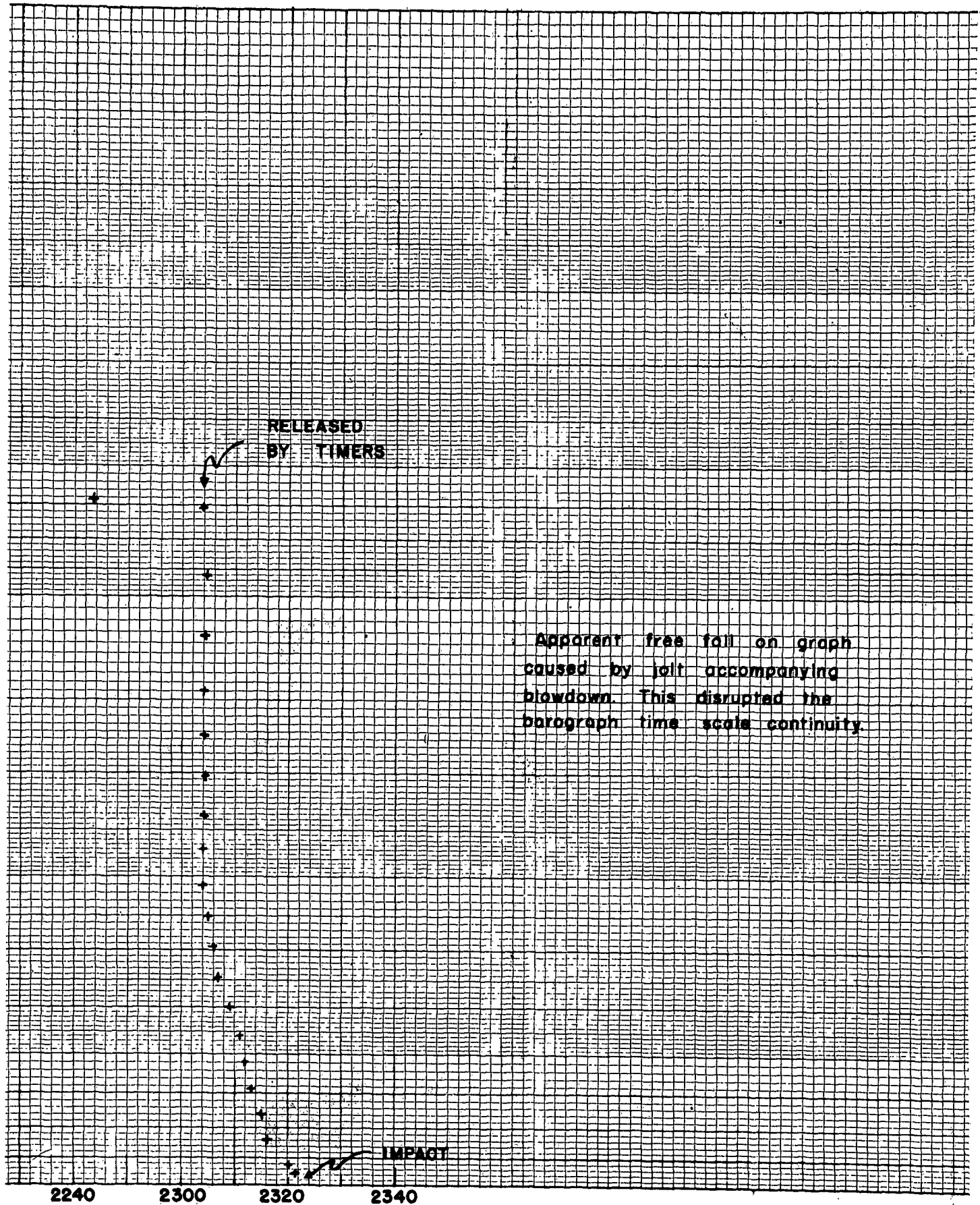
14

CENTRAL STANDARD TIME

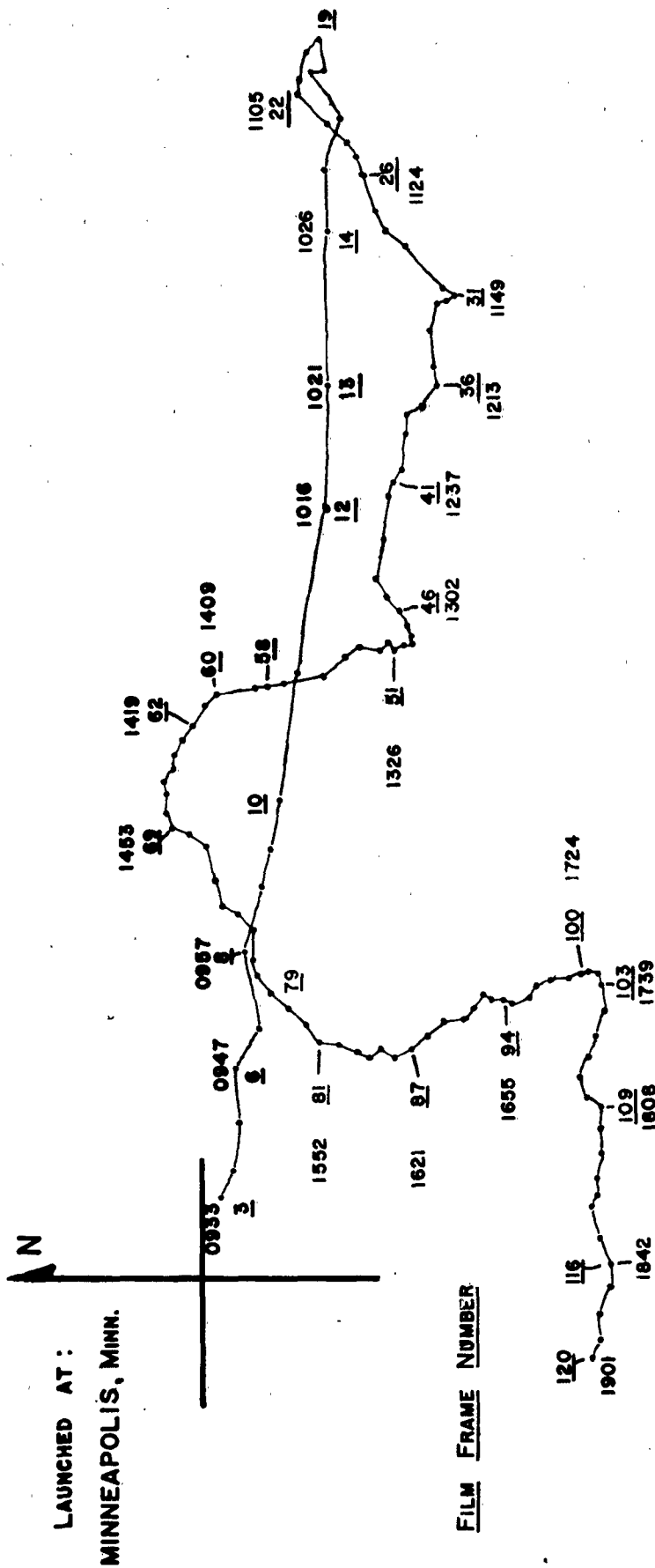








CONFIDENTIAL



FLIGHT NO. 31

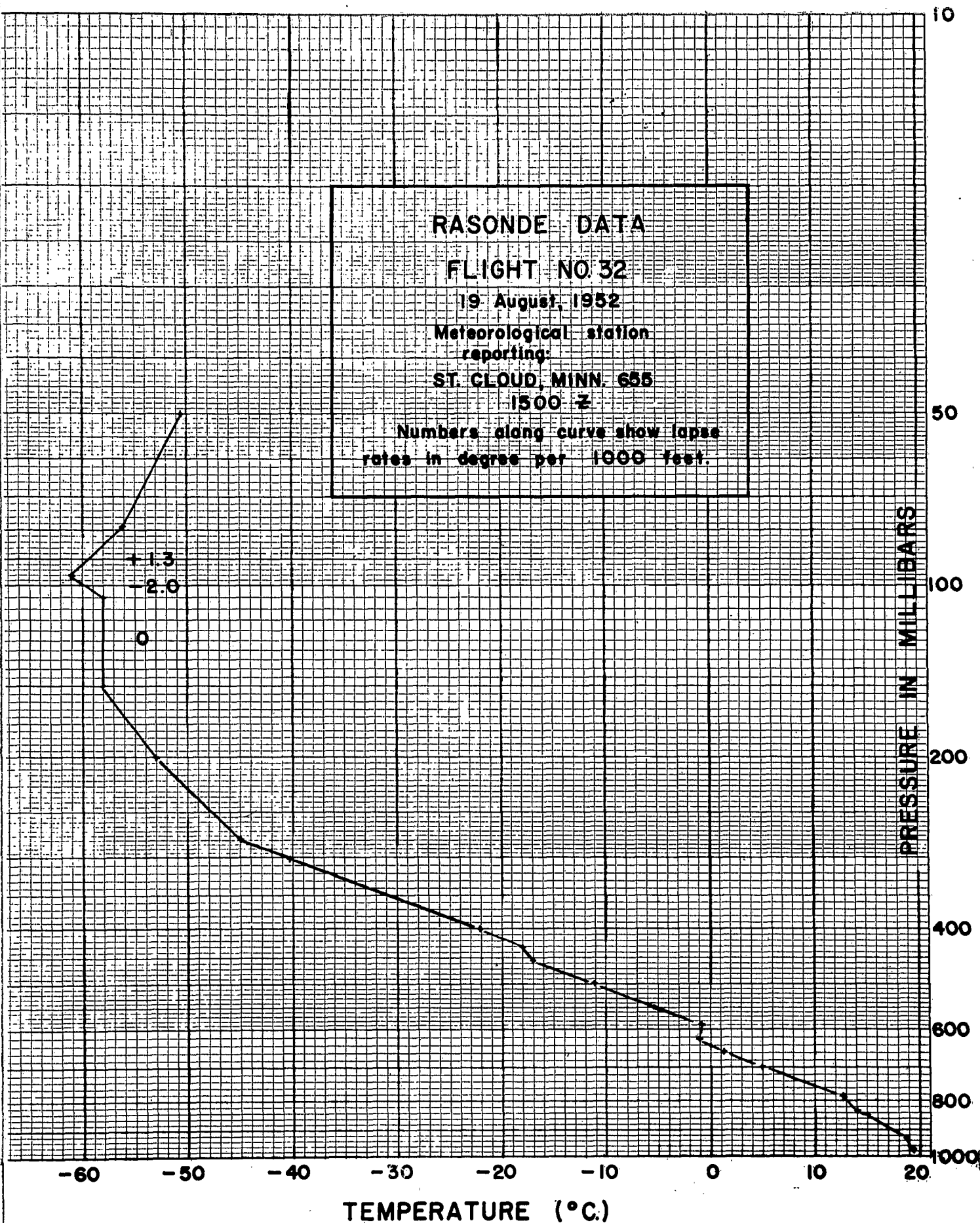
LAUNCHED 0918 CST

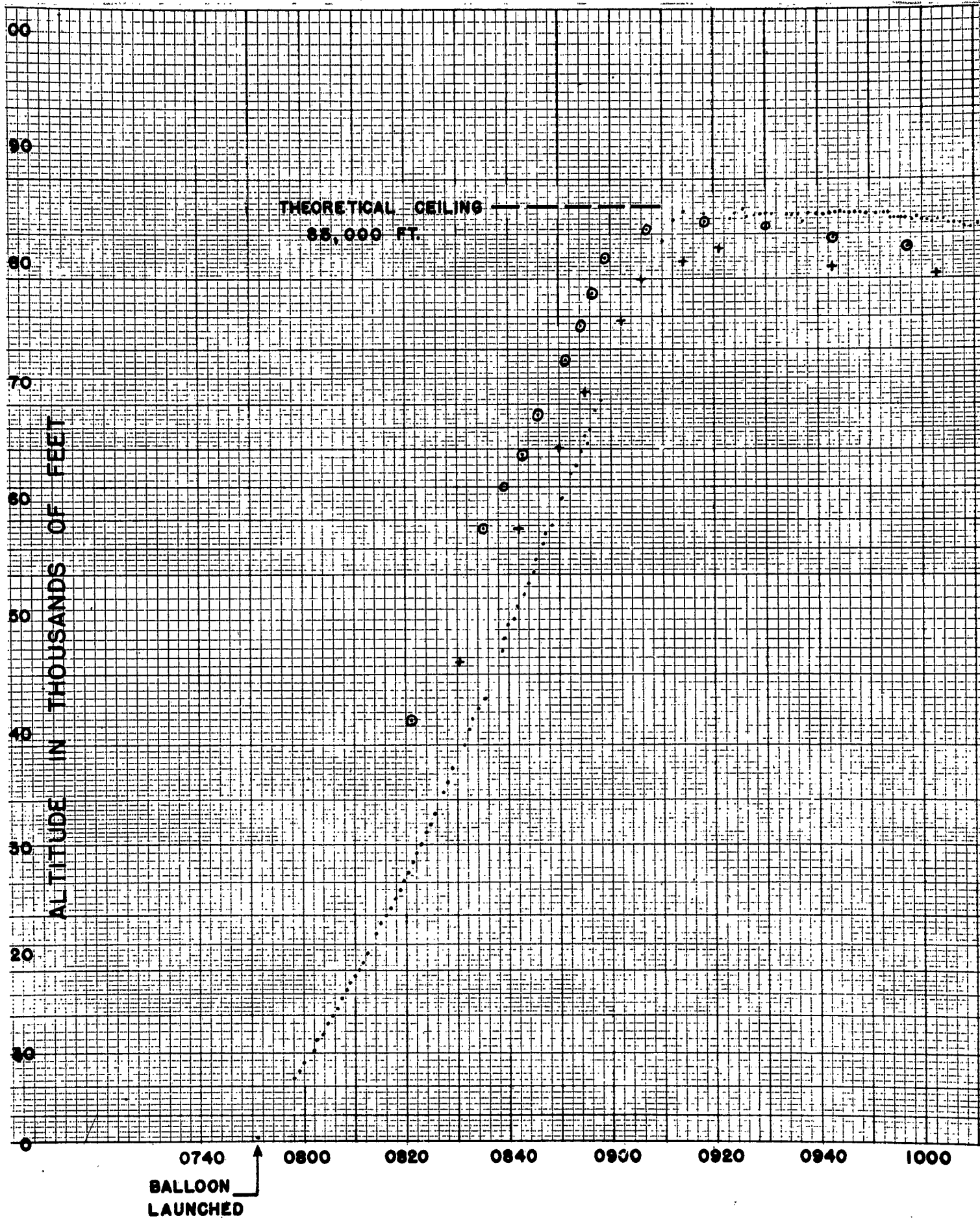
12 AUGUST, 1952

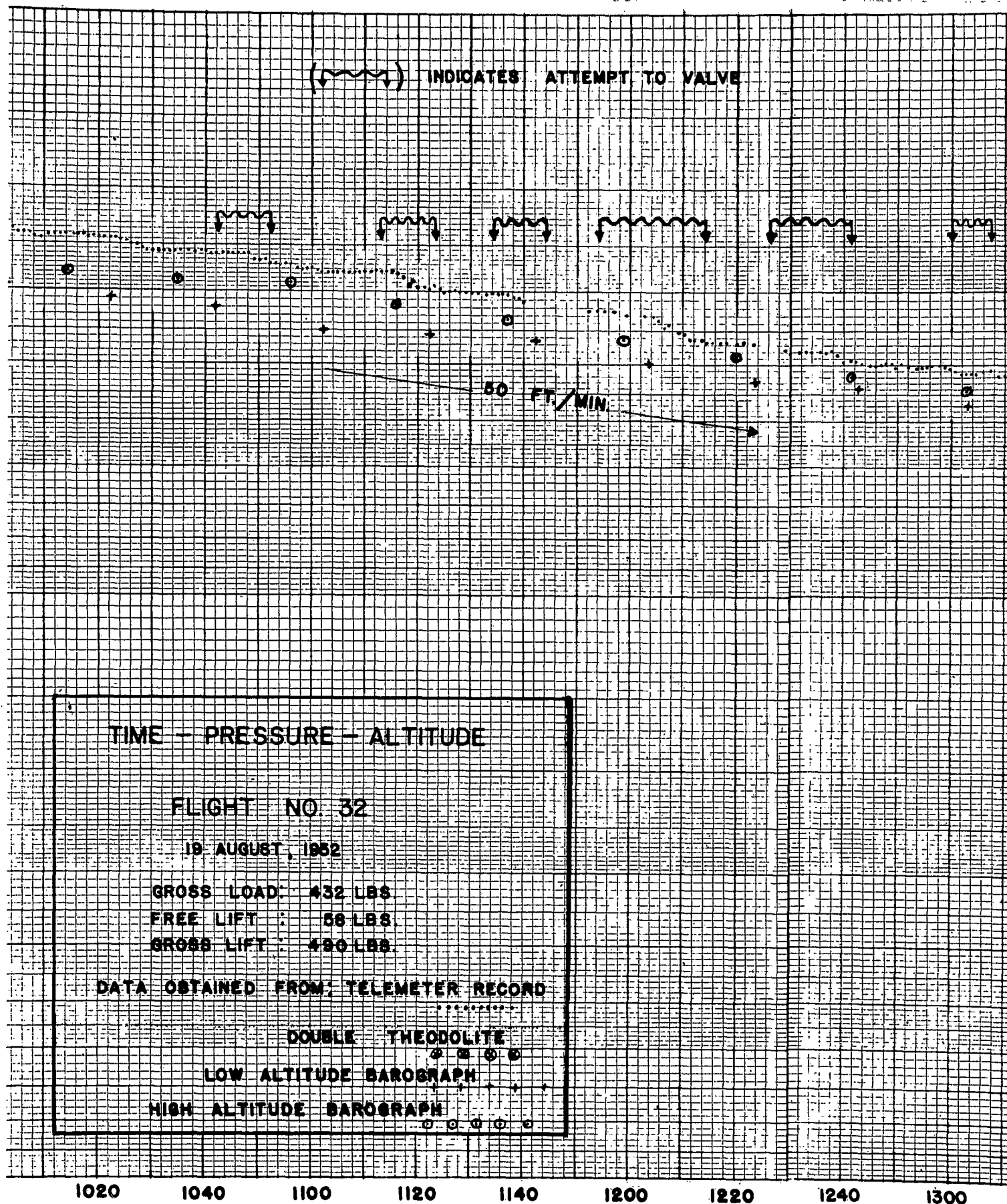
TRAJECTORY FROM DOWN PICTURES

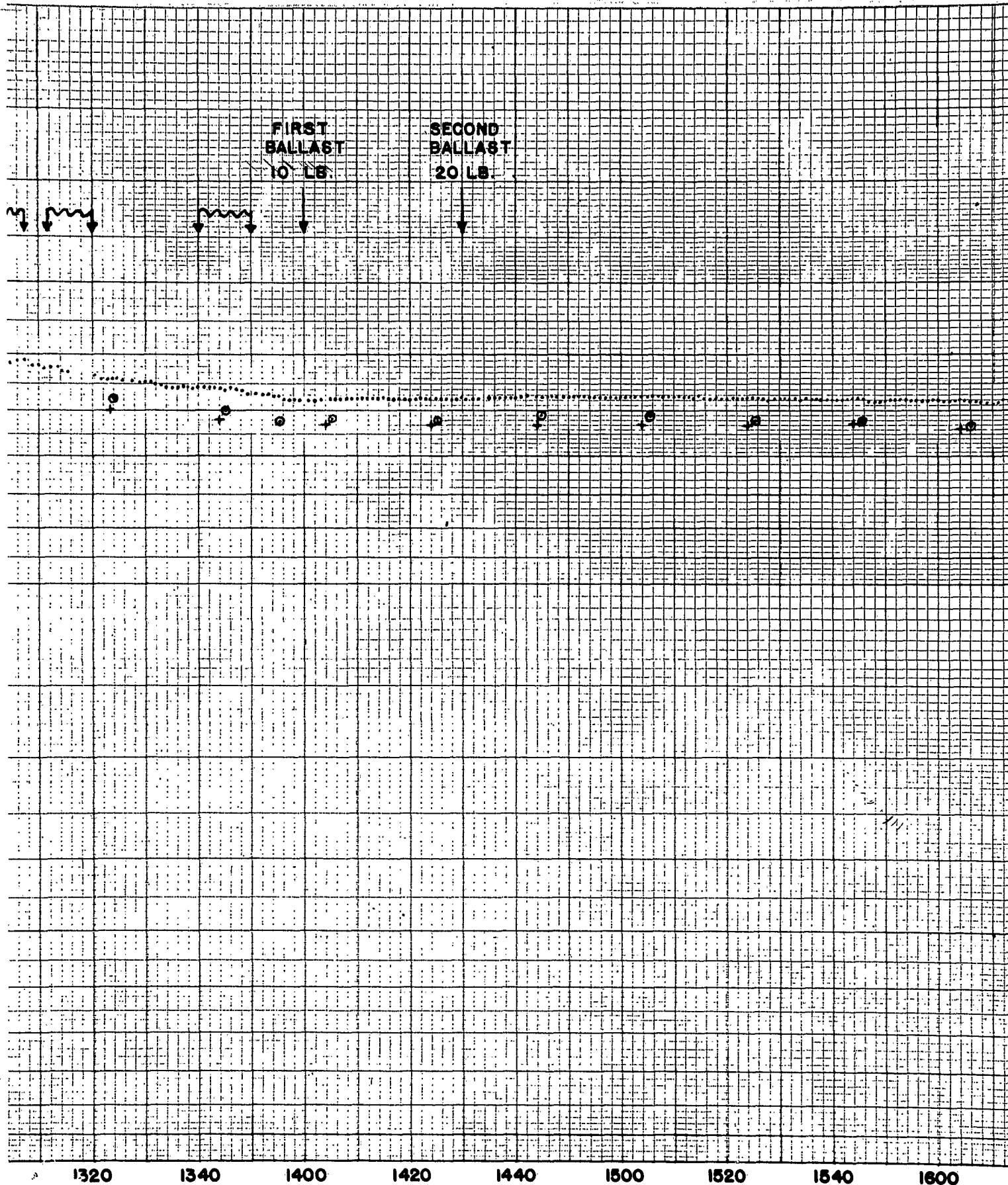
SCALE 1:5 x 10⁵

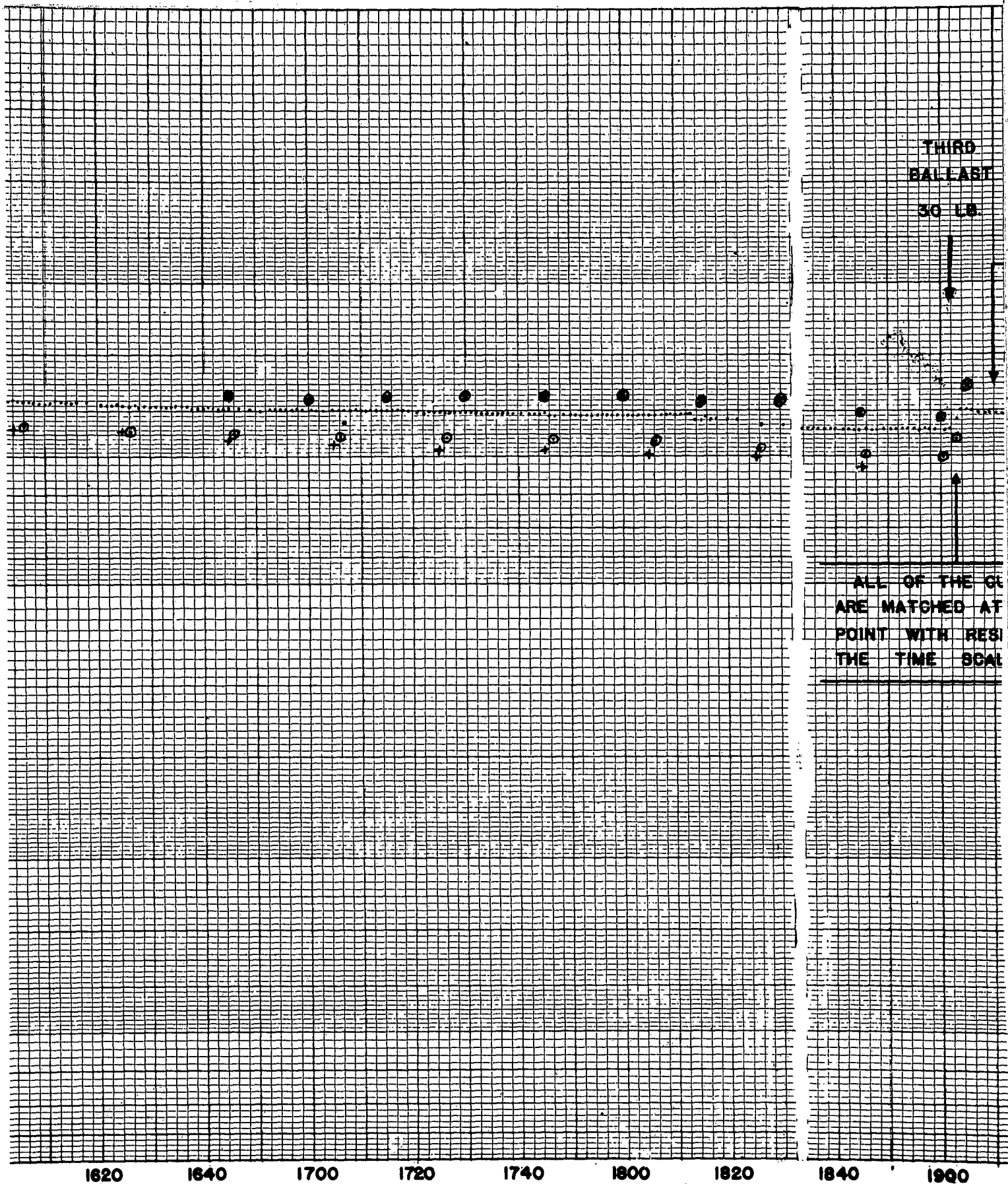


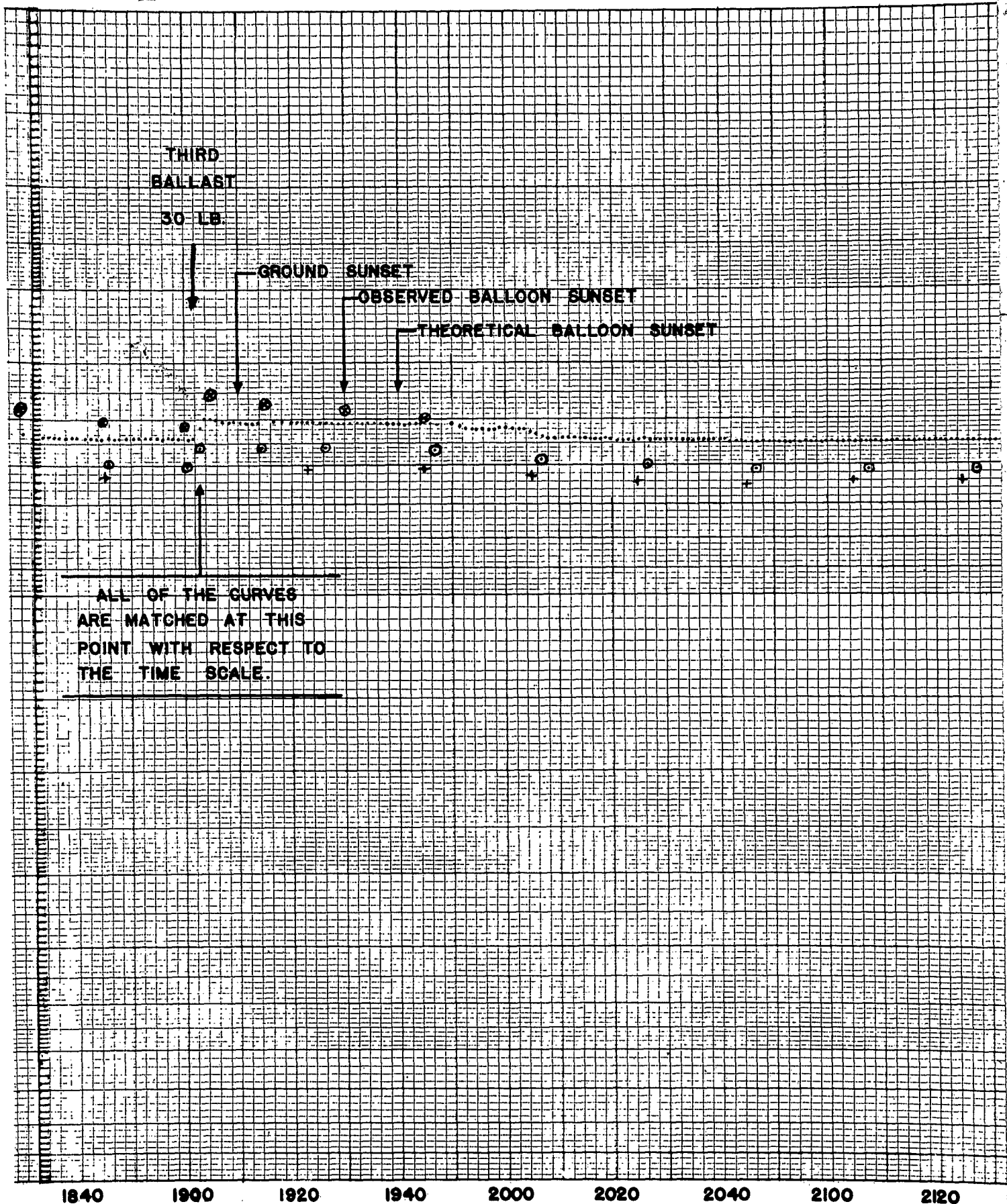


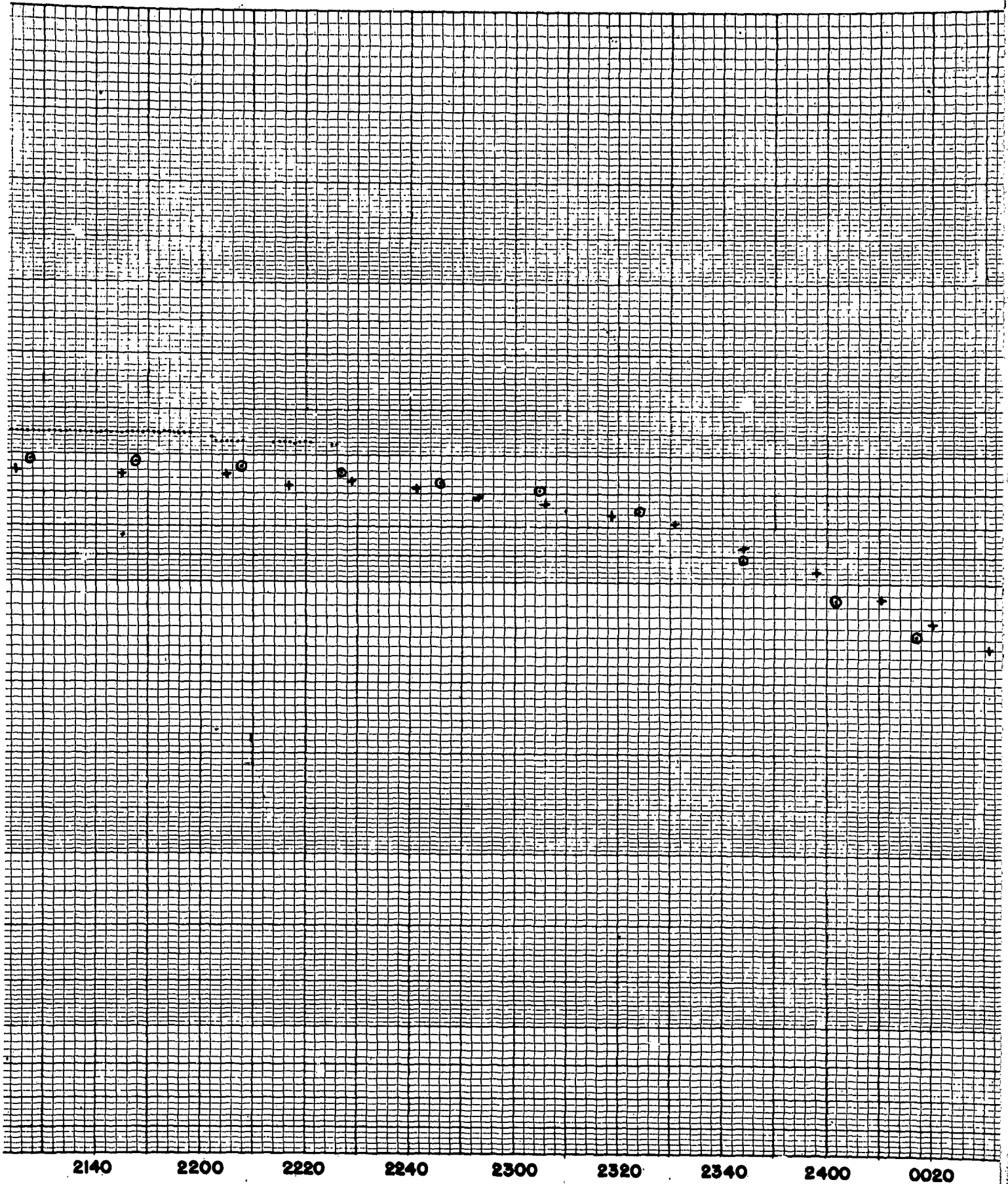


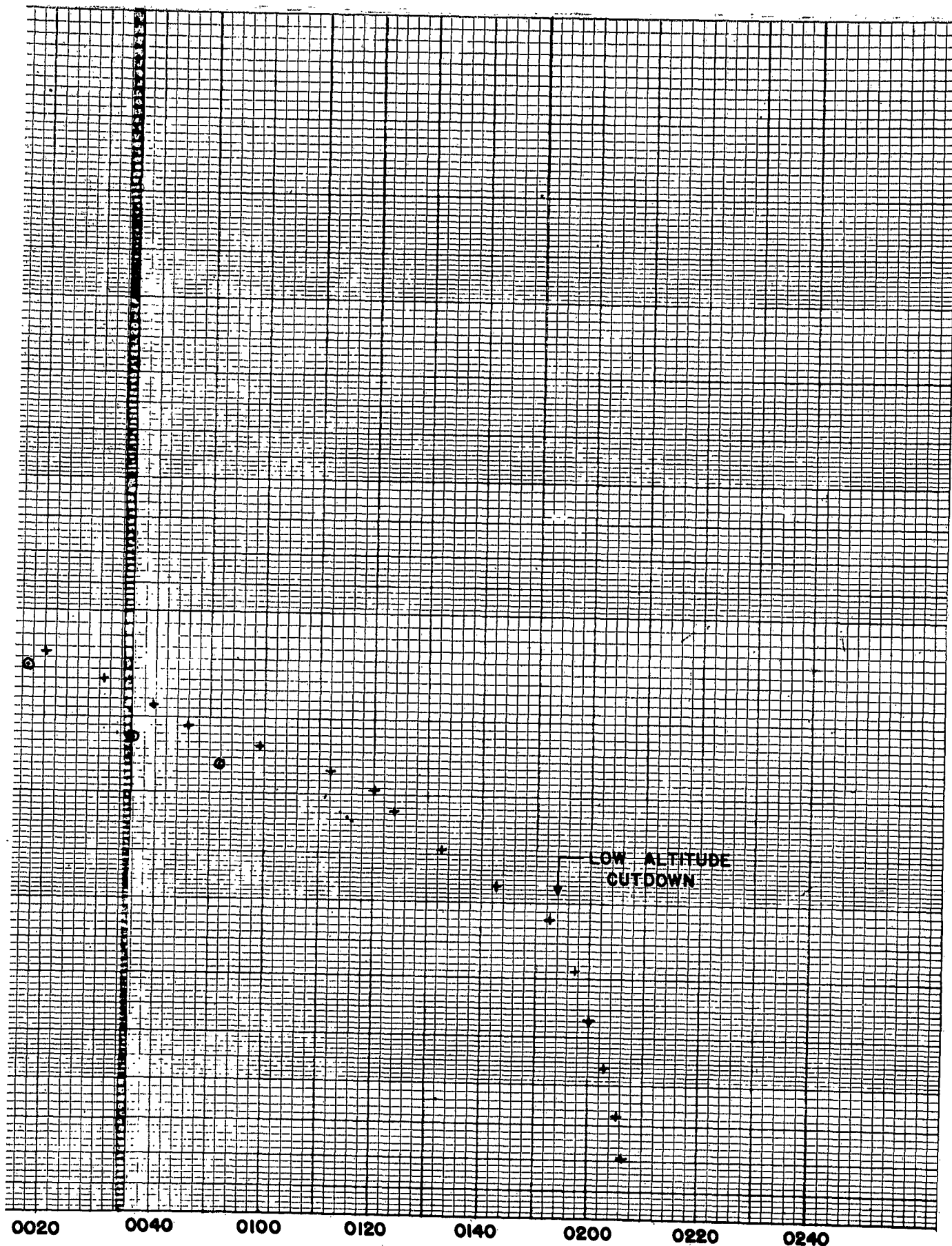




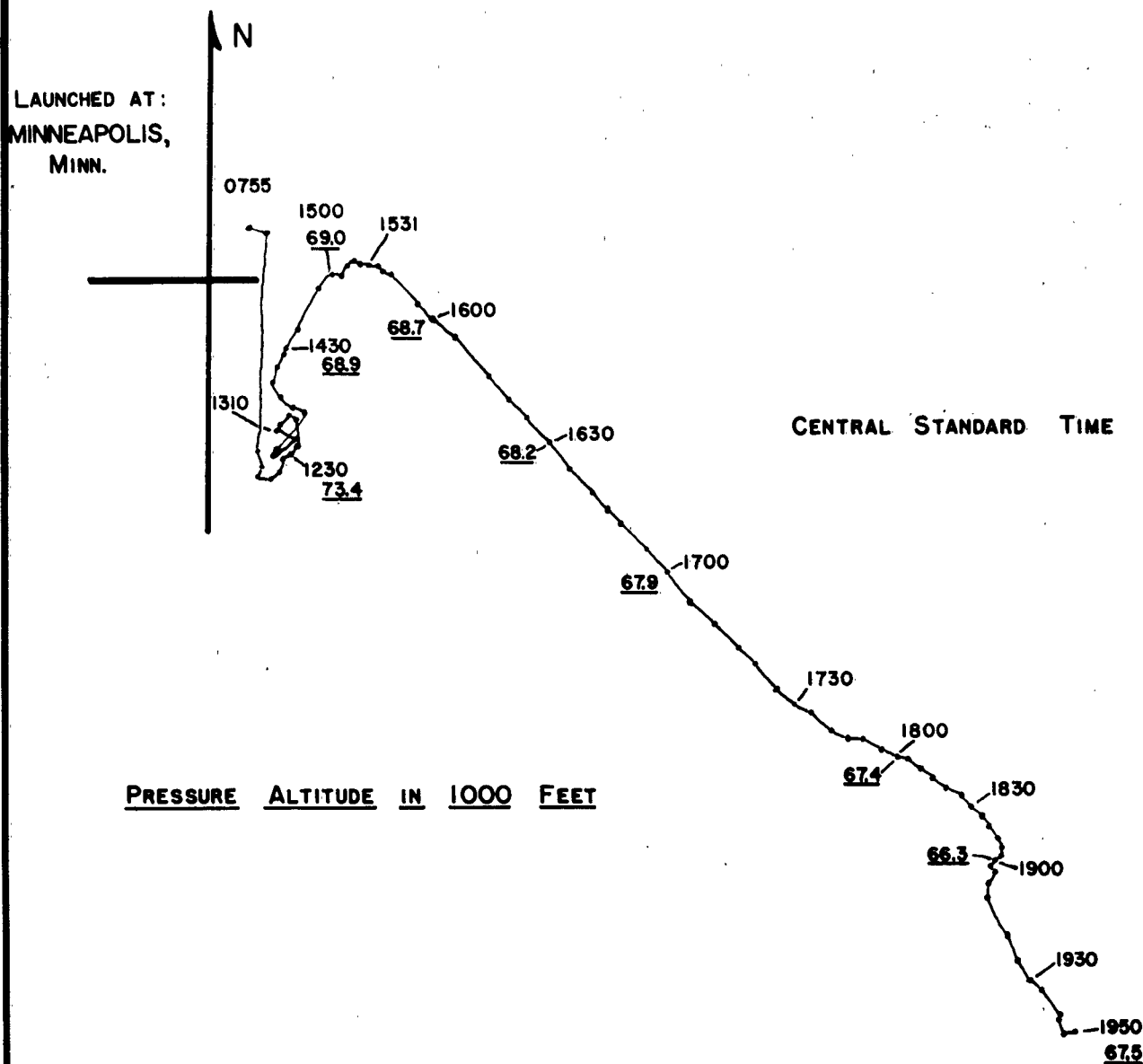








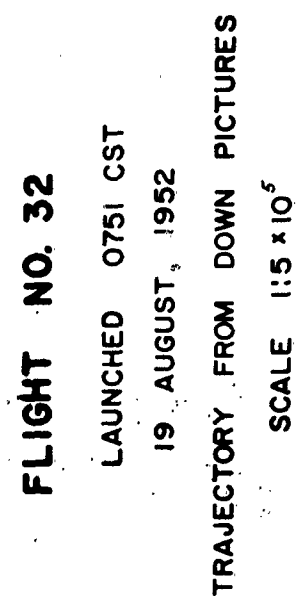
~~CONFIDENTIAL~~



FLIGHT NO. 32
LAUNCHED 0751 CST
19 AUGUST, 1952
TRAJECTORY FROM THEODOLITE FIXES
SCALE $1:5 \times 10^5$

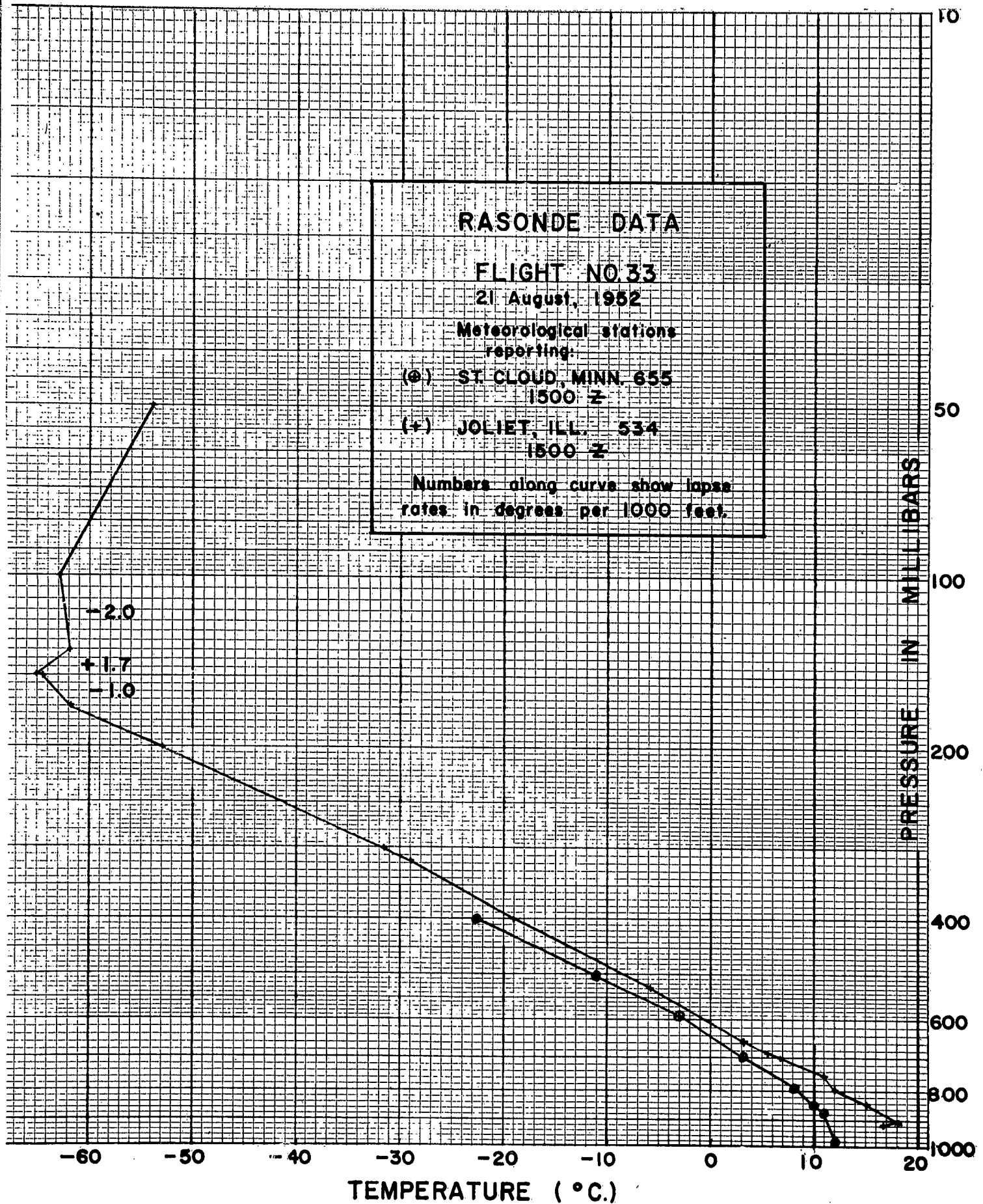
10 0 10 20 STATUTE MILES

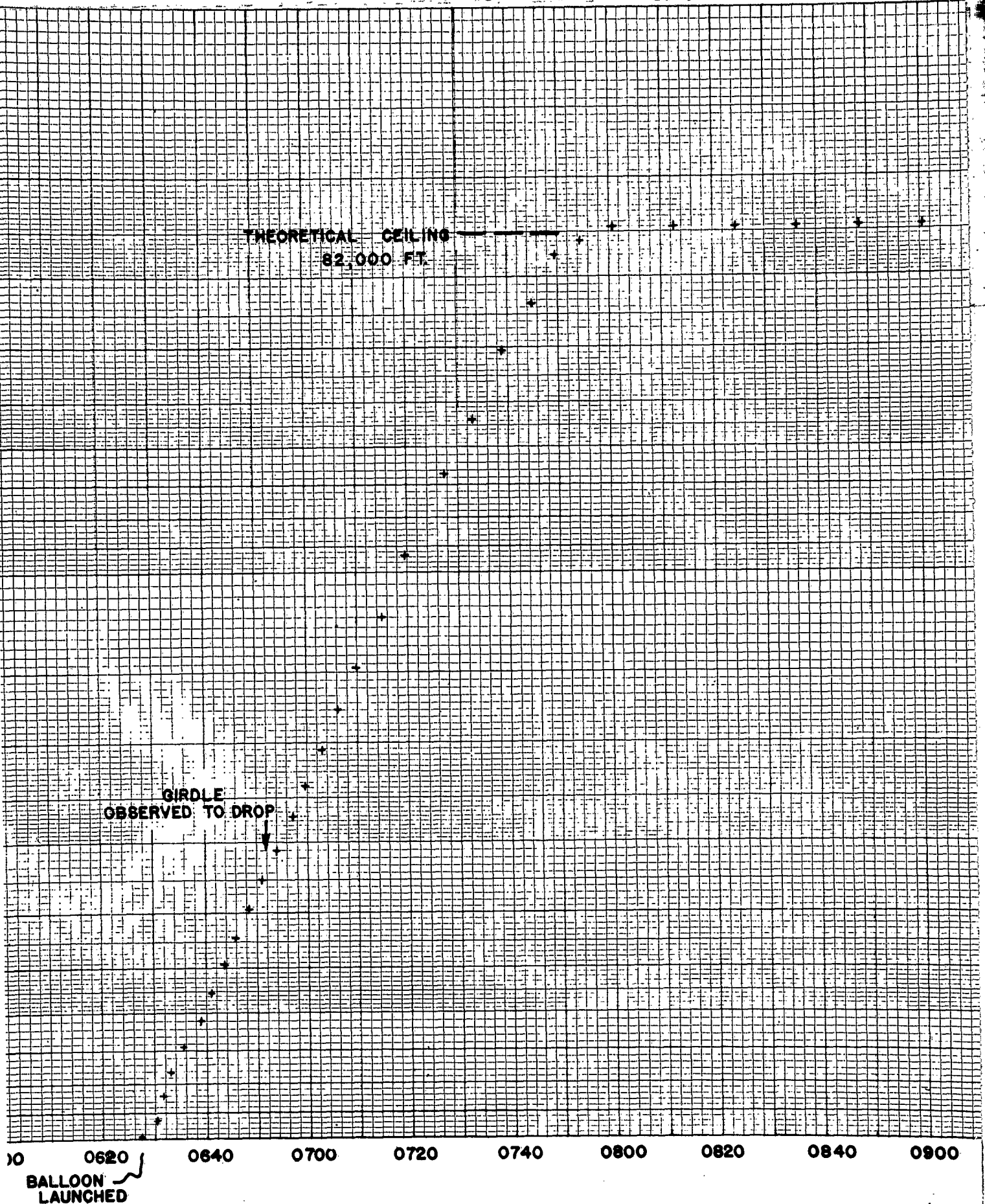
CONFIDENTIAL SECURITY INFORMATION



CONFIDENTIAL **SECURITY** **INFORMATION**

STATUTE				MILES	
10		0	10	20	
10					





TIME - PRESSURE - ALTITUDE

FLIGHT NO. 33

21 AUGUST, 1952

GROSS LOAD: 487 LBS.

FREE LIFT: 66 LBS.

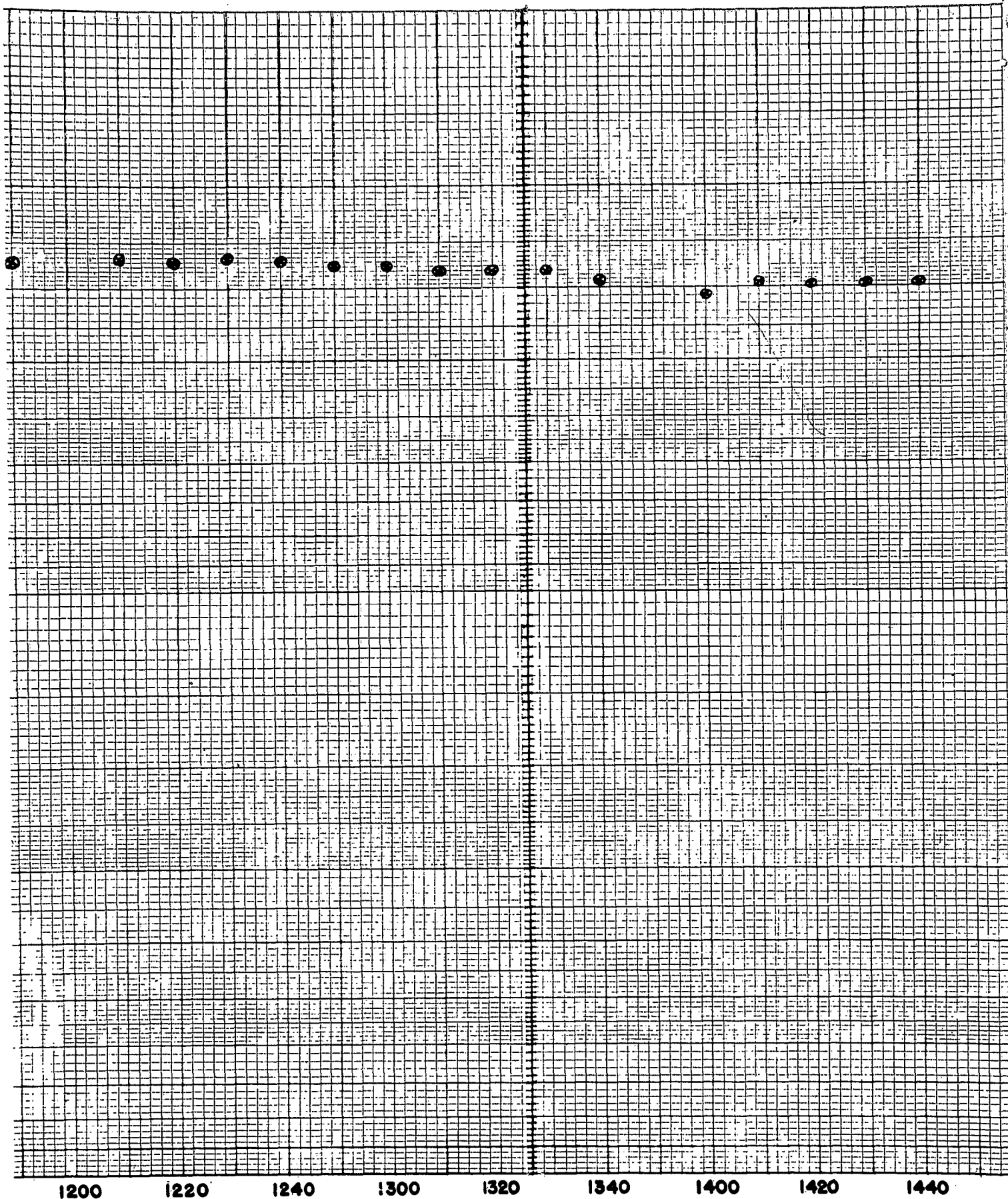
GROSS LIFT: 553 LBS.

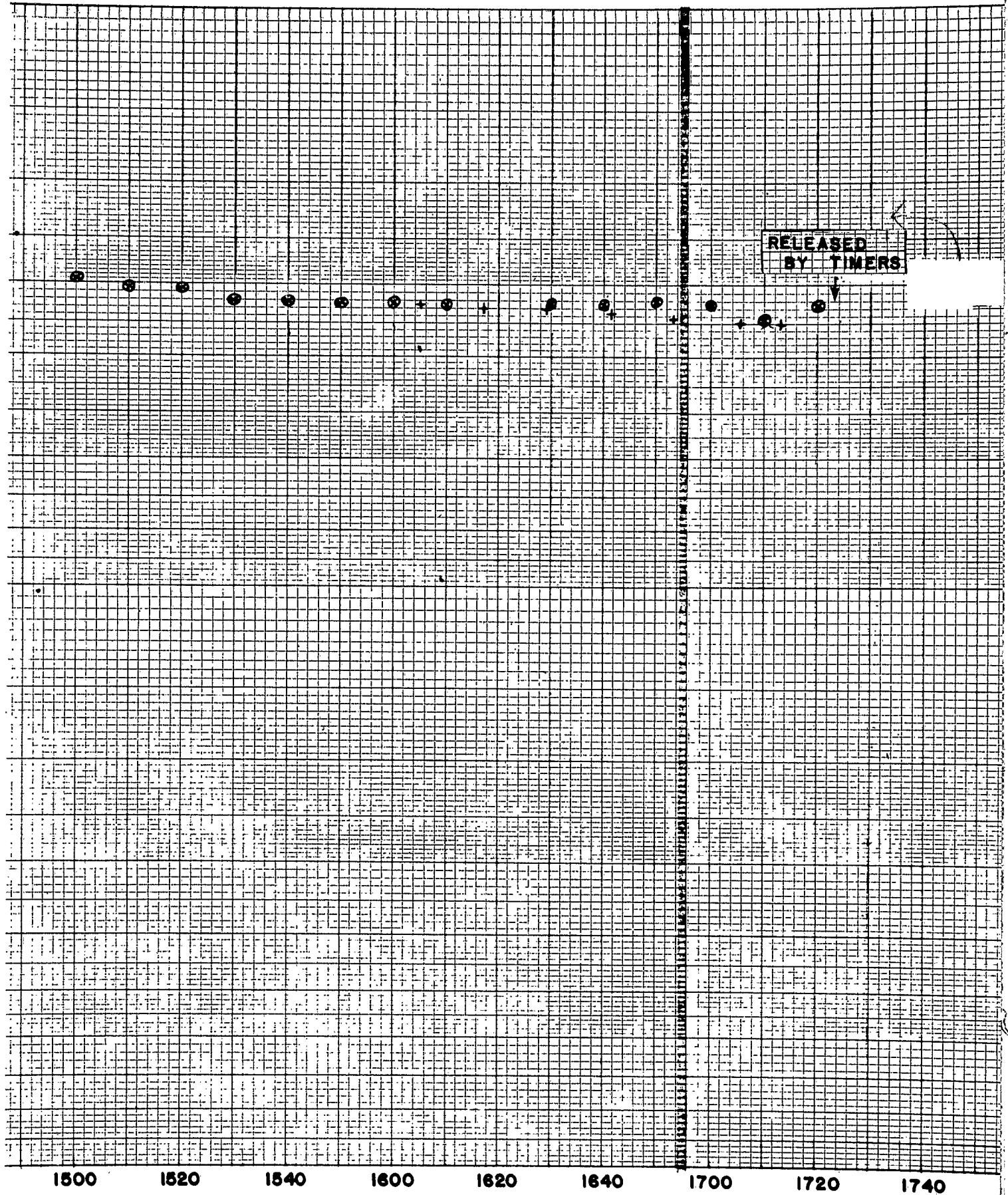
DATA OBTAINED FROM:

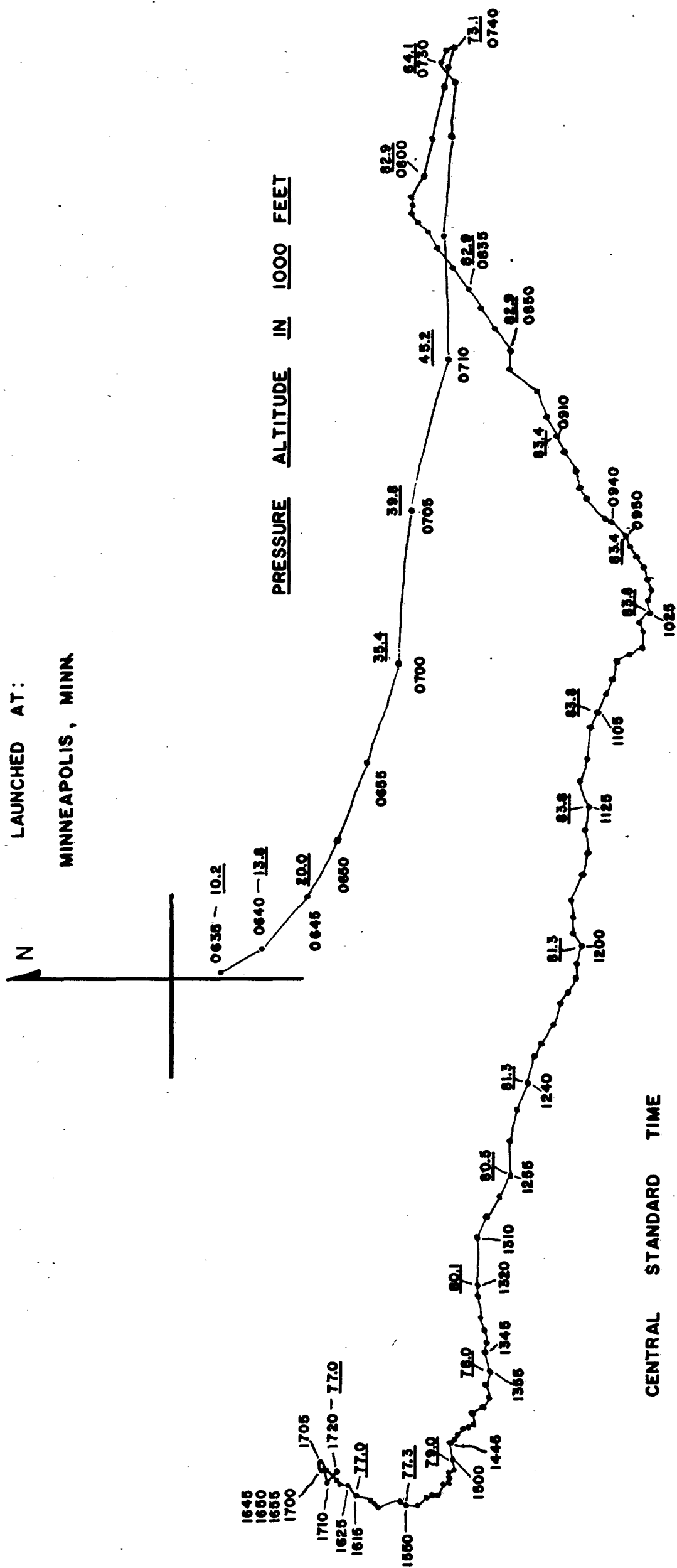
+ + + + BAROGRAPH RECORD
@ @ @ @ DOUBLE THEODOLITE

0900 0920 0940 1000 1020 1040 1100 1120 1140 1200

CENTRAL STANDARD TIME

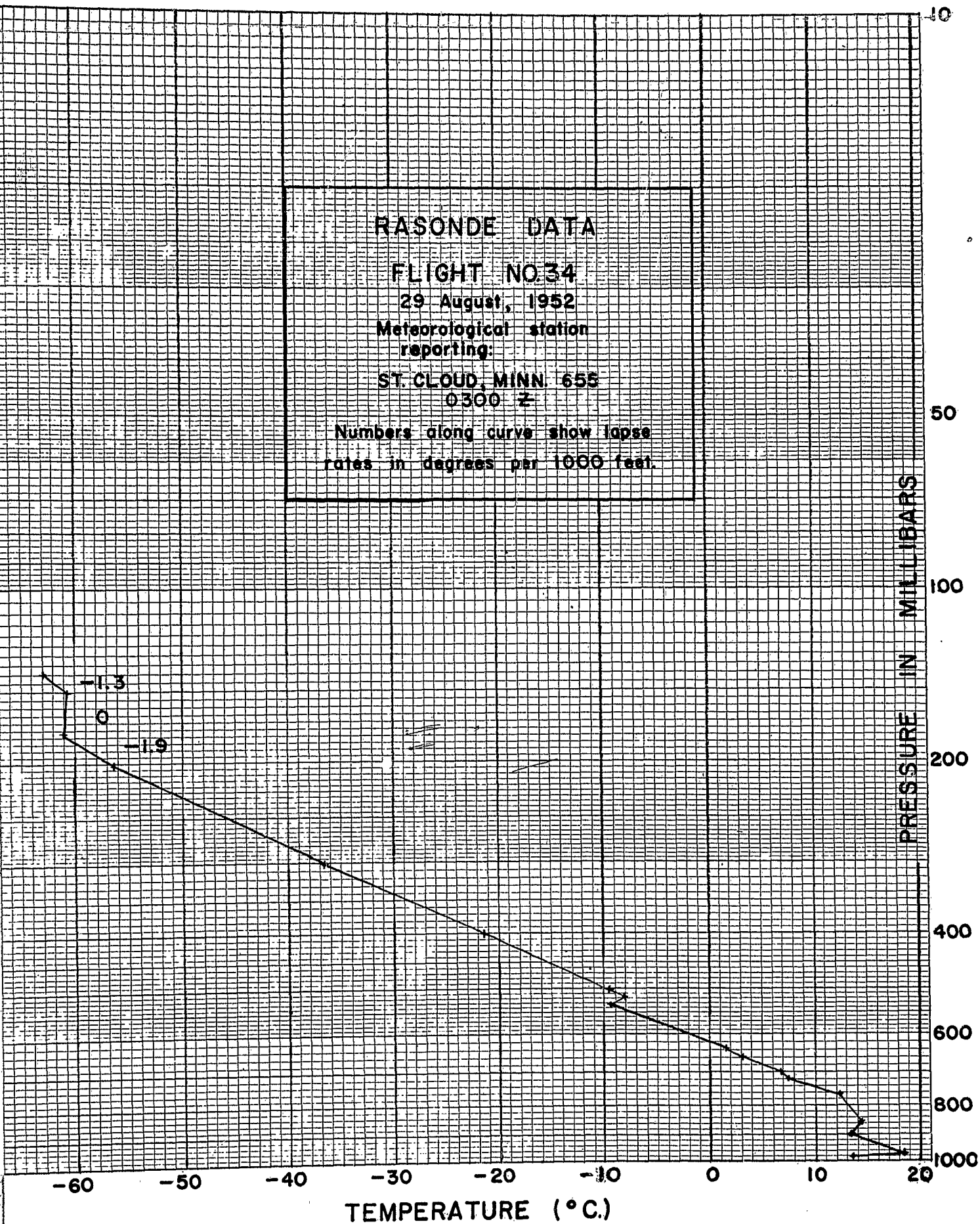




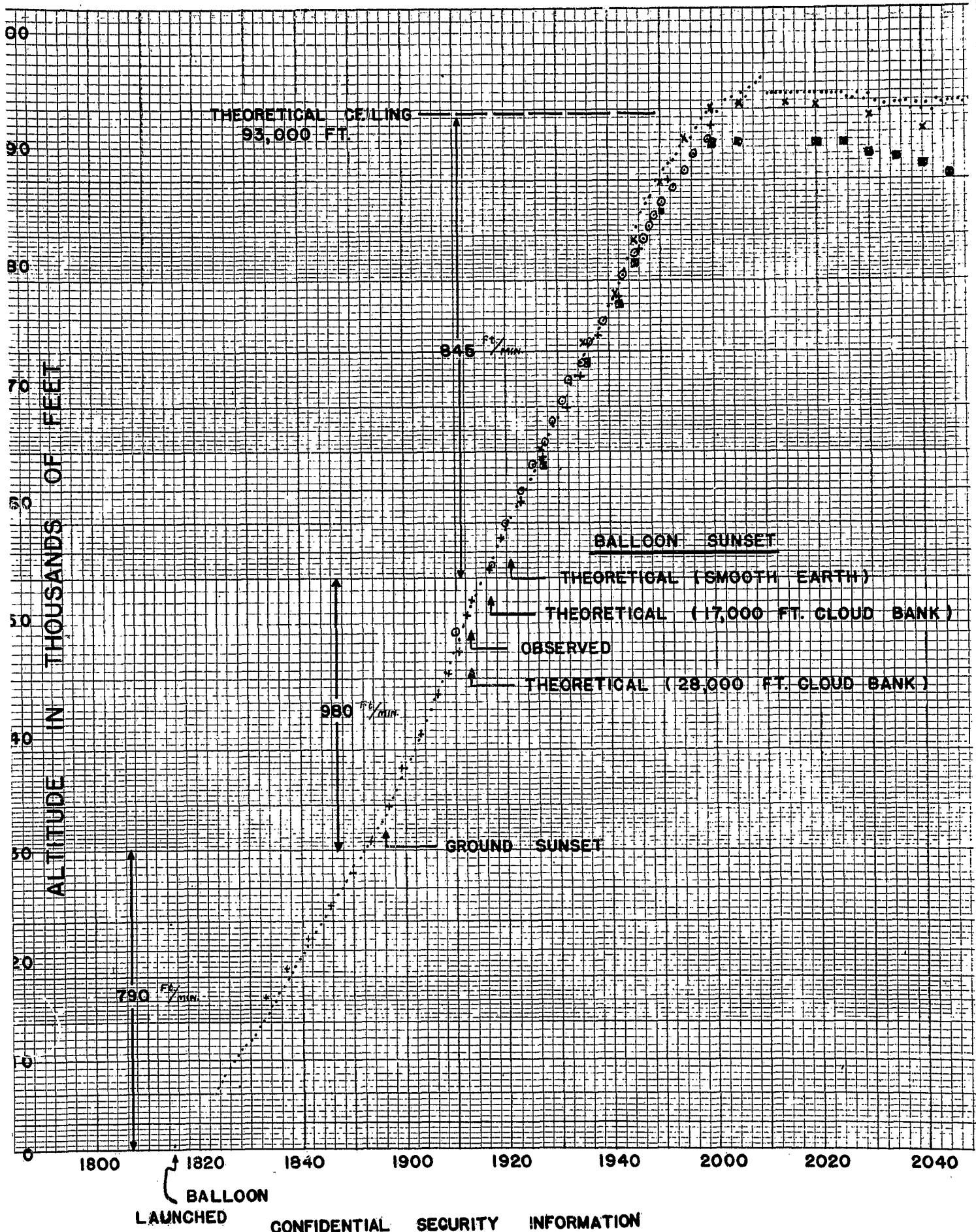


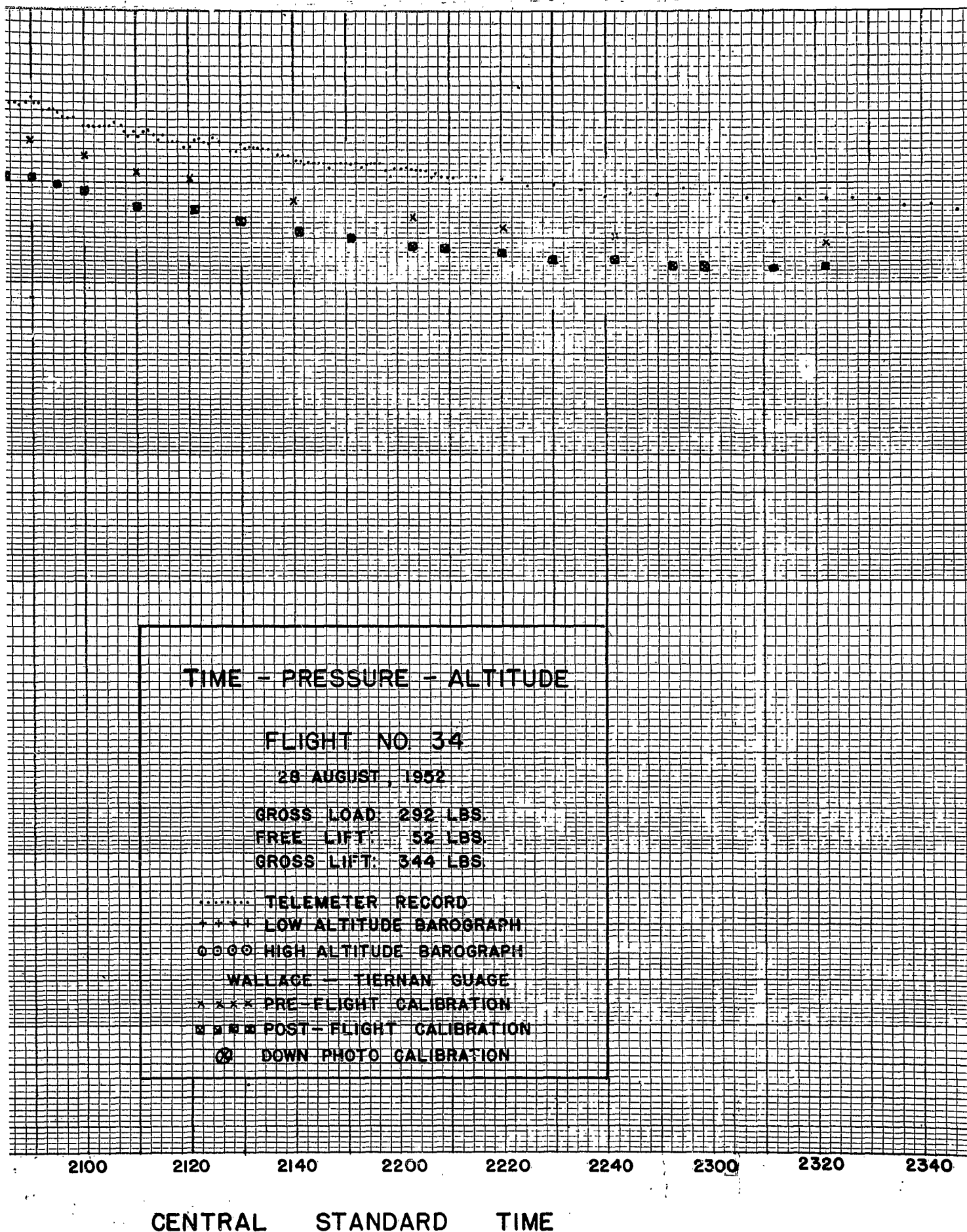
FLIGHT NO. 33
LAUNCHED 0627 CST
21 AUGUST, 1952
TRAJECTORY FROM THEODOLITE FIXES

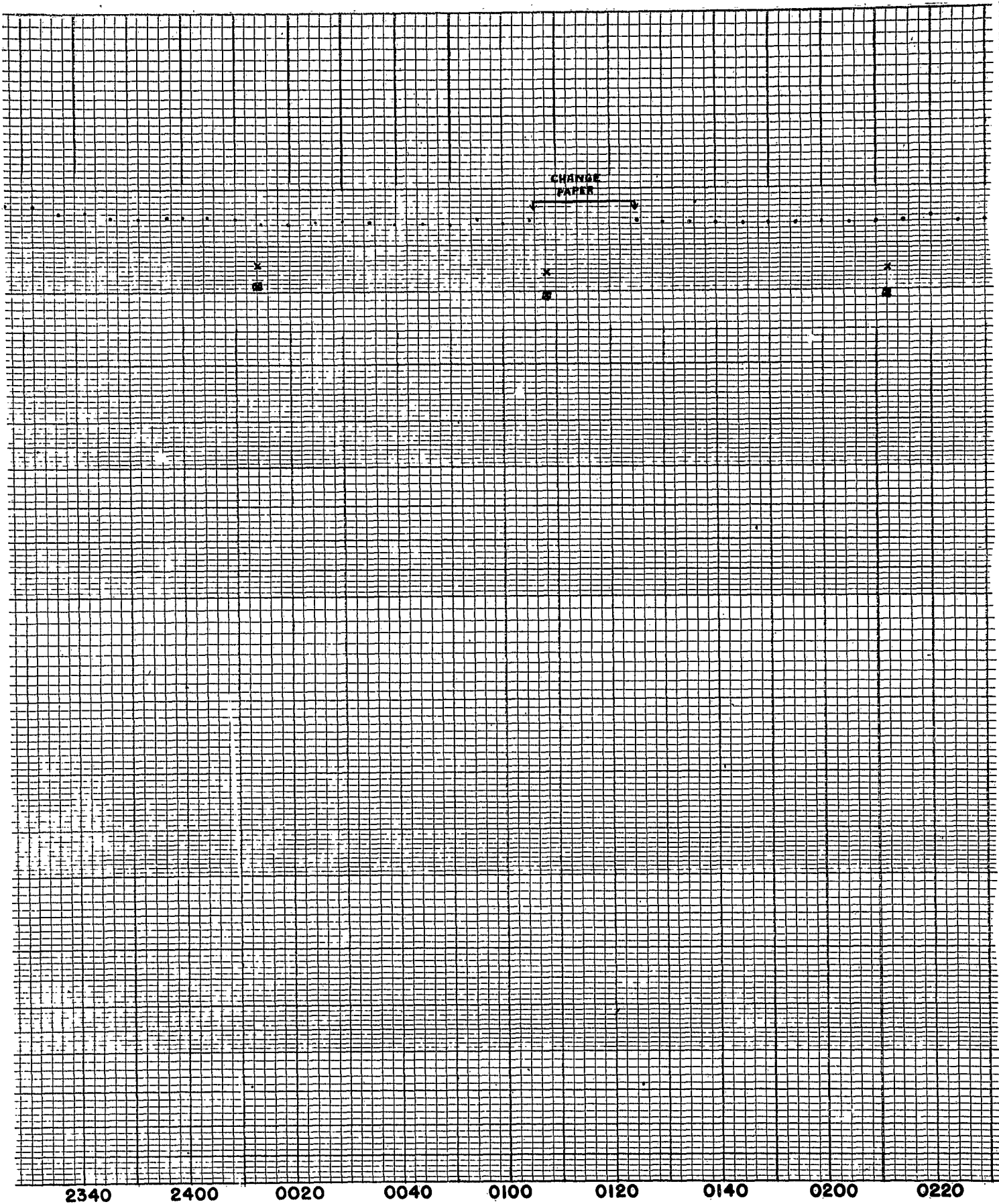
Confidential



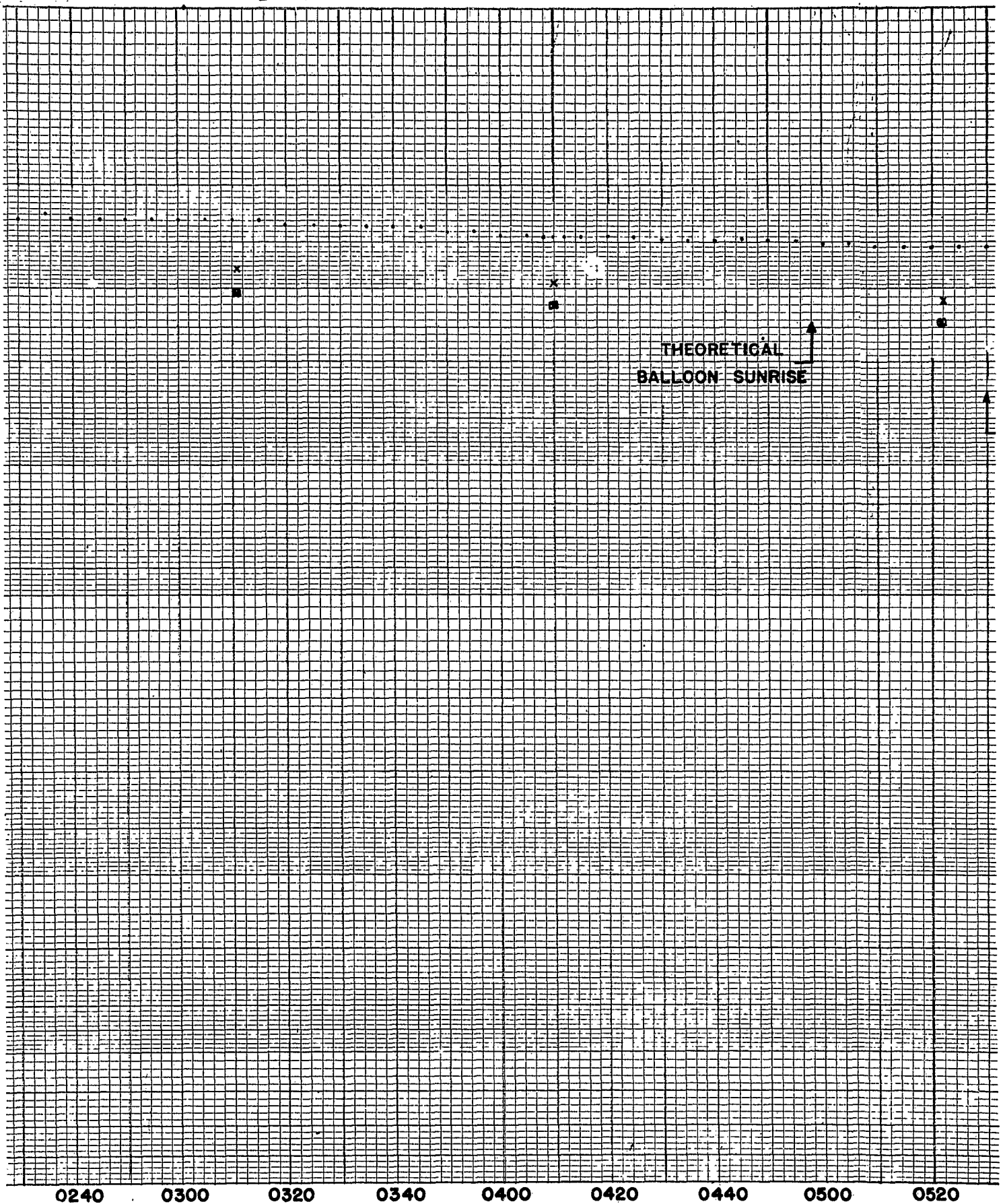
Confidential Security Information

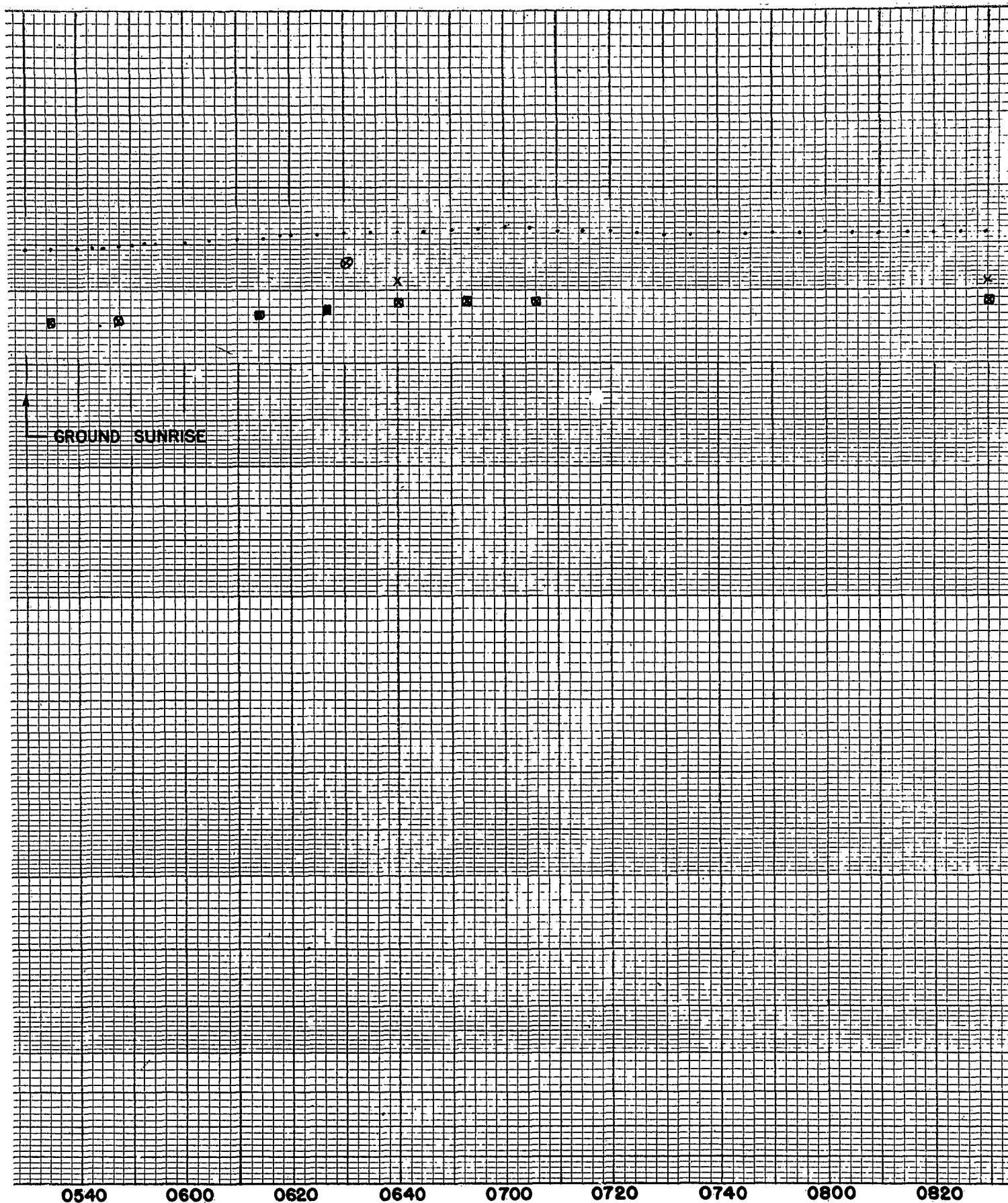


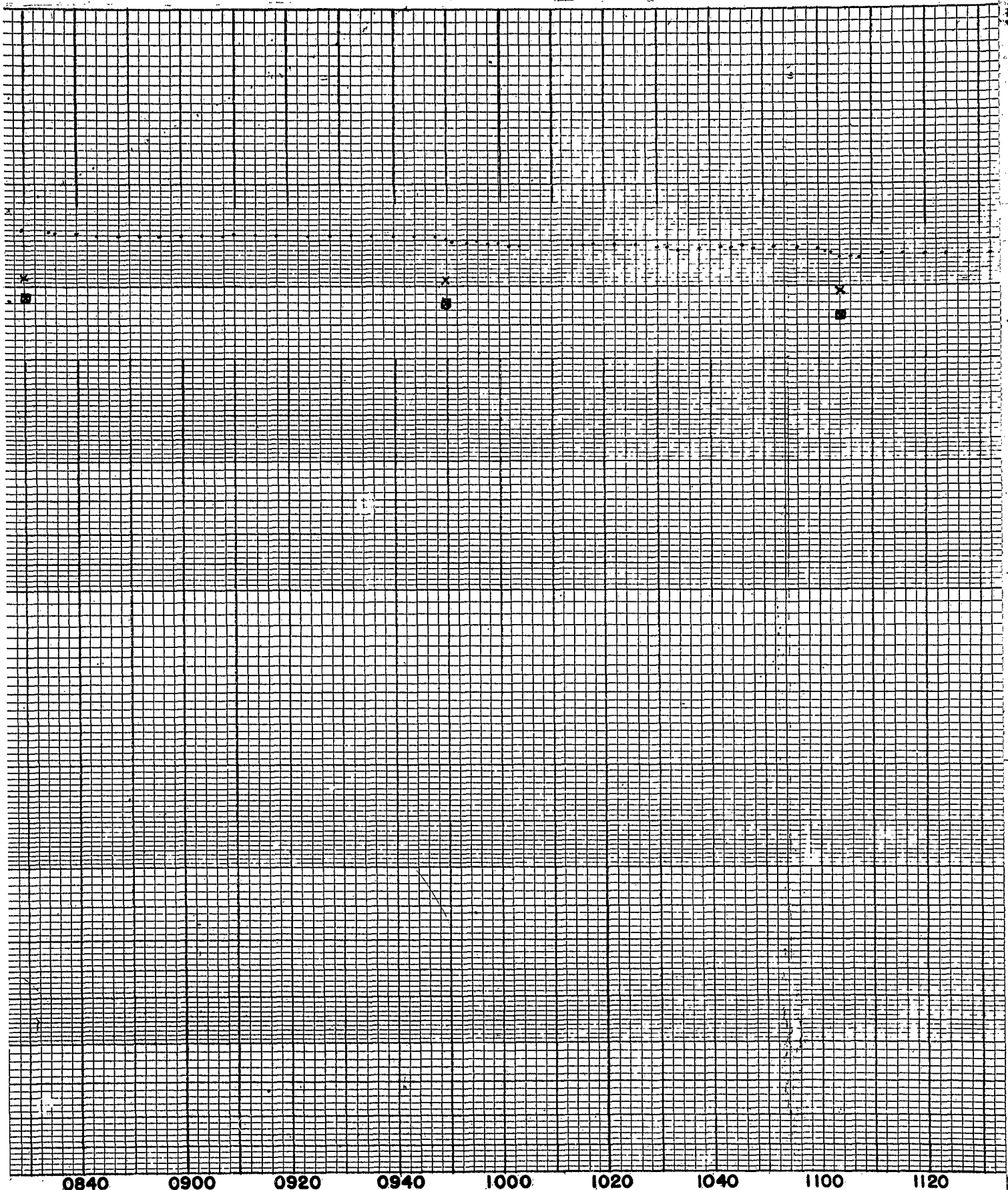


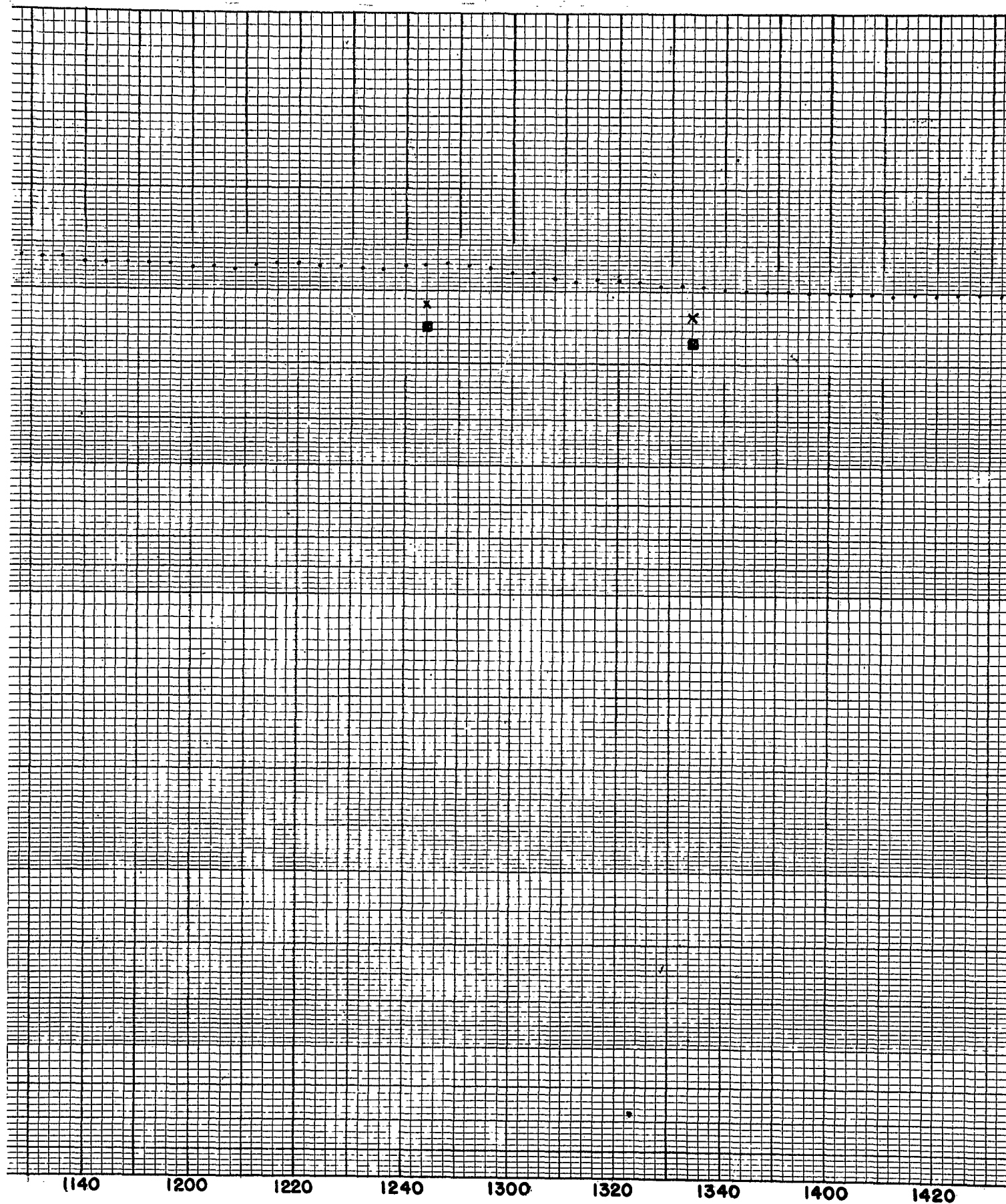


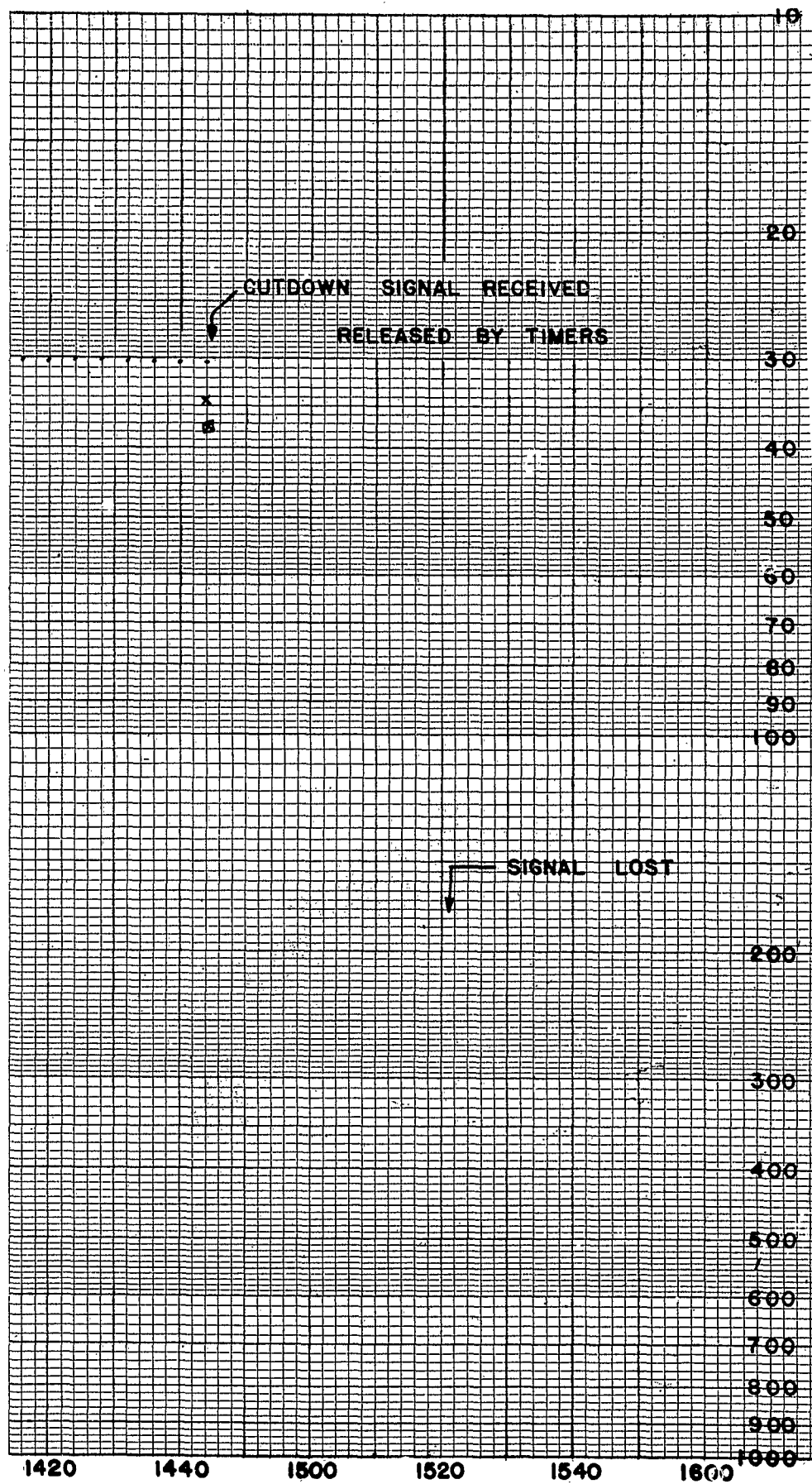
29 AUGUST



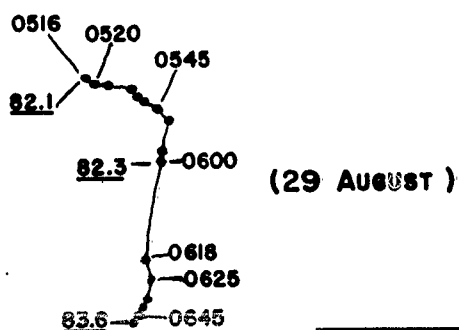
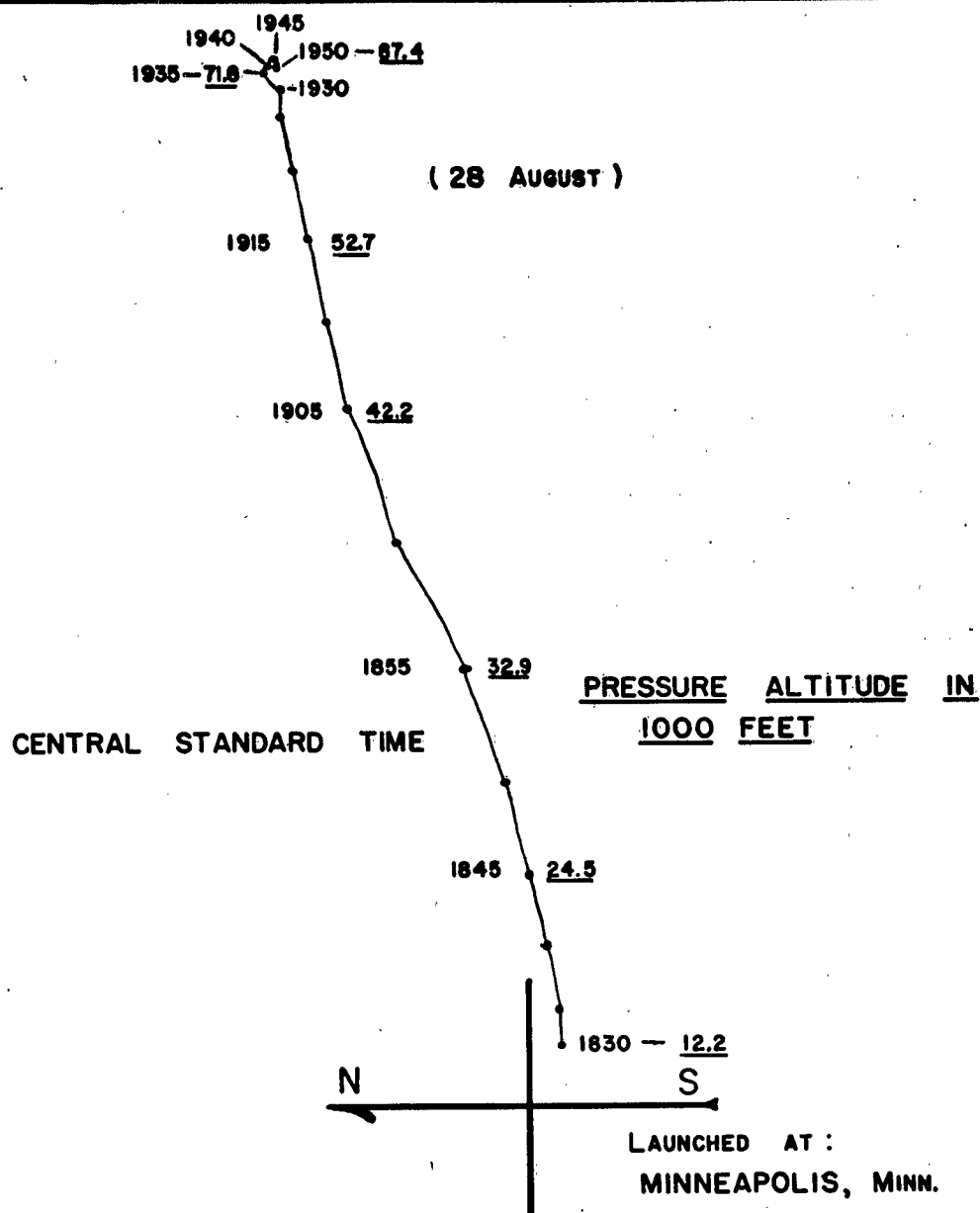








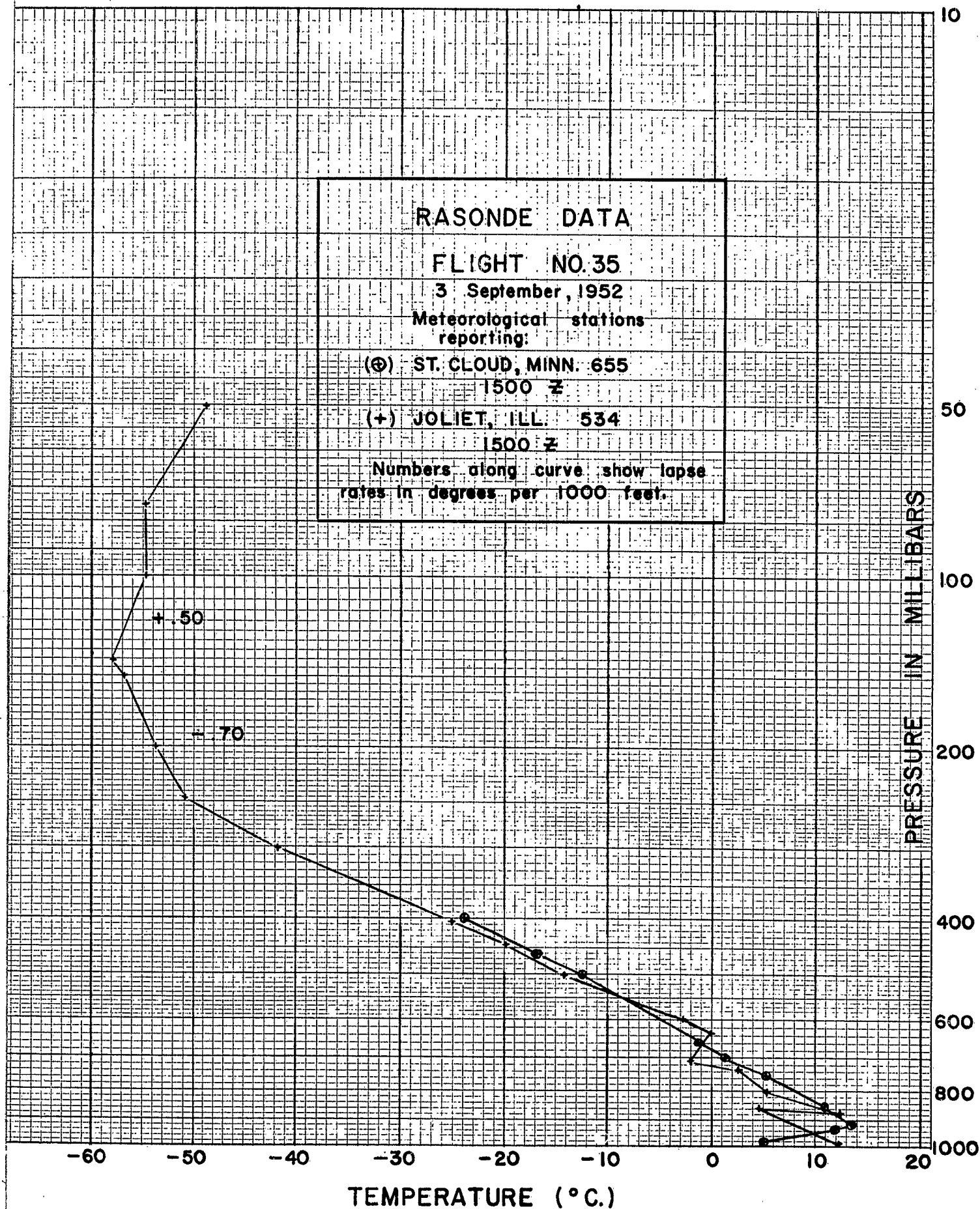
CONFIDENTIAL

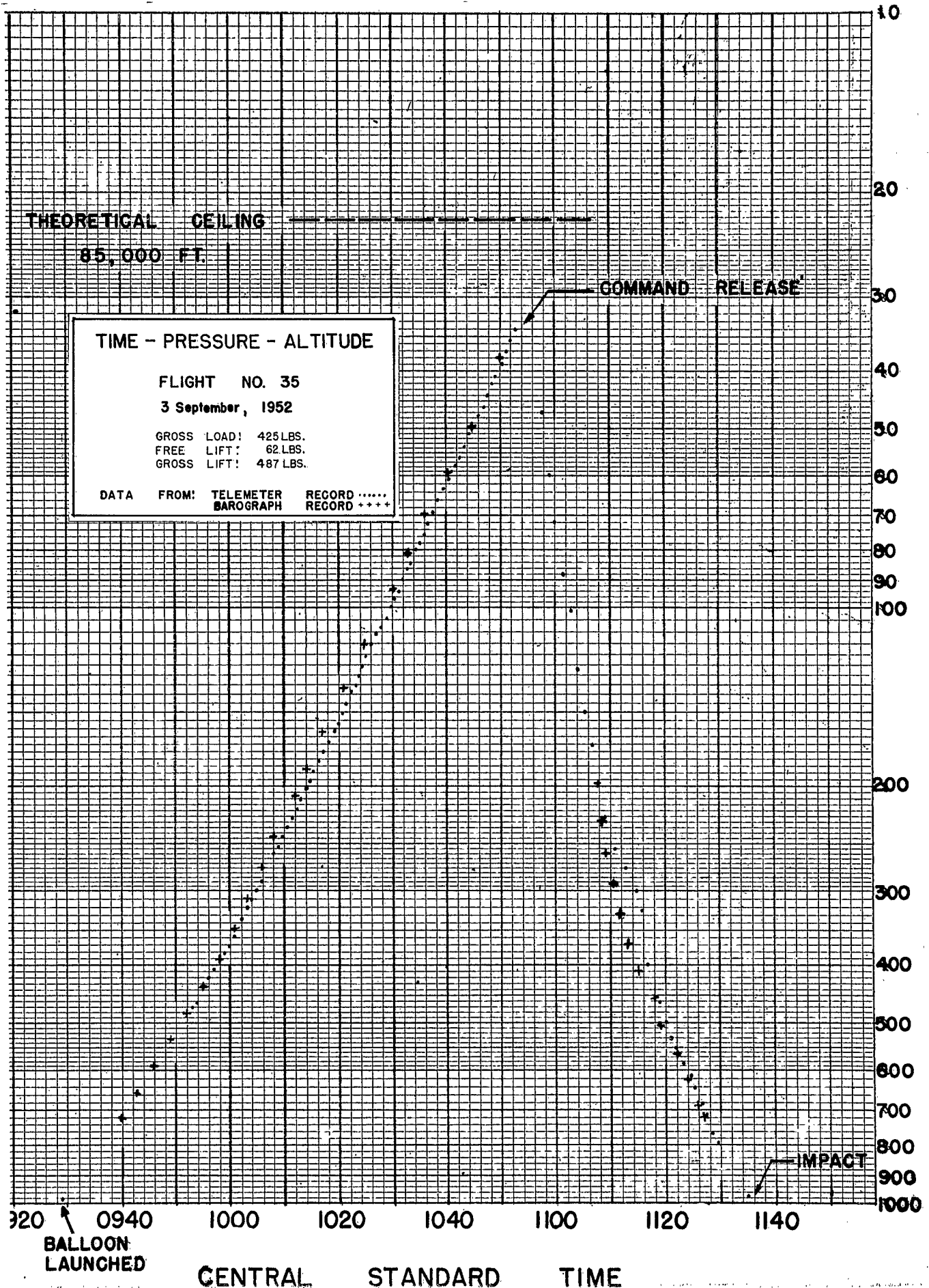


FLIGHT NO. 34
LAUNCHED 1815 CST
28 AUGUST, 1952
TRAJECTORY FROM THEODOLITE FIXES
SCALE $1:5 \times 10^5$

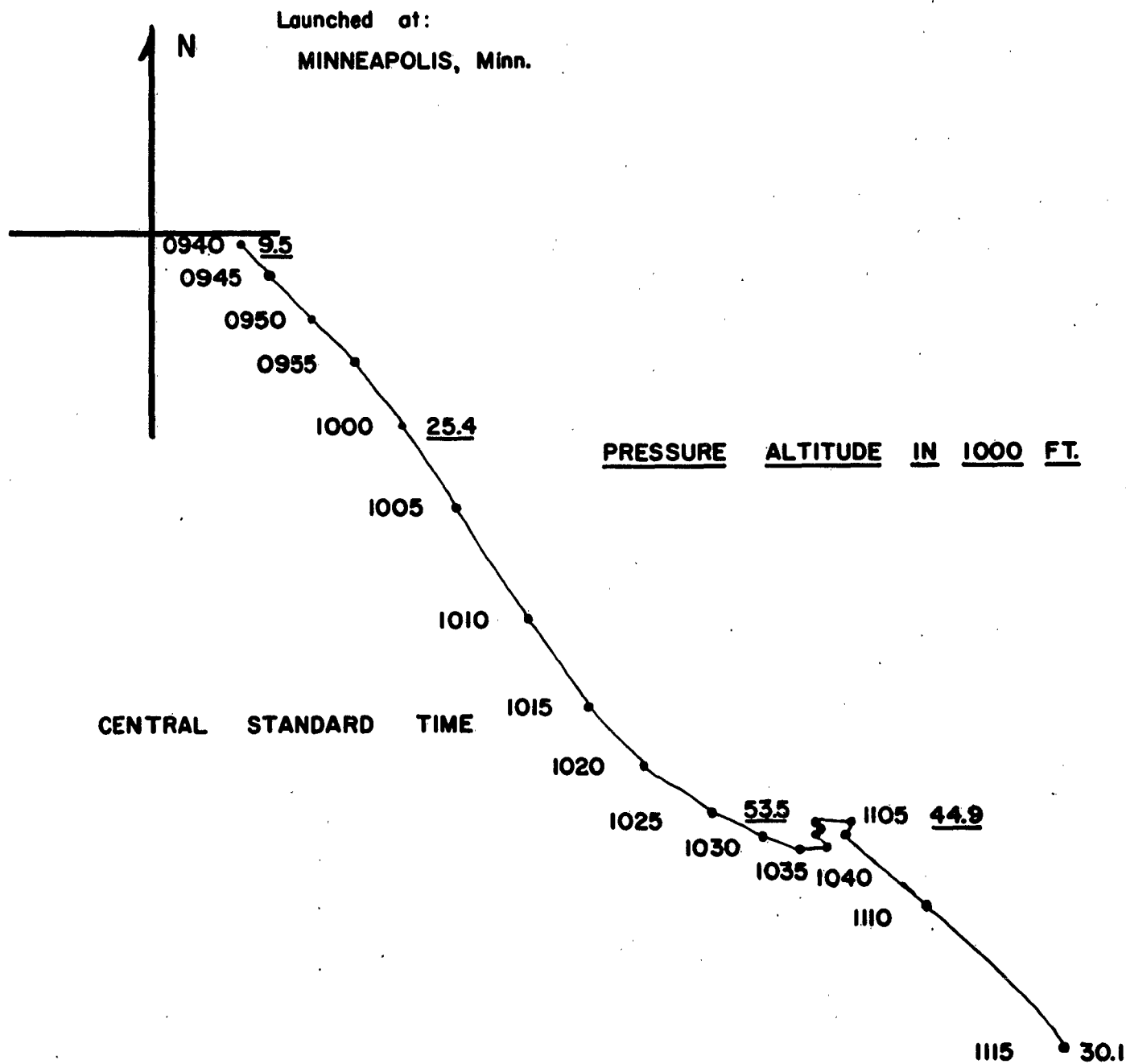
10 0 10 20 STATUTE MILES

CONFIDENTIAL SECURITY INFORMATION





CONFIDENTIAL



FLIGHT NO. 35

LAUNCHED 0929 CST

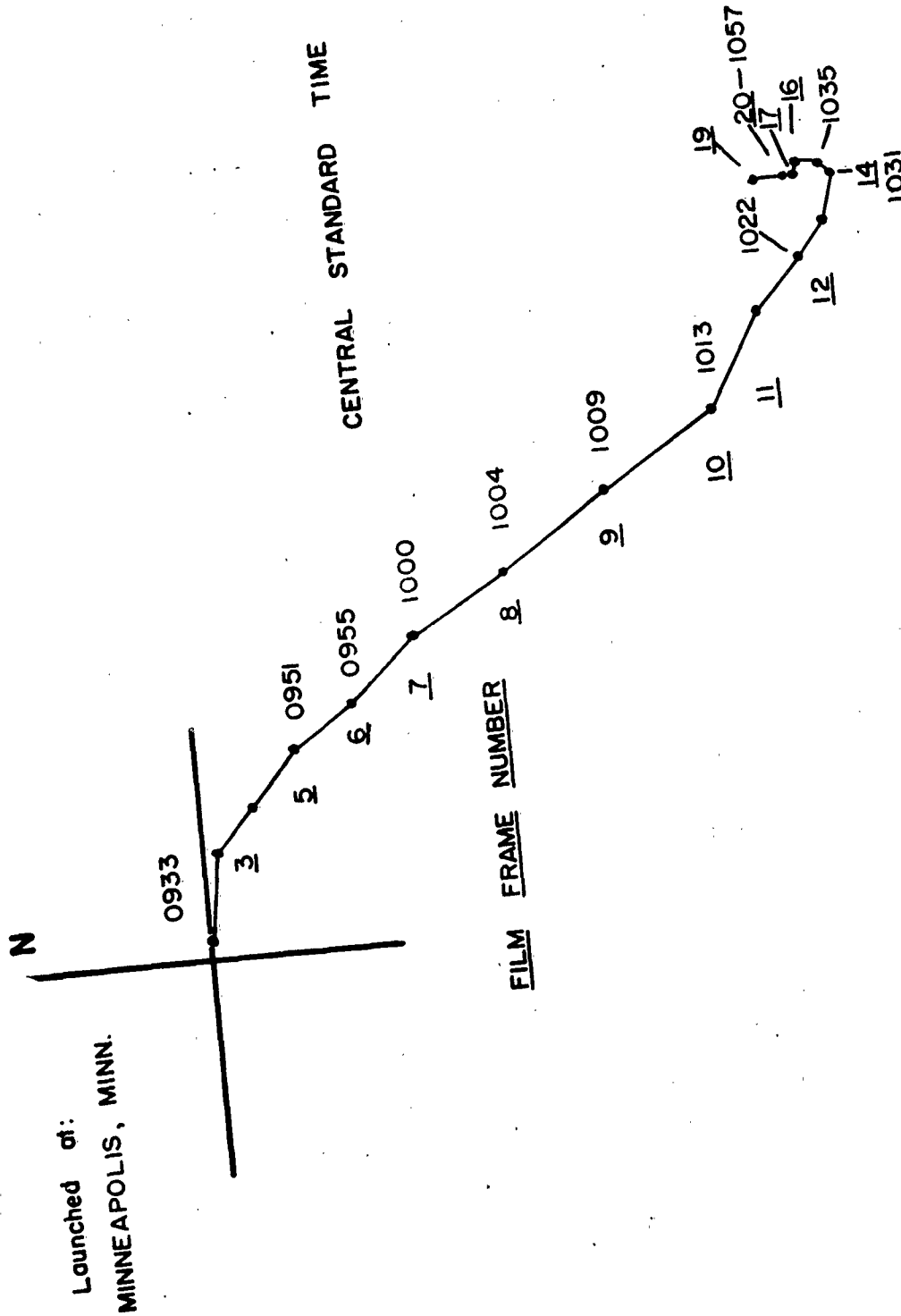
3 SEPTEMBER, 1952

TRAJECTORY FROM THEODOLITE FIXES

SCALE $1:5 \times 10^5$

10 0 10 20 STATUTE MILES

CONFIDENTIAL



FLIGHT NO. 35

LAUNCHED 0929 CST.

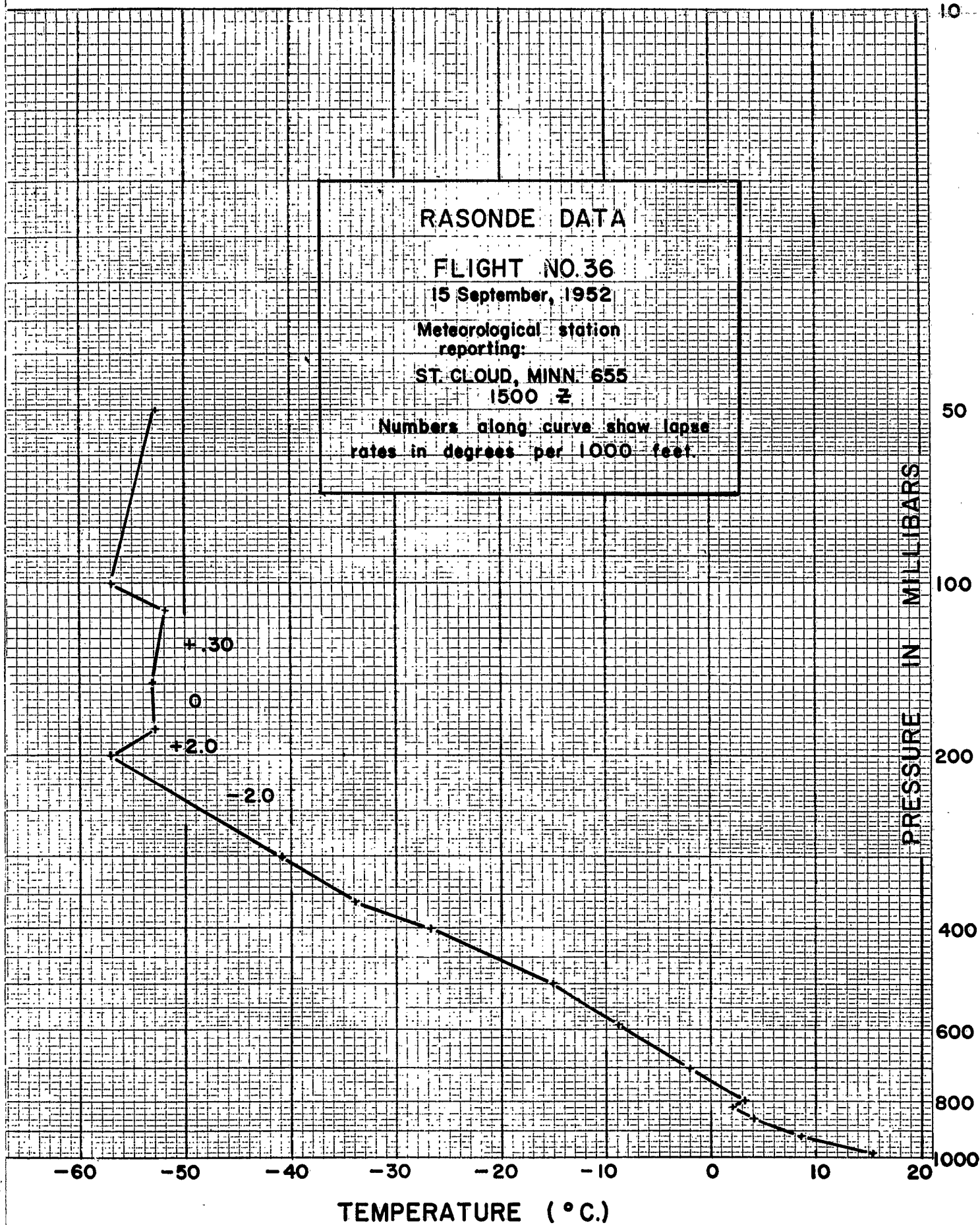
3 SEPTEMBER, 1952

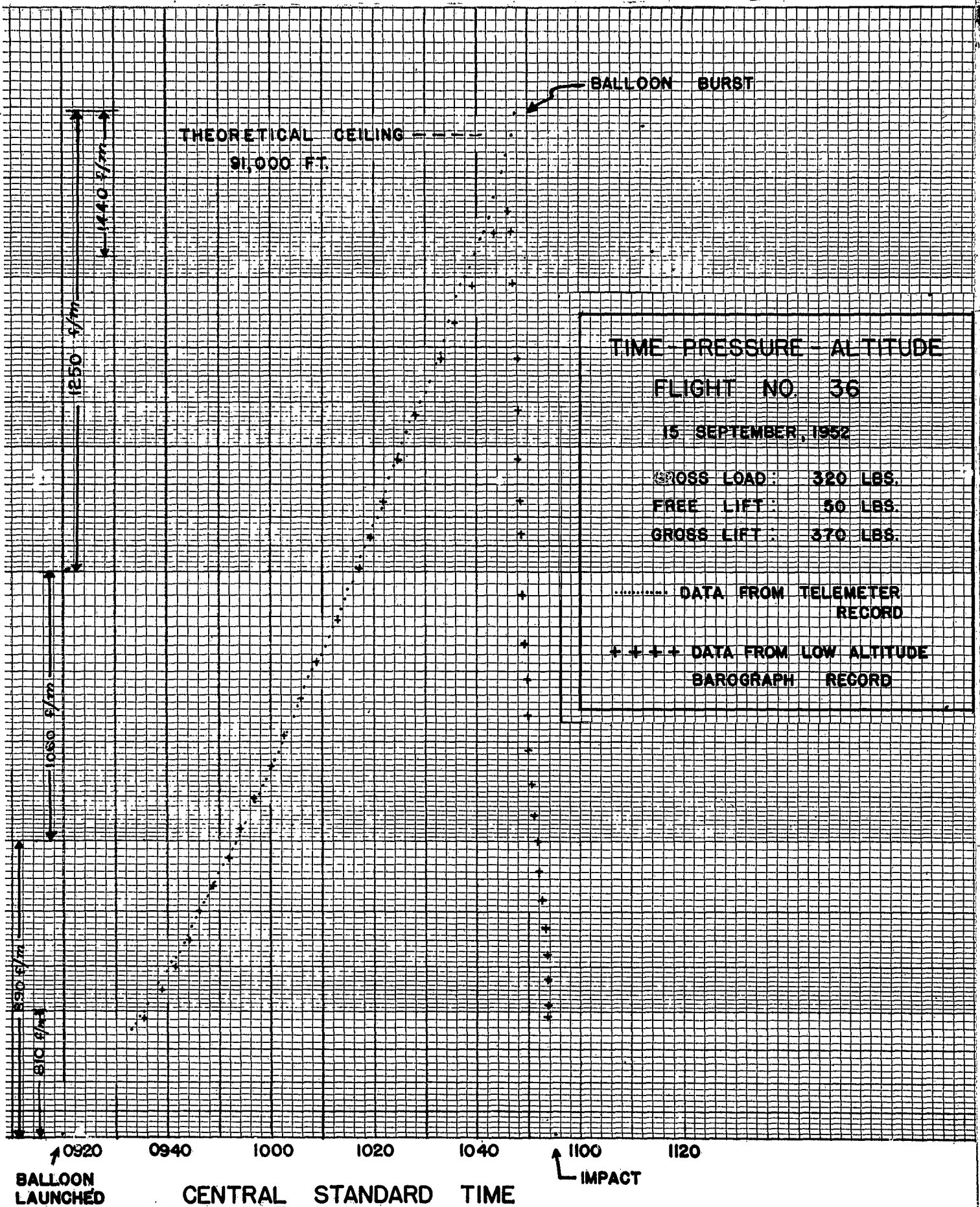
TRAJECTORY FROM DOWN PICTURES

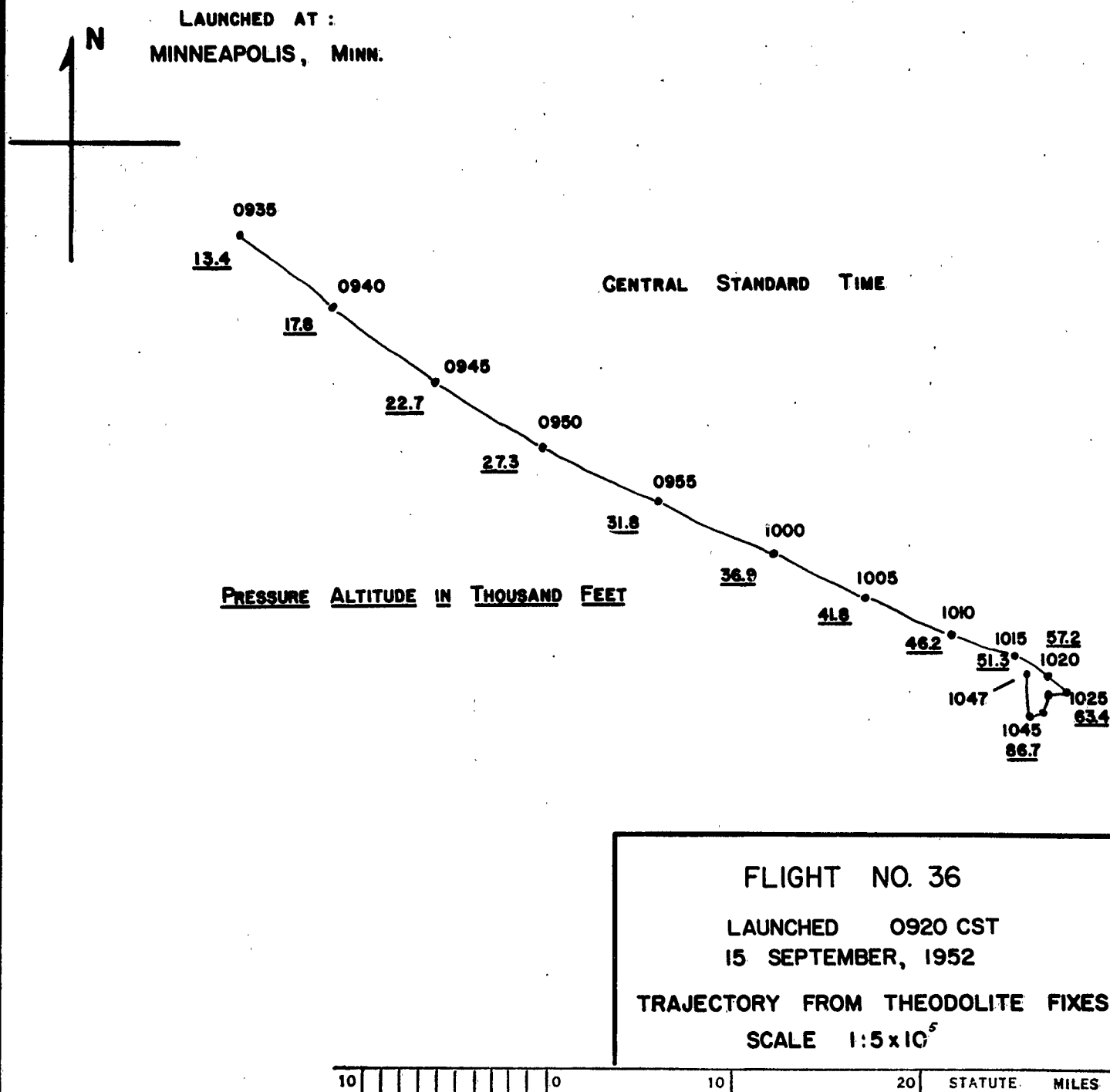
SCALE 1:5 x 10⁵

CONFIDENTIAL SECURITY INFORMATION



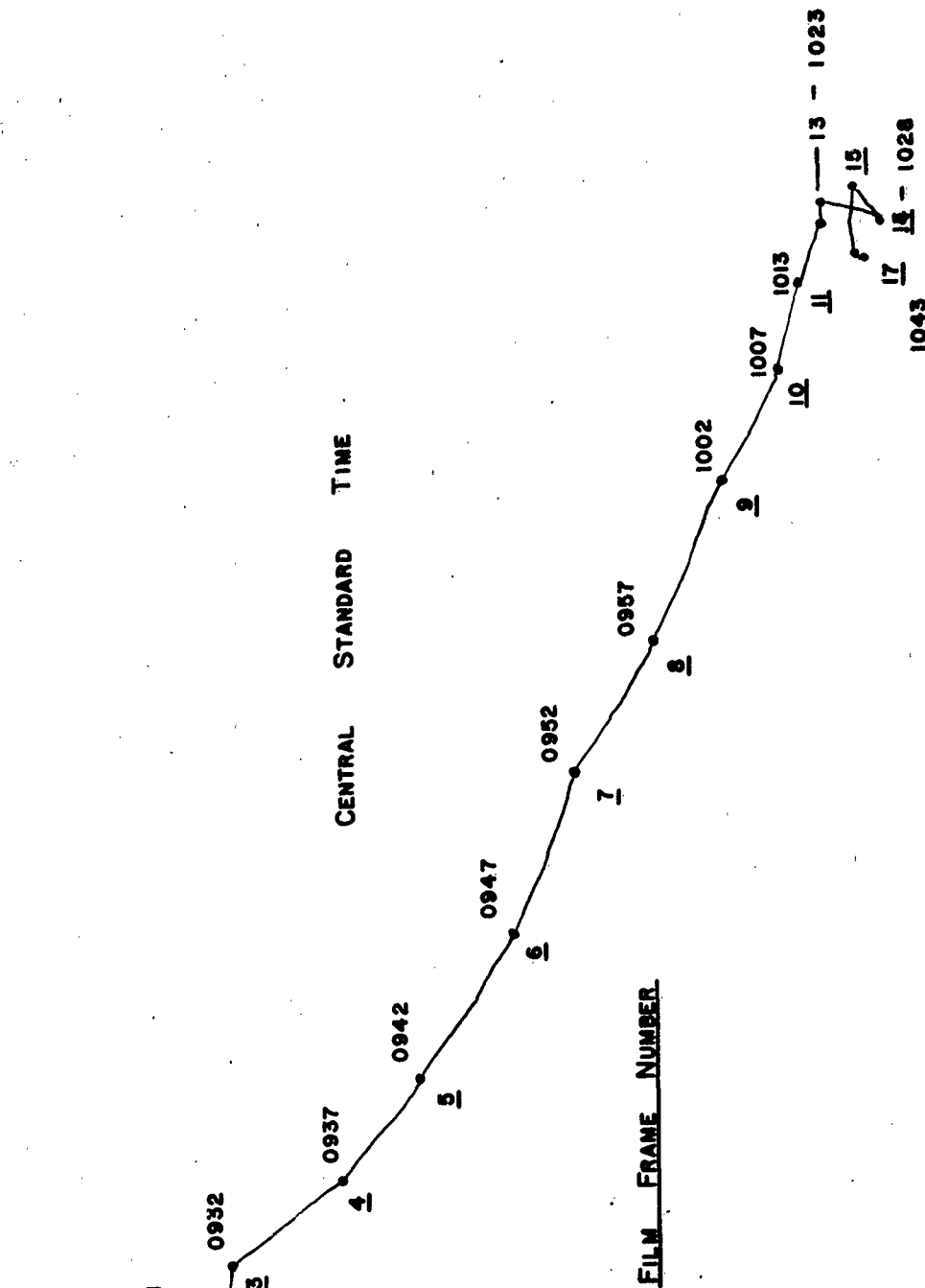




CONFIDENTIAL**CONFIDENTIAL SECURITY INFORMATION**

CONFIDENTIAL

LAUNCHED AT:
MINNEAPOLIS, MINN.



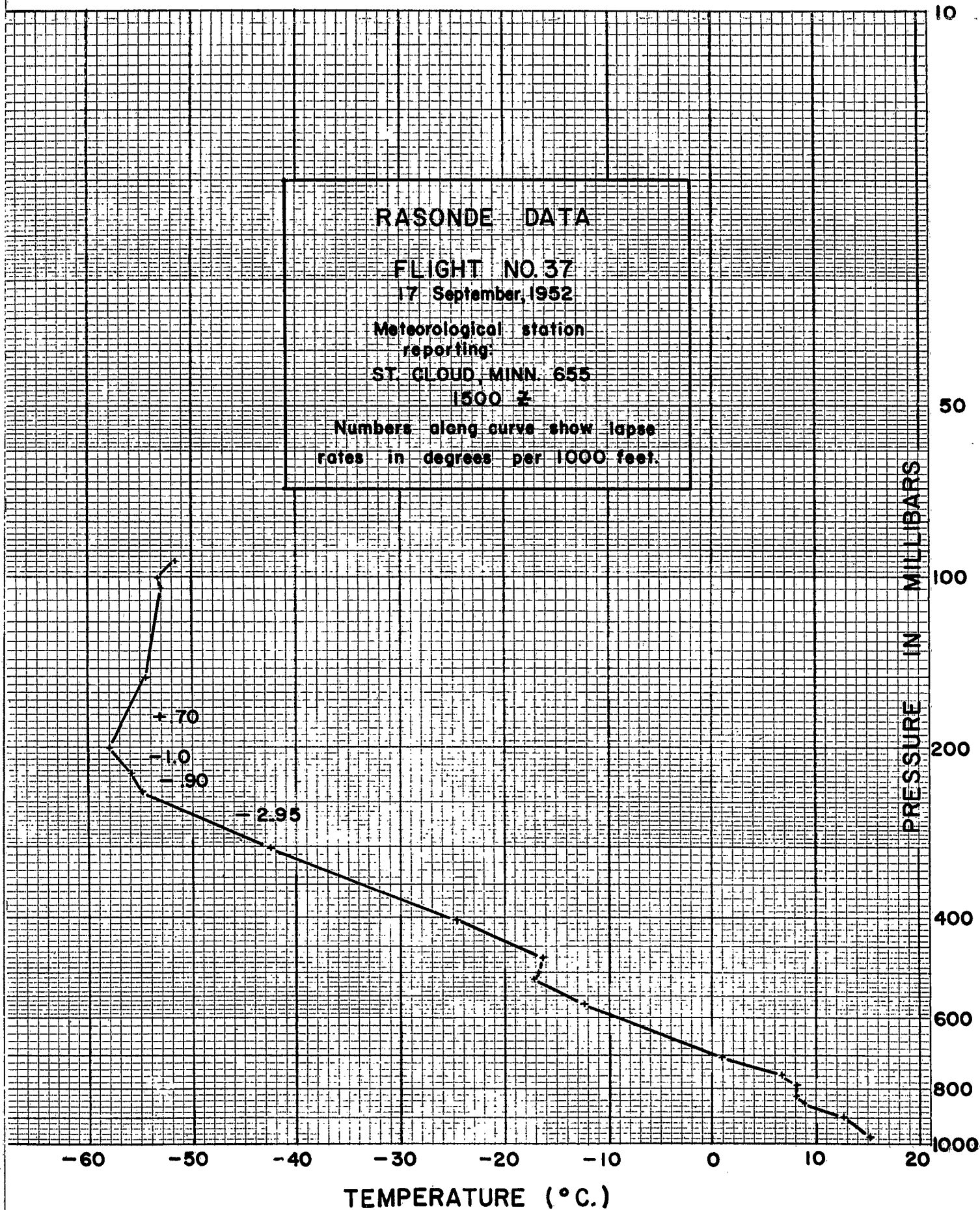
FLIGHT NO. 36

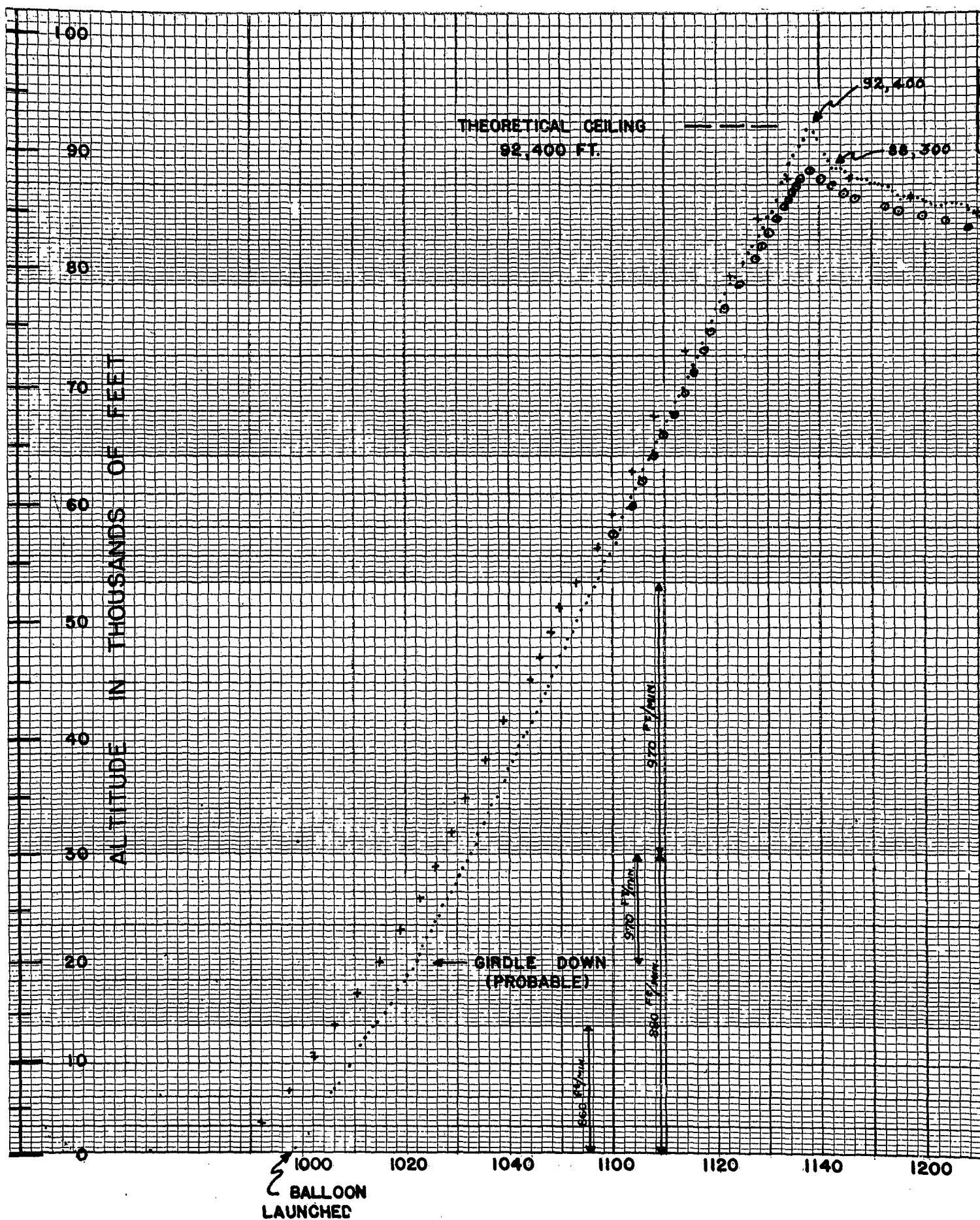
LAUNCHED 0920 CST

15 SEPTEMBER, 1952

TRAJECTORY FROM DOWN PICTURES

SCALE 1:5 x 10⁵





TEMPERATURE CHANGE
FROM BOUNCE

$$4.1(4) = 16.4^{\circ}\text{C.}$$

+ 1.6 (FROM CONVECTION WARMING)

$$= 18^{\circ}\text{C.}$$

$$\frac{\Delta T}{T} = 8.0\%$$

$$\text{INITIAL } \frac{F}{G} = 11.4\%$$

11.4

8.0

3.4%

AERO DRAG AT ALTITUDE
FROM CHANGE IN ALTITUDE
AND INITIAL FREE LIFT

TIME - PRESSURE - ALTITUDE

FLIGHT NO 37

17 SEPTEMBER, 1952

GROSS LOAD: 312 LBS.

FREE LIFT: 48 LBS.

GROSS LIFT: 360 LBS.

TELEMETER RECORD

+++ LOW ALTITUDE BAROGRAPH

ooo HIGH ALTITUDE BAROGRAPH

LOW ALTITUDE BAROGRAPH TIME DIFFERENCE
DUE TO CALIBRATION ERROR.

1220

1240

1300

1320

1340

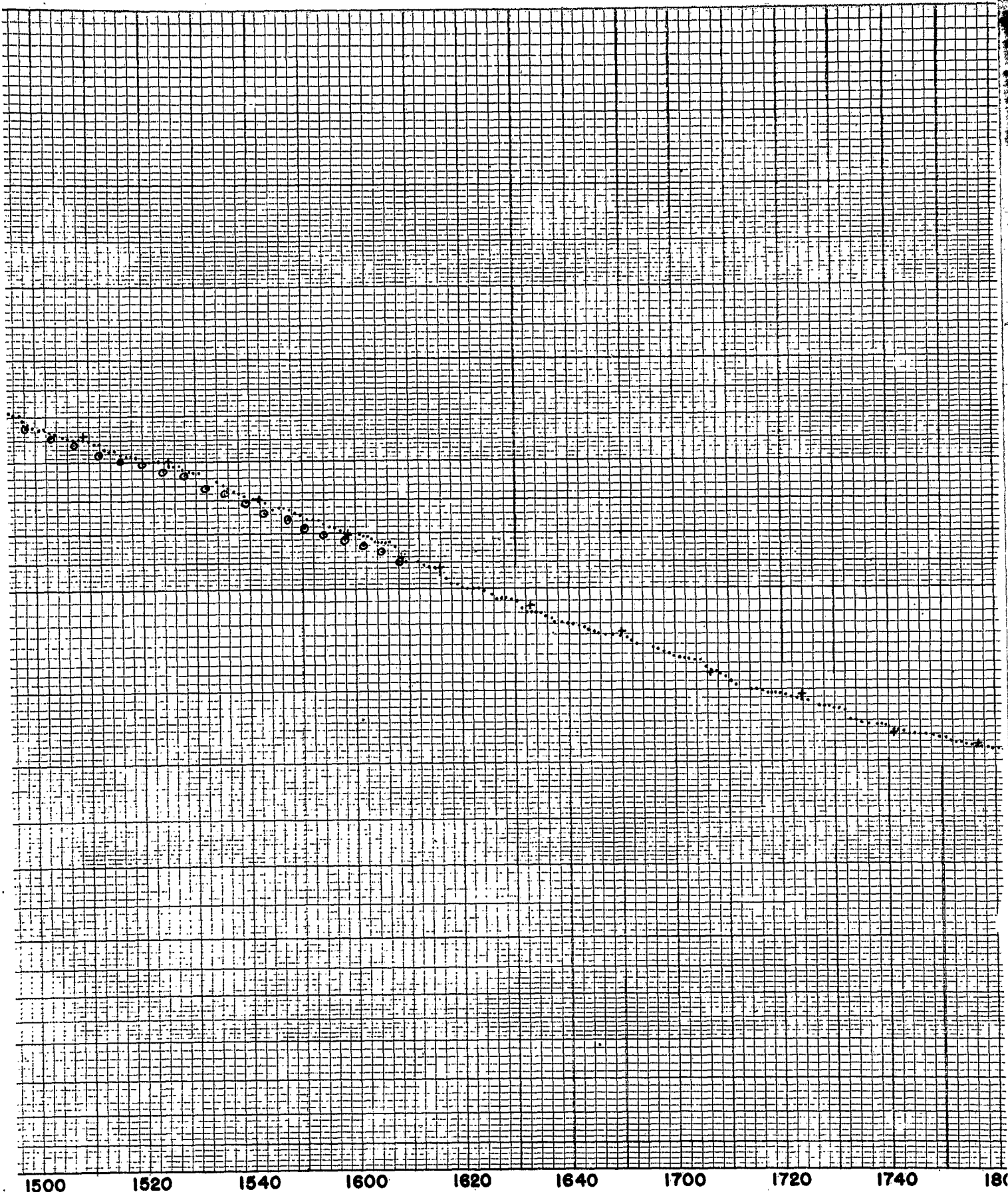
1400

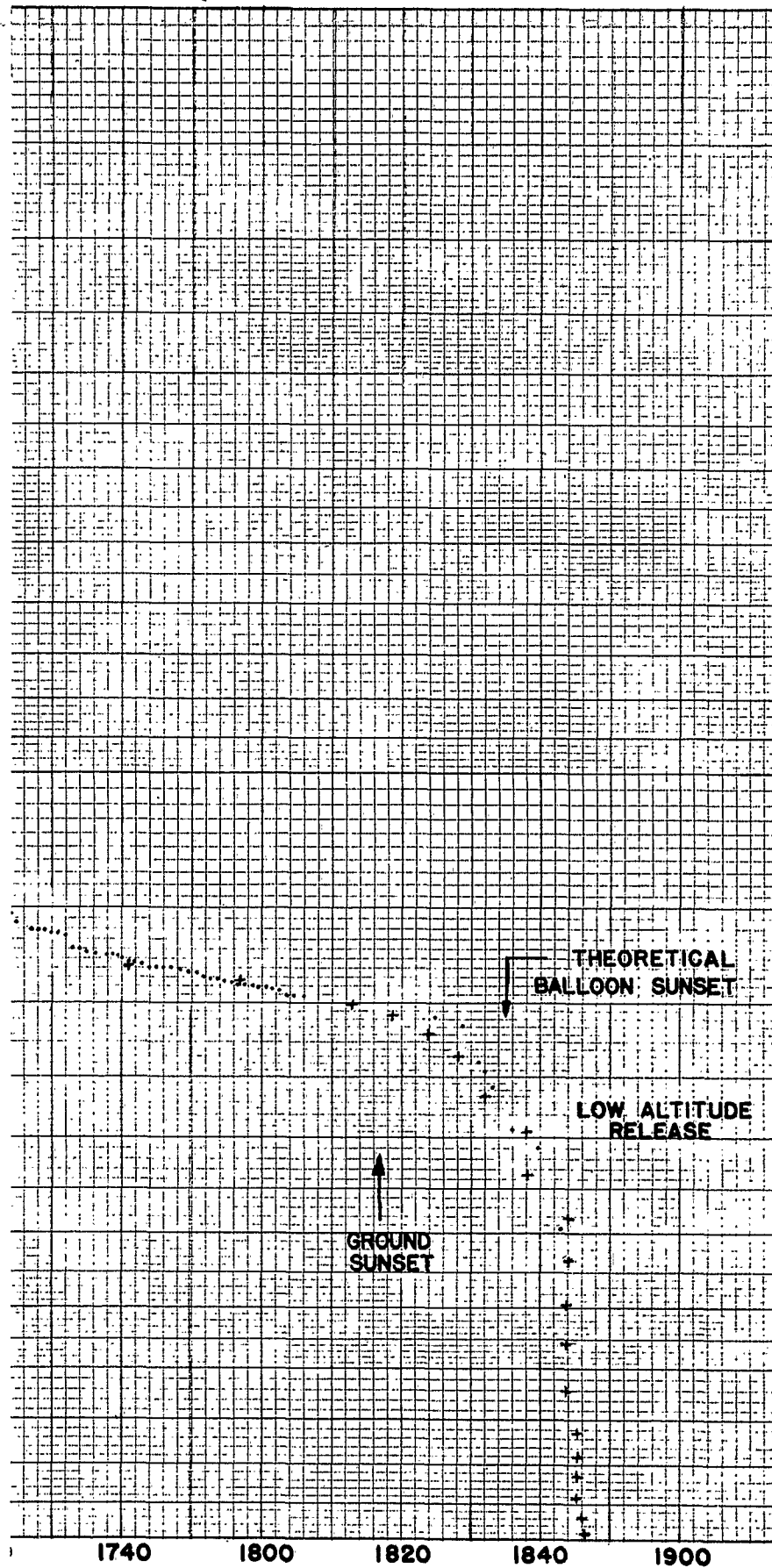
1420

1440

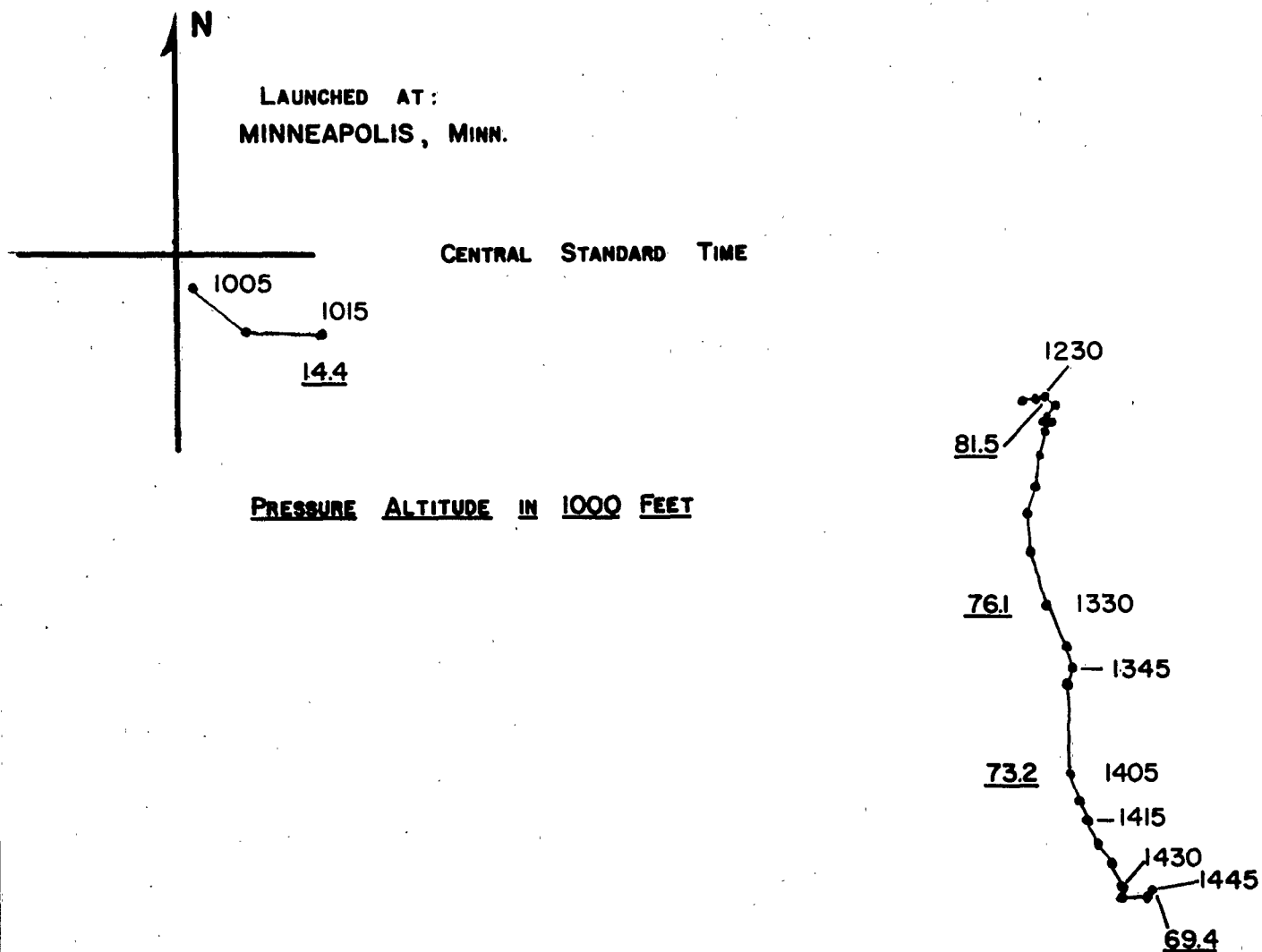
1500

CENTRAL STANDARD TIME



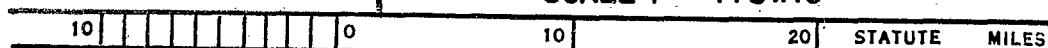


CONFIDENTIAL



FLIGHT NO 37
LAUNCHED 0958 CST
17 SEPTEMBER, 1952

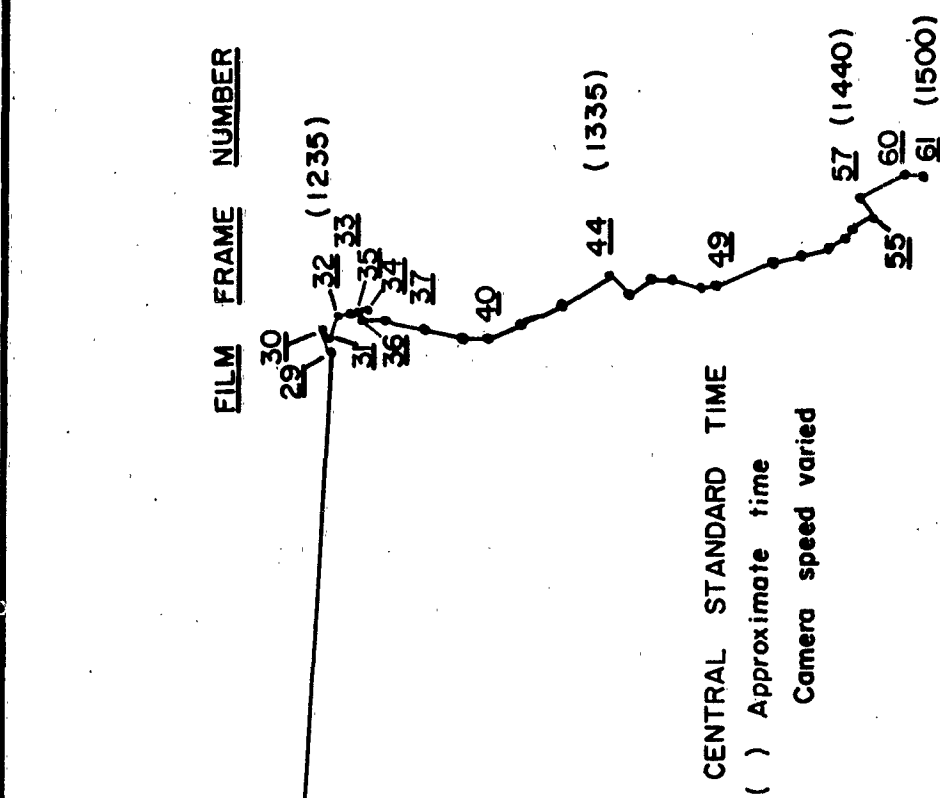
TRAJECTORY FROM THEODOLITE FIXES
SCALE : $1:5 \times 10^5$



CONFIDENTIAL SECURITY INFORMATION

CONFIDENTIAL

Launched at:
MINNEAPOLIS, MINN.



FLIGHT NO. 37

LAUNCHED 0958 C.S.T.

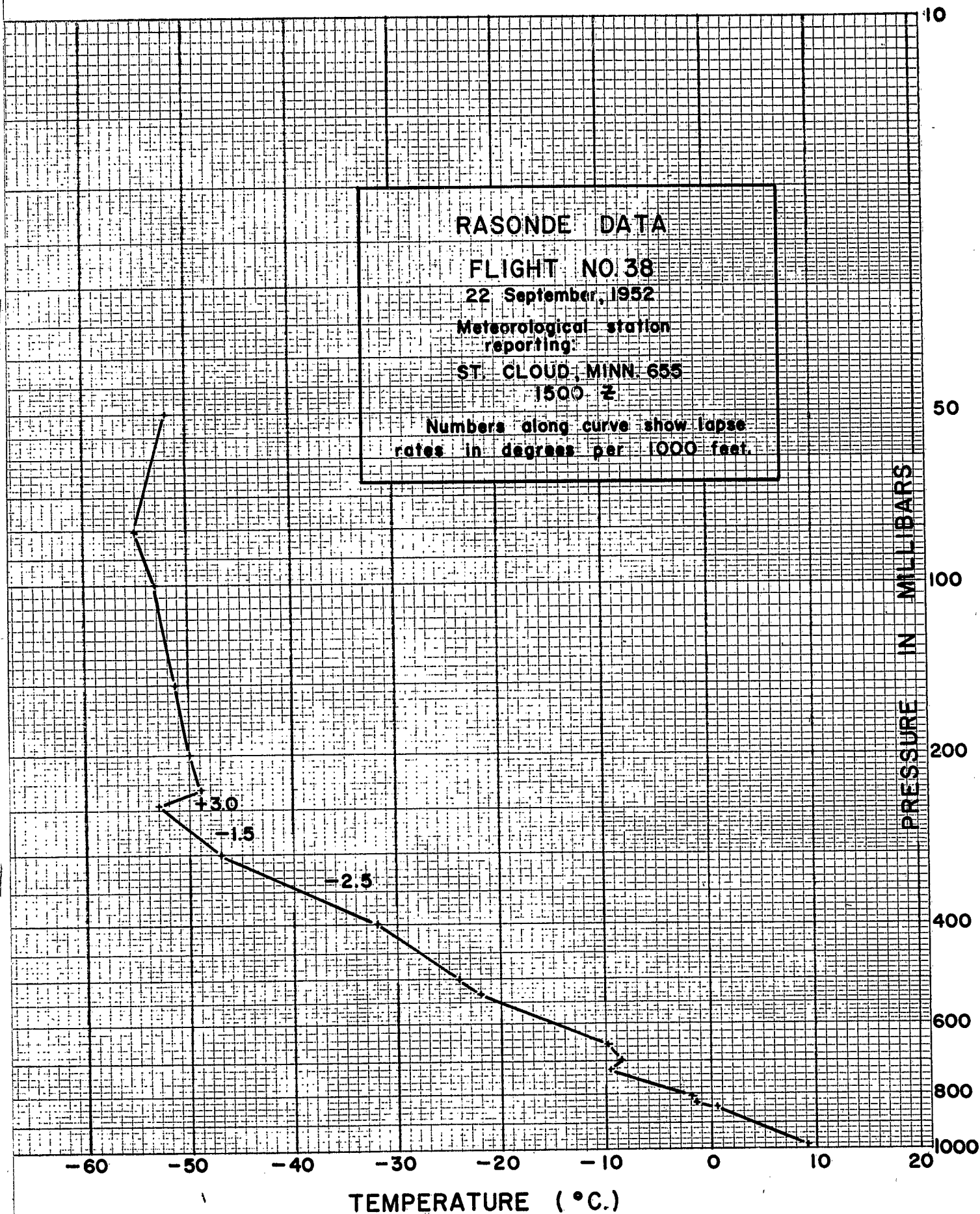
17 SEPTEMBER, 1952

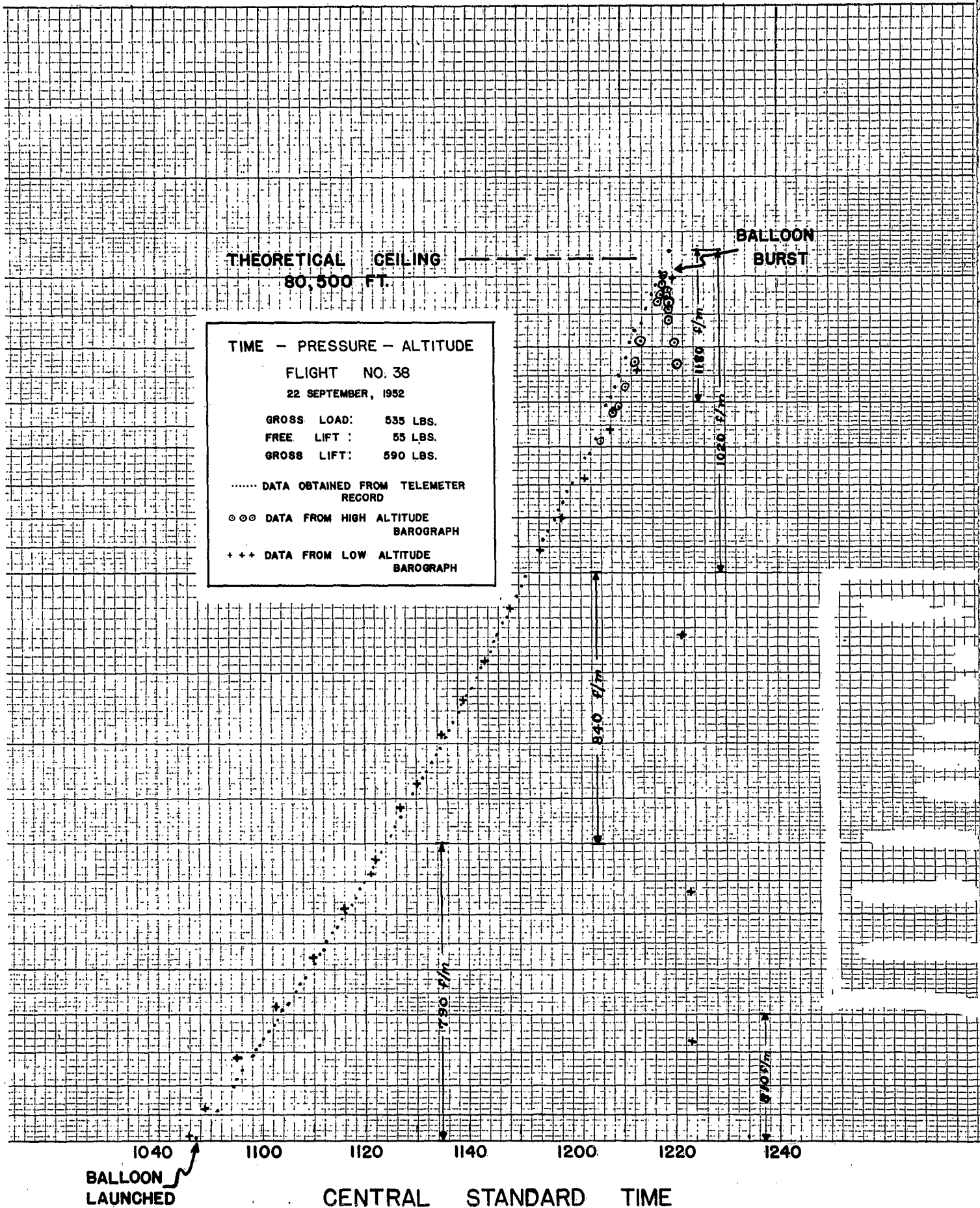
TRAJECTORY FROM DOWN PICTURES

SCALE 1:5 x 10⁵

CONFIDENTIAL **SECURITY** **INFORMATION**

[illegible]

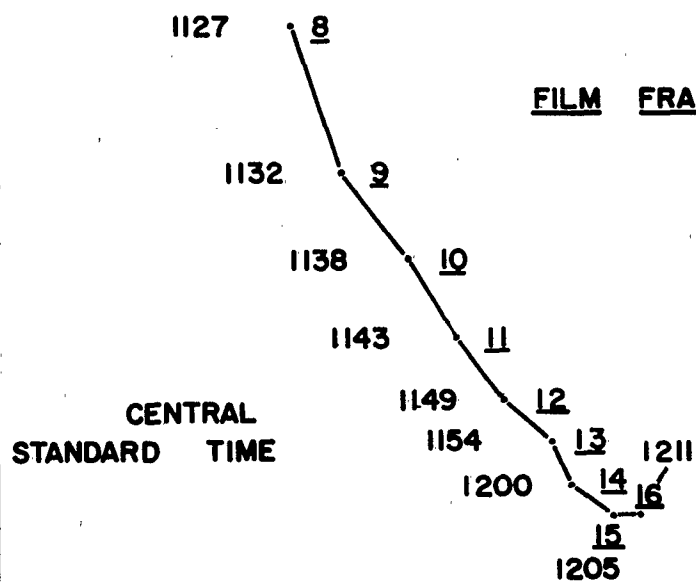




CONFIDENTIAL



Launched at:
MINNEAPOLIS, Minn.

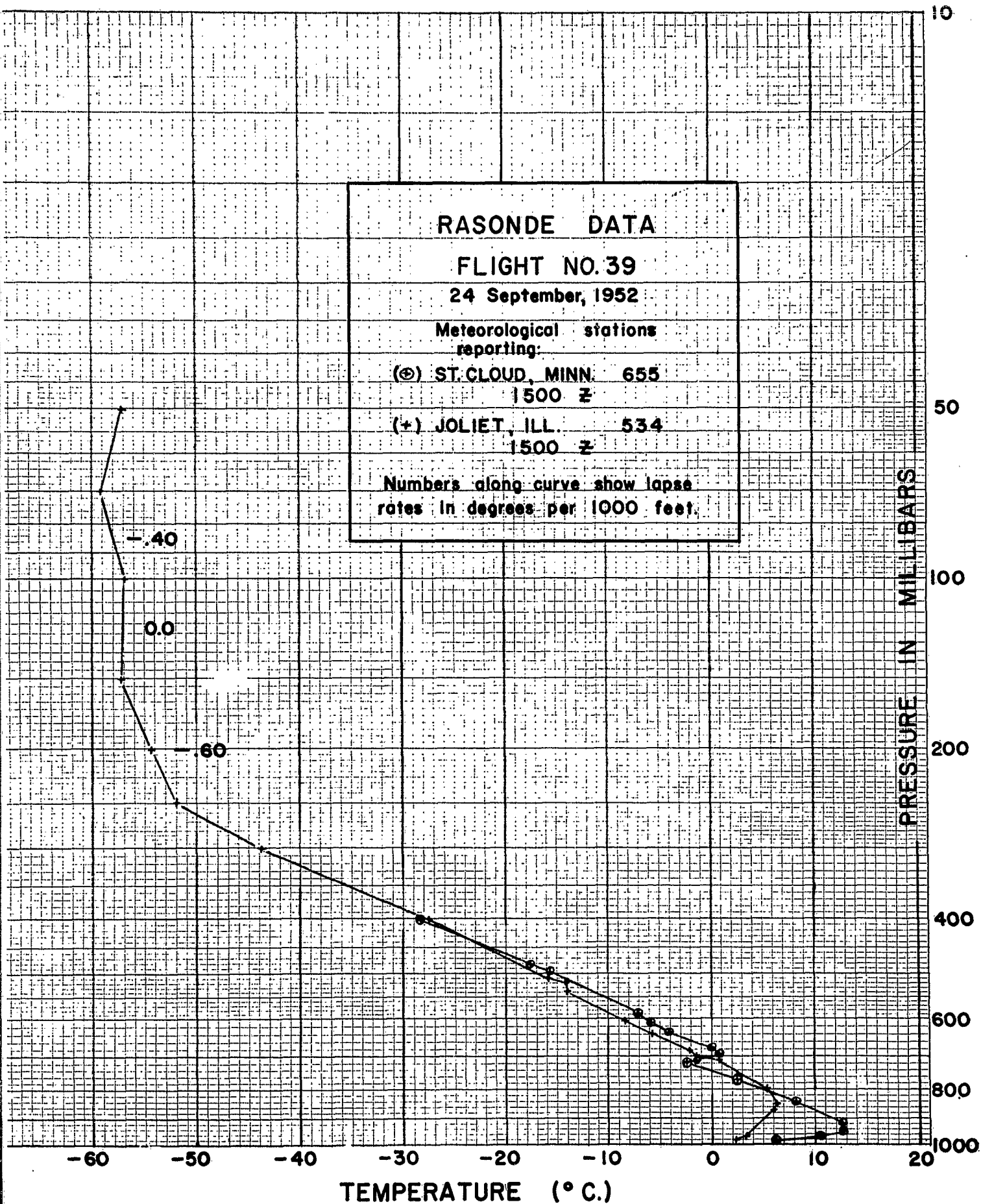


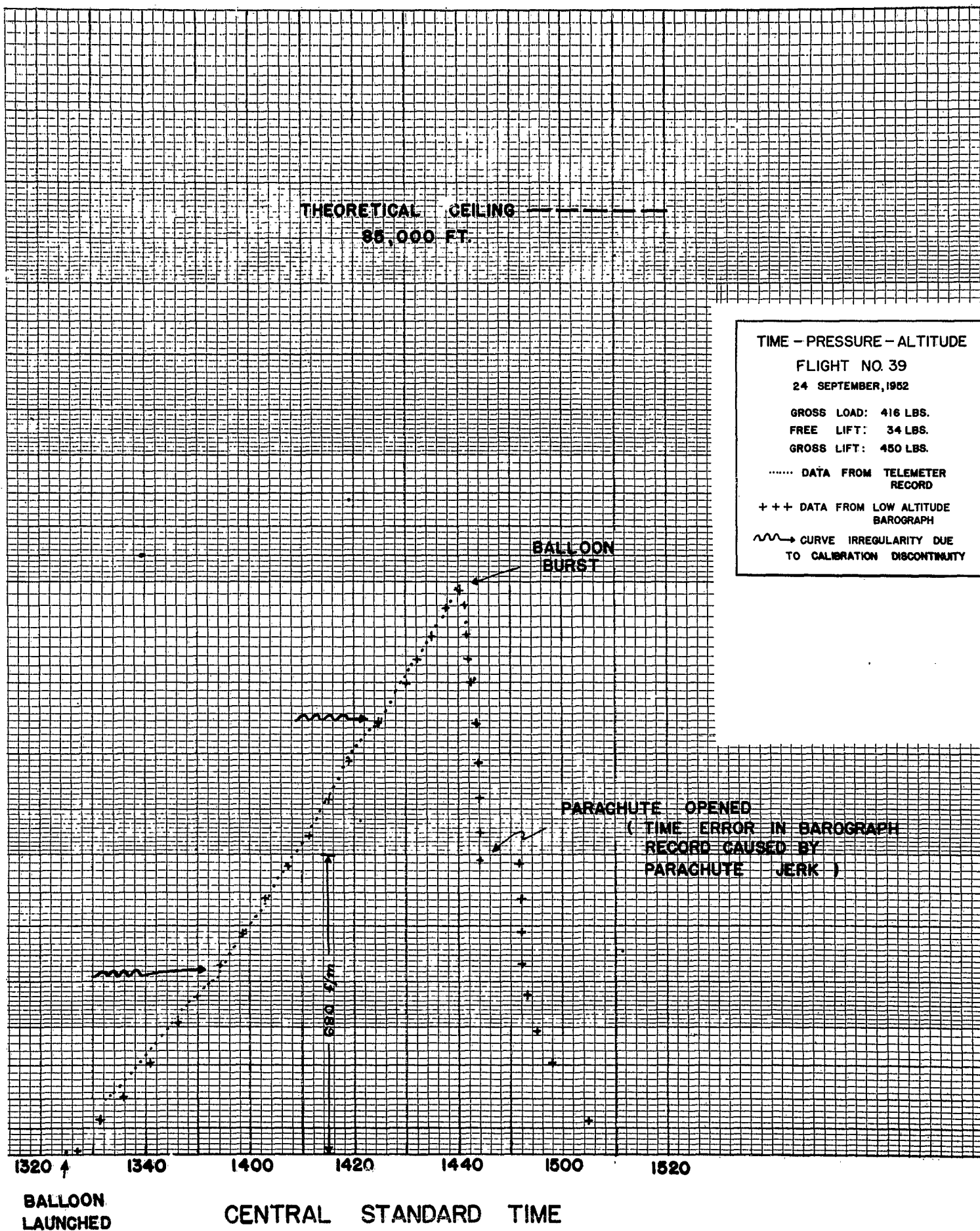
FLIGHT NO. 38
LAUNCHED 1047
22 SEPTEMBER, 1952
TRAJECTORY FROM DOWN PICTURES

CONFIDENTIAL SECURITY INFORMATION

SCALE 1:5 x 10⁵

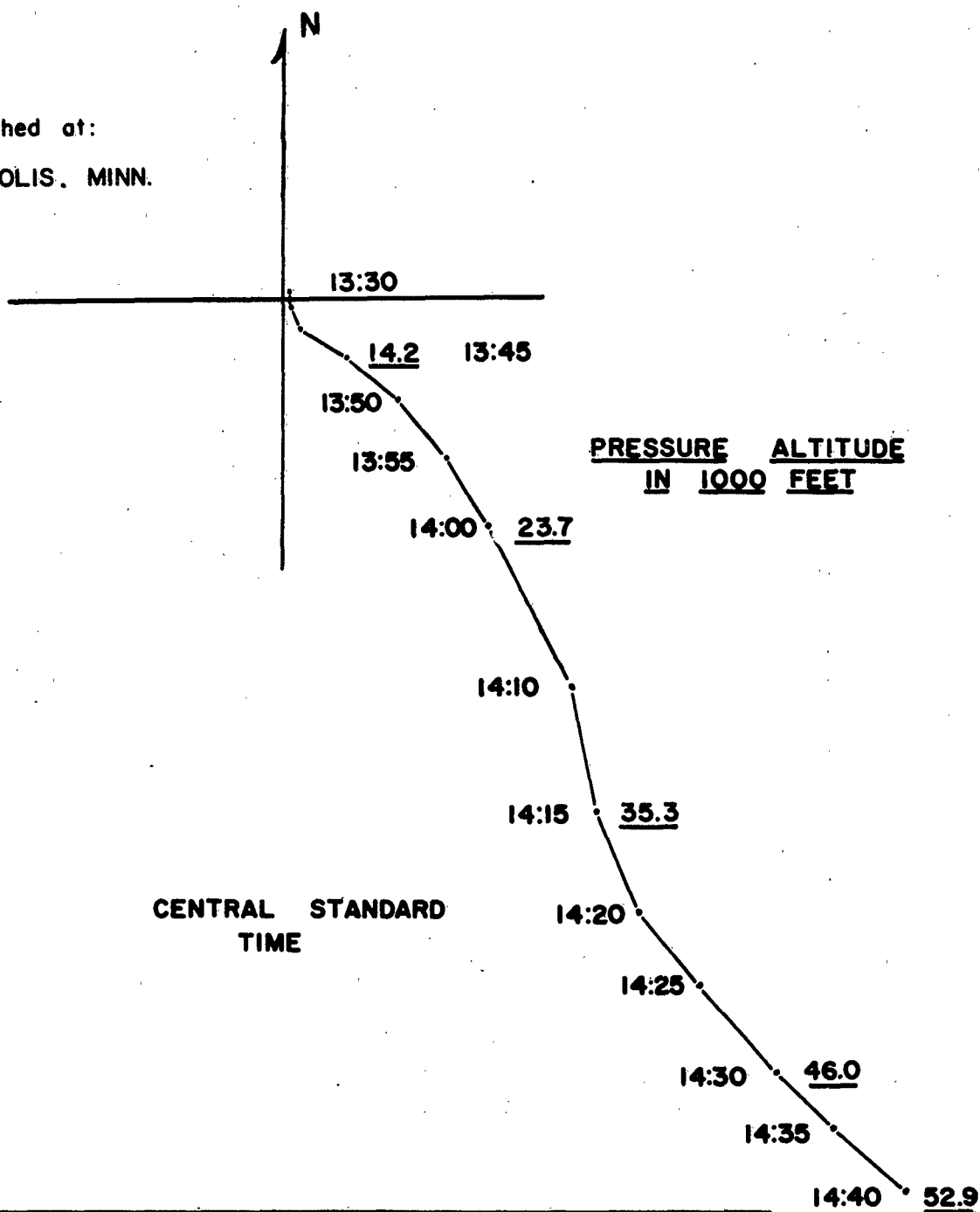






CONFIDENTIAL

Launched at:
MINNEAPOLIS, MINN.



FLIGHT NO. 39

LAUNCHED 1325

24 SEPTEMBER, 1952

TRAJECTORY FROM THEODOLITE FIXES

SCALE: $1:5 \times 10^5$

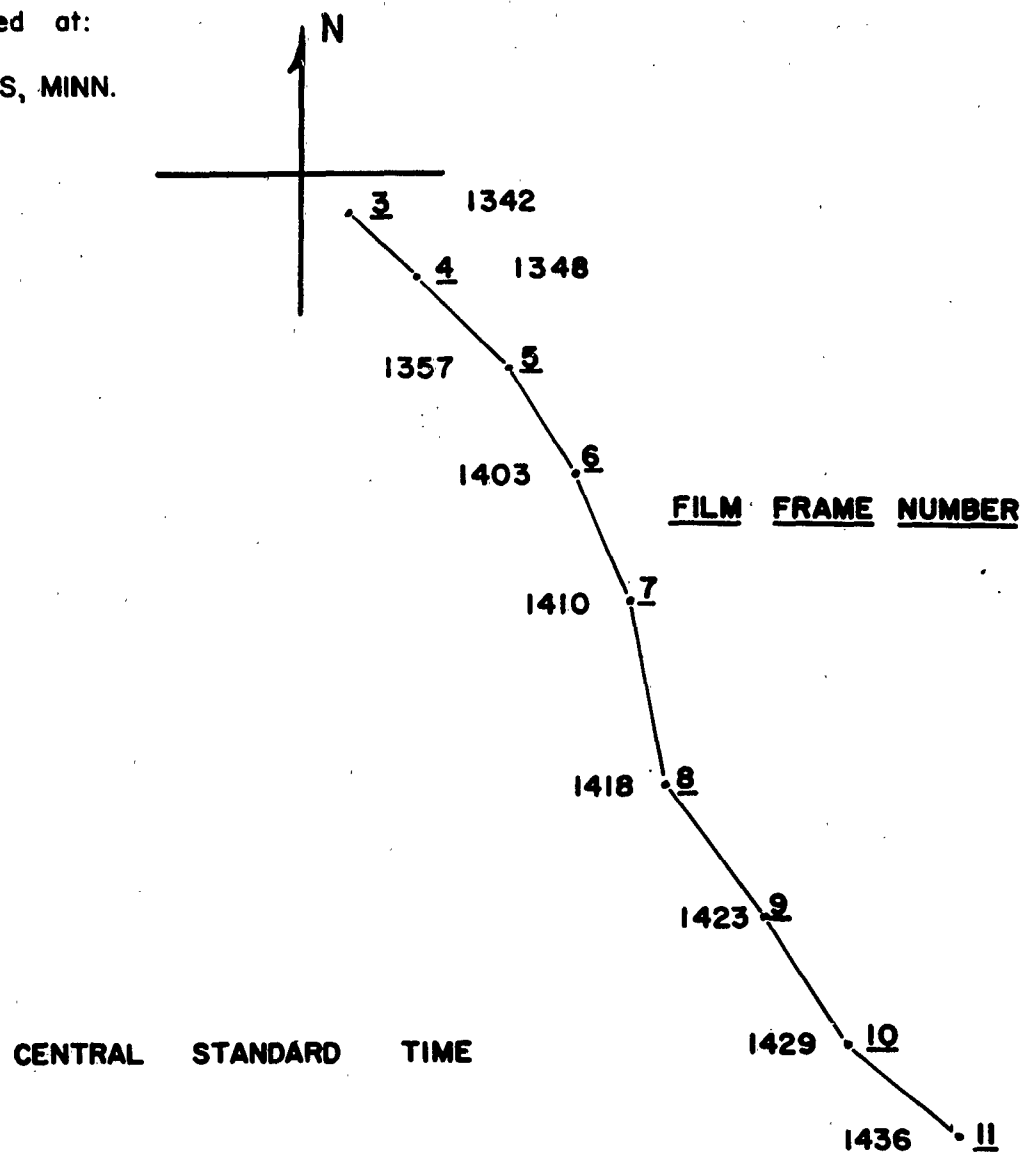
CONFIDENTIAL

SECURITY

INFORMATION

CONFIDENTIAL

Launched at:
MINNEAPOLIS, MINN.



FLIGHT NO. 39

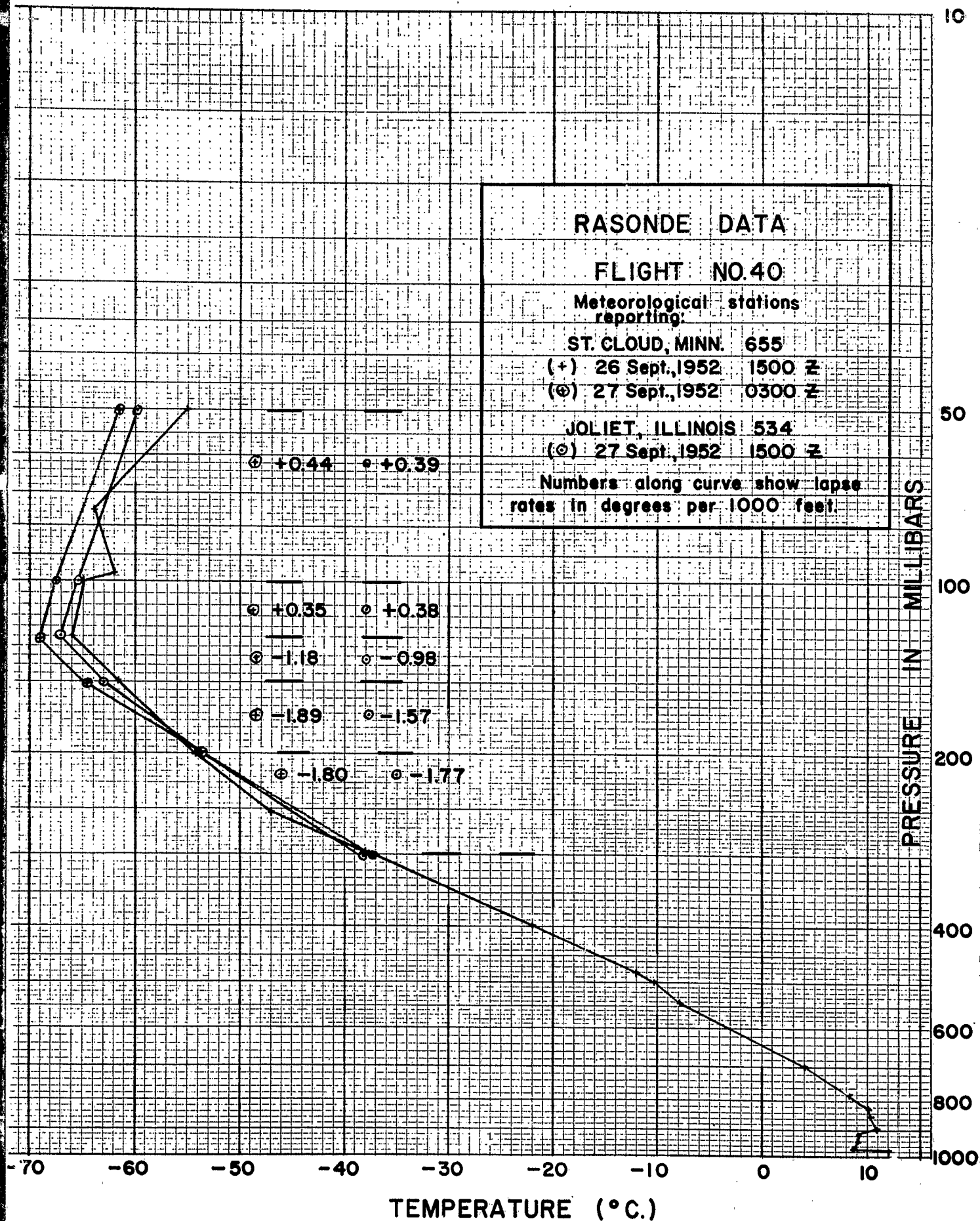
LAUNCHED 13:25 CST

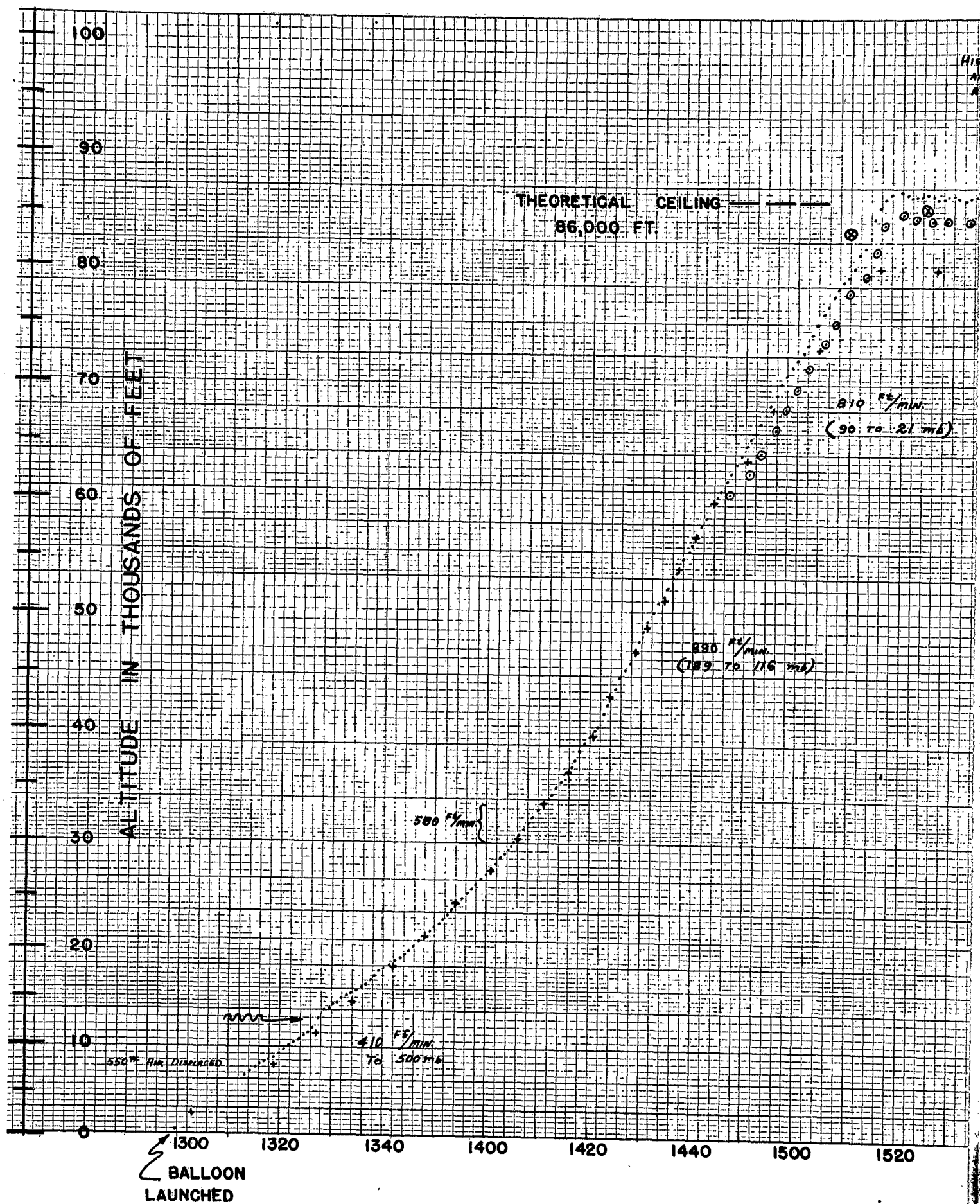
24 NOVEMBER, 1952

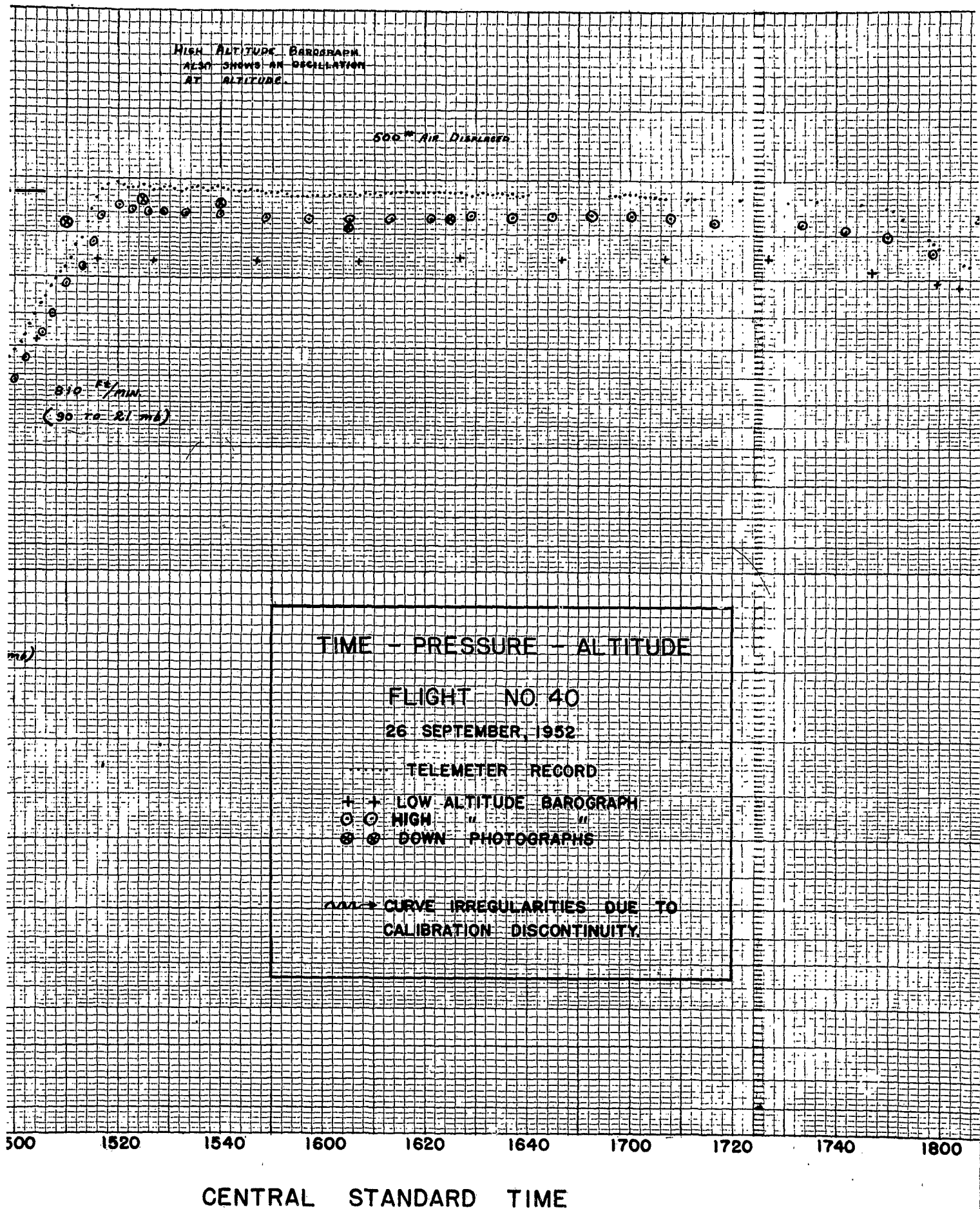
TRAJECTORY FROM DOWN PICTURES

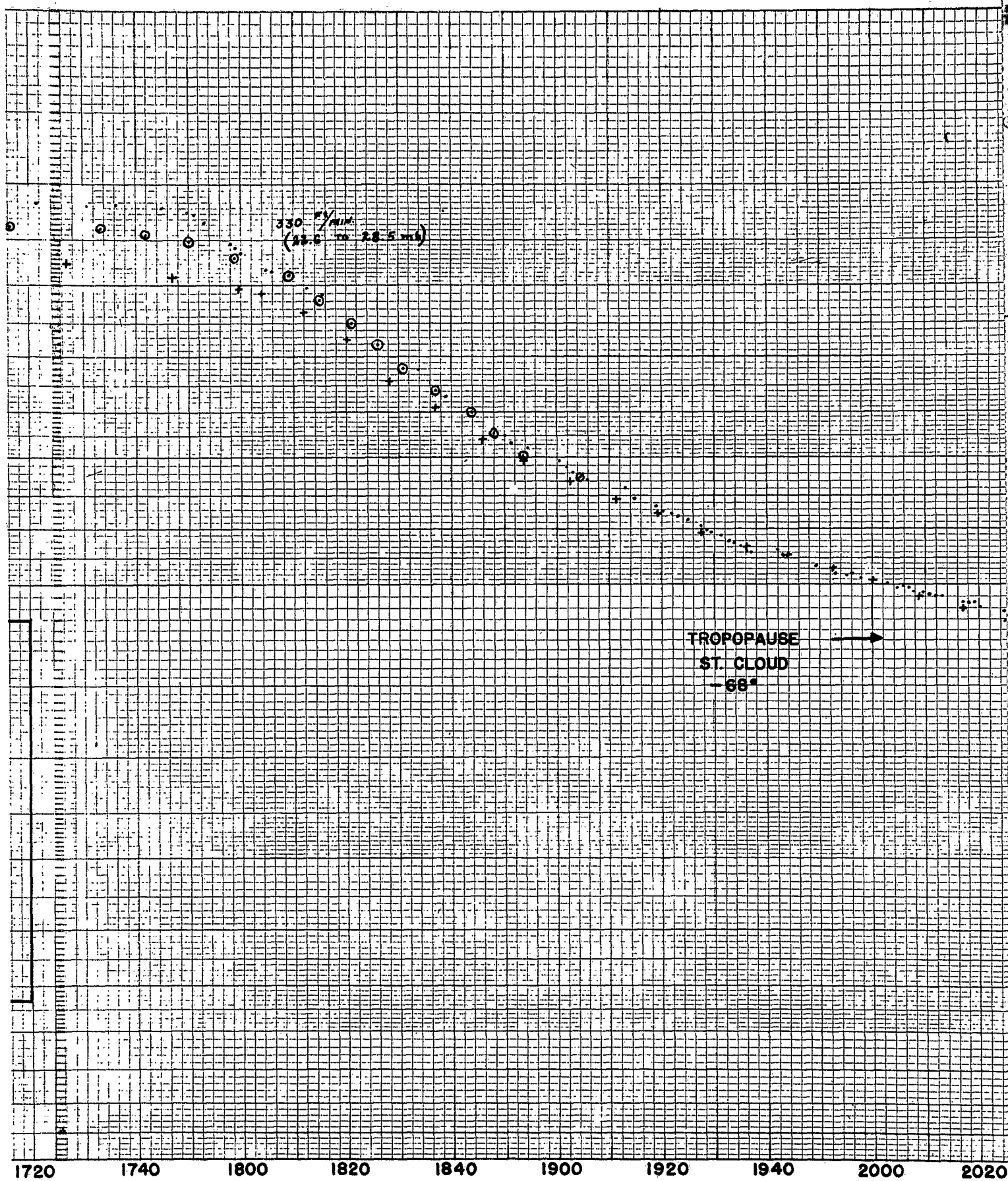
SCALE : $1:5 \times 10^5$

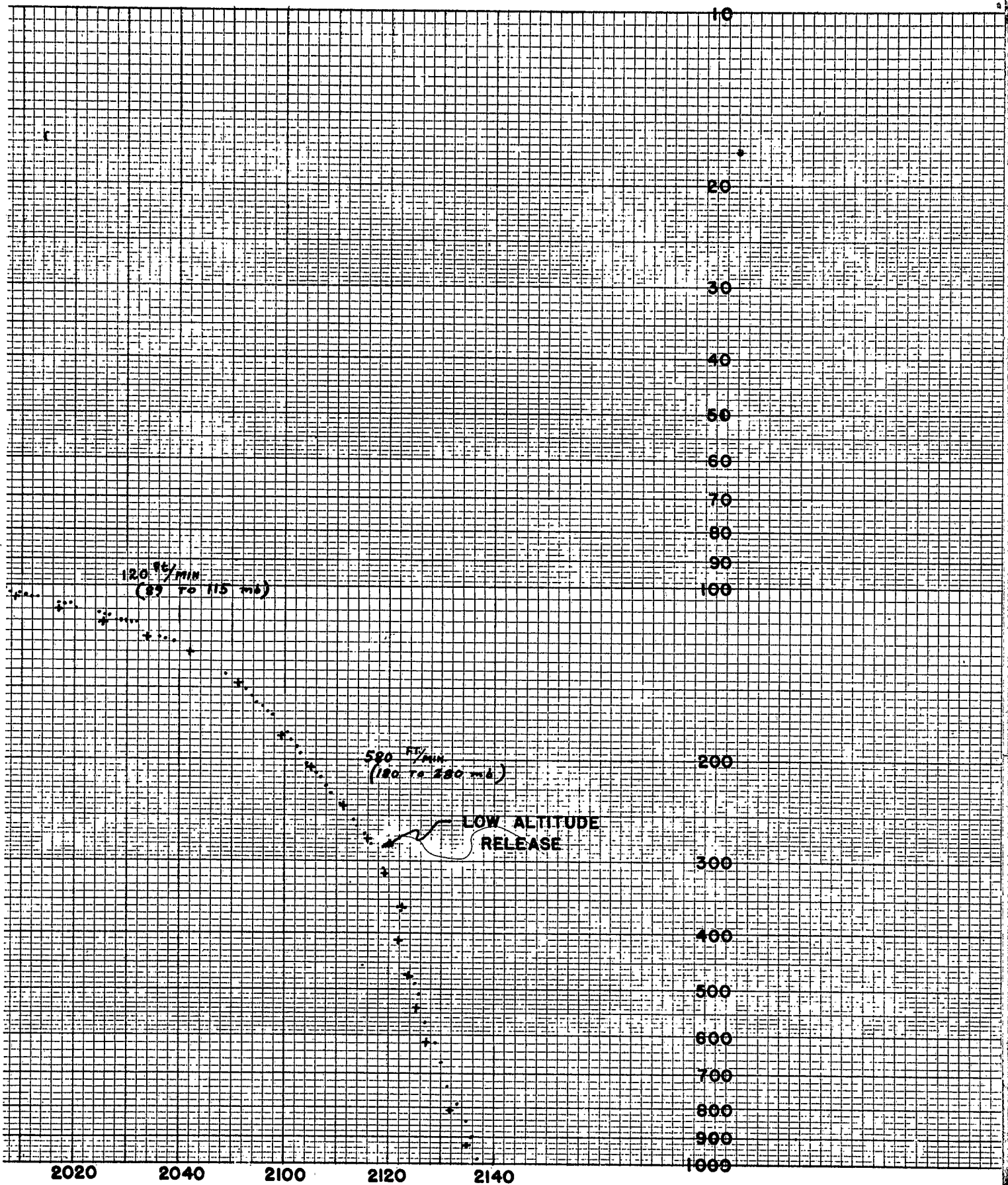
CONFIDENTIAL SECURITY INFORMATION

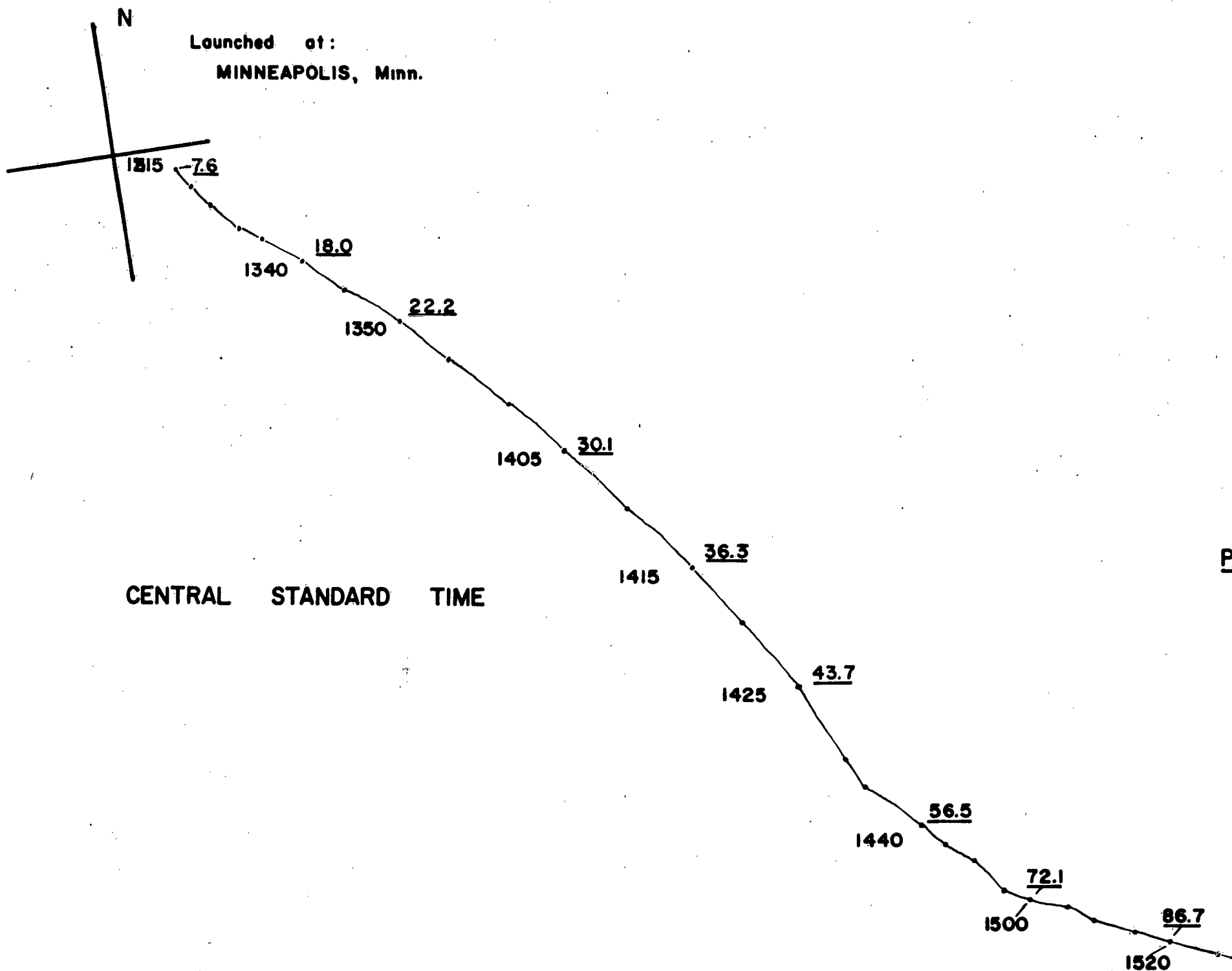












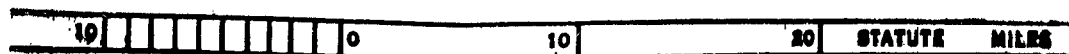
FLIGHT NO. 40

LAUNCHED 1300 CST

26 SEPTEMBER, 1952

1

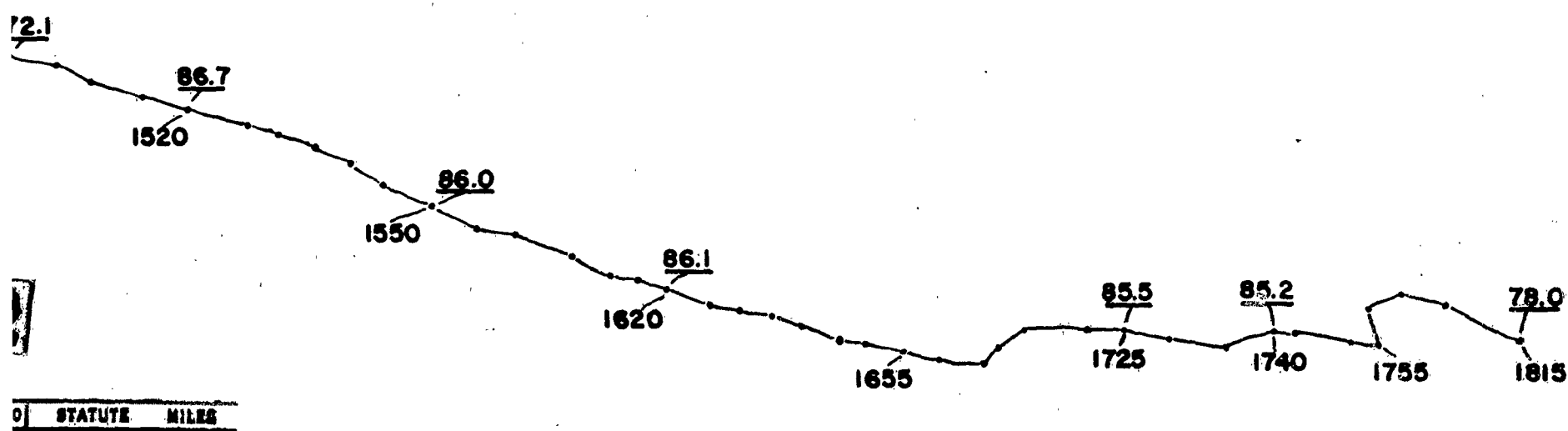
TRAJECTORY FROM THEODOLITE FIXES



CONFIDENTIAL
SECURITY
INFORMATION

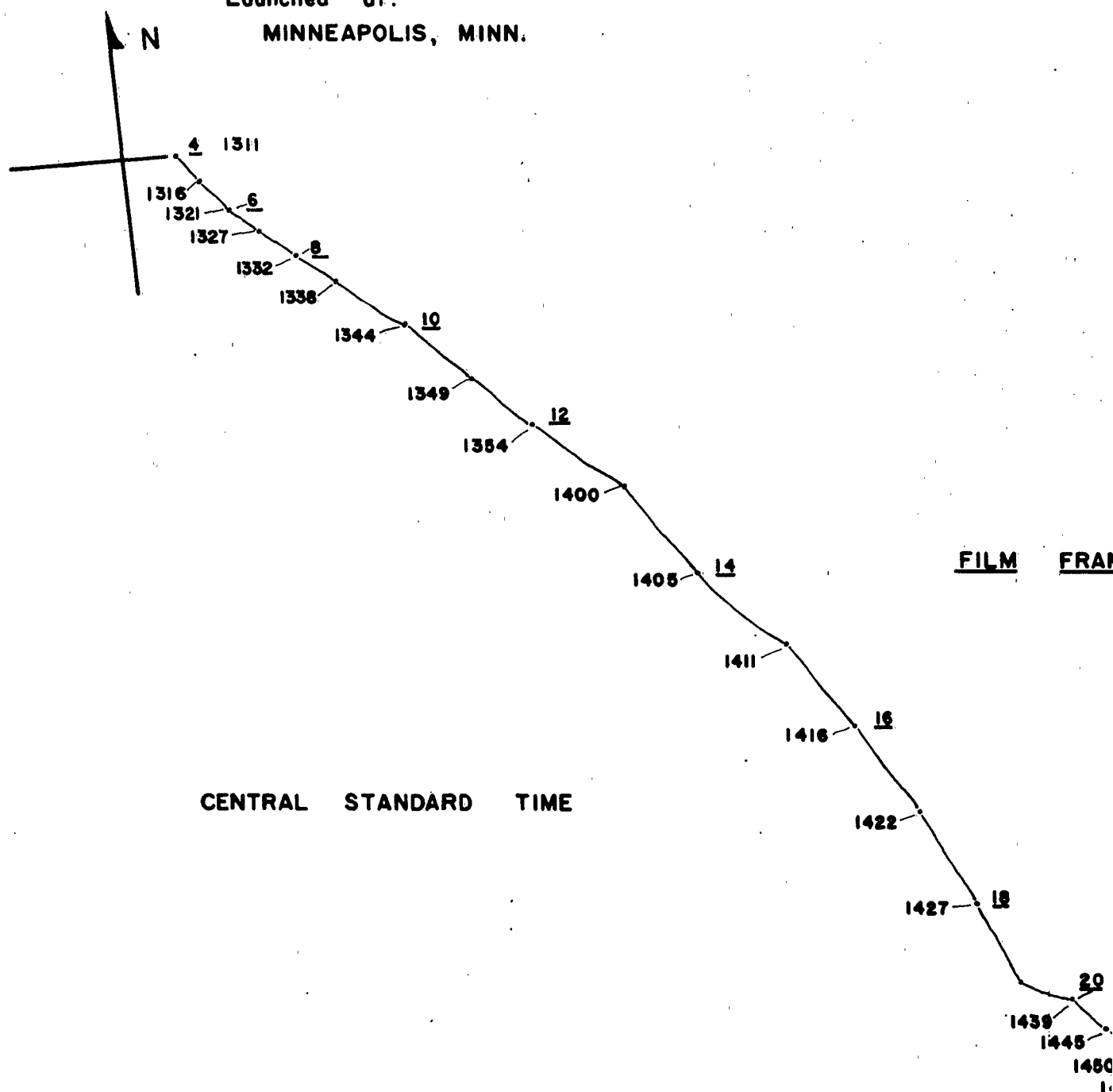
CONFIDENTIAL

PRESSURE ALTITUDE IN 1000 FEET



CONFIDENTIAL SECURITY INFORMATION

Launched at:
MINNEAPOLIS, MINN.



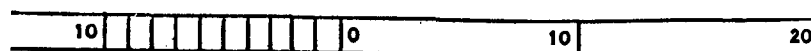
1

FLIGHT NO. 40

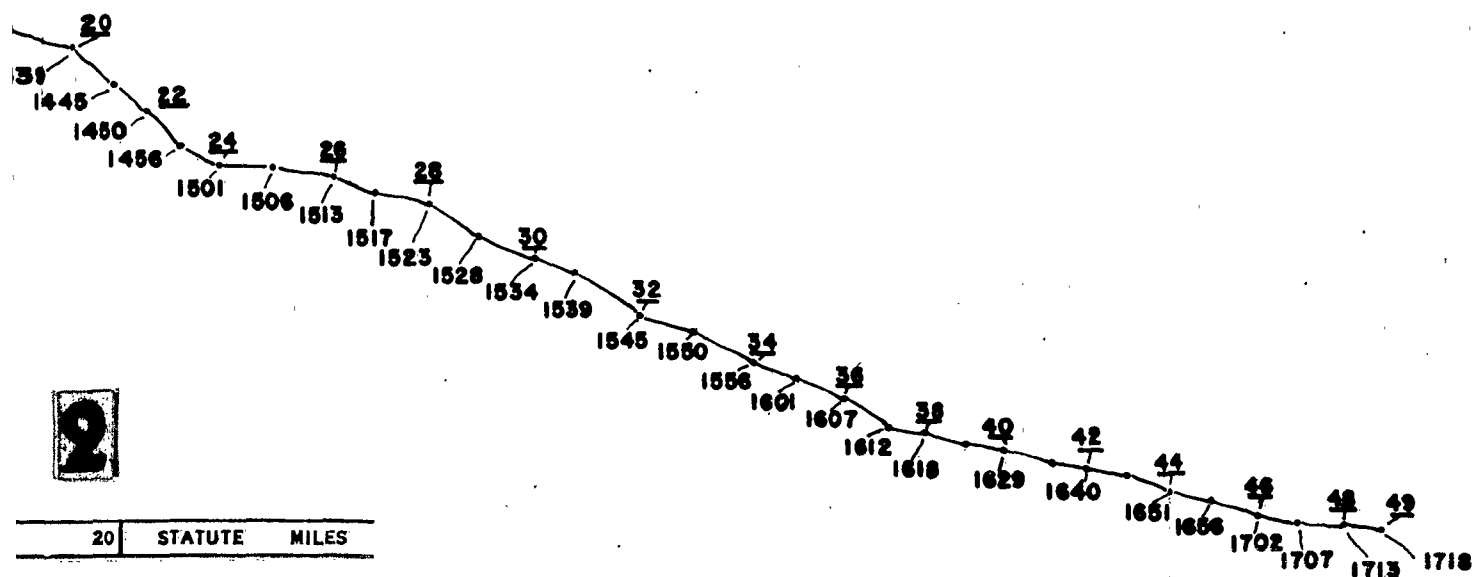
LAUNCHED 1300 CST

26 SEPTEMBER, 1952

TRAJECTORY FROM DOWN PICTURES



FRAME NUMBER



RASONDE DATA

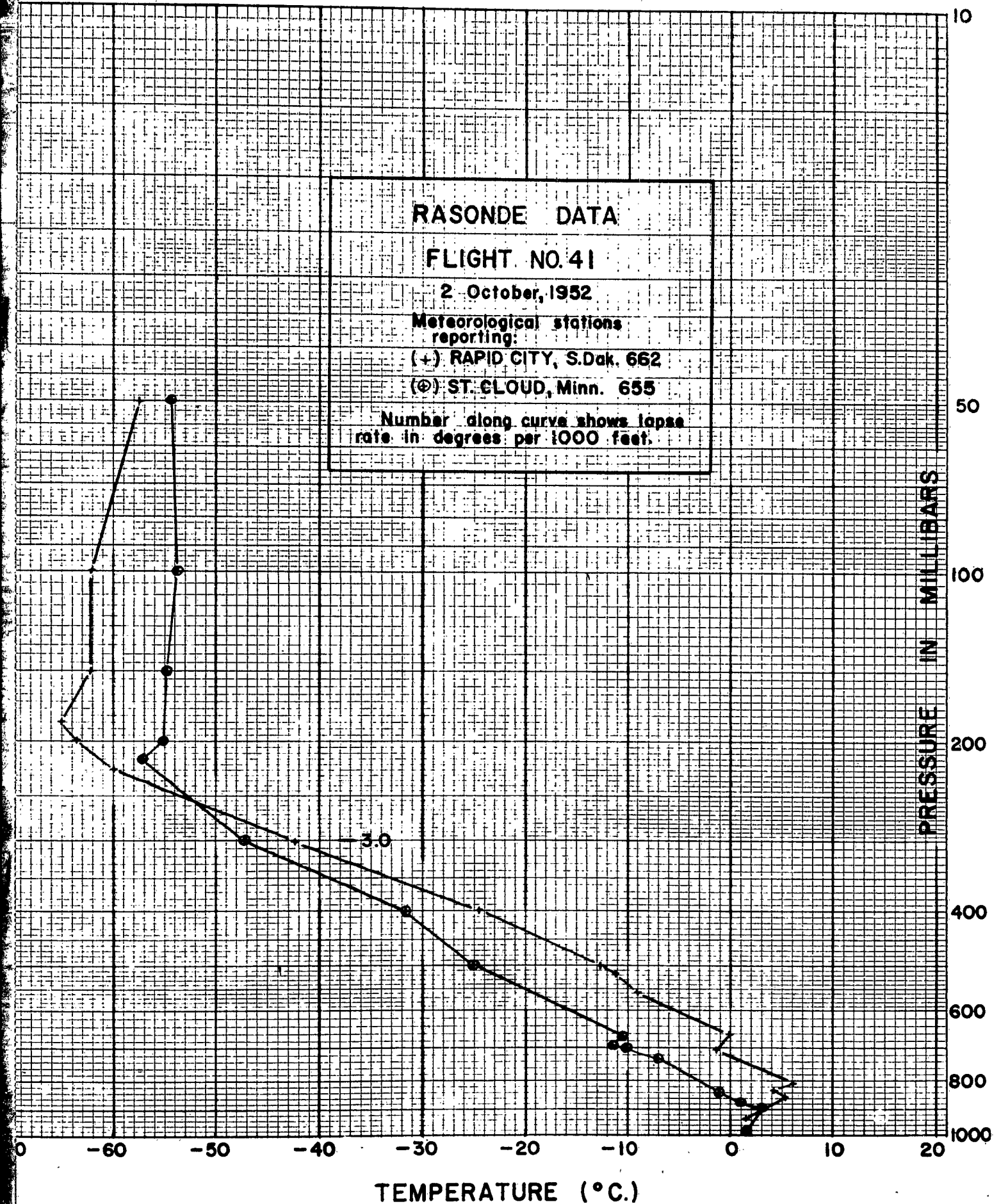
FLIGHT NO. 41

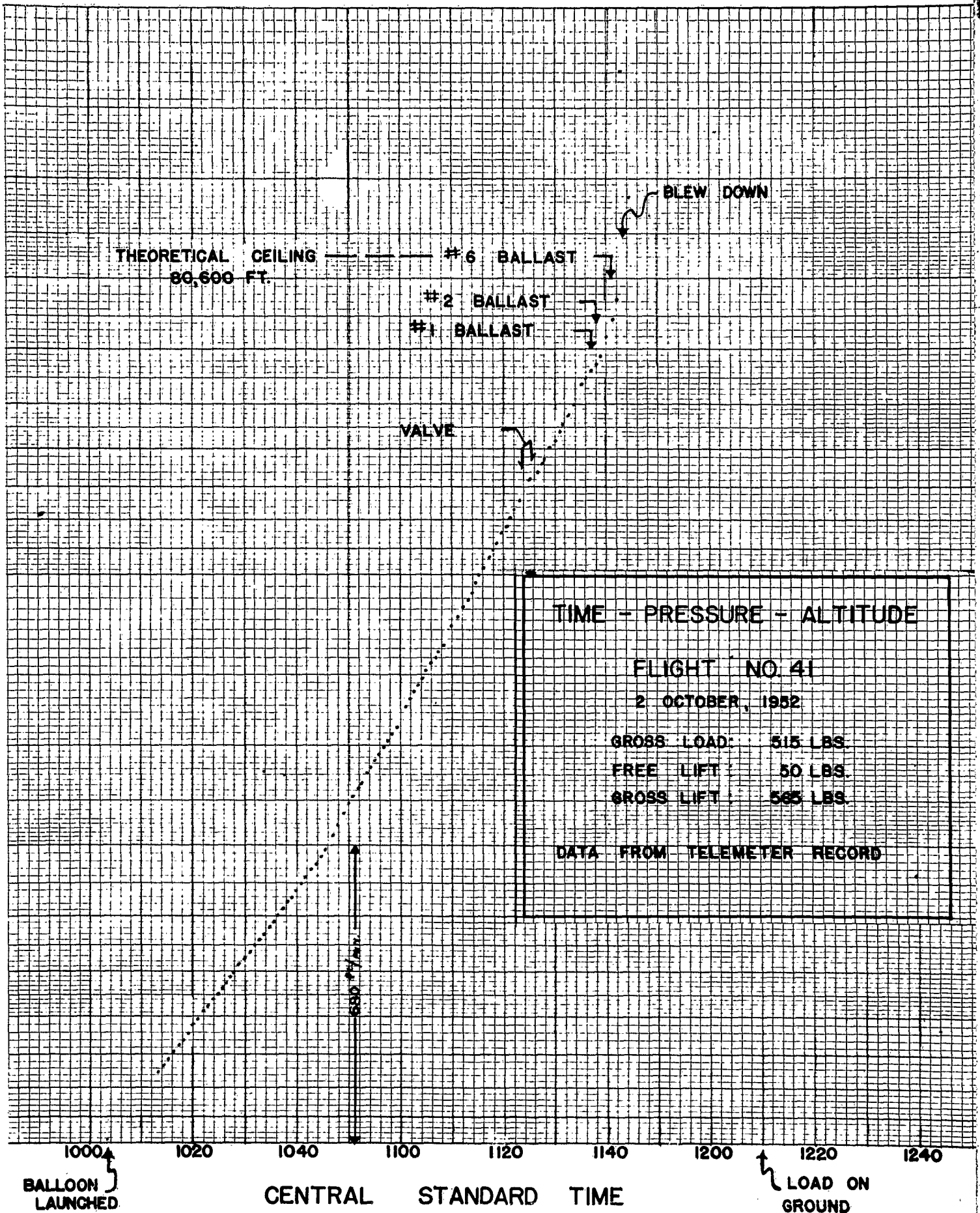
2 October, 1952

Meteorological stations
reporting:

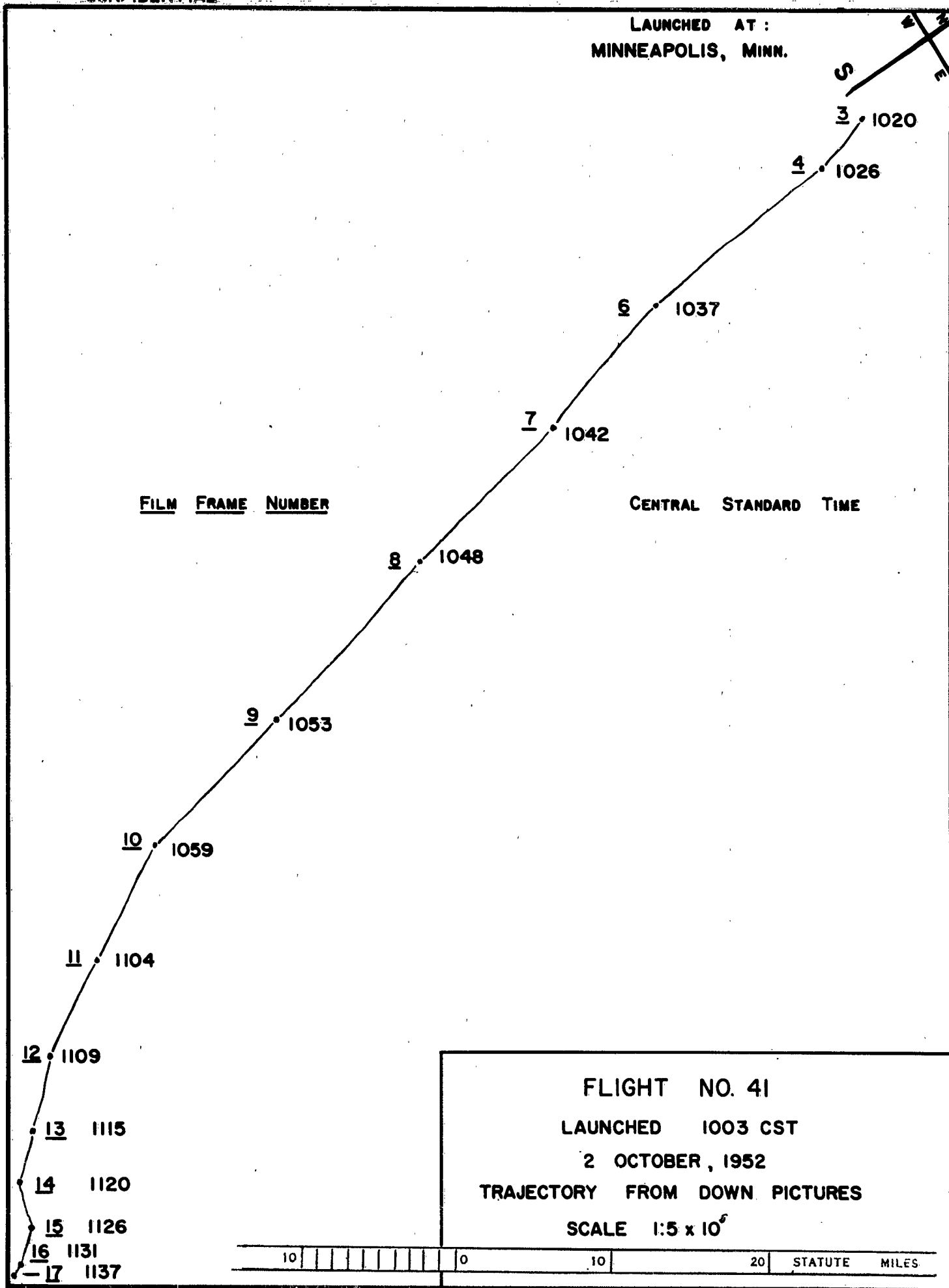
(+) RAPID CITY, S.Dak. 662

(@) ST. CLOUD, Minn. 655

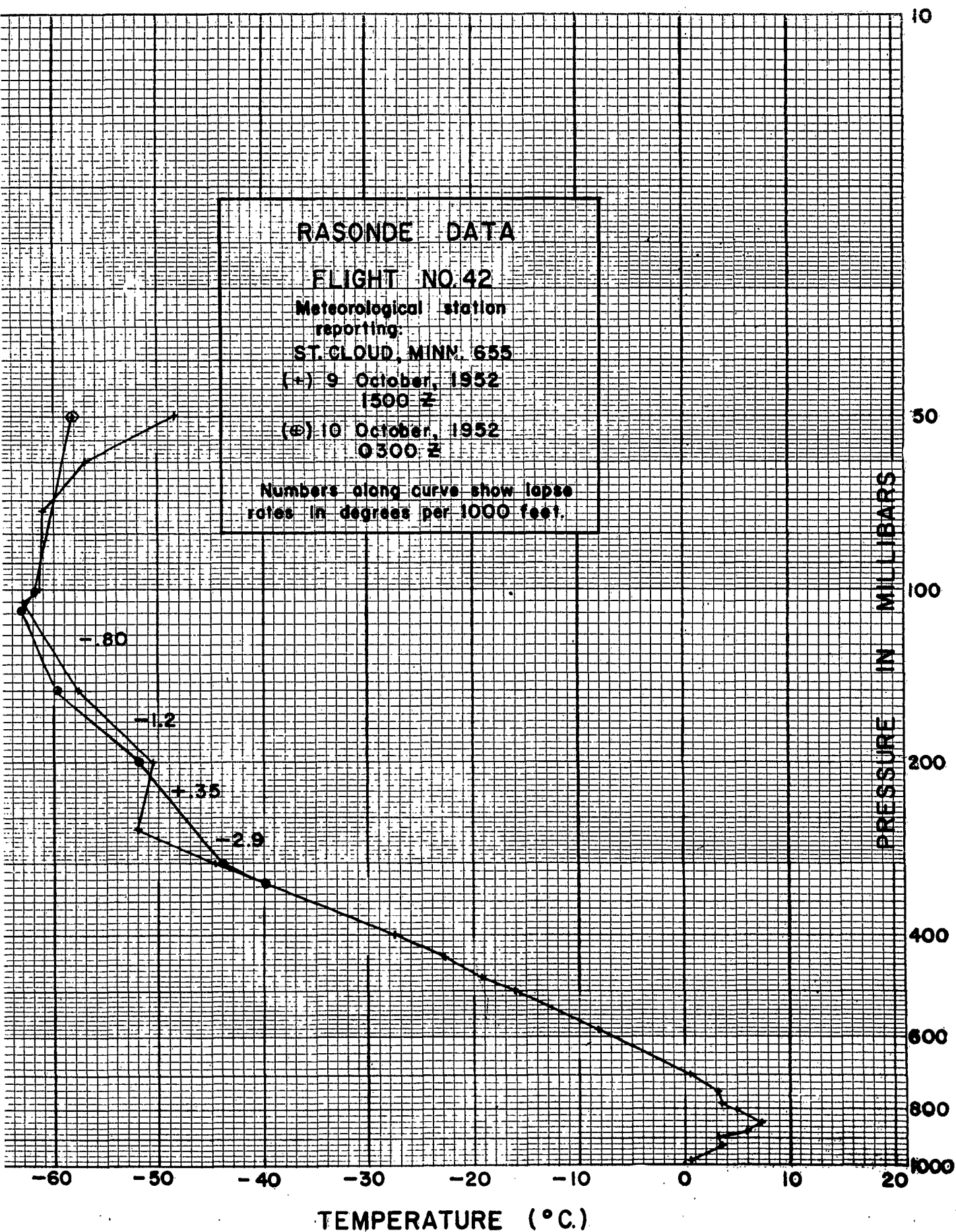
Number along curve shows lapse
rate in degrees per 1000 feet.

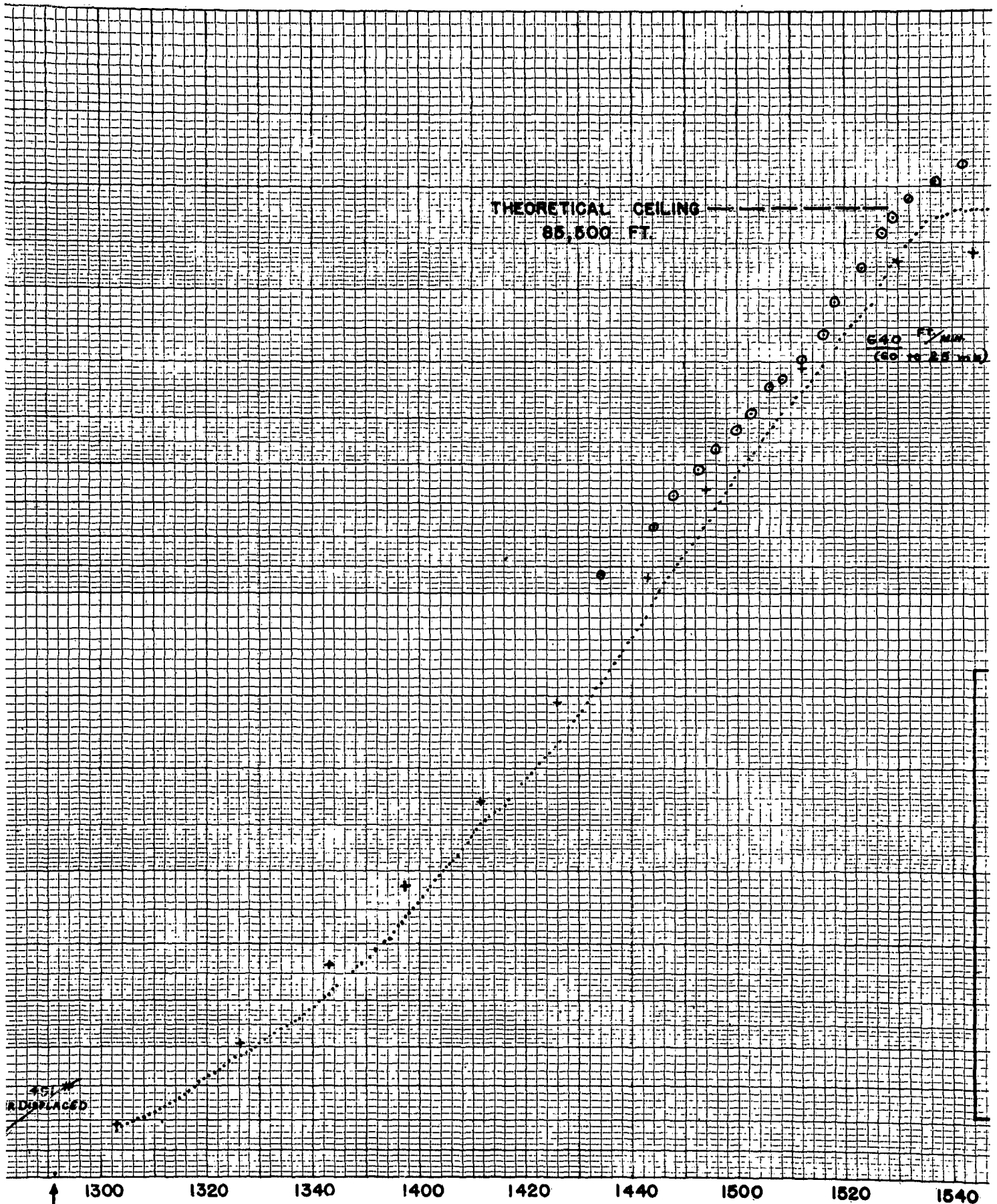


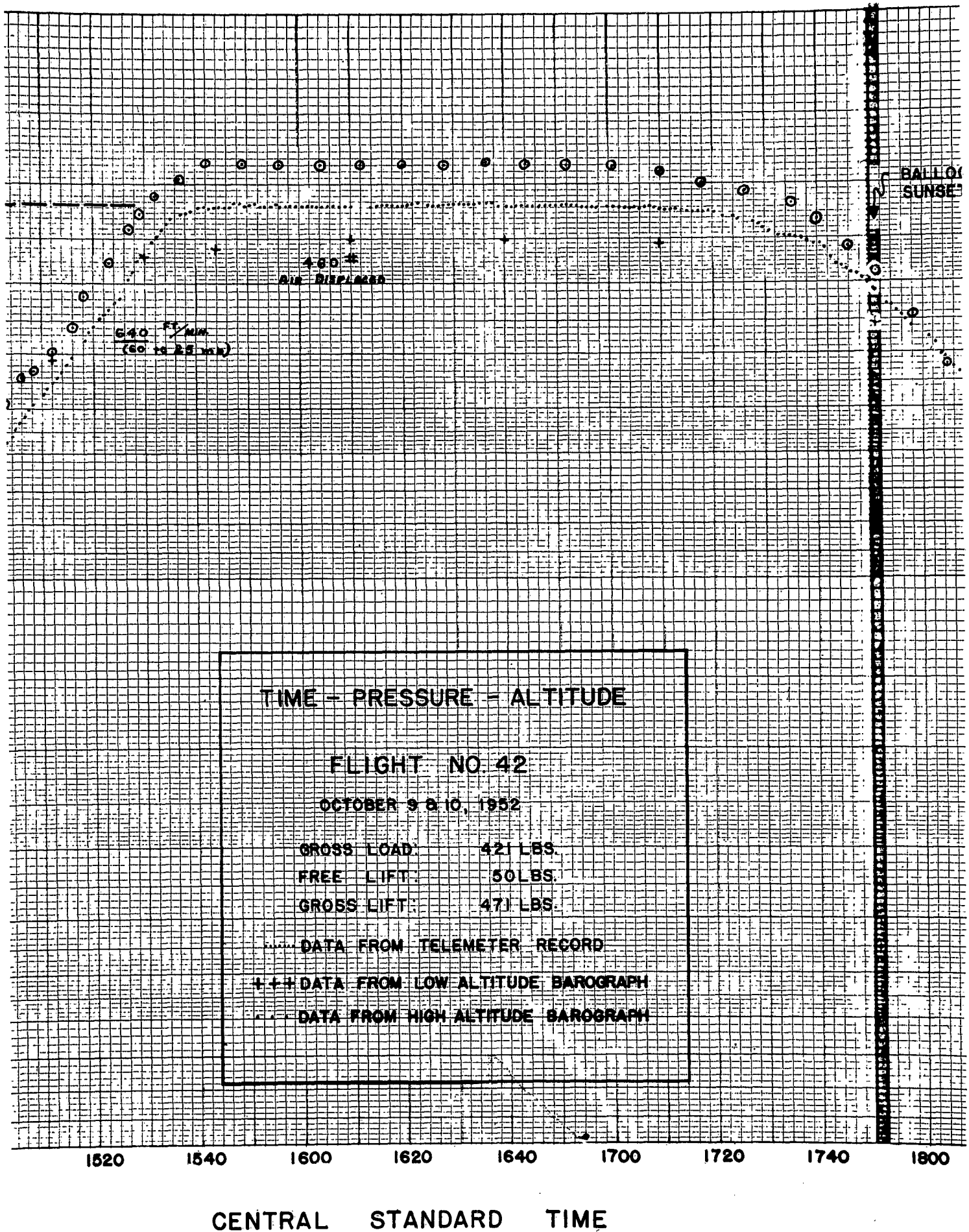
CONFIDENTIAL

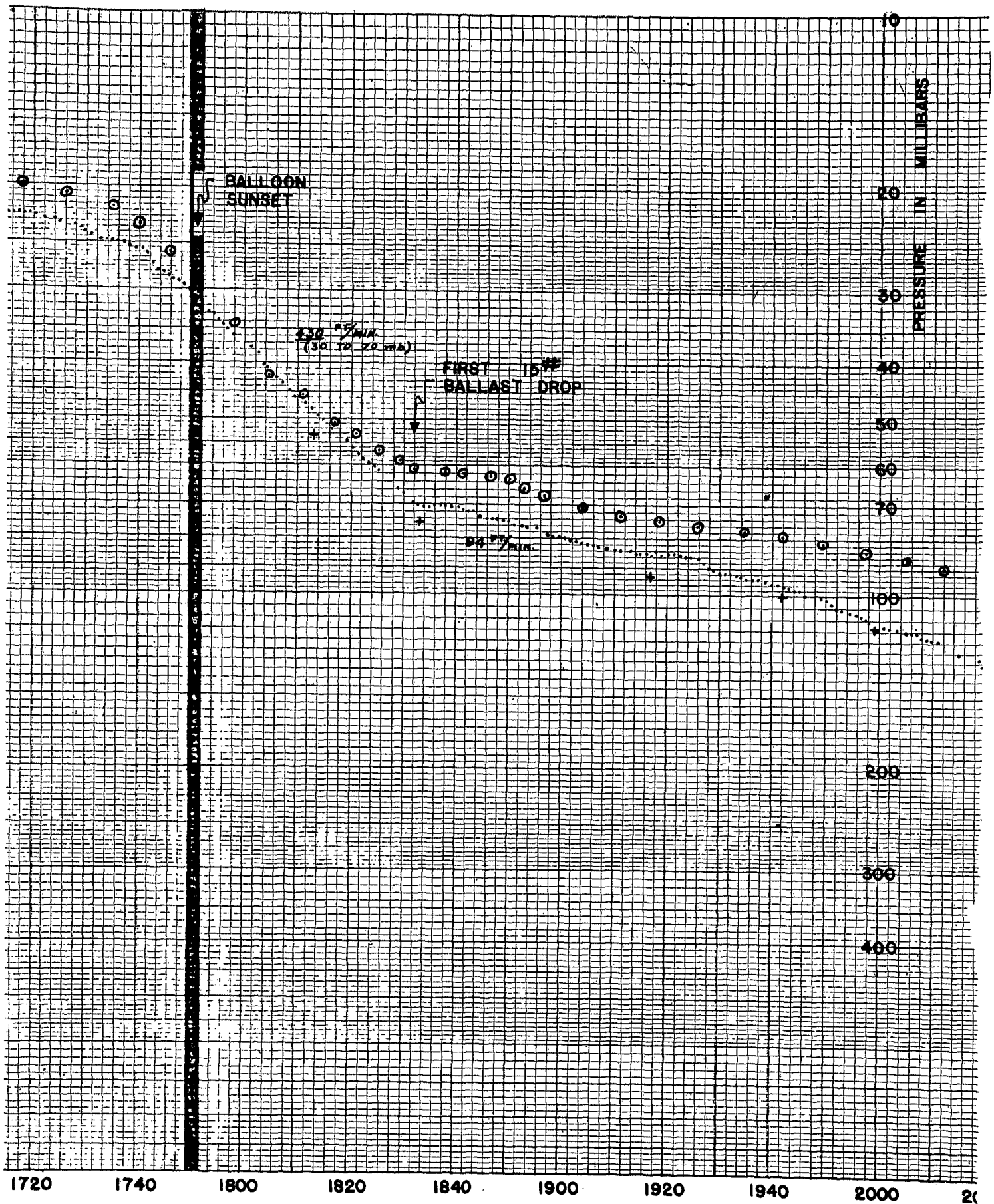
LAUNCHED AT:
MINNEAPOLIS, MINN.

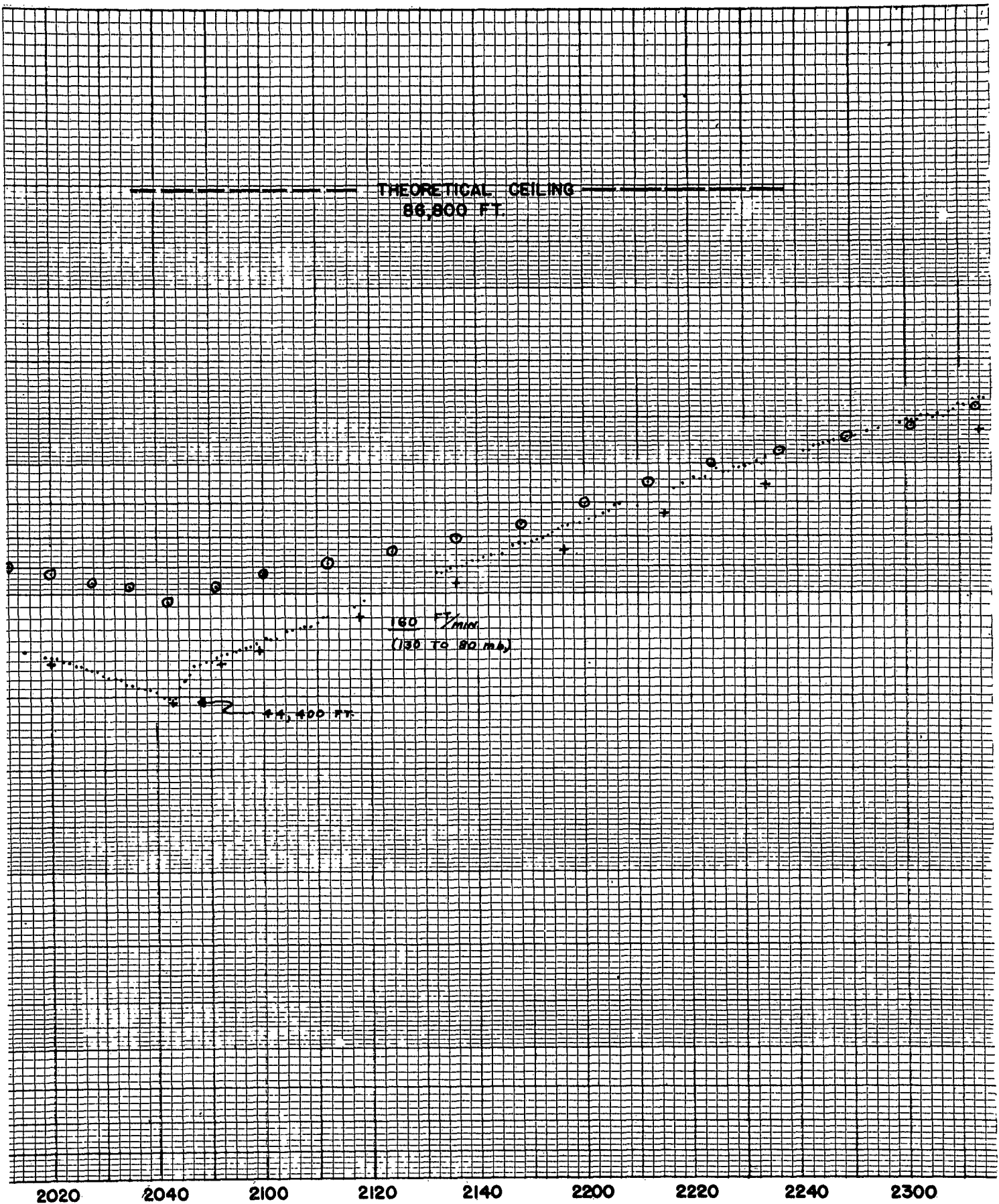
CONFIDENTIAL SECURITY INFORMATION

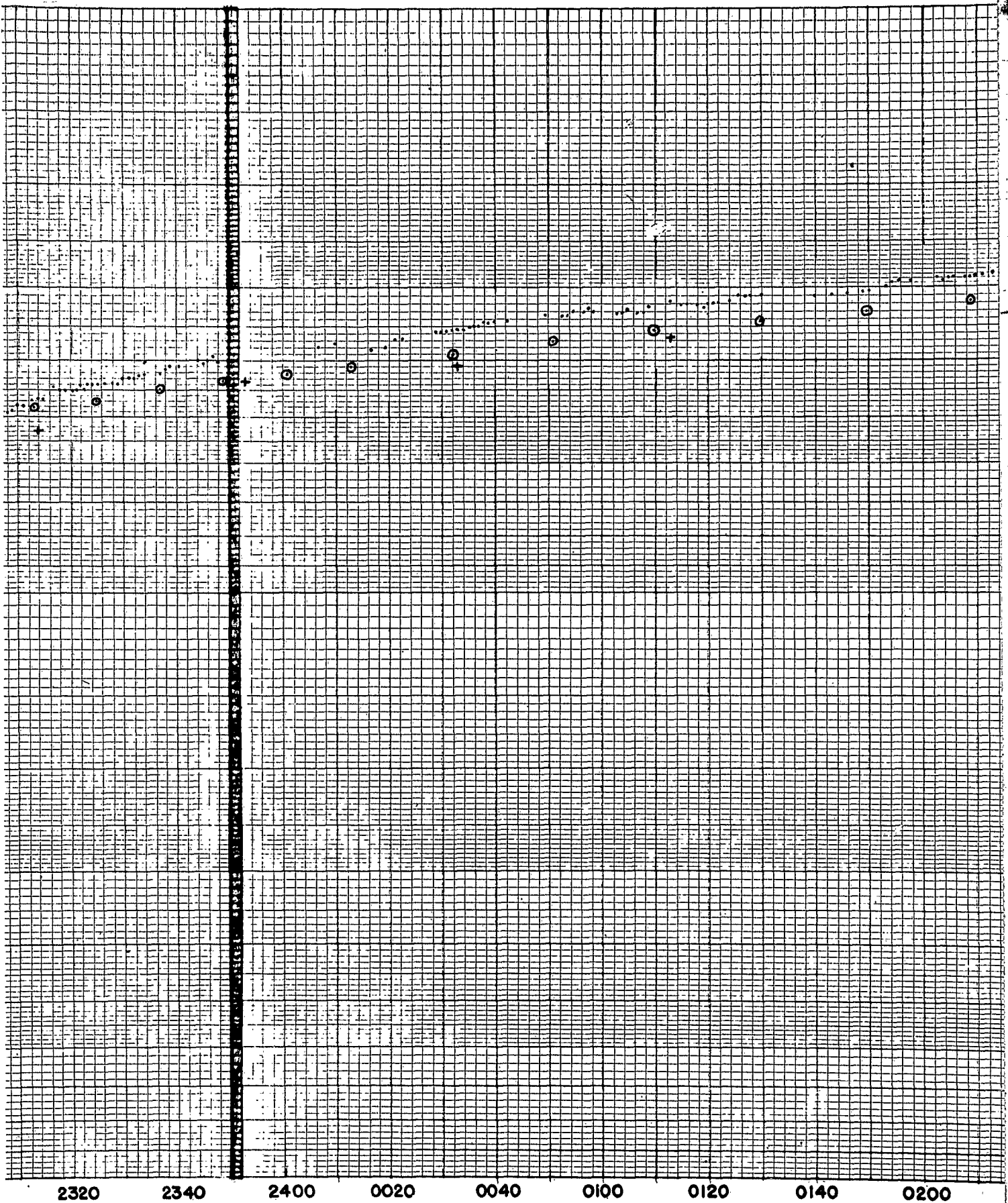




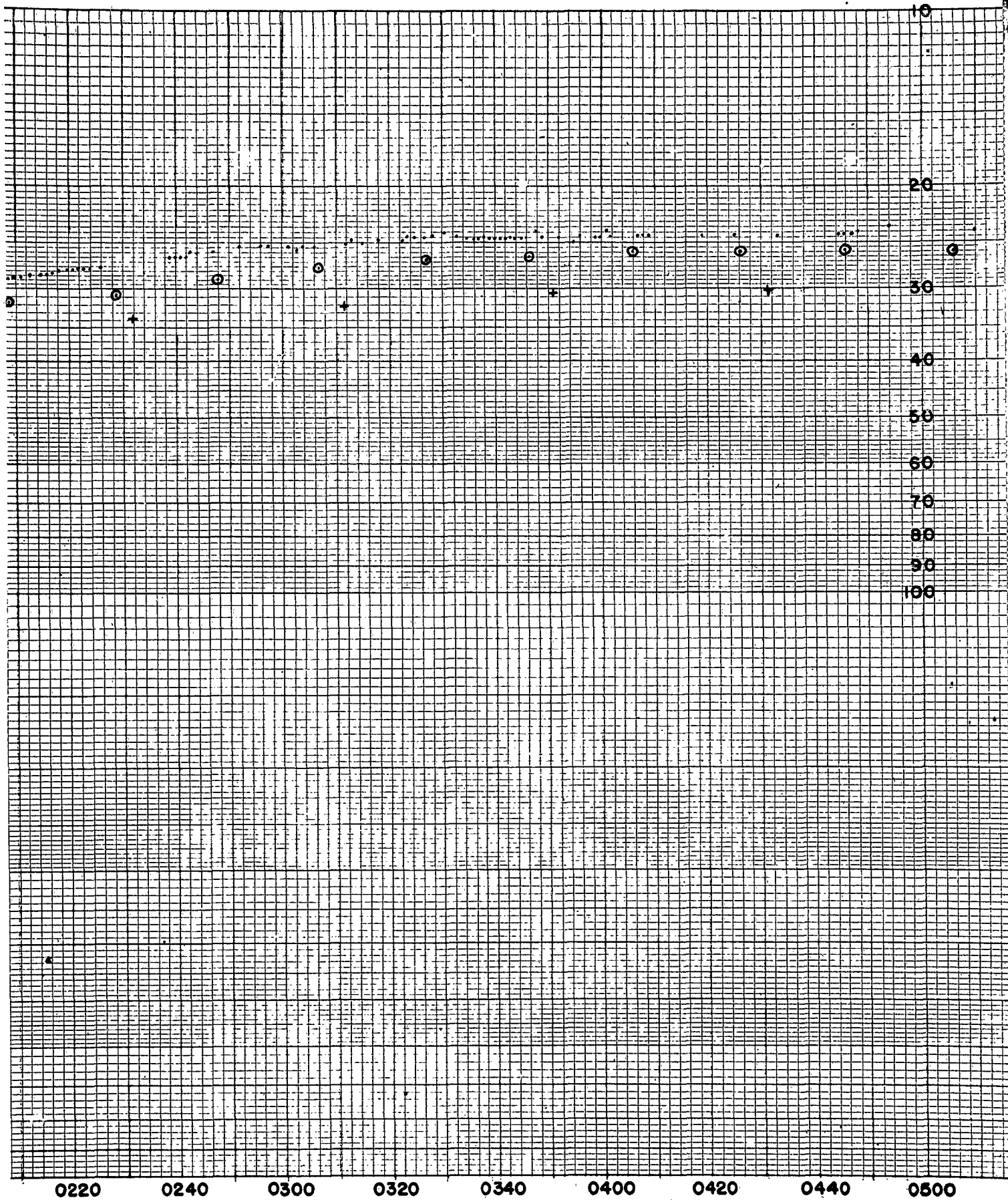


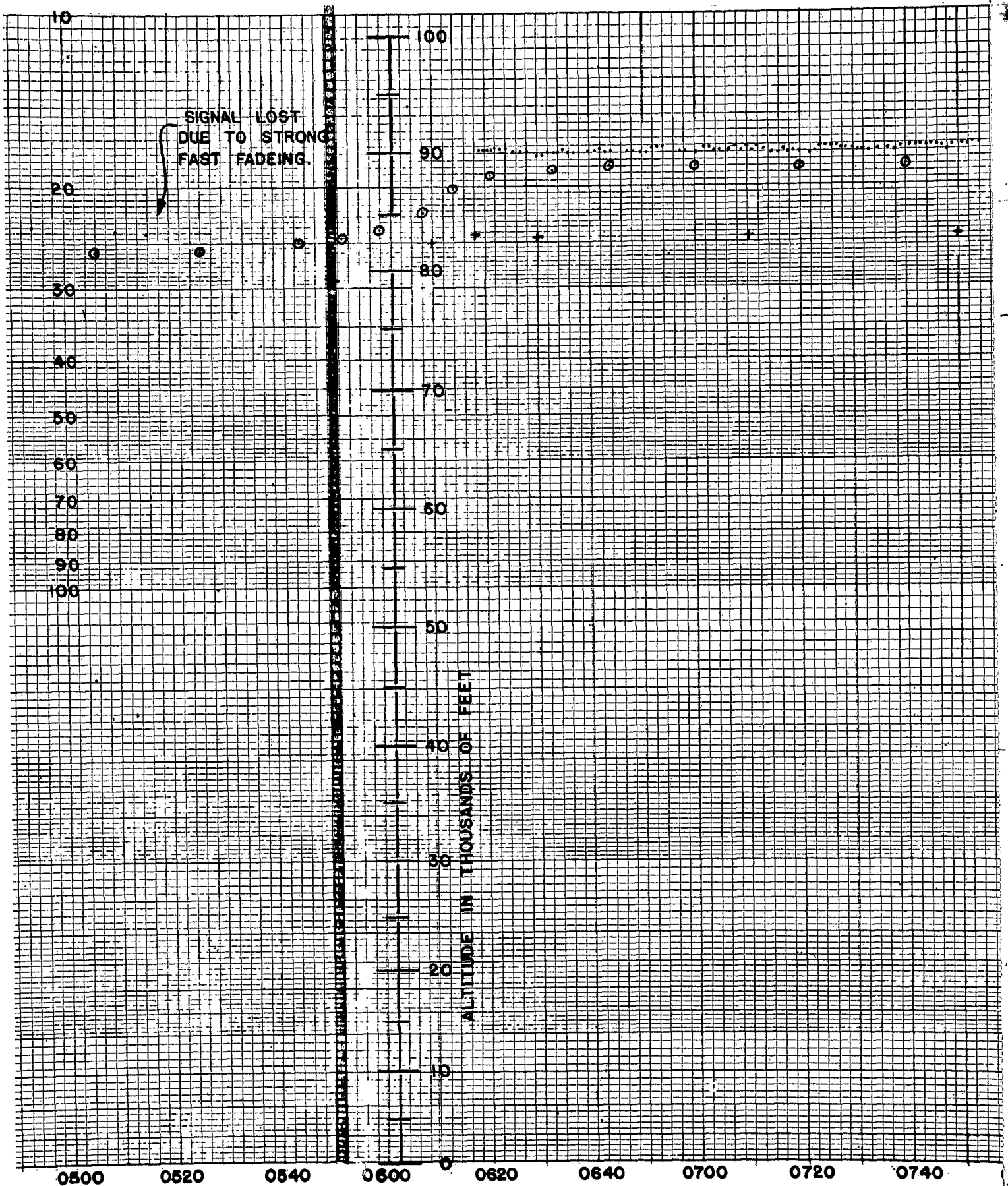


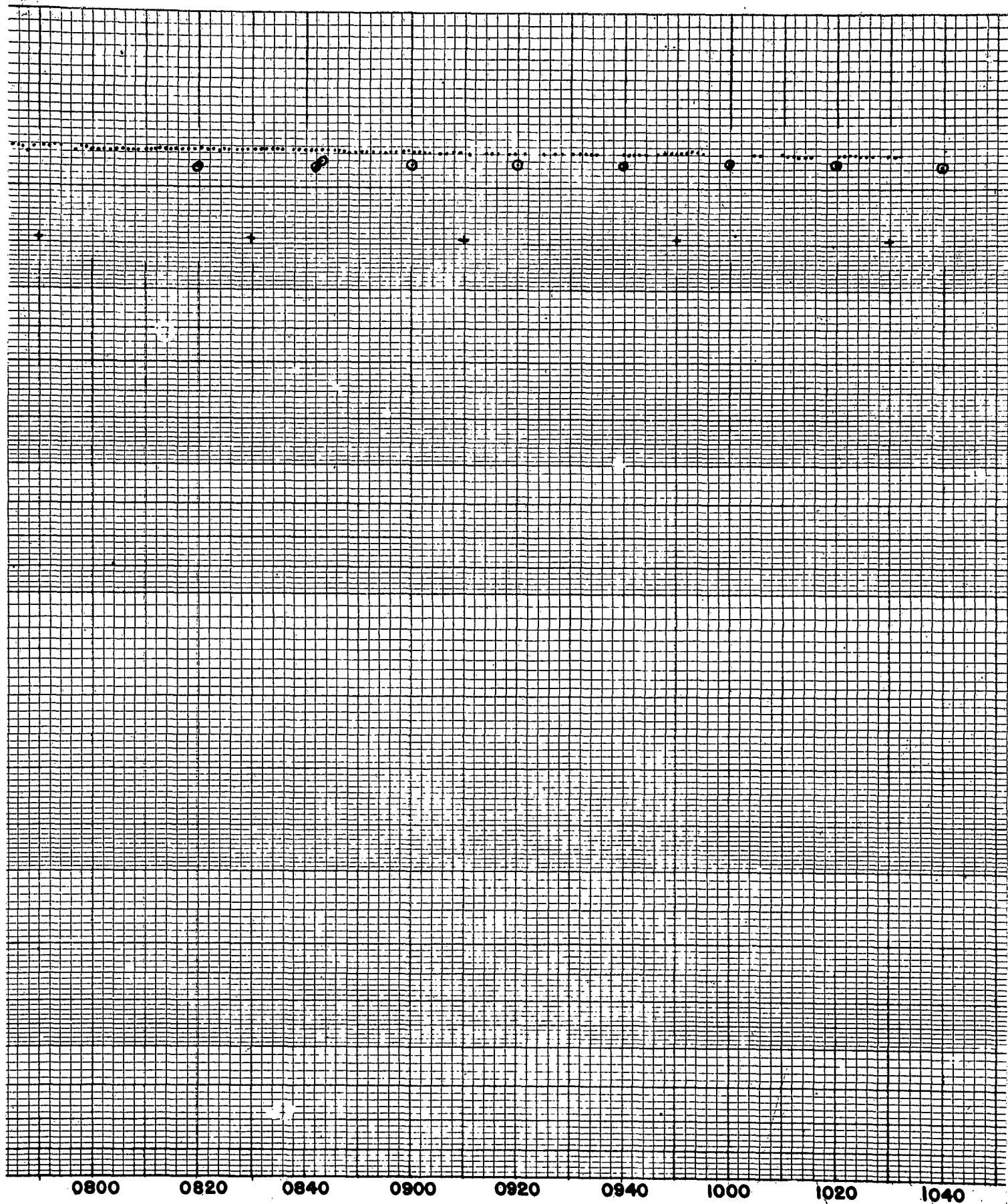


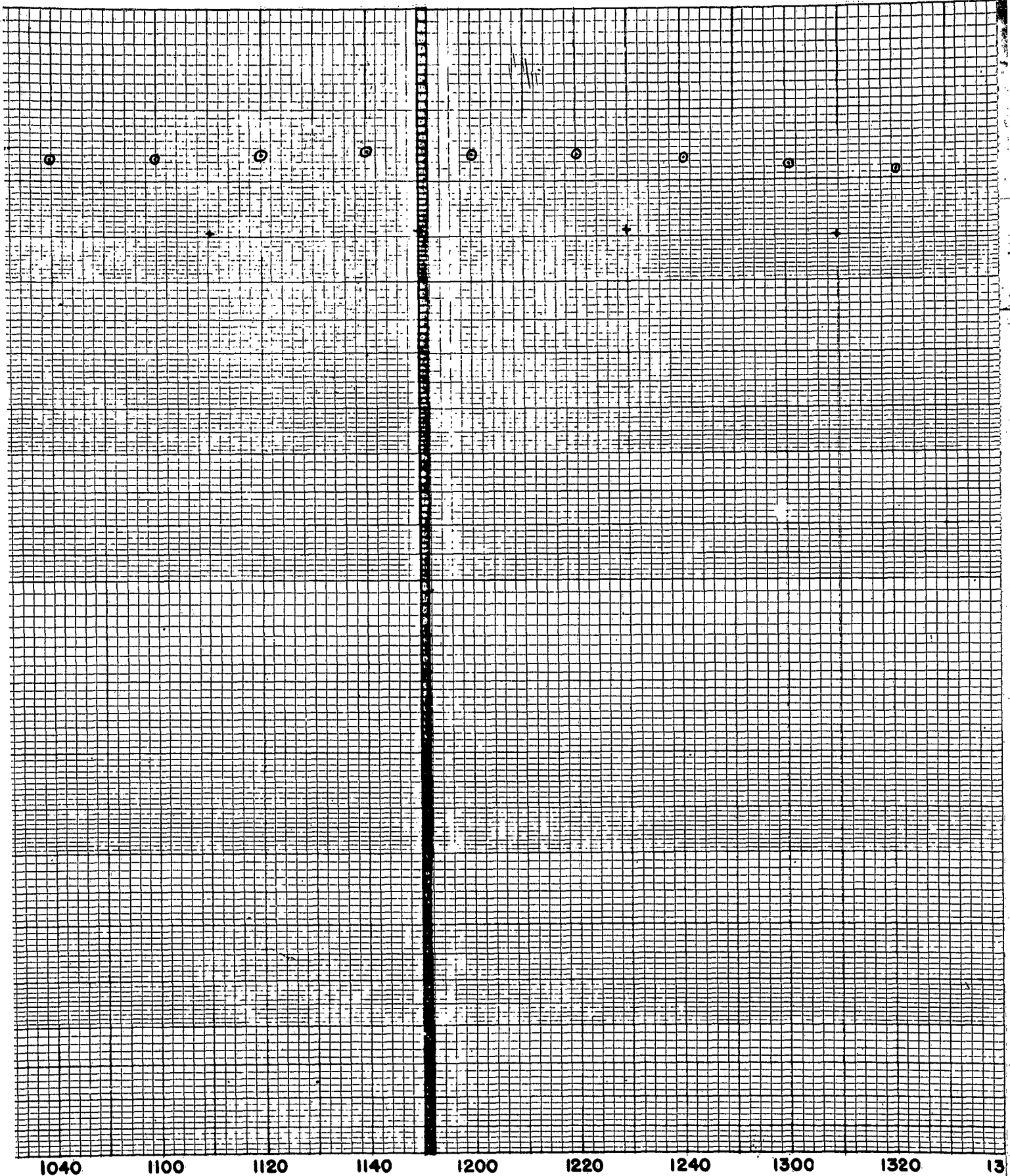


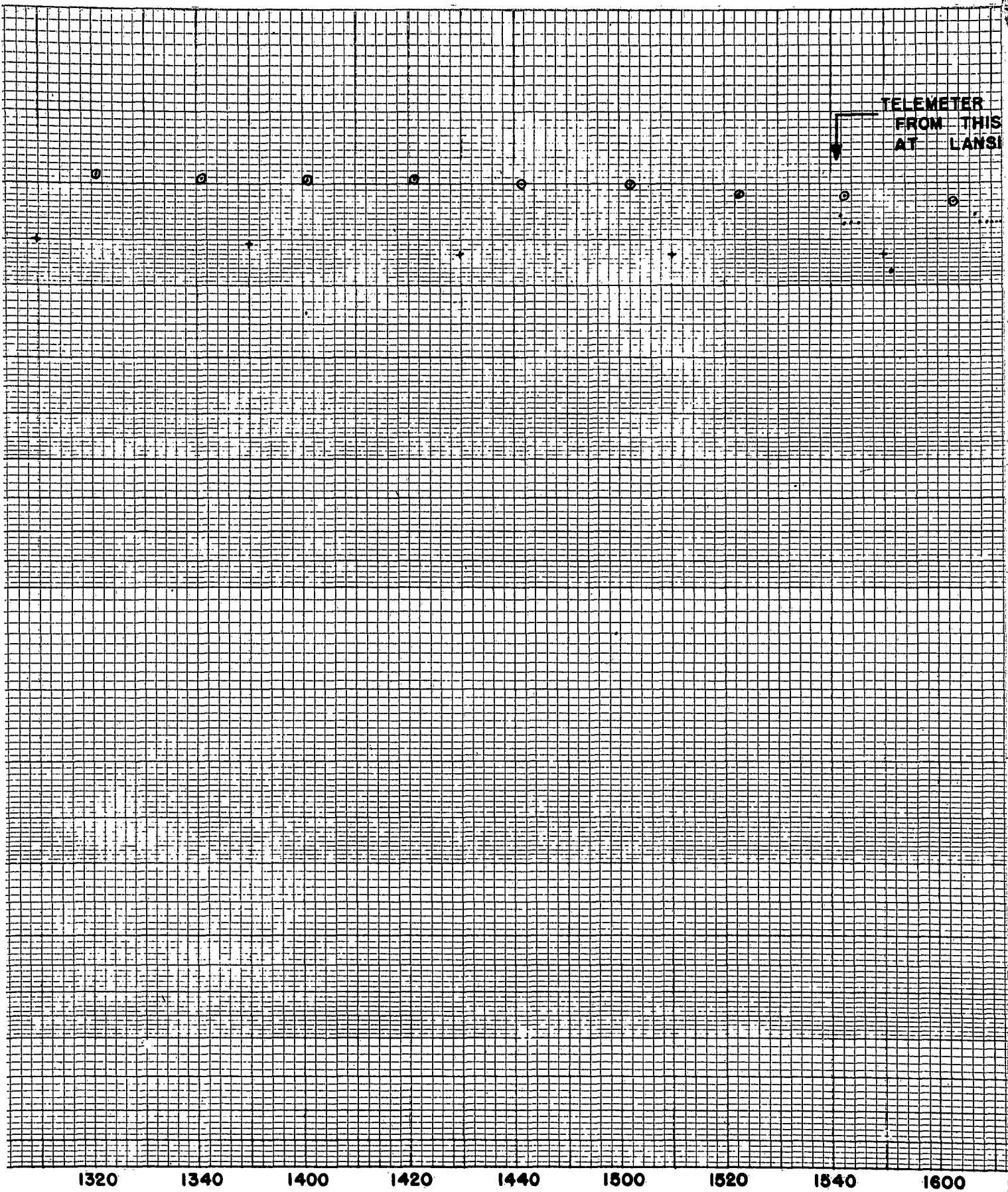
→ 10 OCTOBER











TELEMETER READINGS
FROM THIS POINT ON TAKEN
AT LANSING, MICHIGAN

372 FT/MIN.
(35 TO 50 mb)

1520

1540

1600

1620

1640

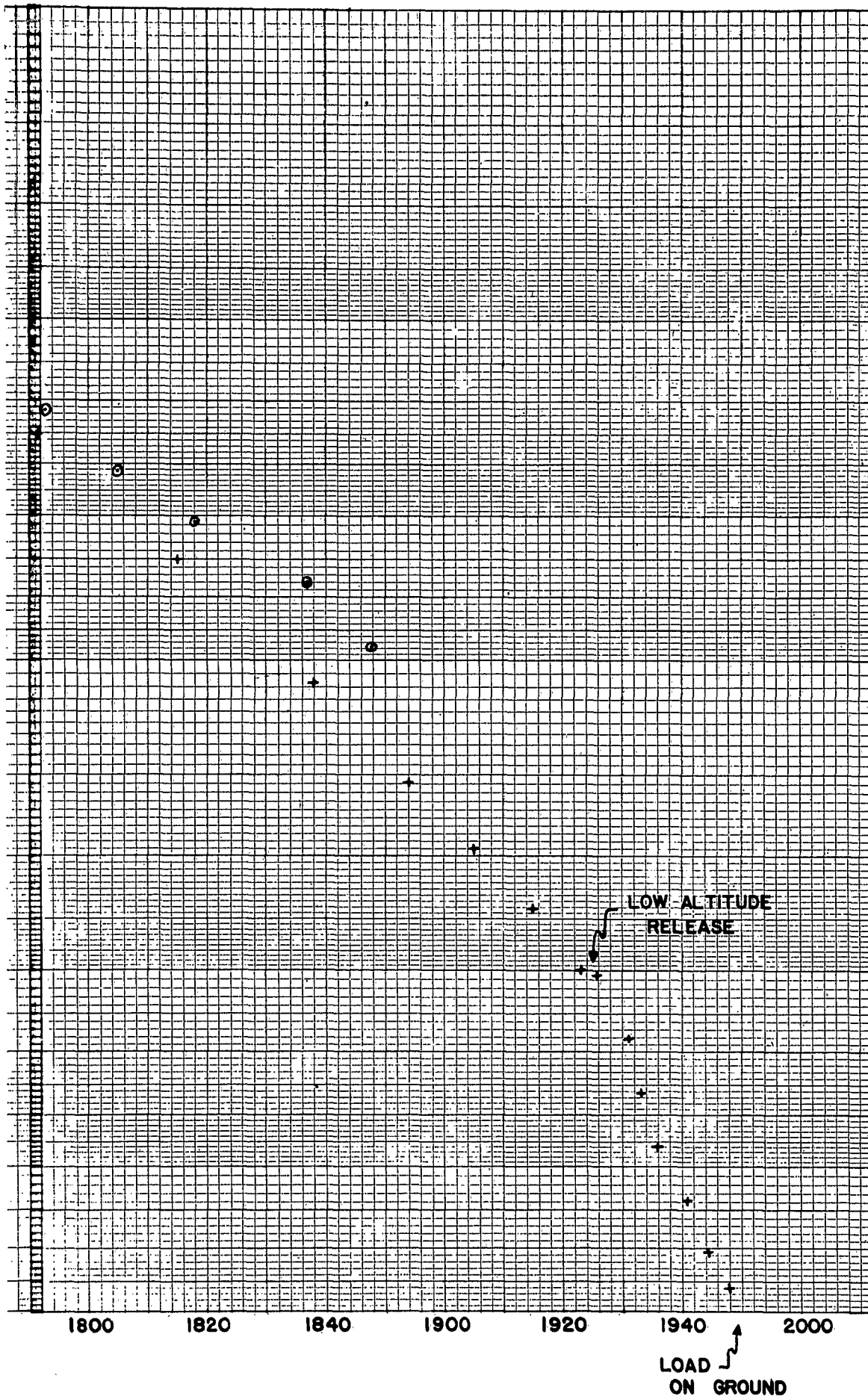
1700

1720

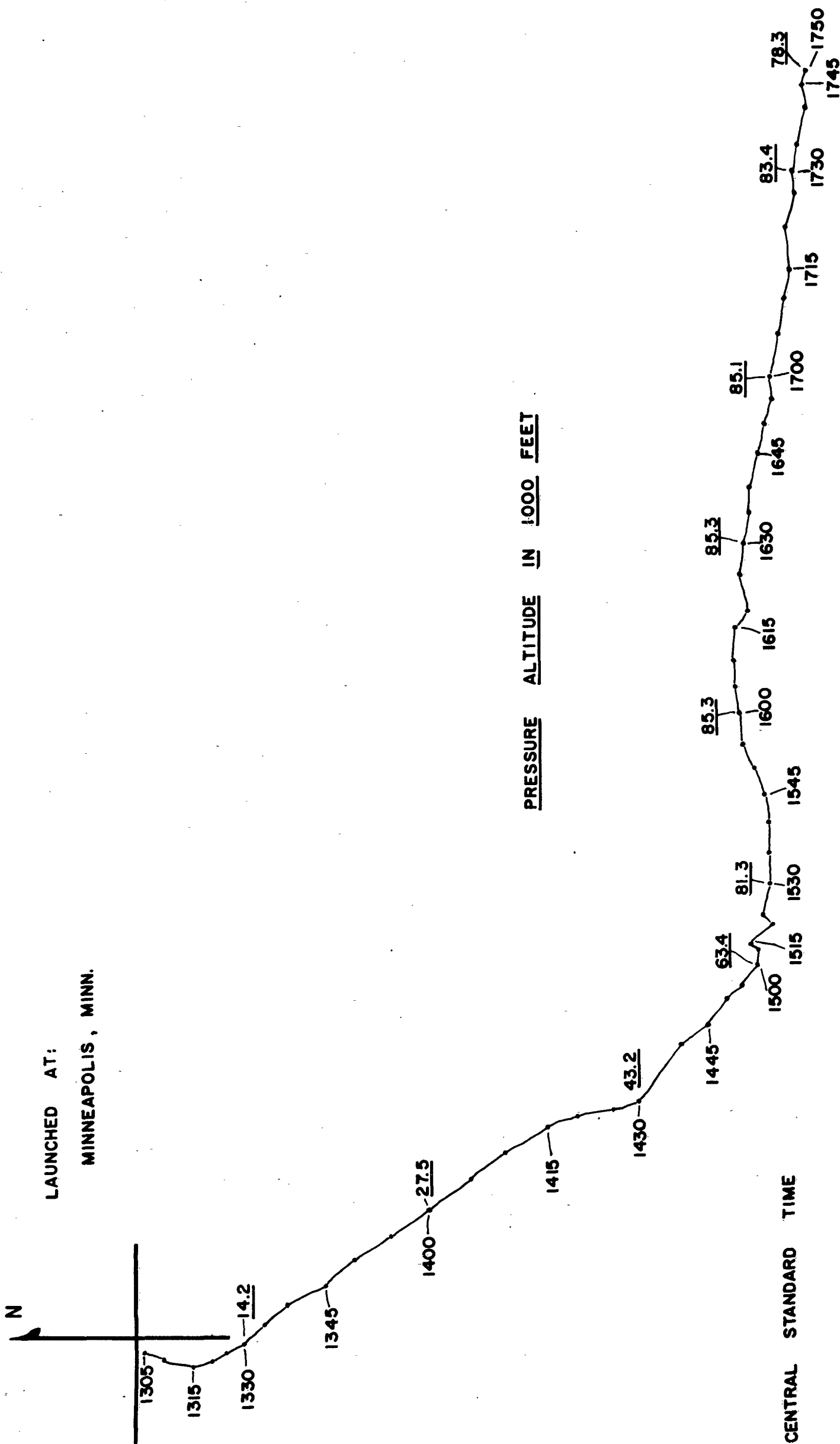
1740

1800

1820



CONFIDENTIAL

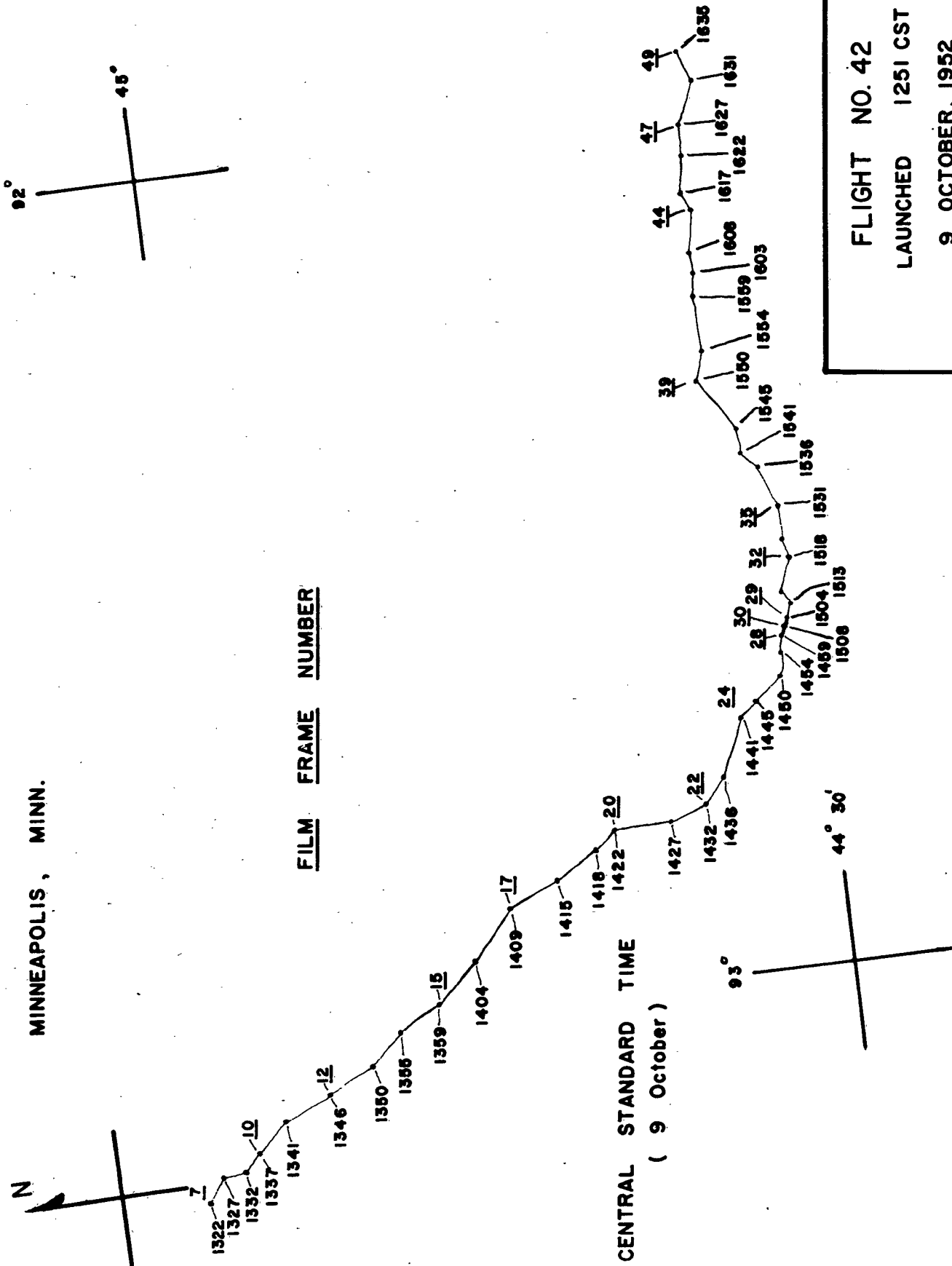


FLIGHT NO. 42
LAUNCHED 1251 CST
3 OCTOBER, 1953
TRAJECTORY FROM THEODOLITE FIXES



CONFIDENTIAL SECURITY INFORMATION

LAUNCHED AT:
MINNEAPOLIS, MINN.

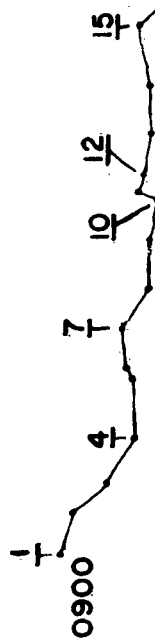


FLIGHT NO. 42
LAUNCHED 1251 CST
9 OCTOBER, 1952
TRAJECTORY FROM DOWN PICTURES

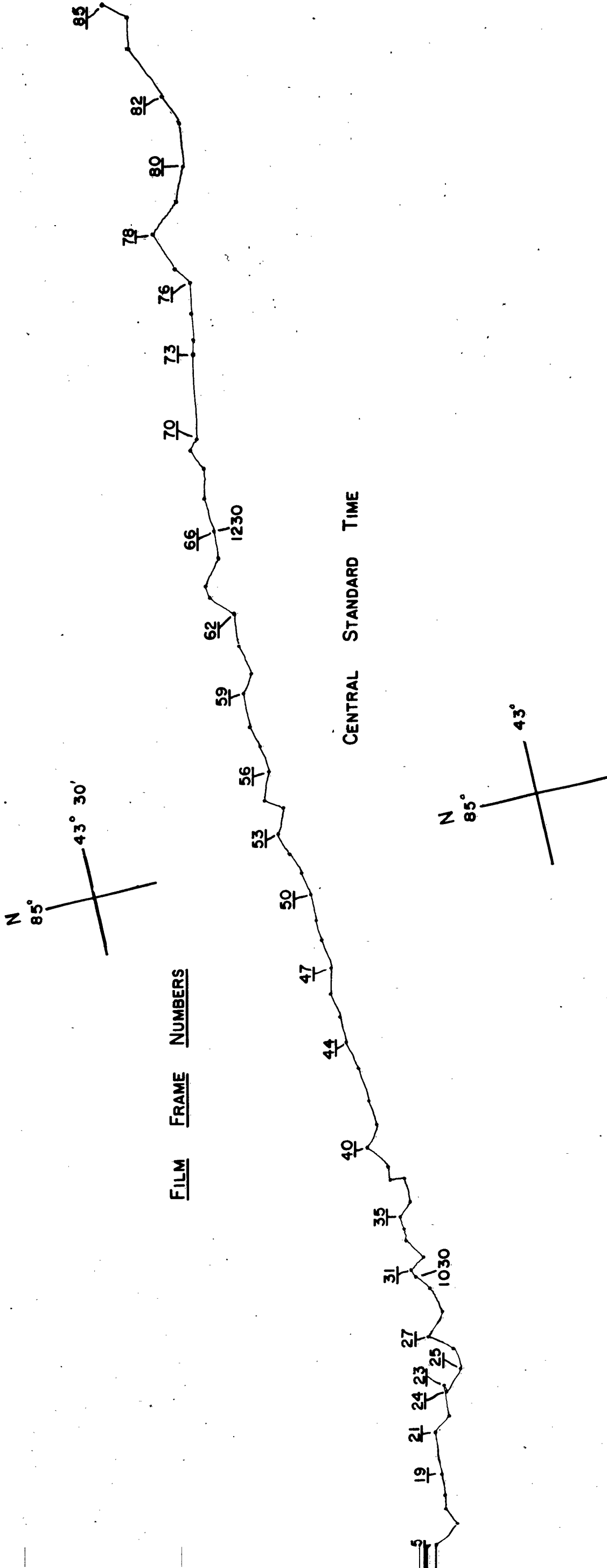


(flt. 42 trajectory cont'd on next page)

TRAJECTORY OF
10 OCTOBER



(CONT'D FROM PREVIOUS PAGE)



FLIGHT NO. 42

10 OCTOBER, 1952

TRACTORY FROM DOWN PICTURES
TAKEN DURING SECOND DAY
OF FLIGHT.



RASONDE DATA

FLIGHT NO.43

Meteorological station
reporting:

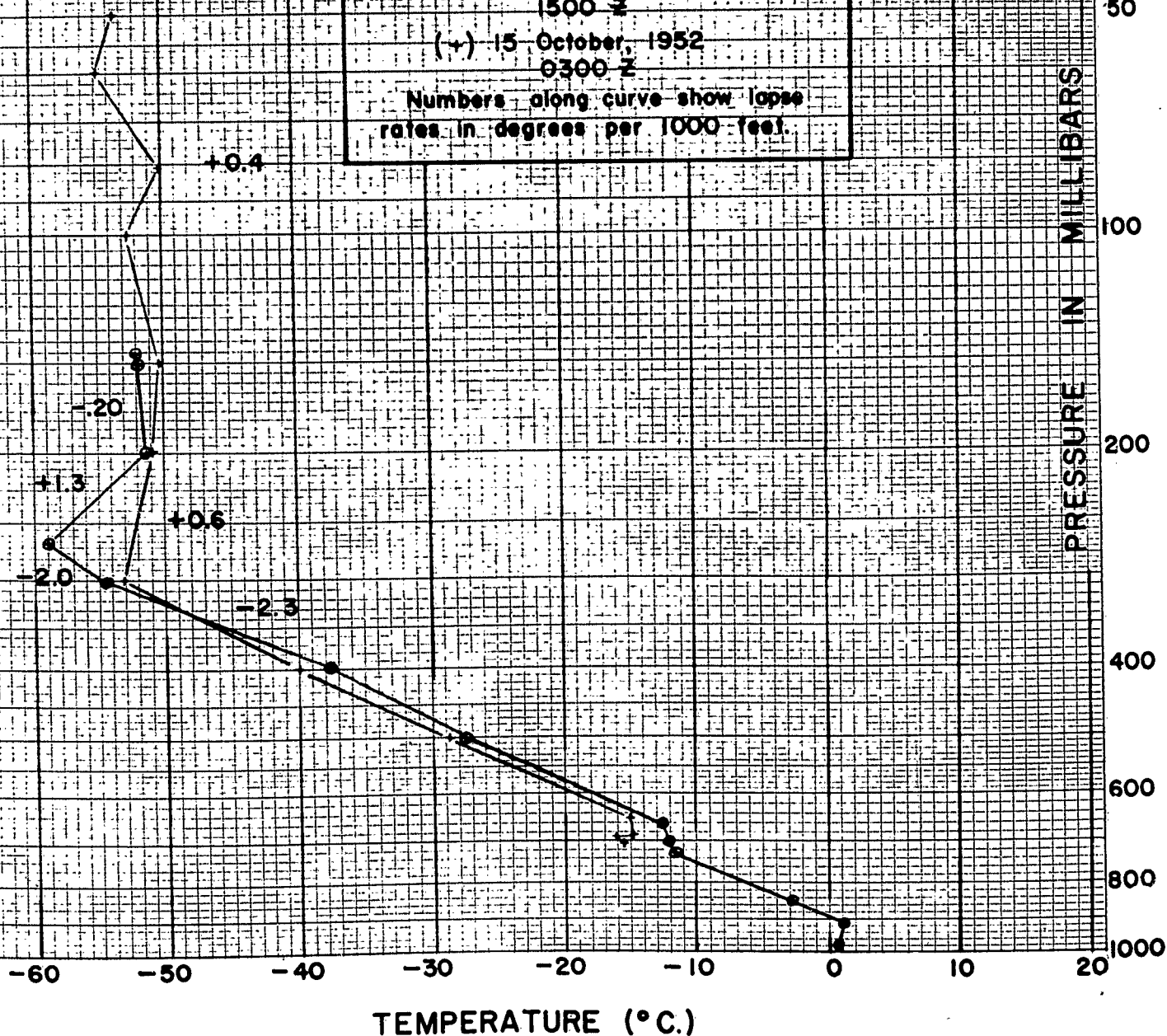
ST. CLOUD, MINN. 655

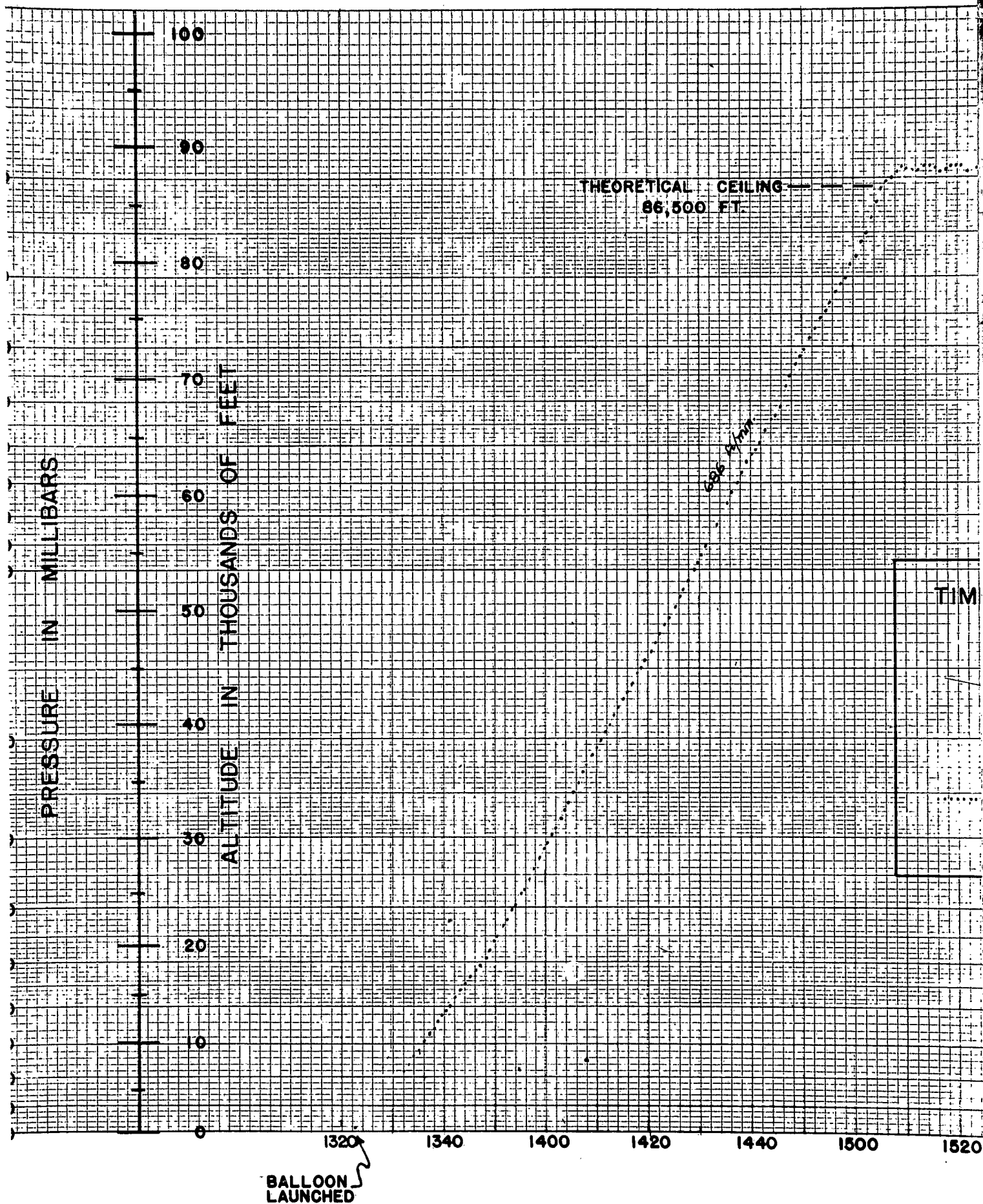
(-) 14 October, 1952

1500 Z

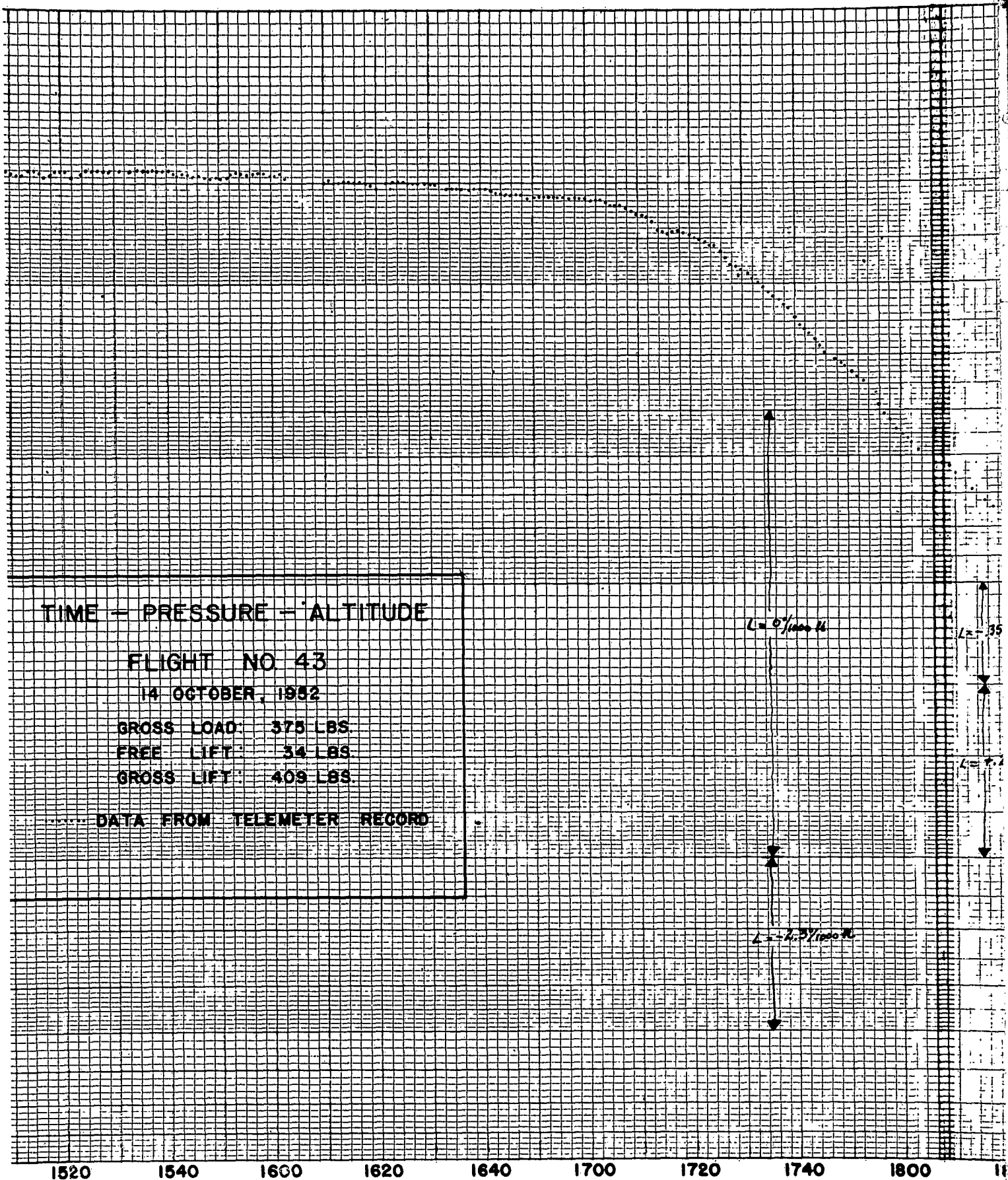
(+) 15 October, 1952

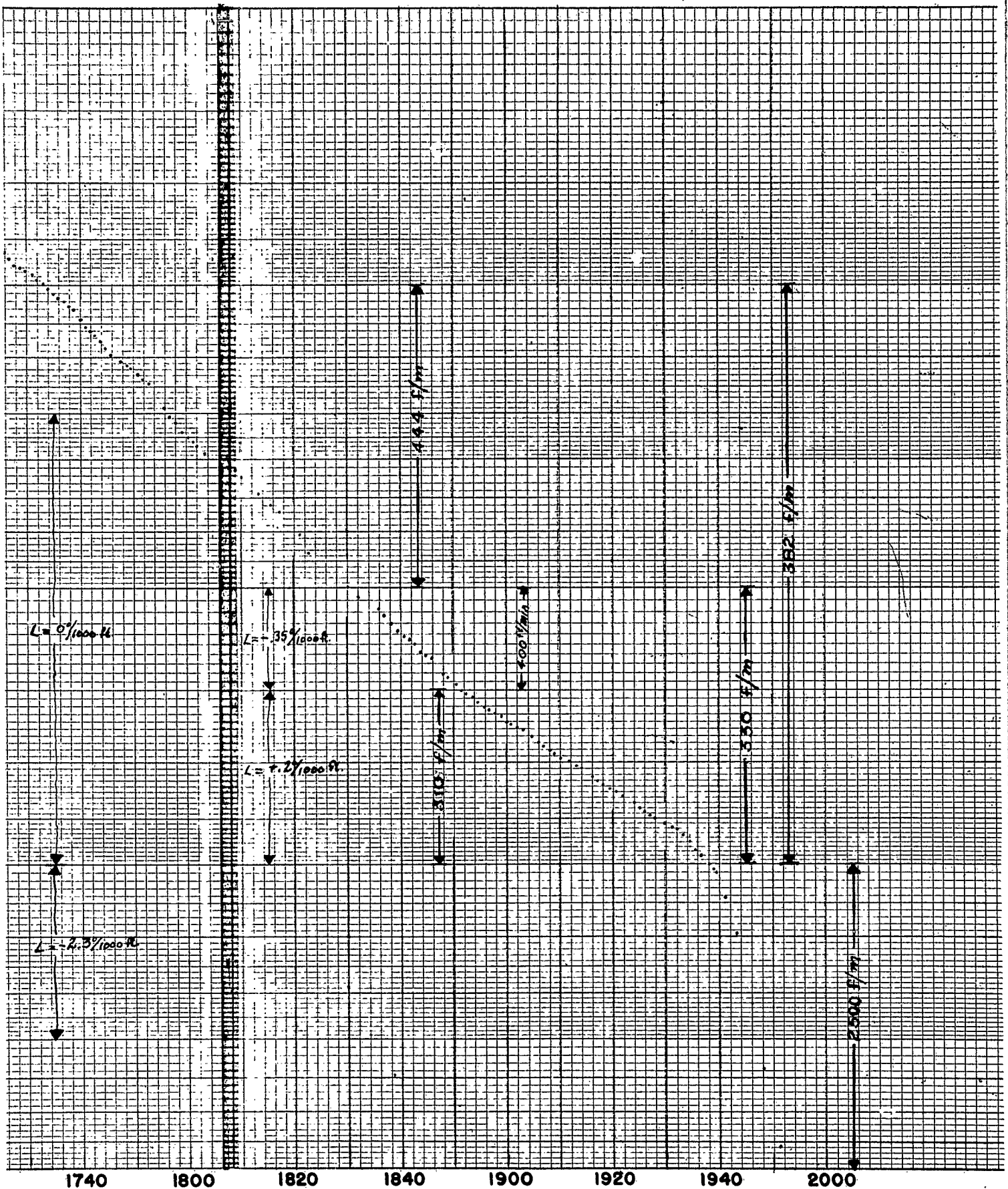
0300 Z

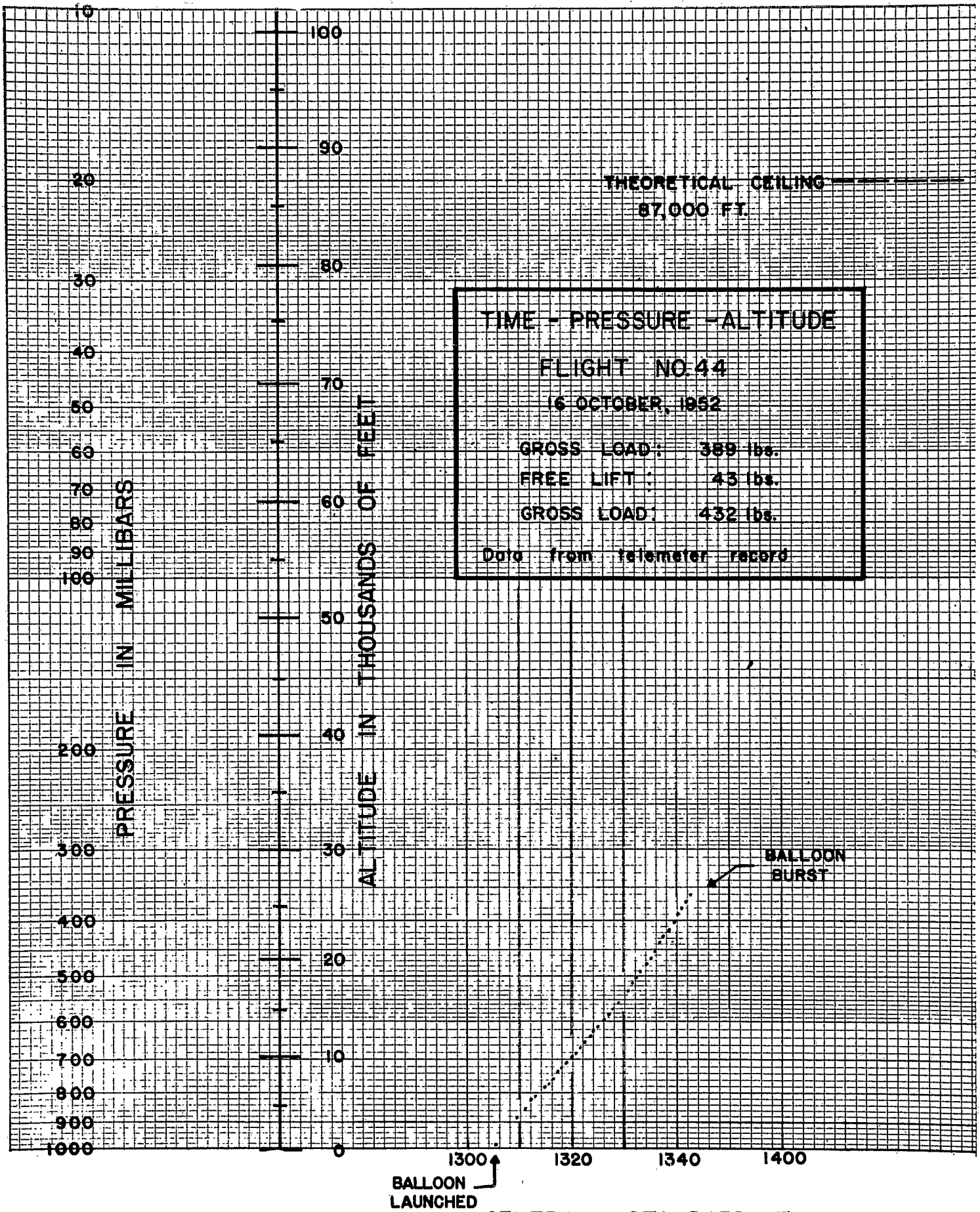
Numbers along curve show lapse
rates in degrees per 1000 feet.



BALLOON LAUNCHED



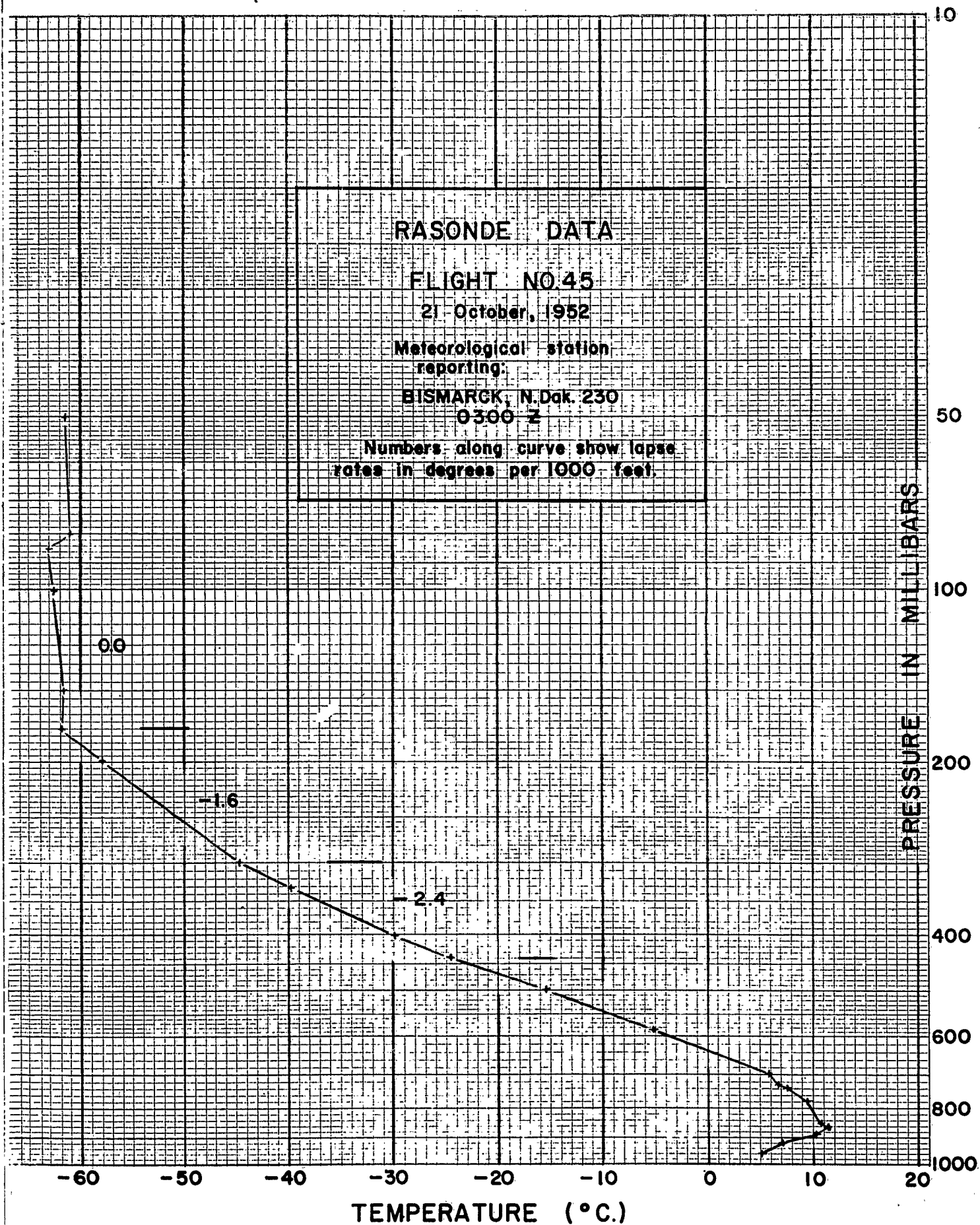


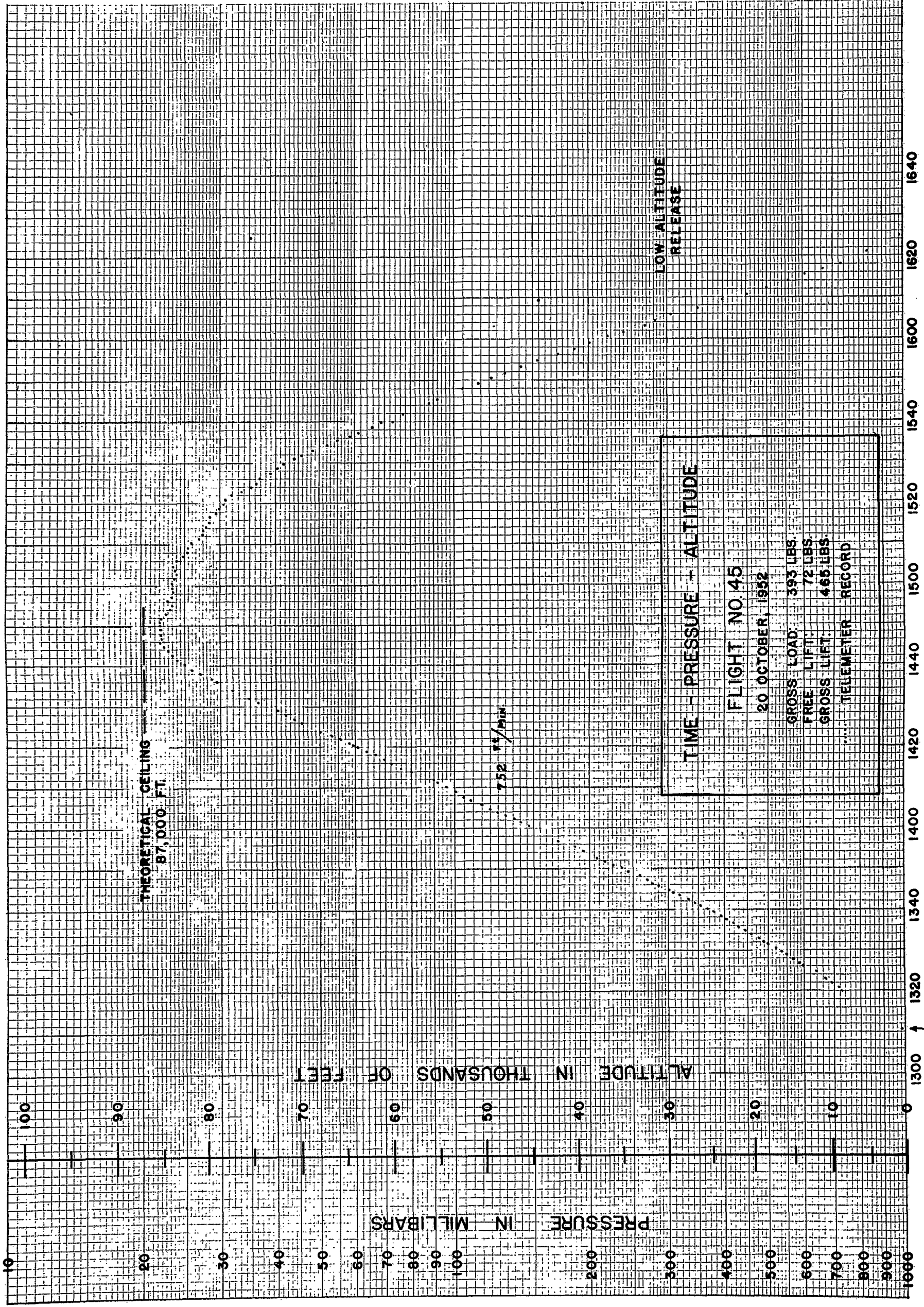


RASONDE DATA

FLIGHT NO. 45

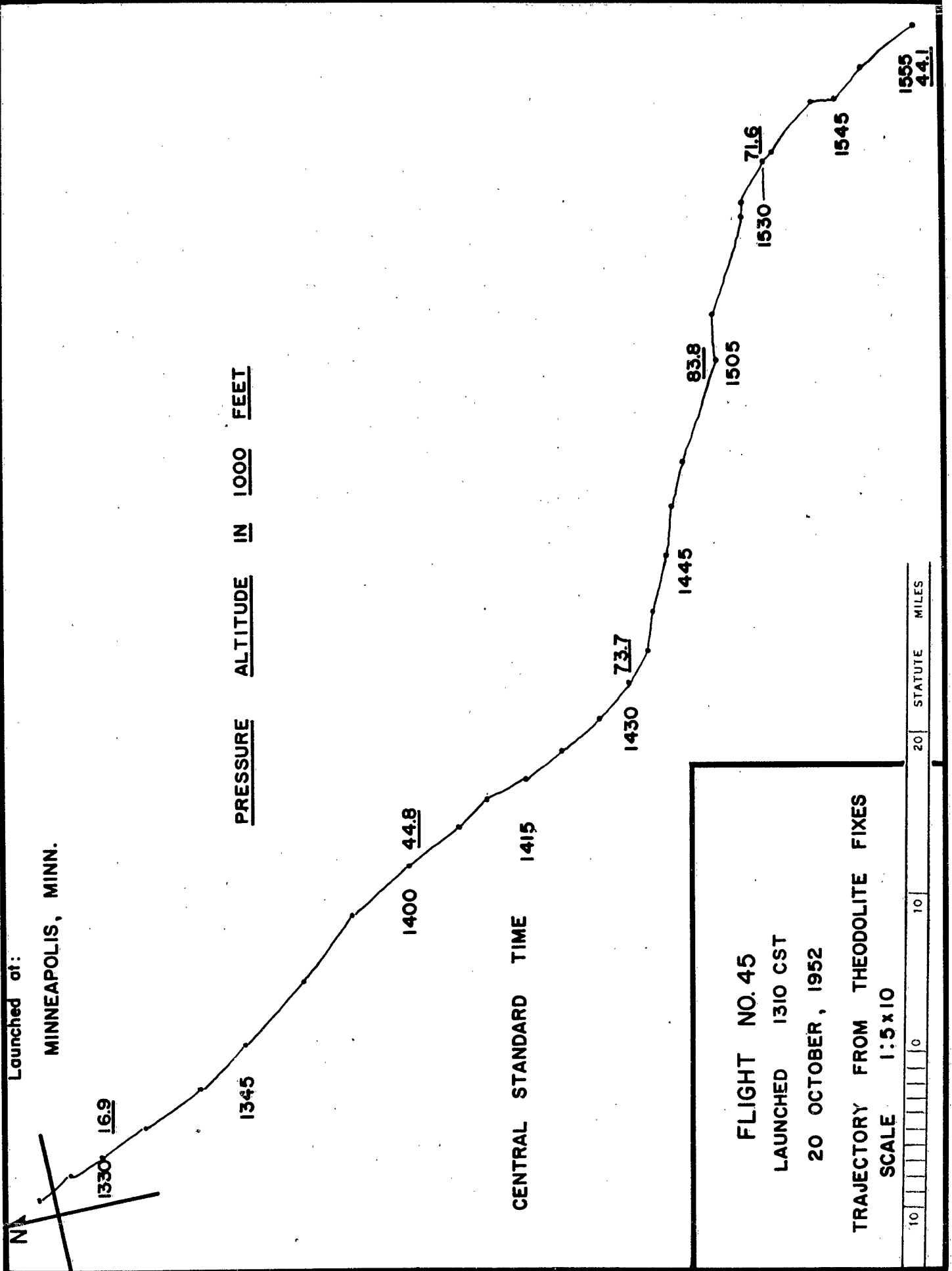
21 October, 1952

Meteorological station
reporting:BISMARCK, N. Dak. 230
0300 ZNumbers along curve show lapse
rates in degrees per 1000 feet.



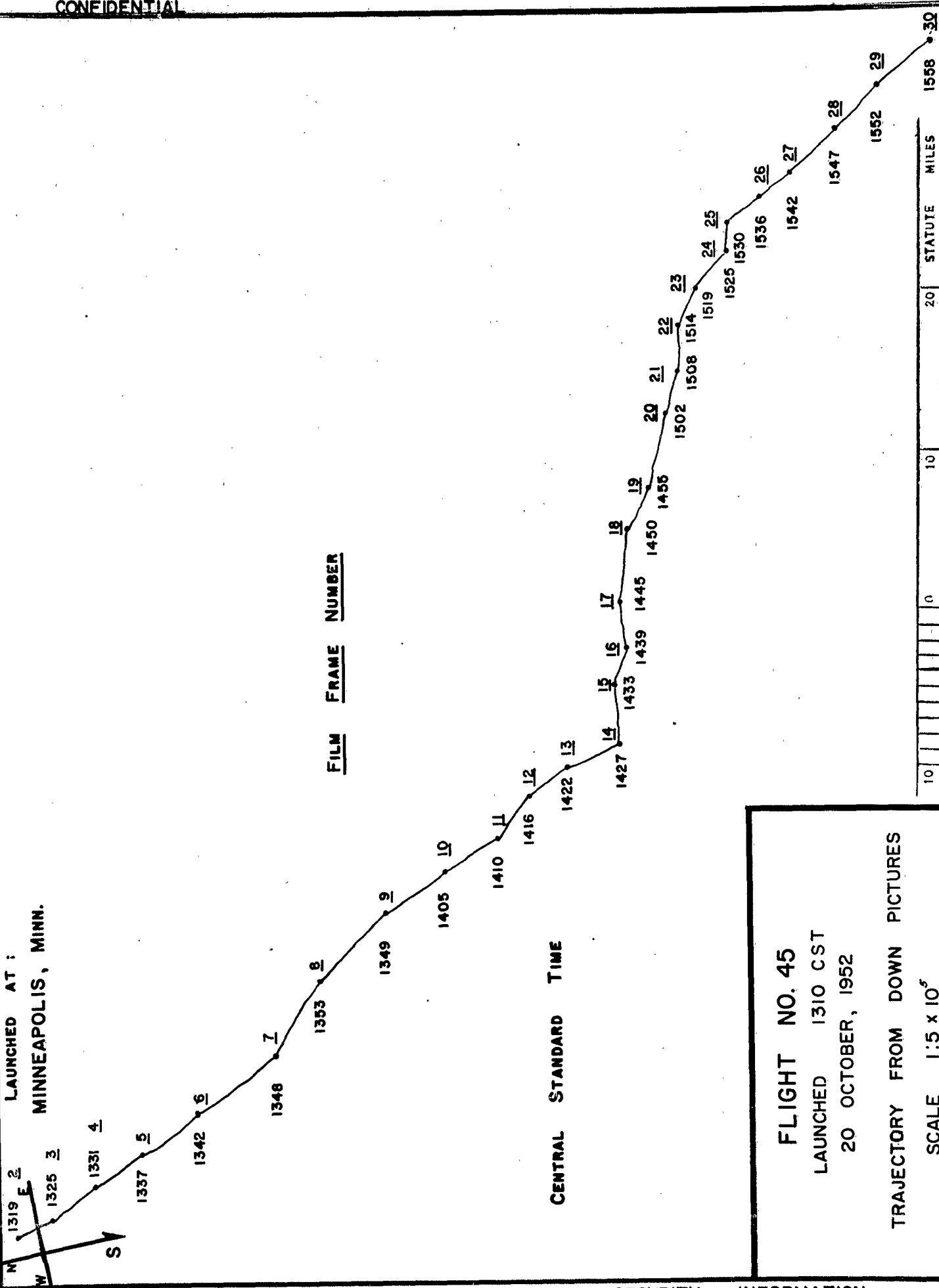
BALLOON
LAUNCHED

CONFIDENTIAL



CONFIDENTIAL

LAUNCHED AT :
MINNEAPOLIS, MINN.



FLIGHT NO. 45
LAUNCHED 1310 CST
20 OCTOBER, 1952
TRAJECTORY FROM DOWN PICTURES
SCALE 1:5 x 10⁵

RASONDE DATA

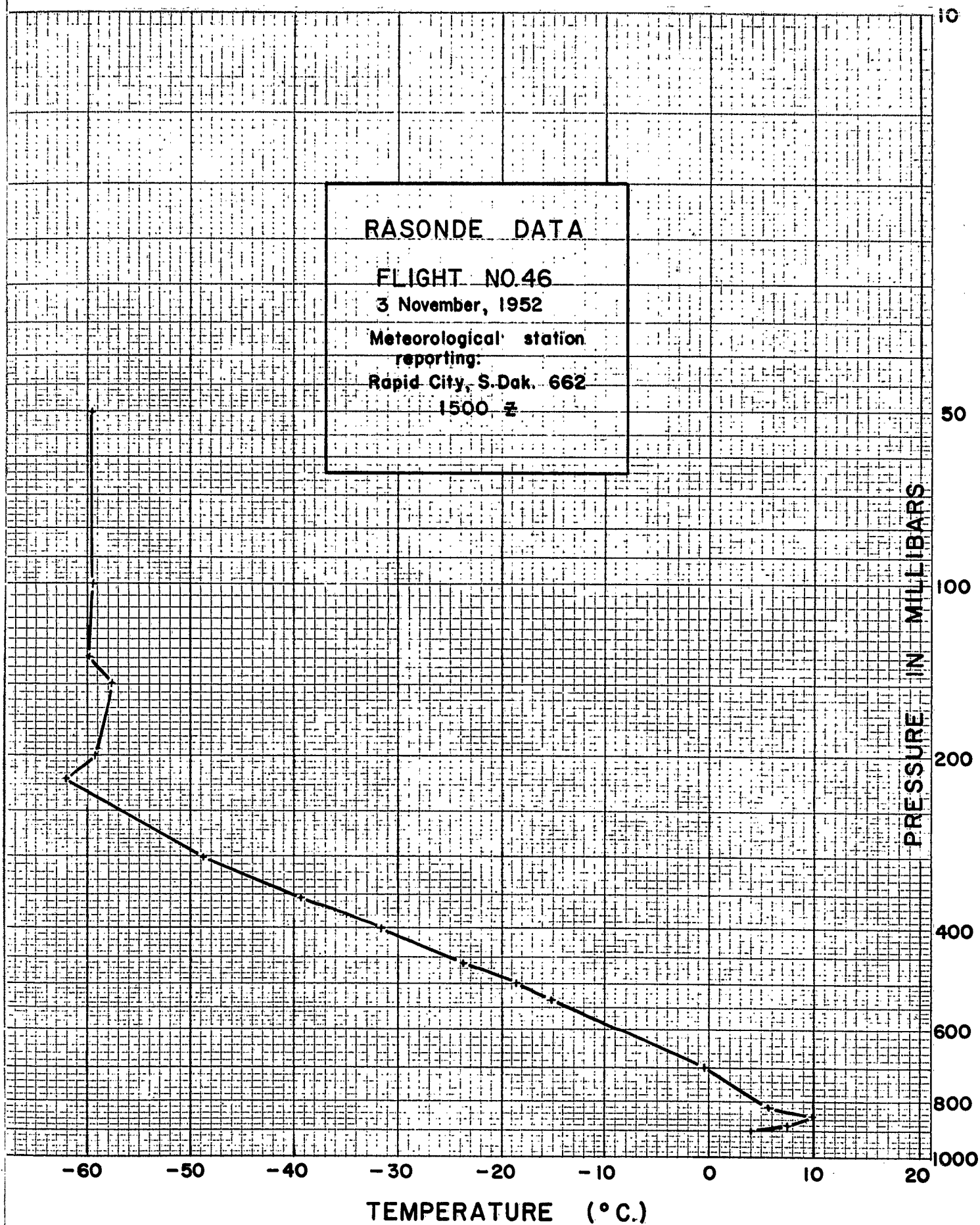
FLIGHT NO.46

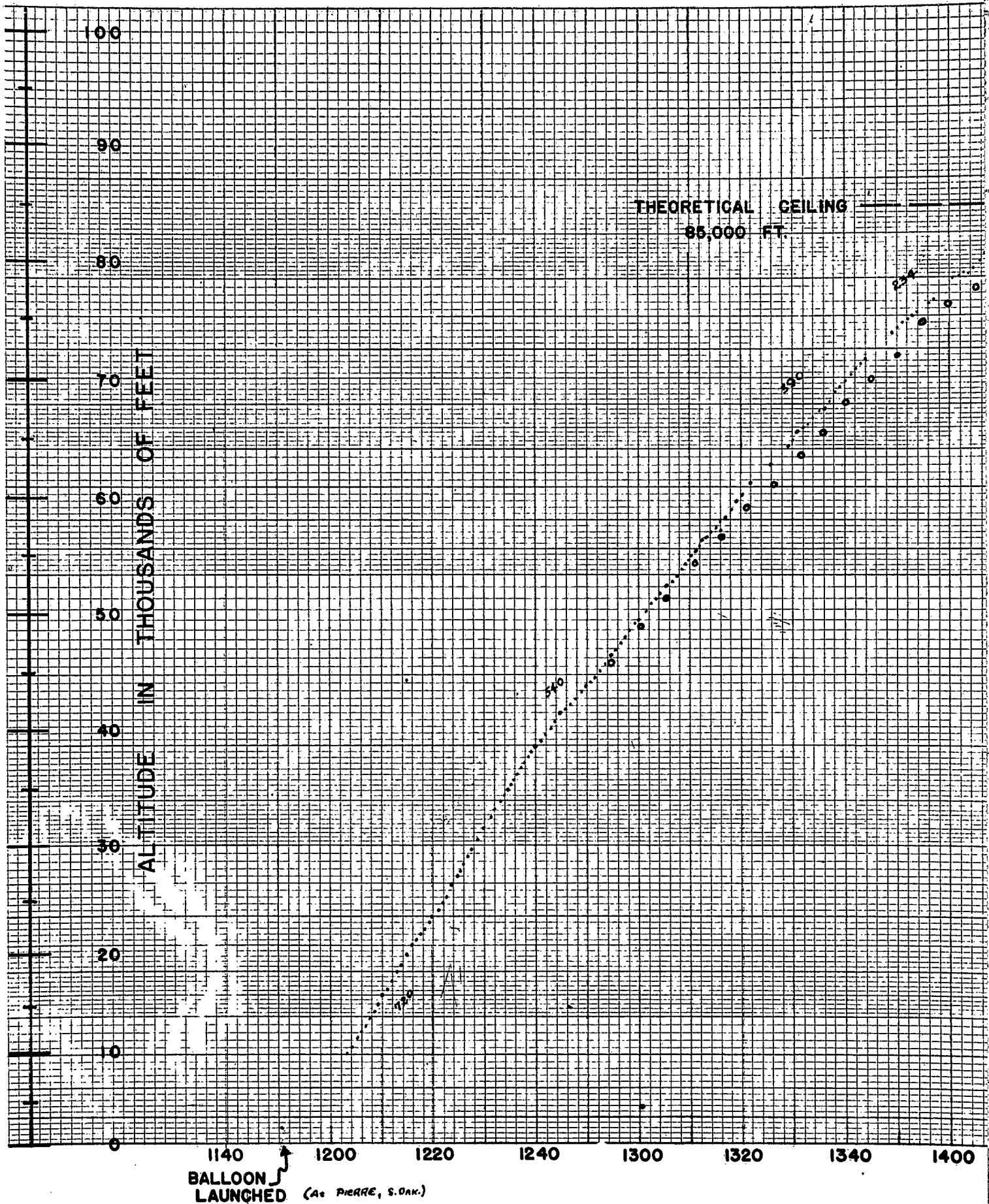
3 November, 1952

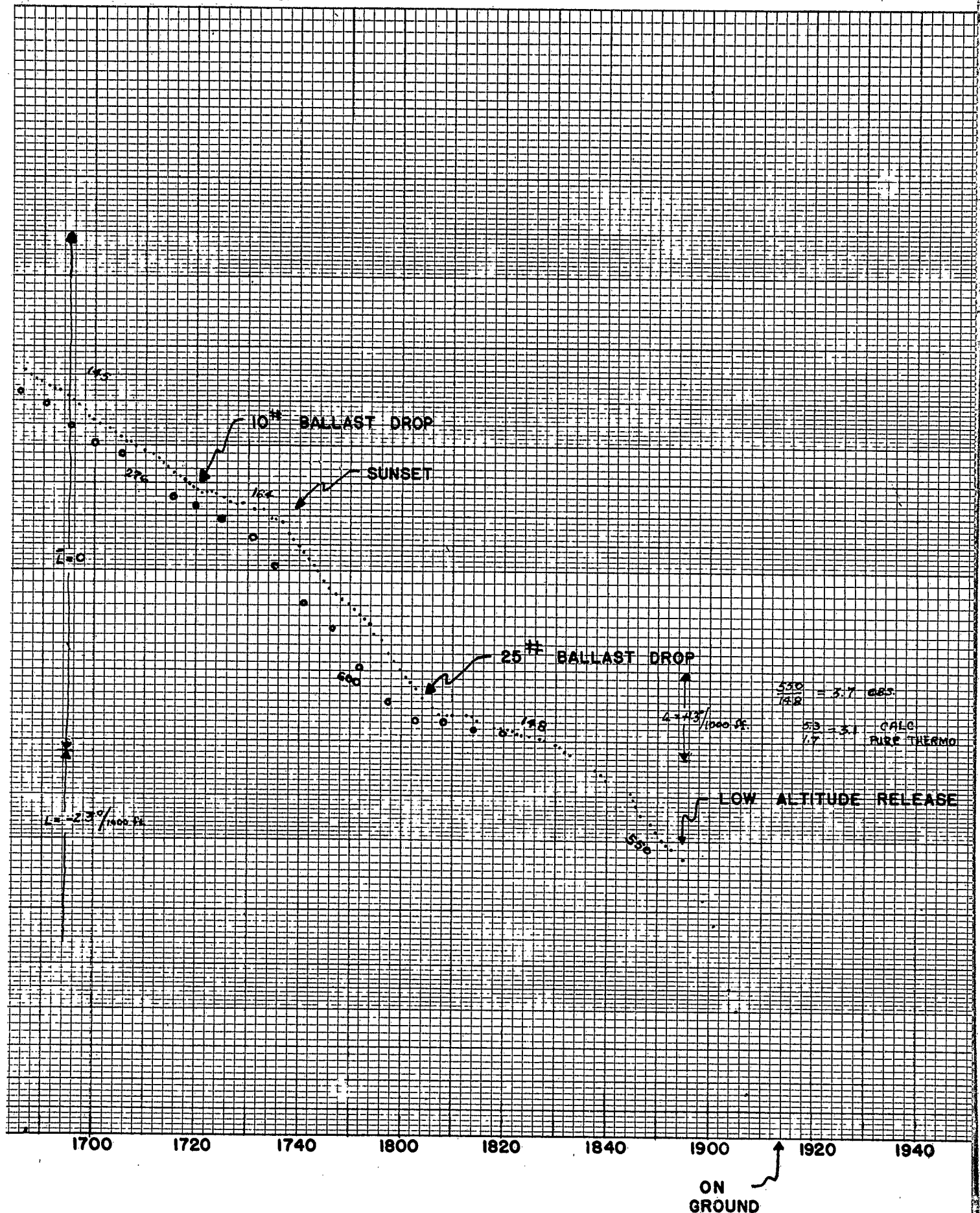
Meteorological station
reporting:

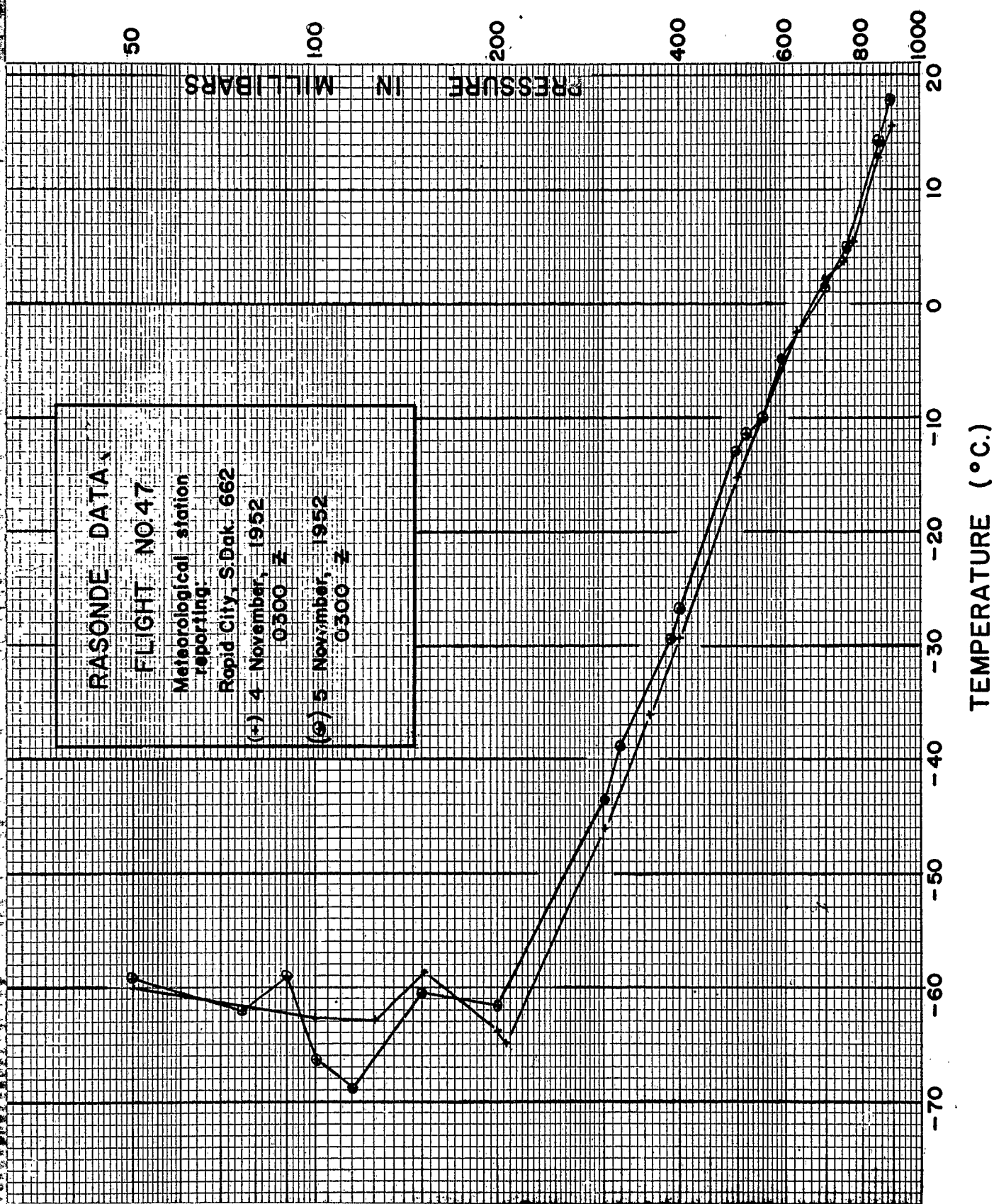
Rapid City, S.Dak. 662

1500 z

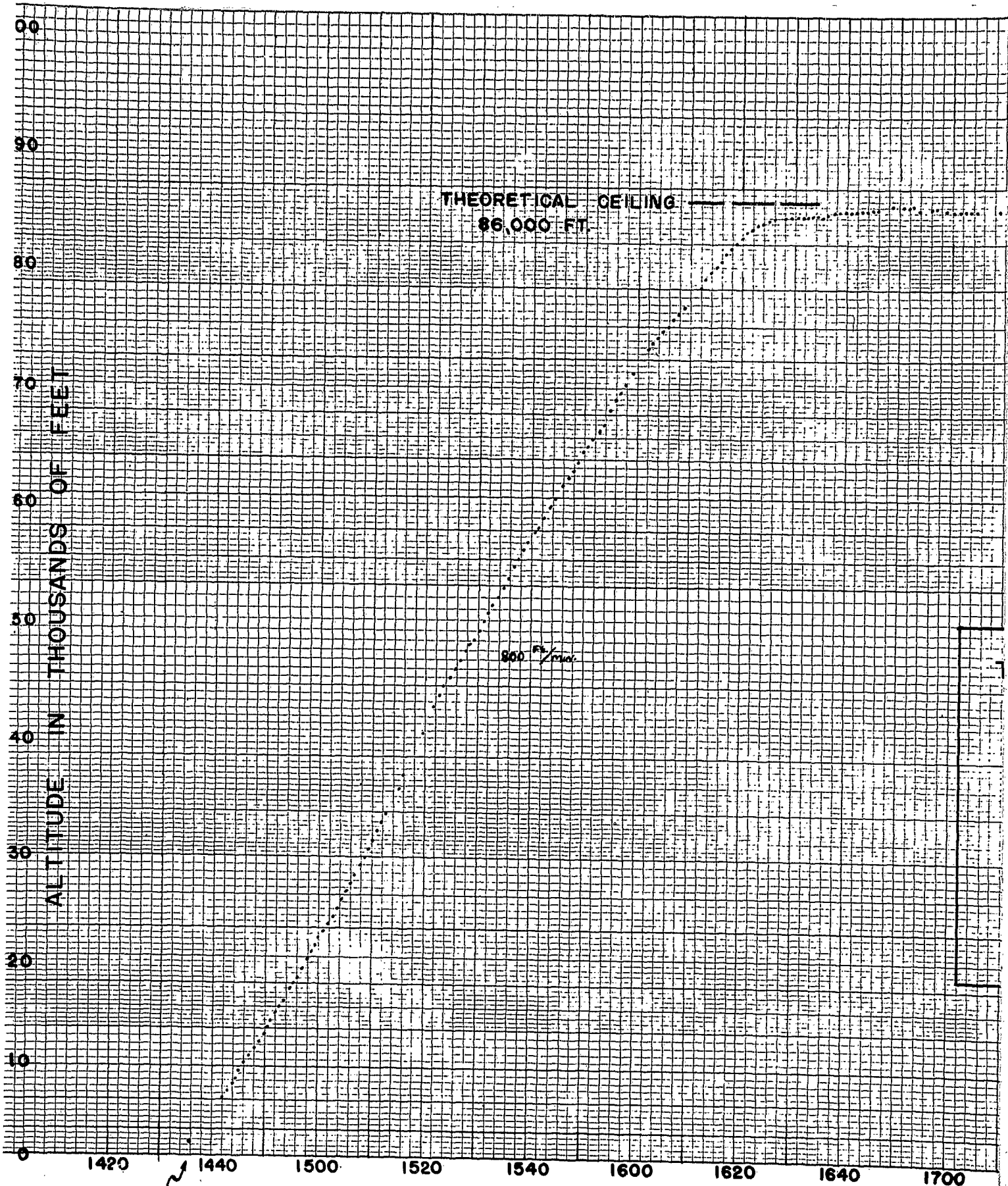




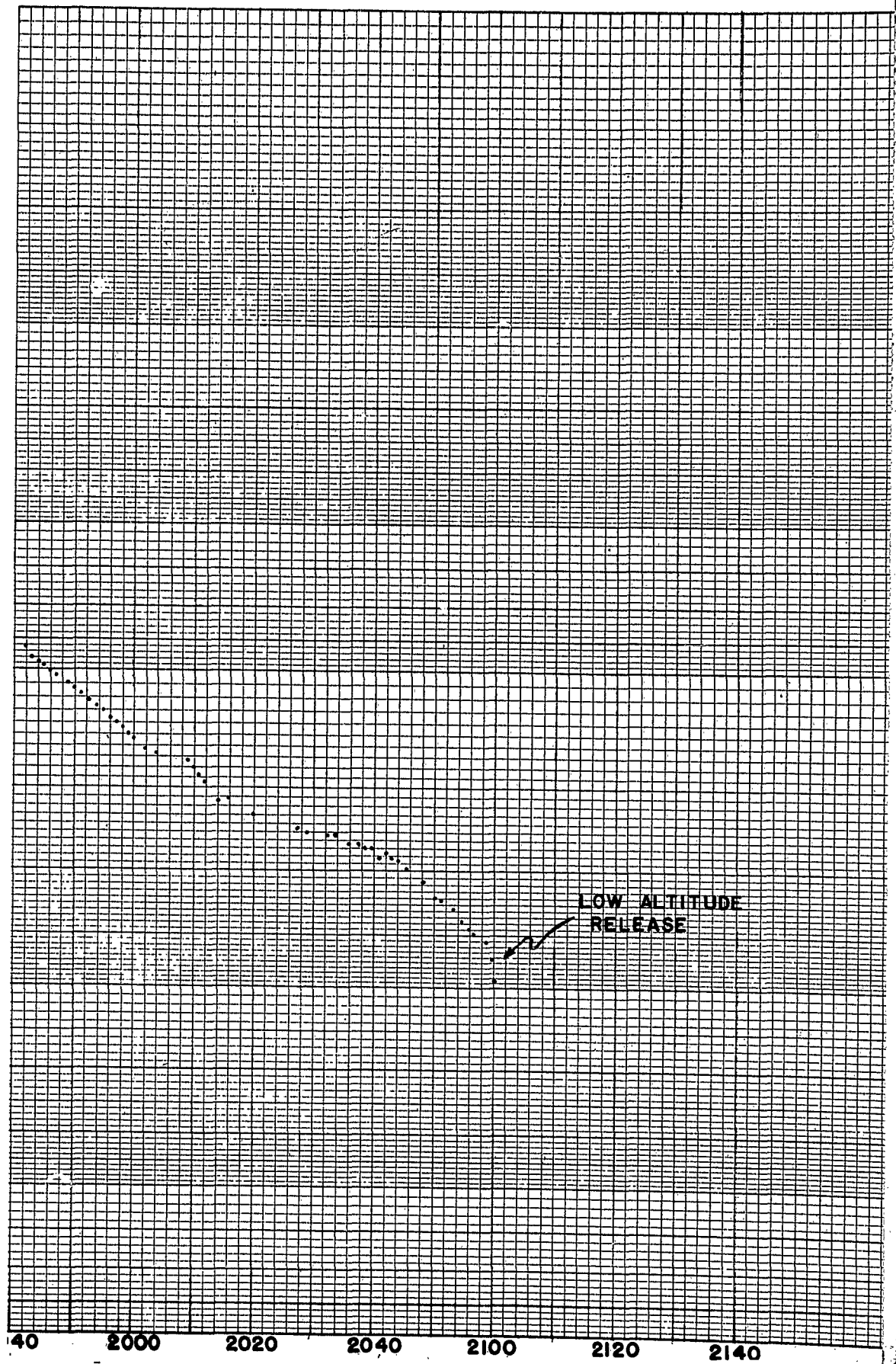




Confidential Security Information

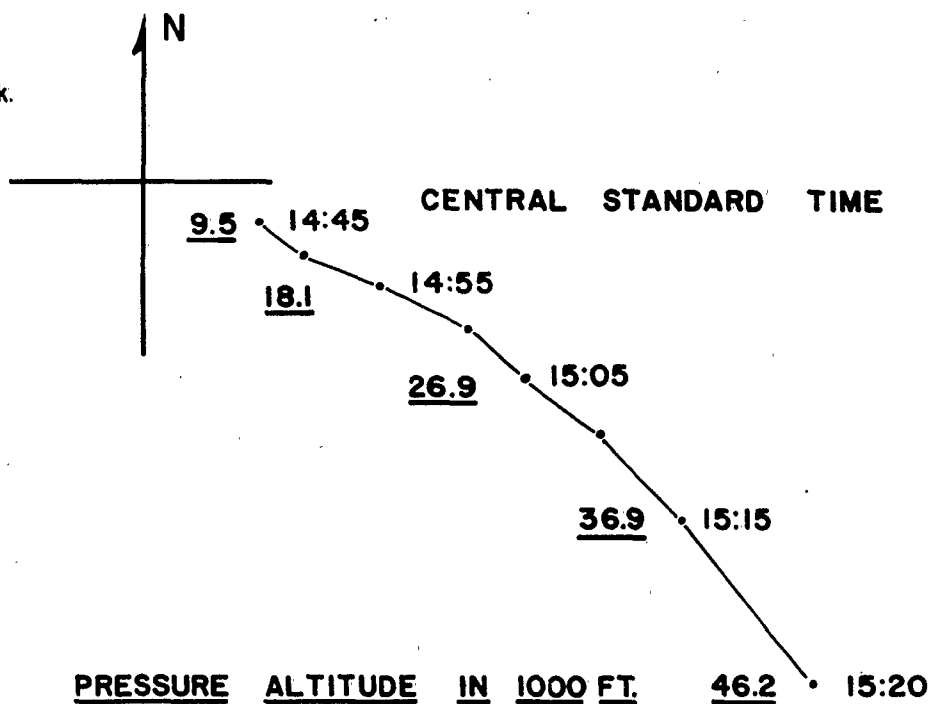


BALLOON LAUNCHED (AT PIERRE, S.D.)



CONFIDENTIAL

Launched at:
PIERRE, So. Dak.

**FLIGHT NO. 47**

LAUNCHED FROM PIERRE, S.D.
at 1436 C.S.T.

4 NOVEMBER, 1952

TRAJECTORY FROM THEODOLITE FIXES

SCALE - $1:5 \times 10^5$

CONFIDENTIAL SECURITY INFORMATION

THEORETICAL CEILING

86,300 FT.

TIME - PRESSURE - ALTITUDE

FLIGHT NO. 48

6 NOVEMBER, 1952

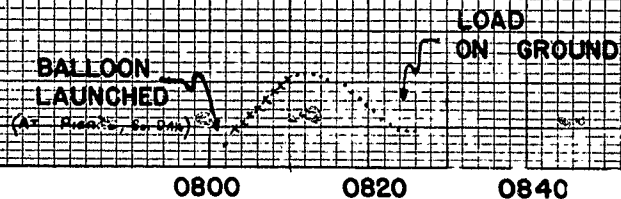
GROSS LOAD: 402 LBS.

FREE LIFT: 32 LBS.

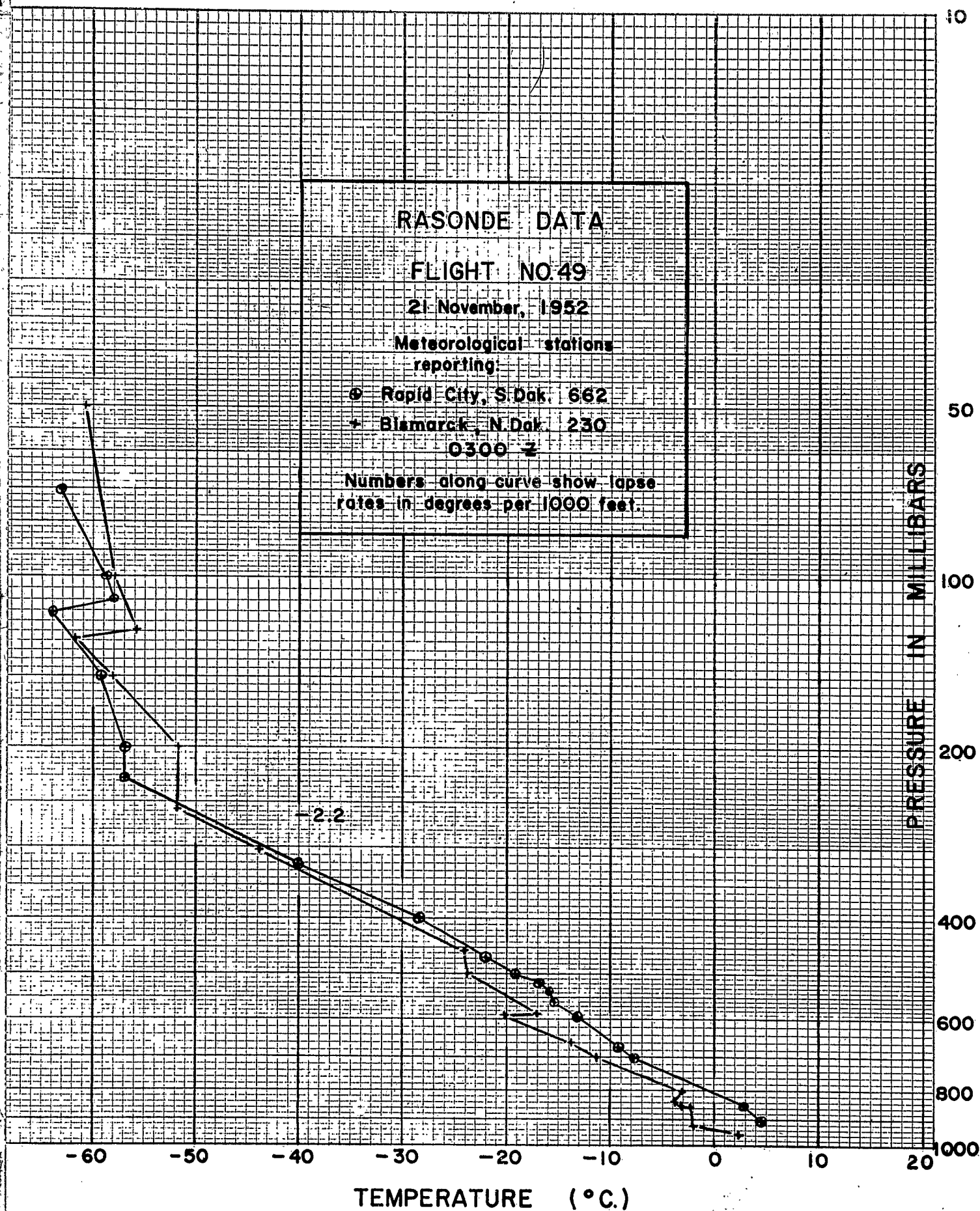
GROSS LIFT: 434 LBS.

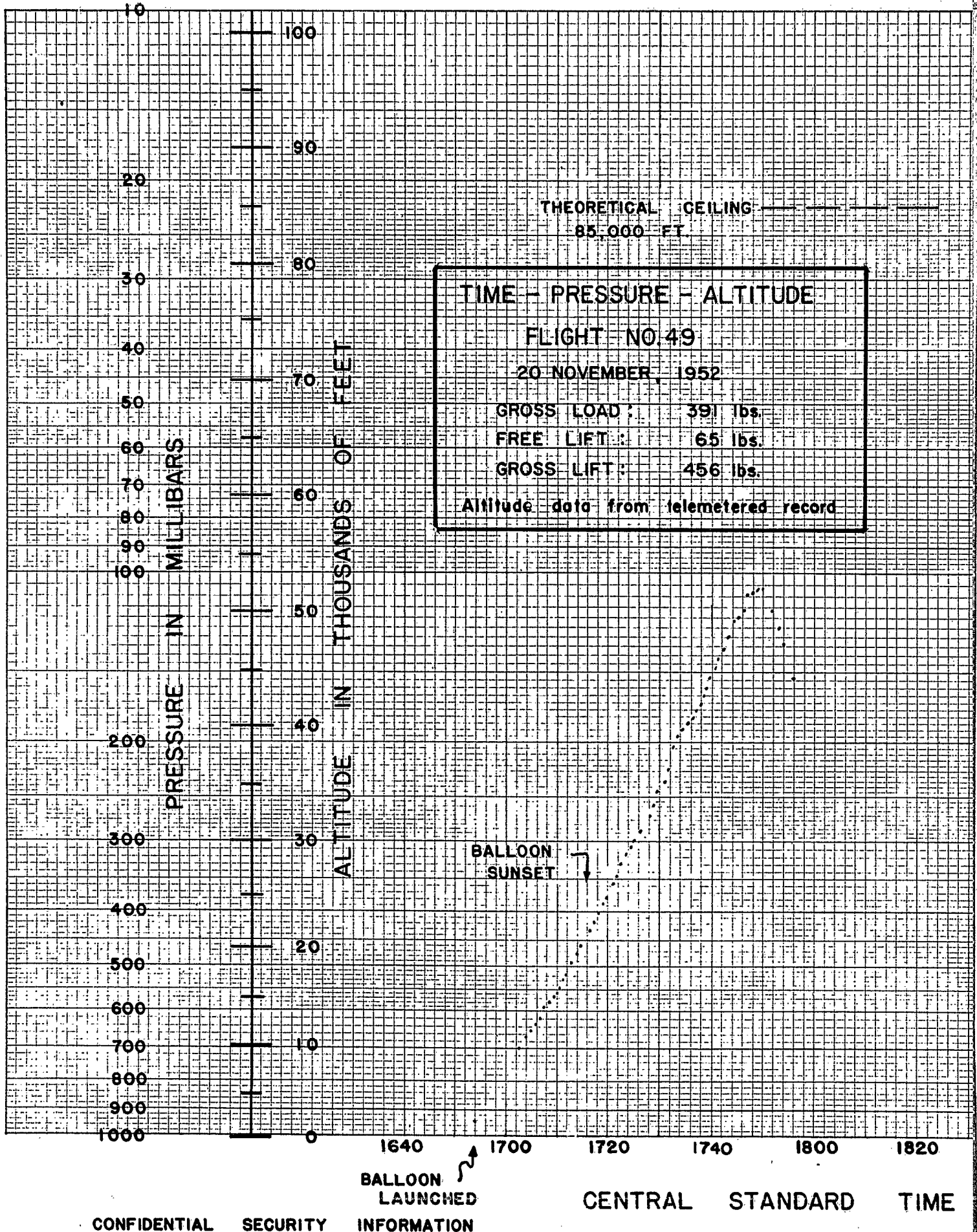
..... DATA FROM TELEMETER RECORD

XXXX DATA FROM A V C RECORDER

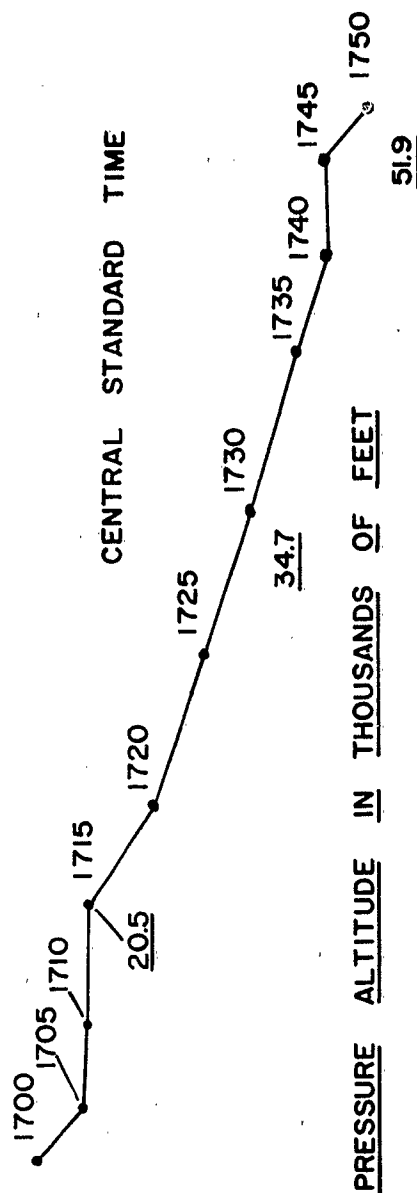
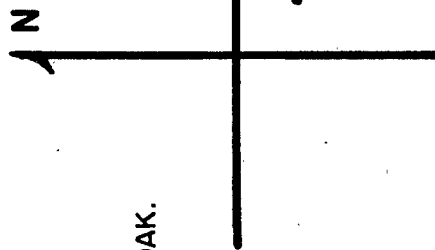


CENTRAL STANDARD TIME





LAUNCHED AT:
PIERRE, SO. DAK.



FLIGHT NO.49

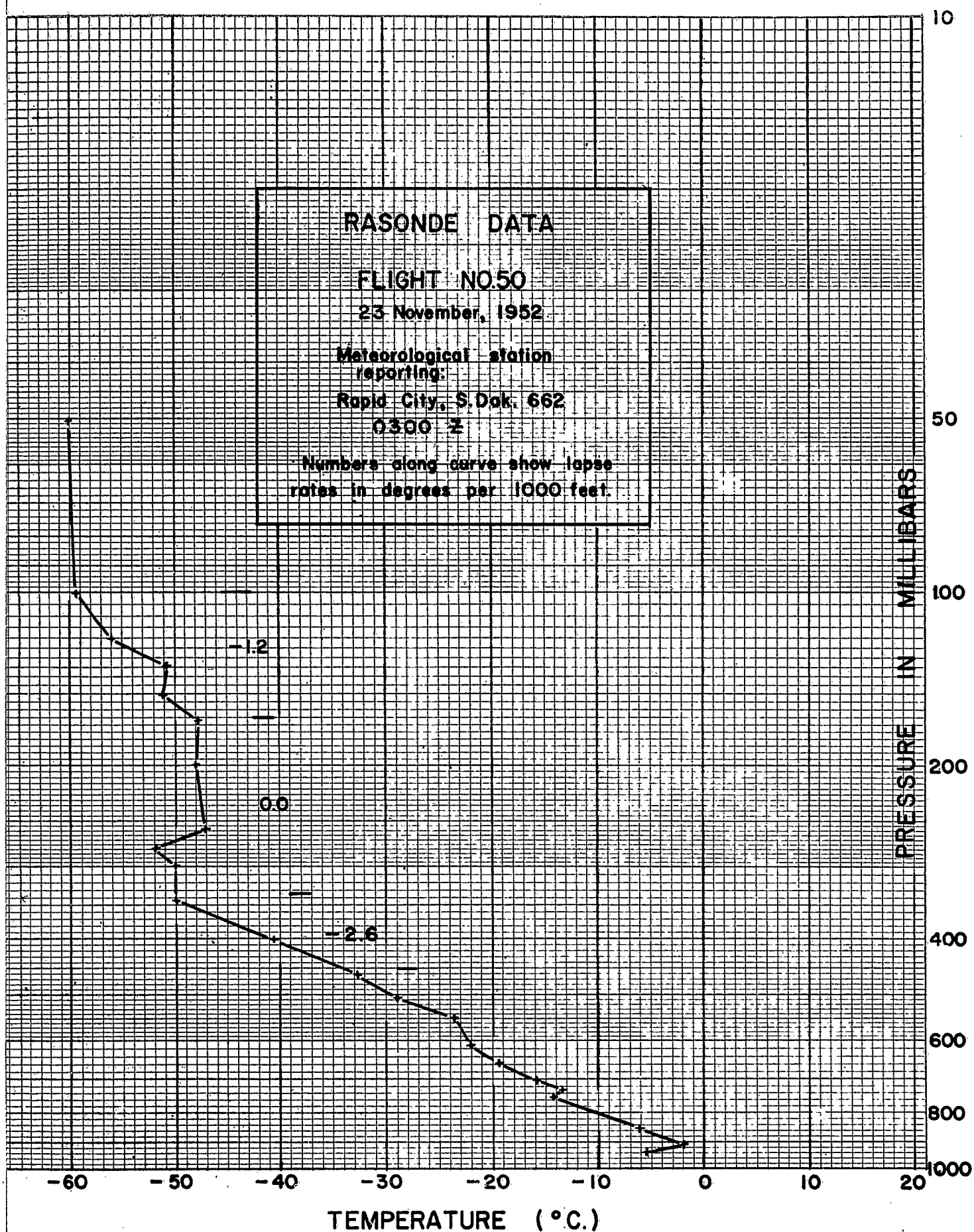
LAUNCHED 1654 CST.

20 NOVEMBER, 1952

TRAJECTORY FROM THEODOLITE FIXES

SCALE 1:5 x 10⁵

10	0	10	20	STATUTE MILES



(Girdle never came off)

TIME - PRESSURE - ALTITUDE

FLIGHT NO. 50

22 NOVEMBER, 1952

GROSS LOAD: 504 LBS.

FREE LIFT: 40 LBS.

GROSS LIFT: 544 LBS.

TRACES FROM DOWN CAMERA
RECORD

TIME BASE FROM
UP CAMERA RECORD

10 1420 1440 1500 1520 1540 1600 1620 1640 1700

CENTRAL STANDARD TIME

CONFIDENTIAL

FLIGHT NO. 50

LAUNCHED 1129 C.S.T.

22 NOVEMBER, 1952

TRAJECTORY FROM THEODOLITE FIXES

SCALE 1:5x10⁵

ALTITUDE IN THOUSANDS OF FEET

CENTRAL STANDARD TIME

47.8

1325

37.2

1300

1250

1205

1150

1320

1315

1310

1305

1255

1245

1240

1235

1230

1225

1220

1215

1210

1205

1150

Launched at:

PIERRE, SO. DAK.

23.0

N

15.3

1210

1205

1150

10 0 10 20 STATUTE MILES

THEORETICAL CEILING
80,000 FT.

TIME - PRESSURE - ALTITUDE

FLIGHT NO. 51

24 NOVEMBER, 1952

GROSS LOAD: 542 LBS.

FREE LIFT: 64 LBS.

GROSS LIFT: 606 LBS.

..... FROM TELEMETER RECORD

BALLOON
LAUNCHED
(AS PLANNED)

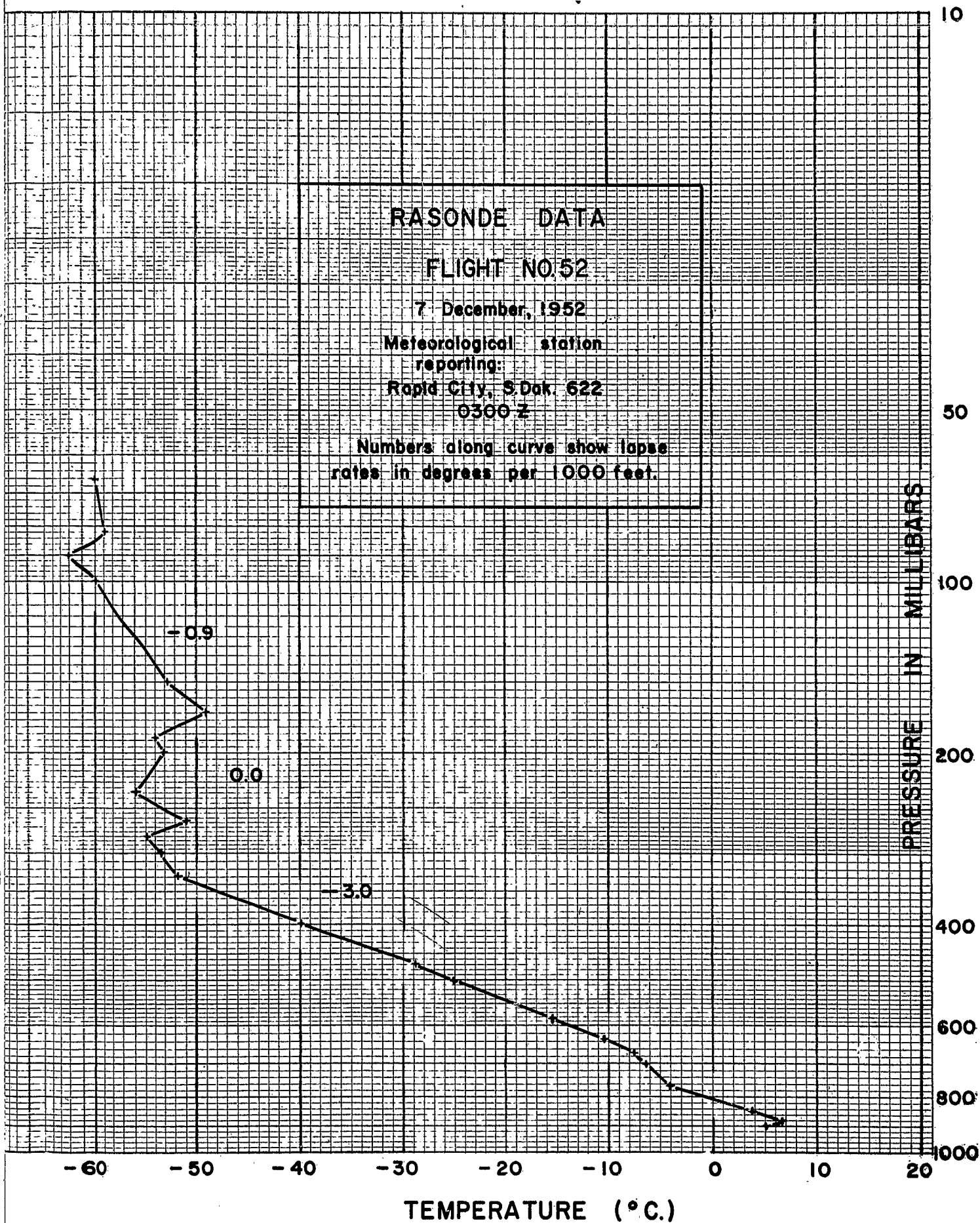
0800

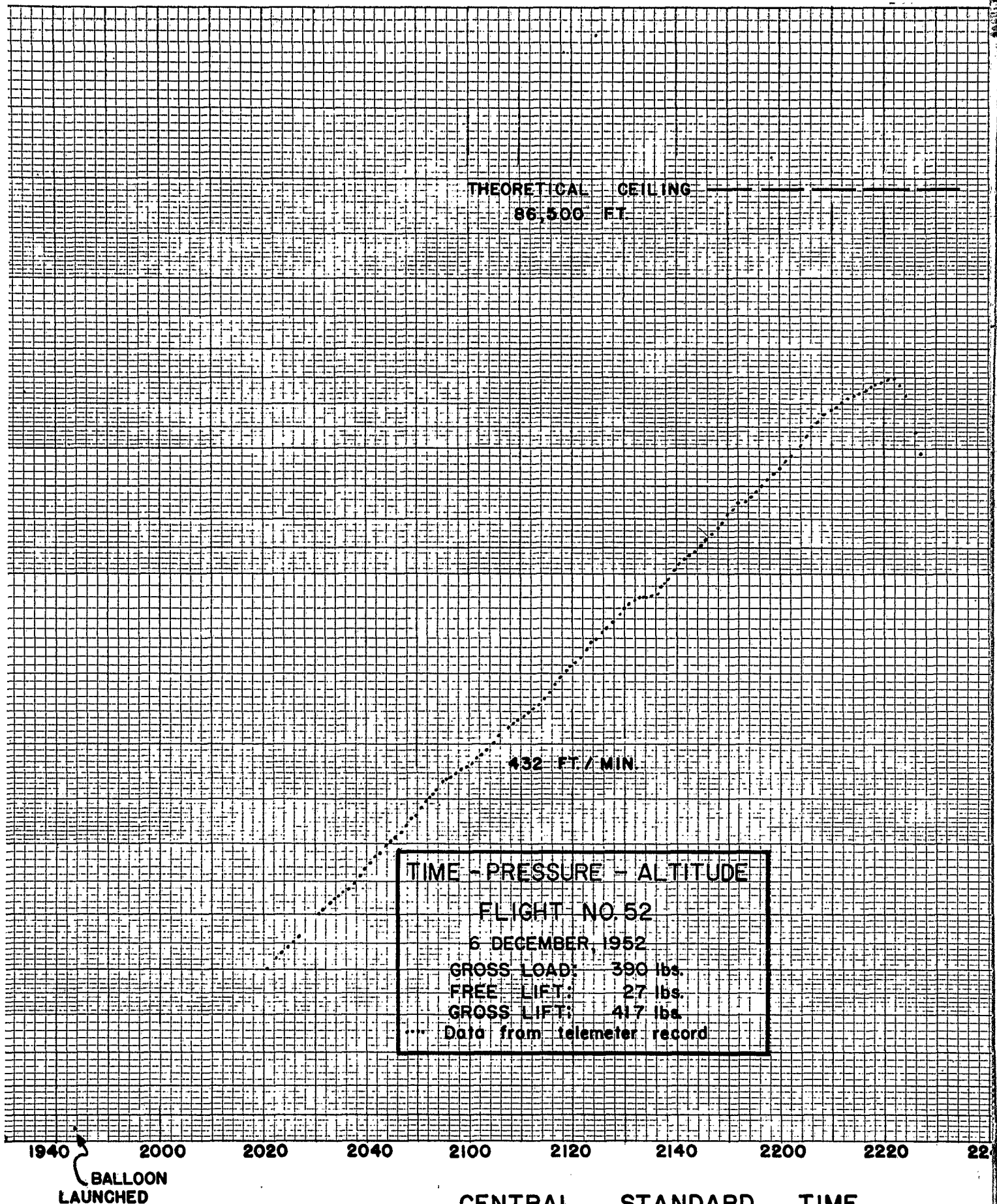
0820

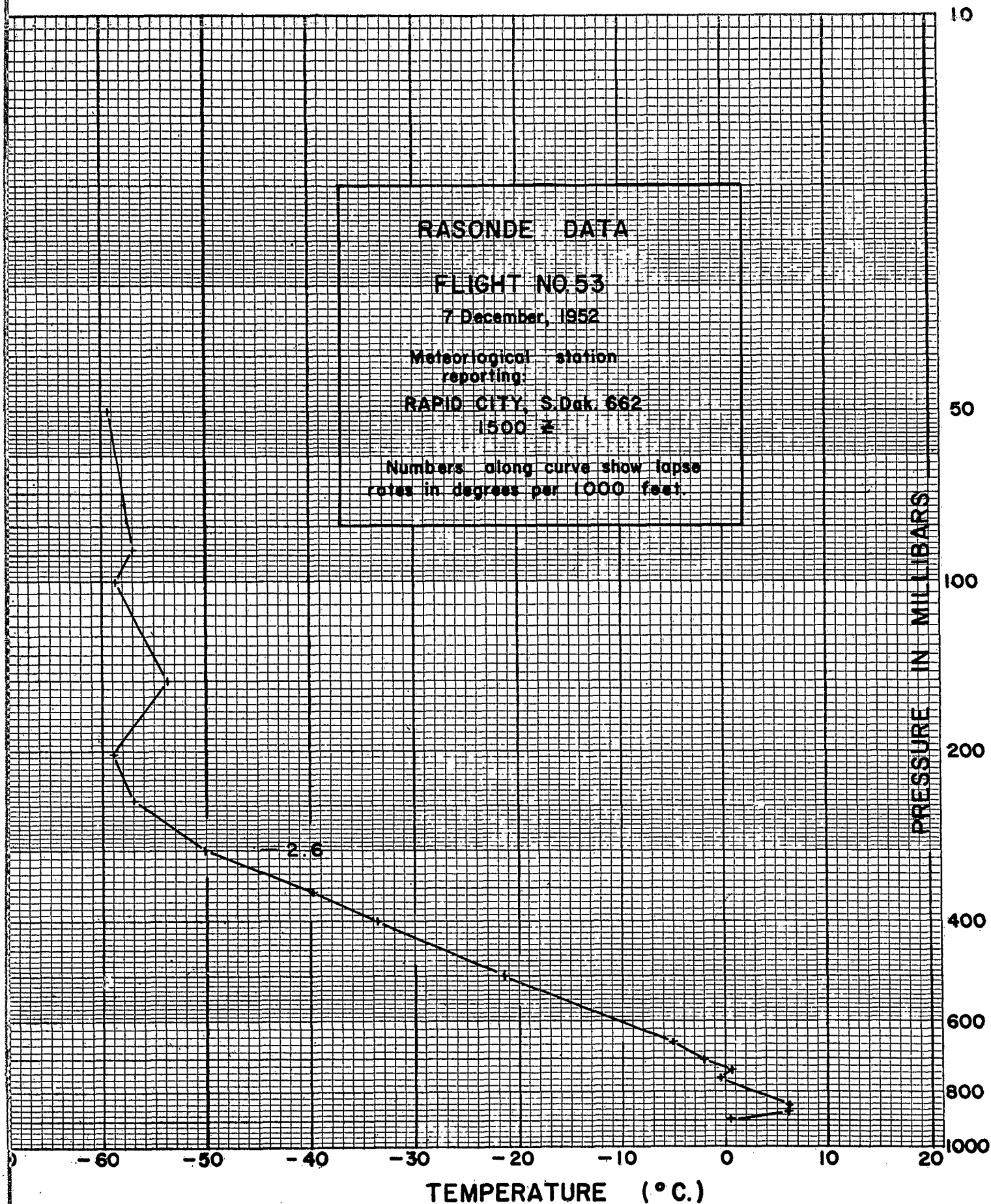
0840

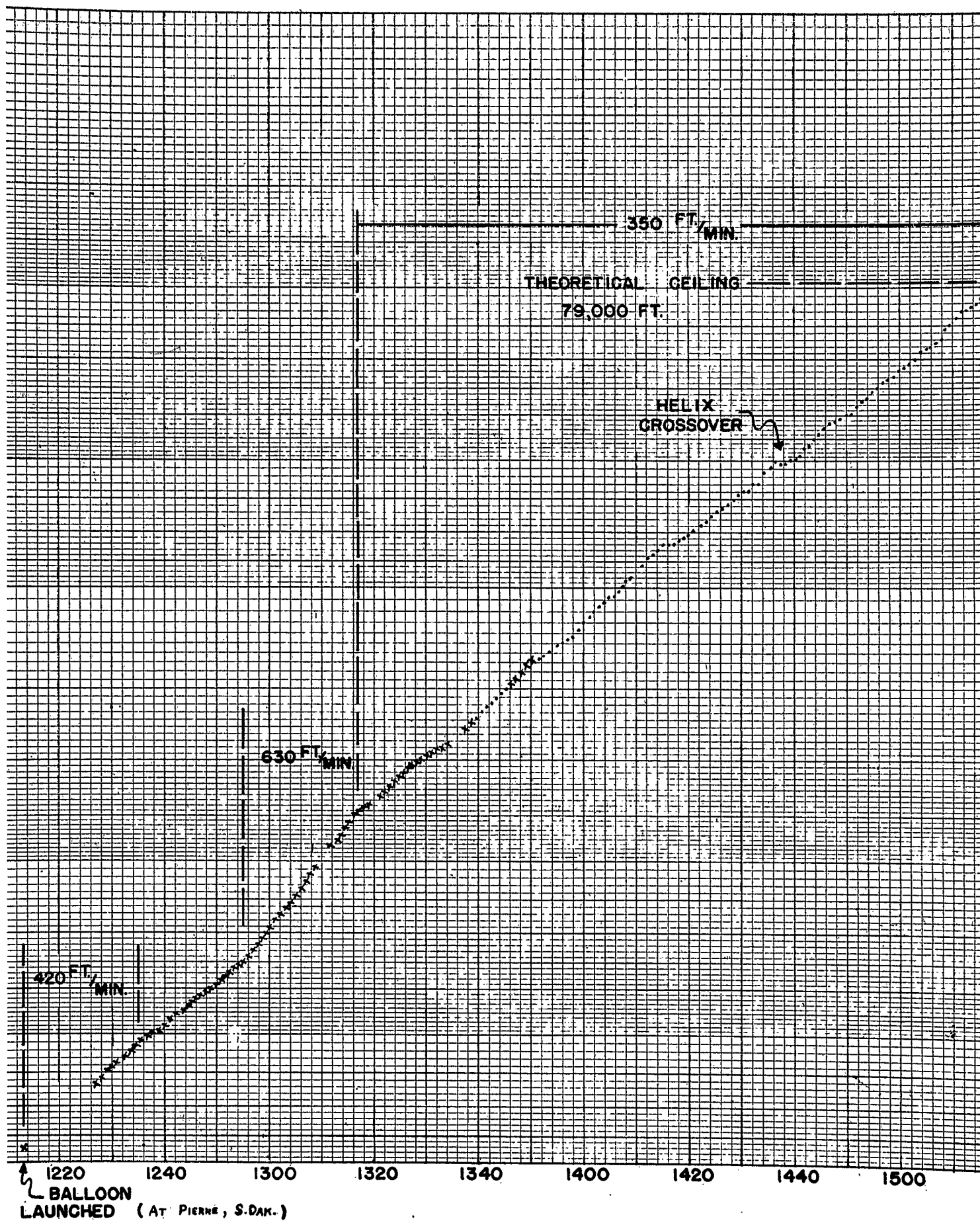
0900

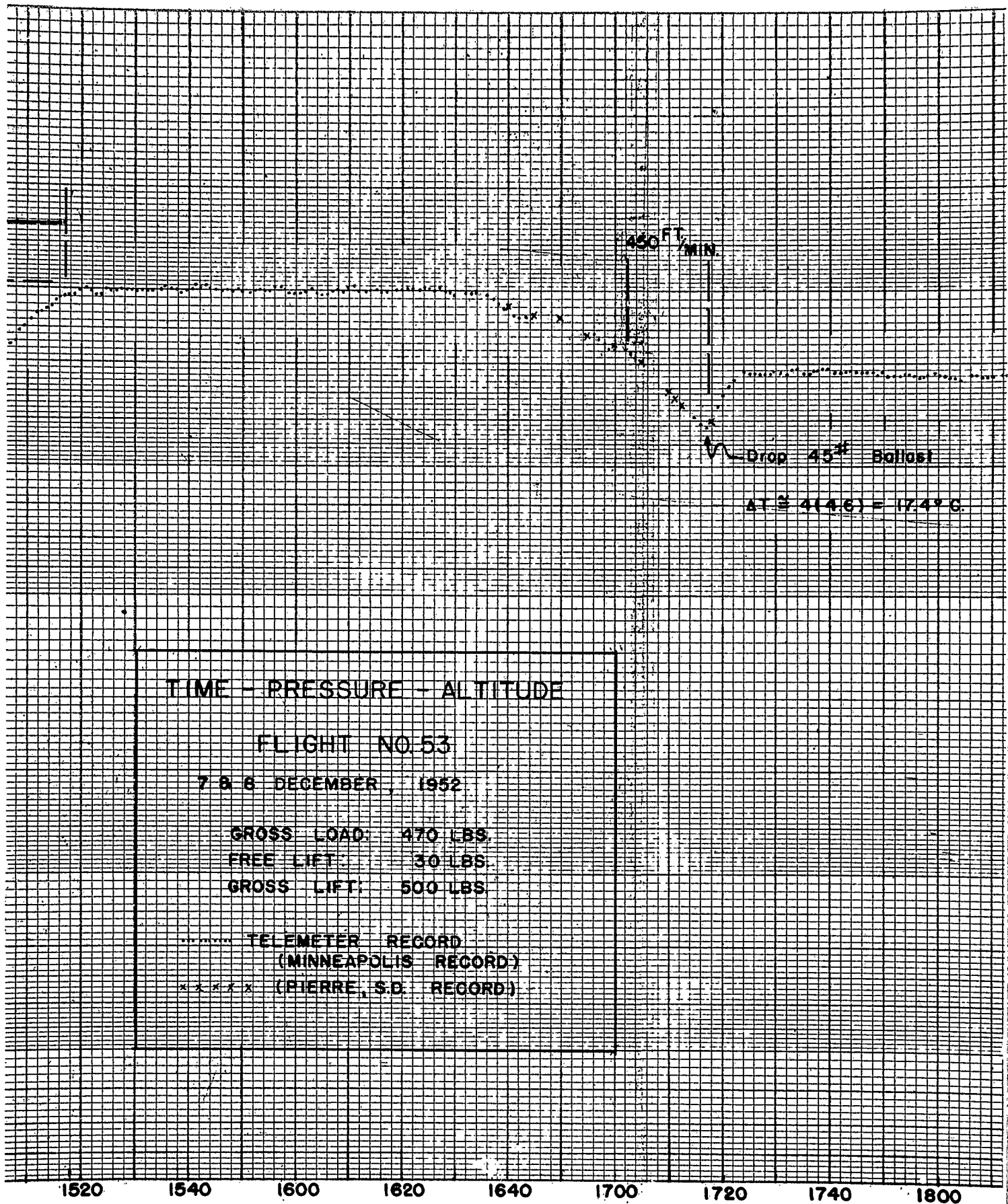
CENTRAL STANDARD TIME

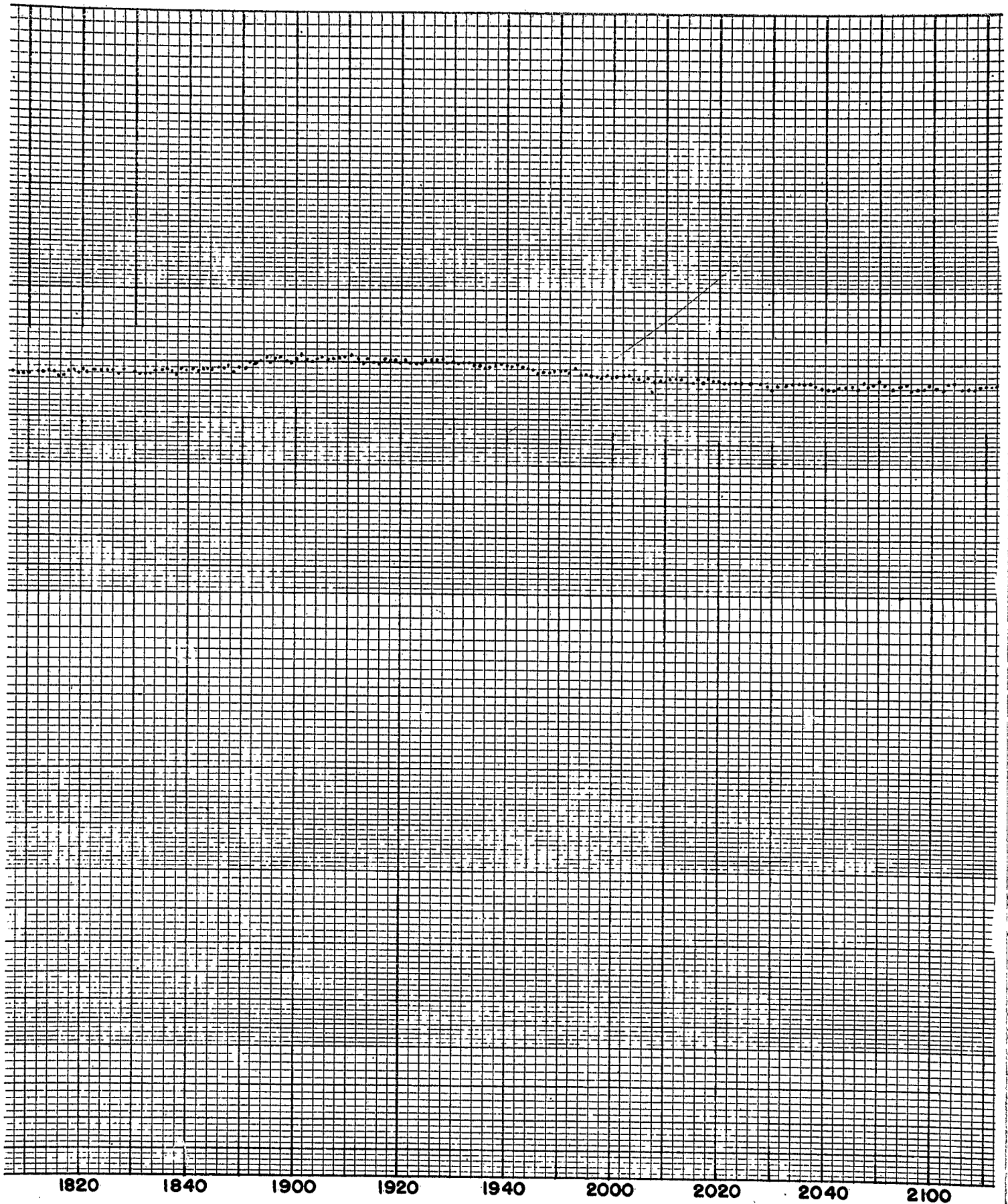


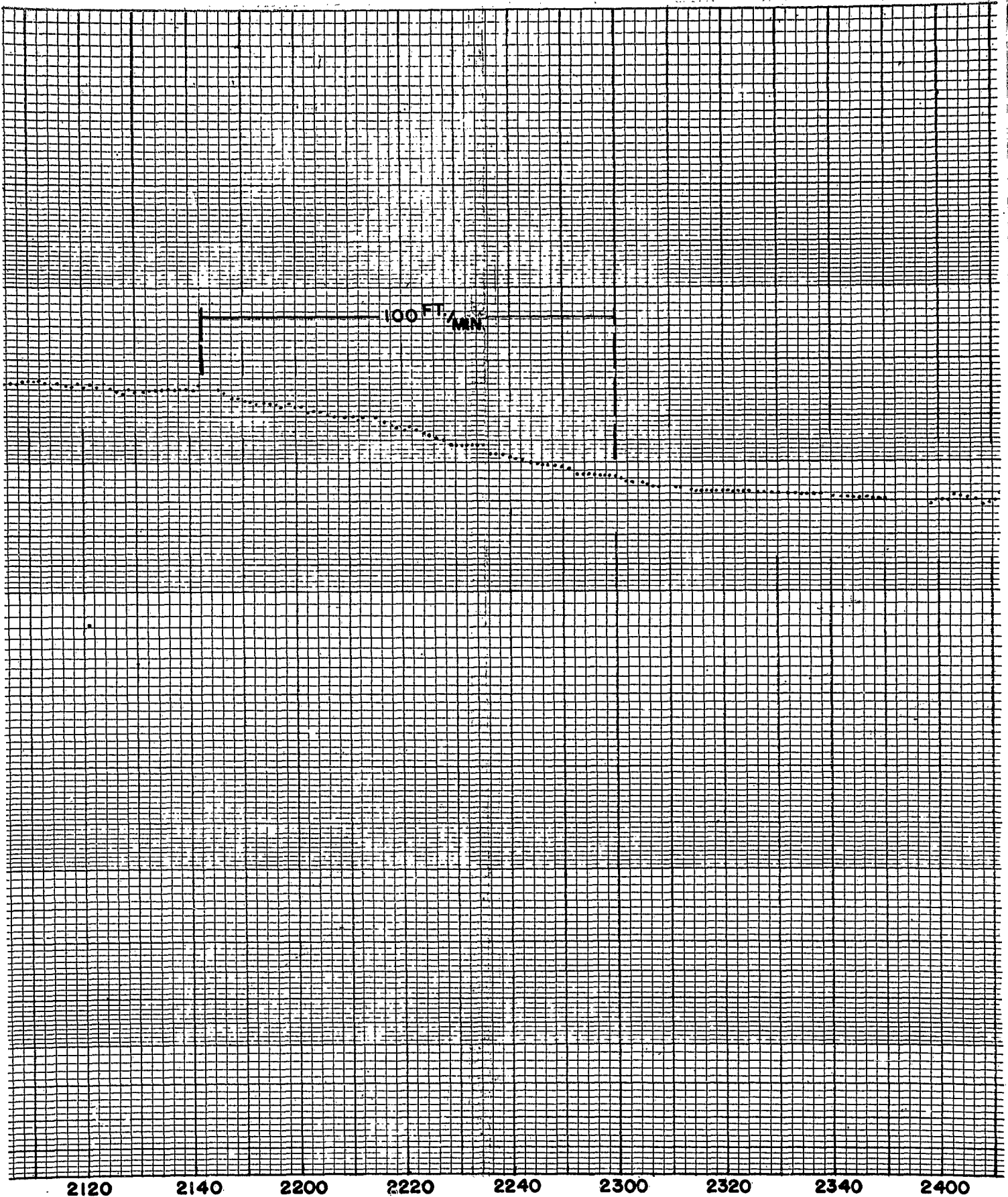


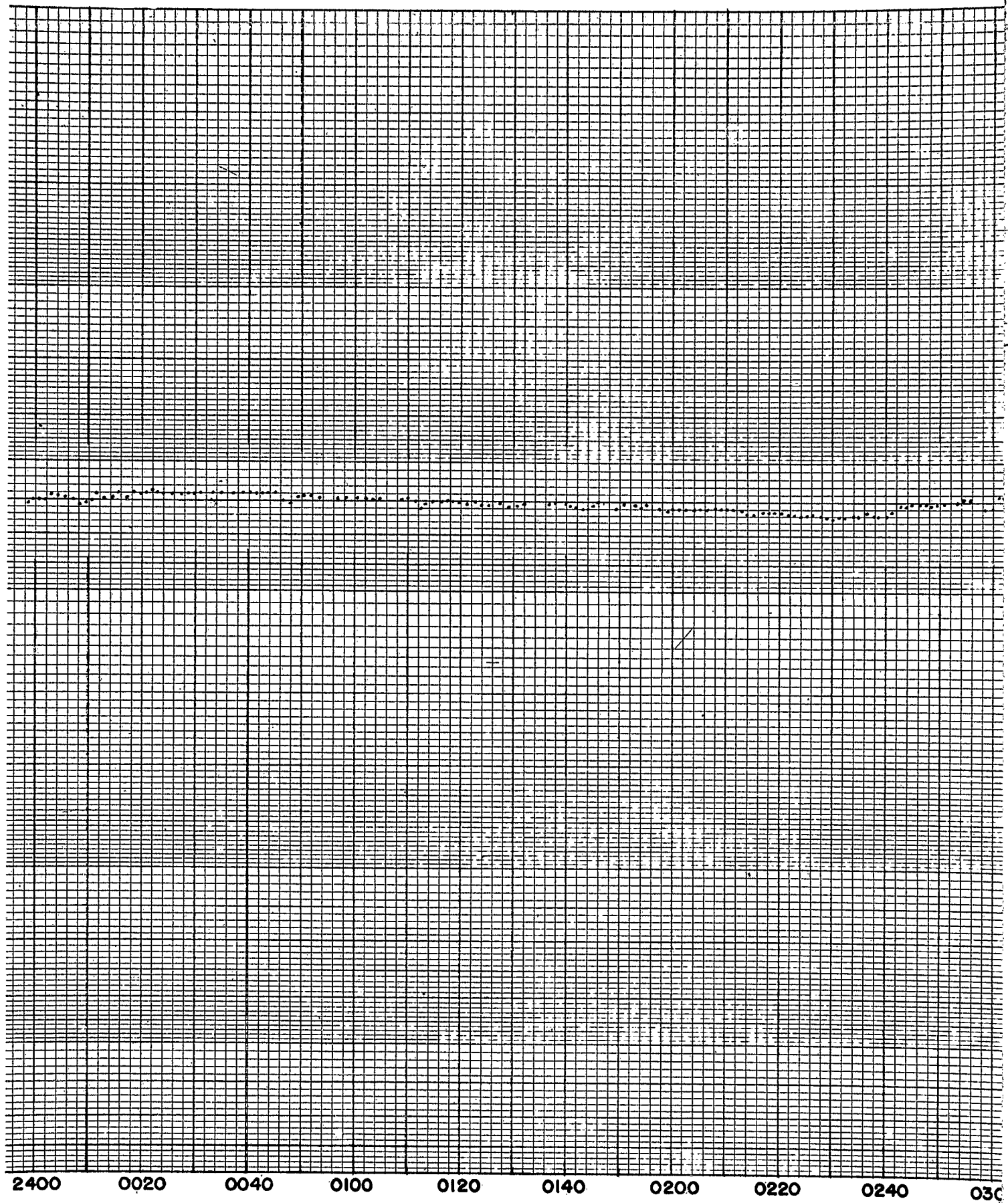






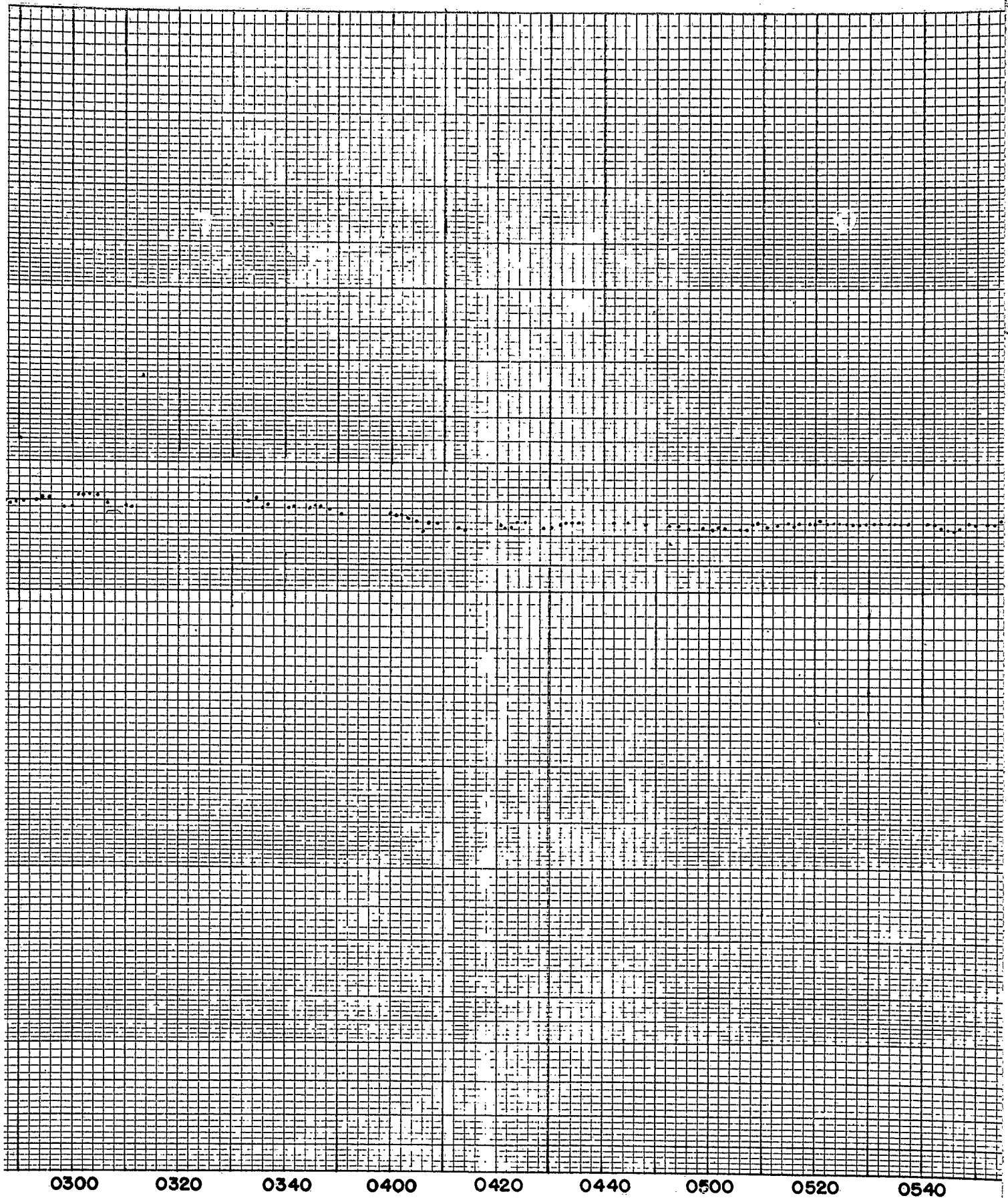


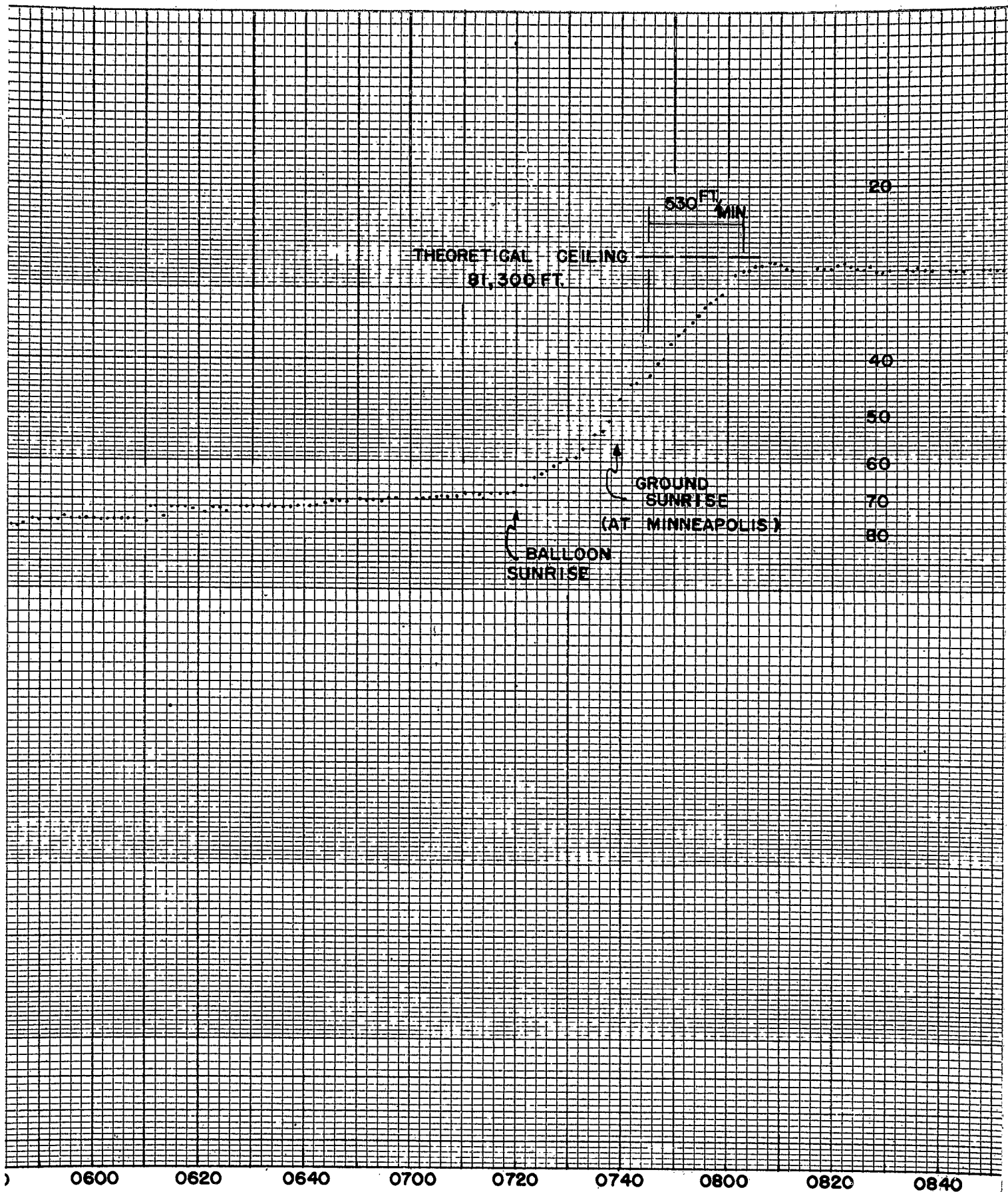




2400 0020 0040 0100 0120 0140 0200 0220 0240 0300

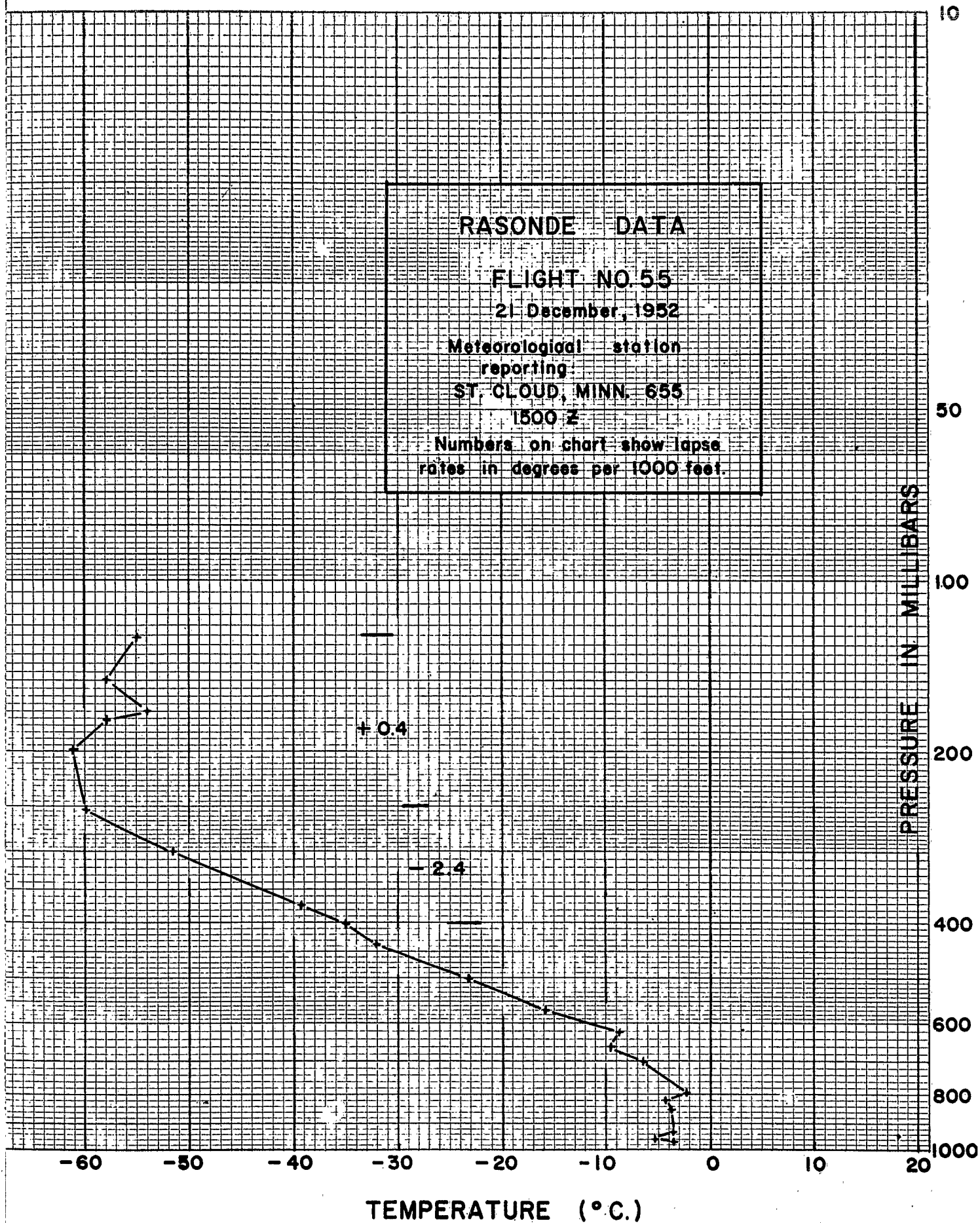
→ 8 DECEMBER





SIGNAL LOST

0840 0900 0920 0940 1000 1020 1040 1100 1120 1140



TIME - PRESSURE - ALTITUDE

FLIGHT NO. 55

21 DECEMBER, 1952

GROSS LOAD: 316 LBS.

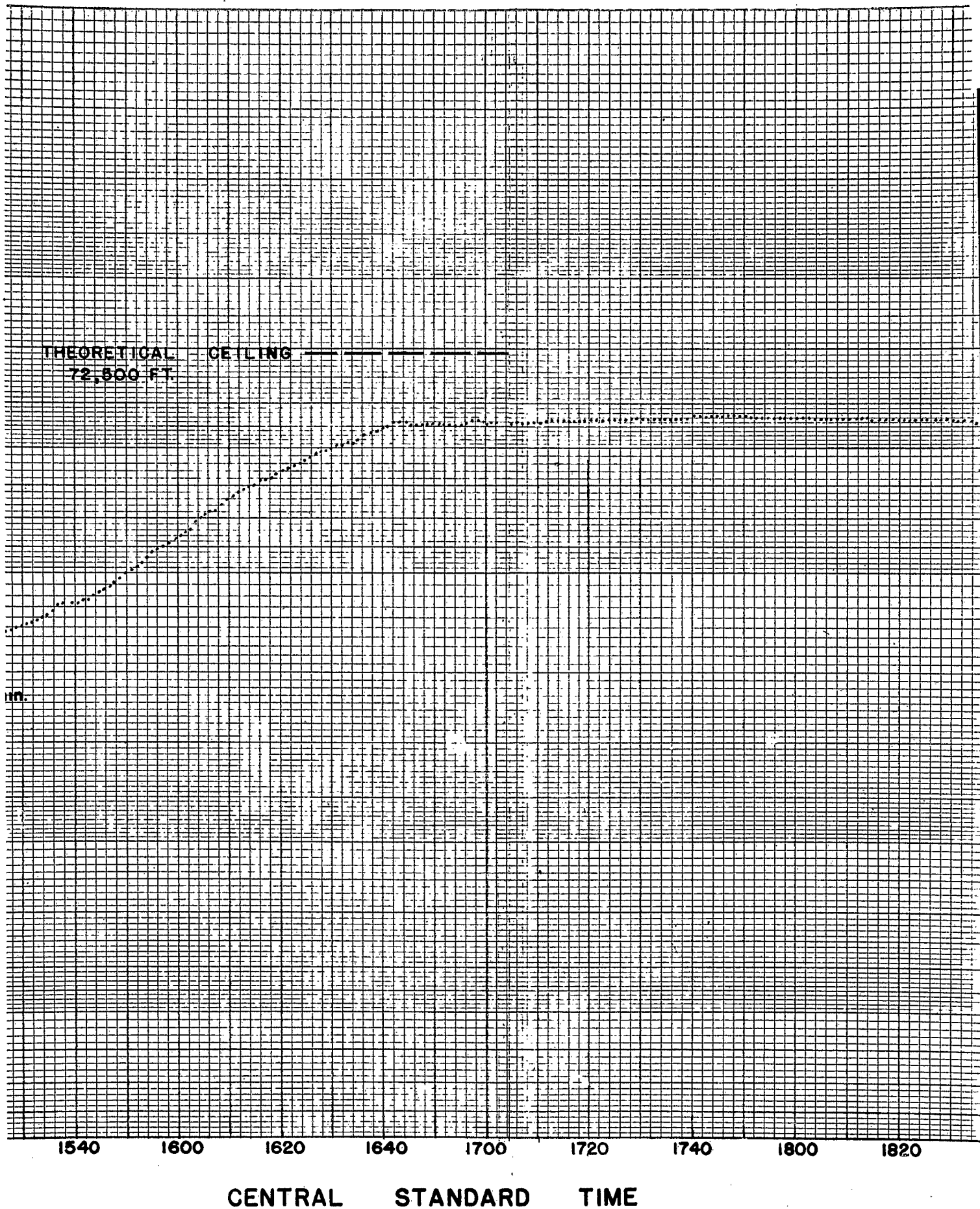
FREE LIFT: 79 LBS.

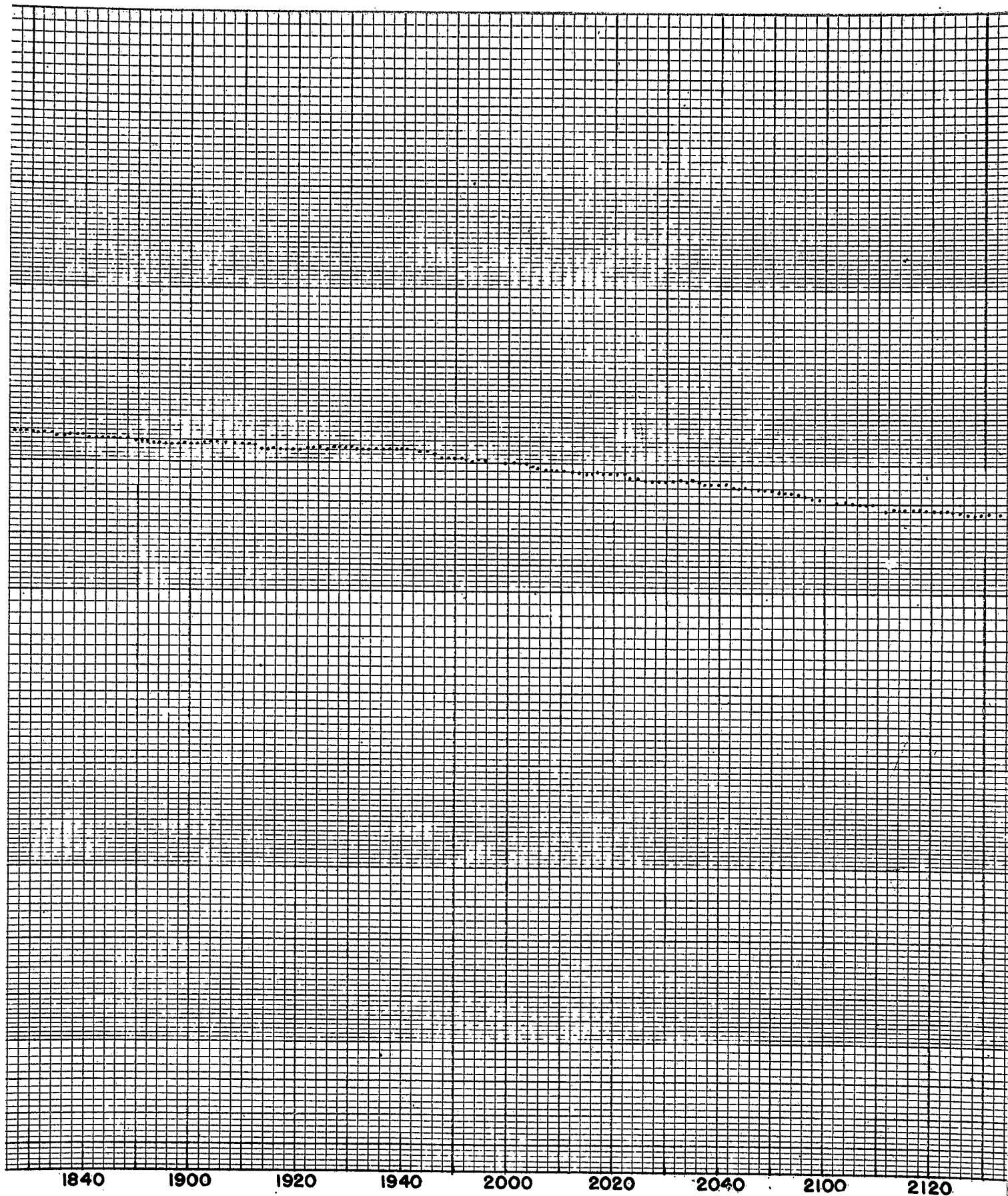
GROSS LIFT: 394 LBS.

FROM TELEMETER RECORD

1240 1300 1320 1340 1400 1420 1440 1500 1520

BALLOON LAUNCHED





1840

1900

1920

1940

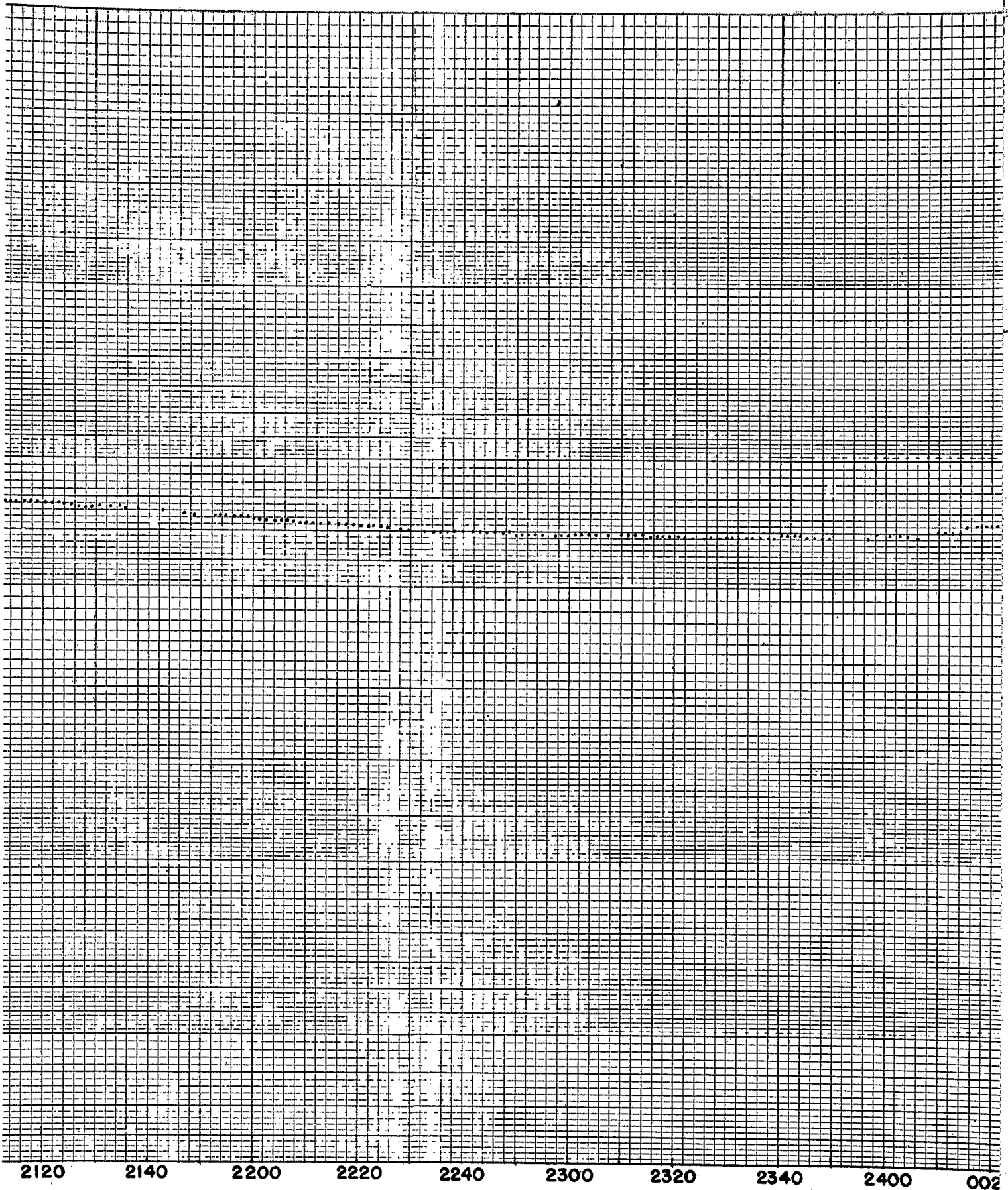
2000

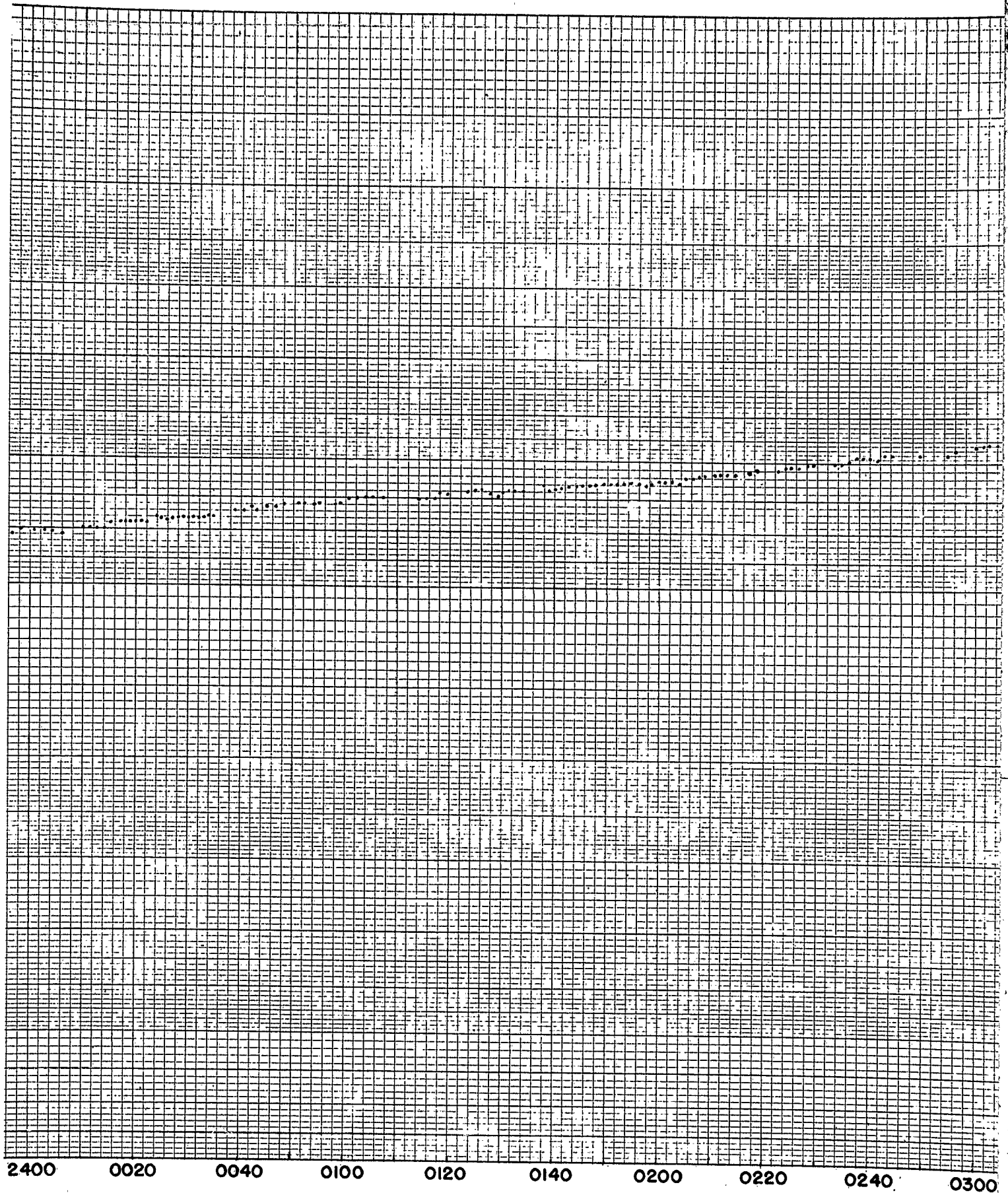
2020

2040

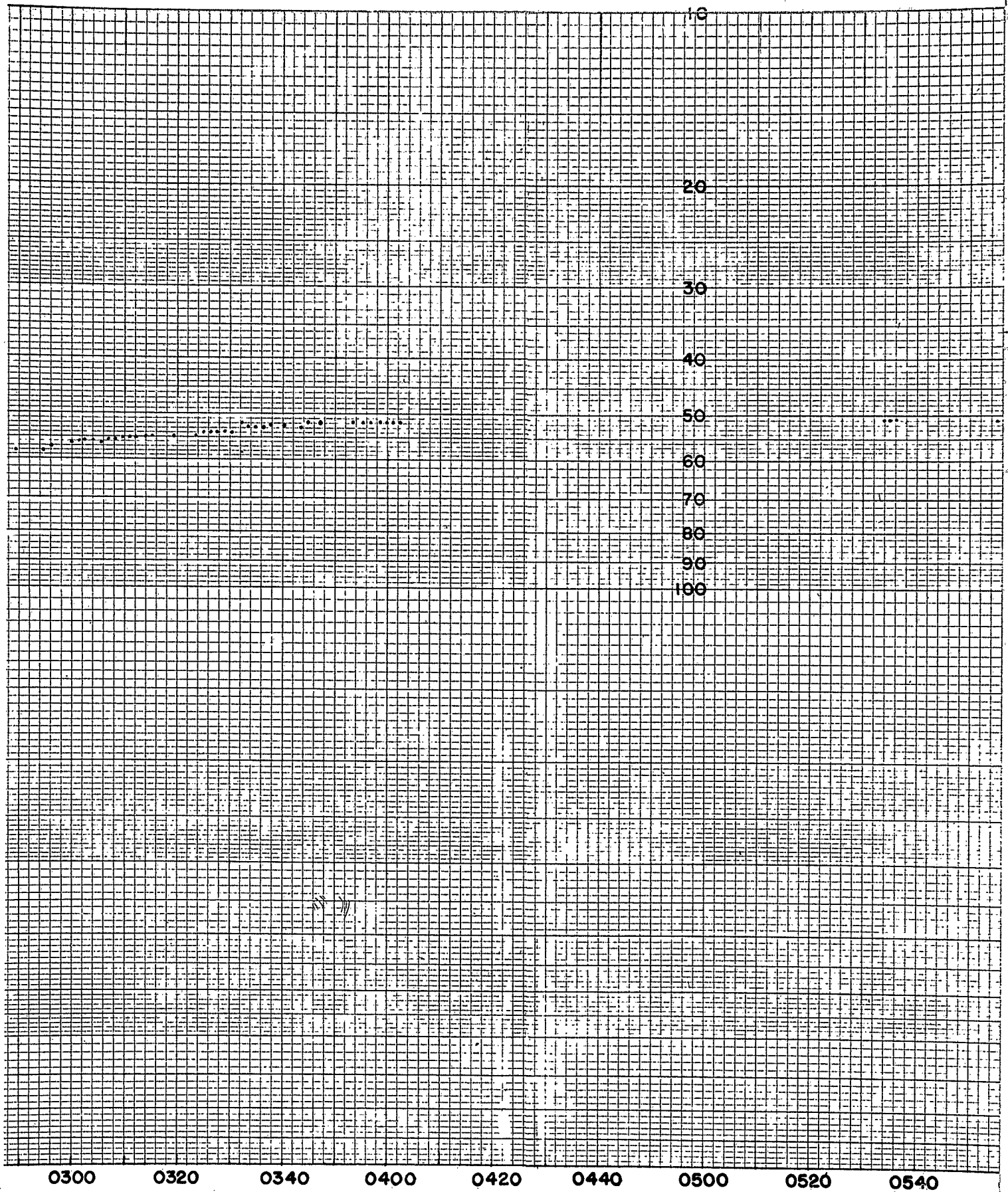
2100

2120





→ 22 DECEMBER



SIGNAL FADED IN
MINNEAPOLIS, MINN.

x x POINTS
KALAMAZOO

0600

0620

0640

0700

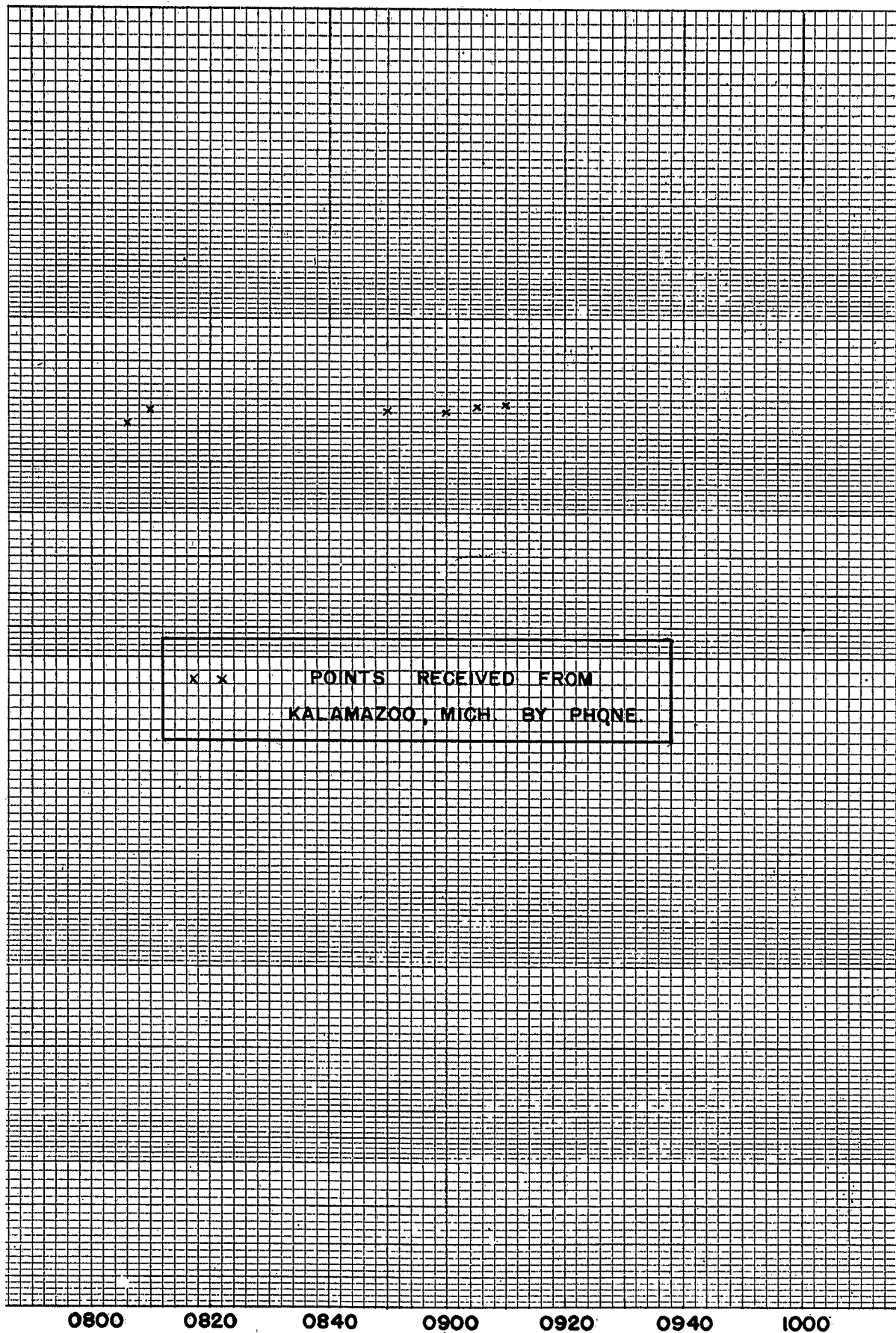
0720

0740

0800

0820

0840



BALLOON
LAUNCHED



1320 1340 1400 1420 1440 1500 1520 1540 1600

Confidential Security Information

TIME — TEMPERATURE

FLIGHT NO.24

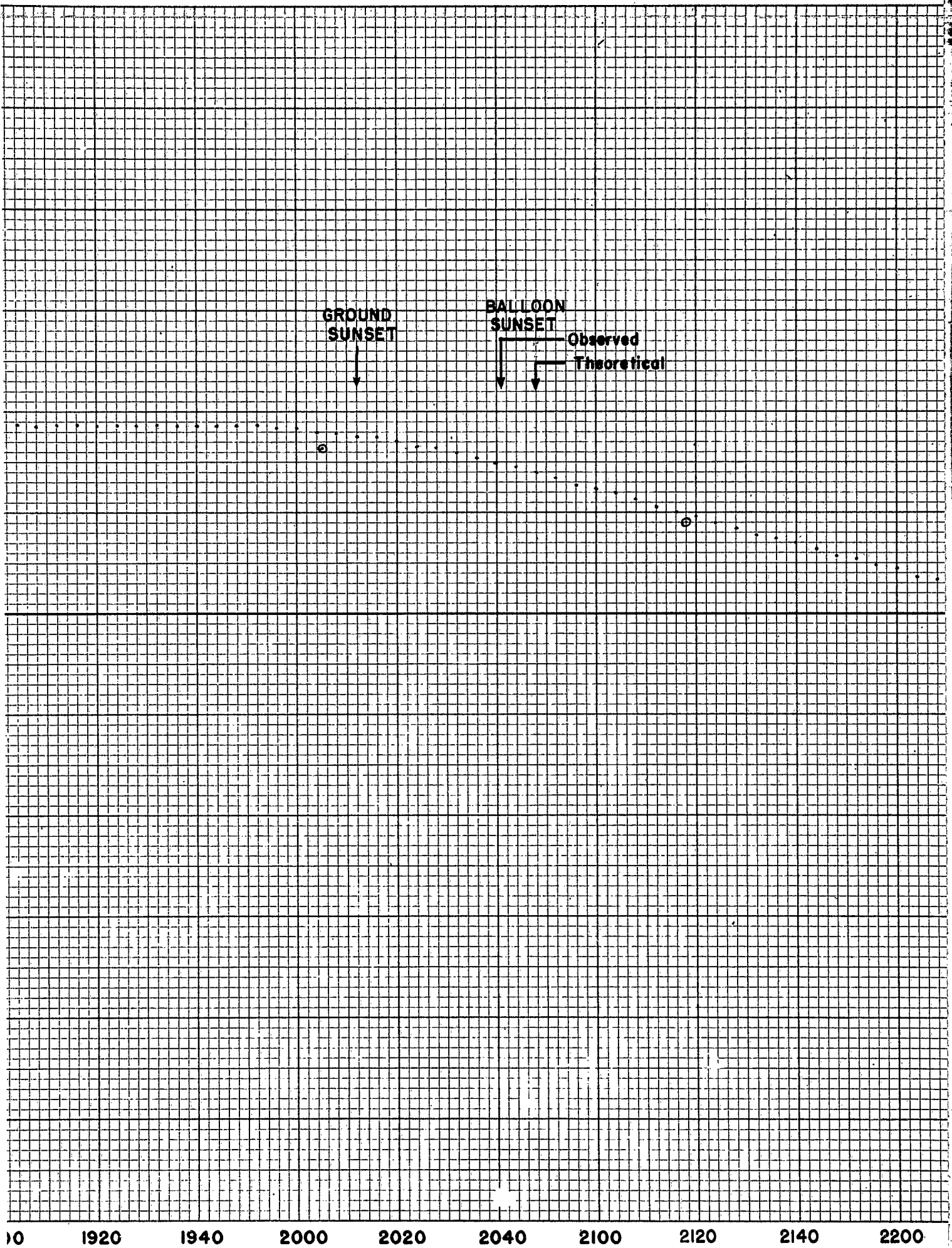
8 & 9 JULY, 1952

DATA FROM THERMOGRAPH RECORD

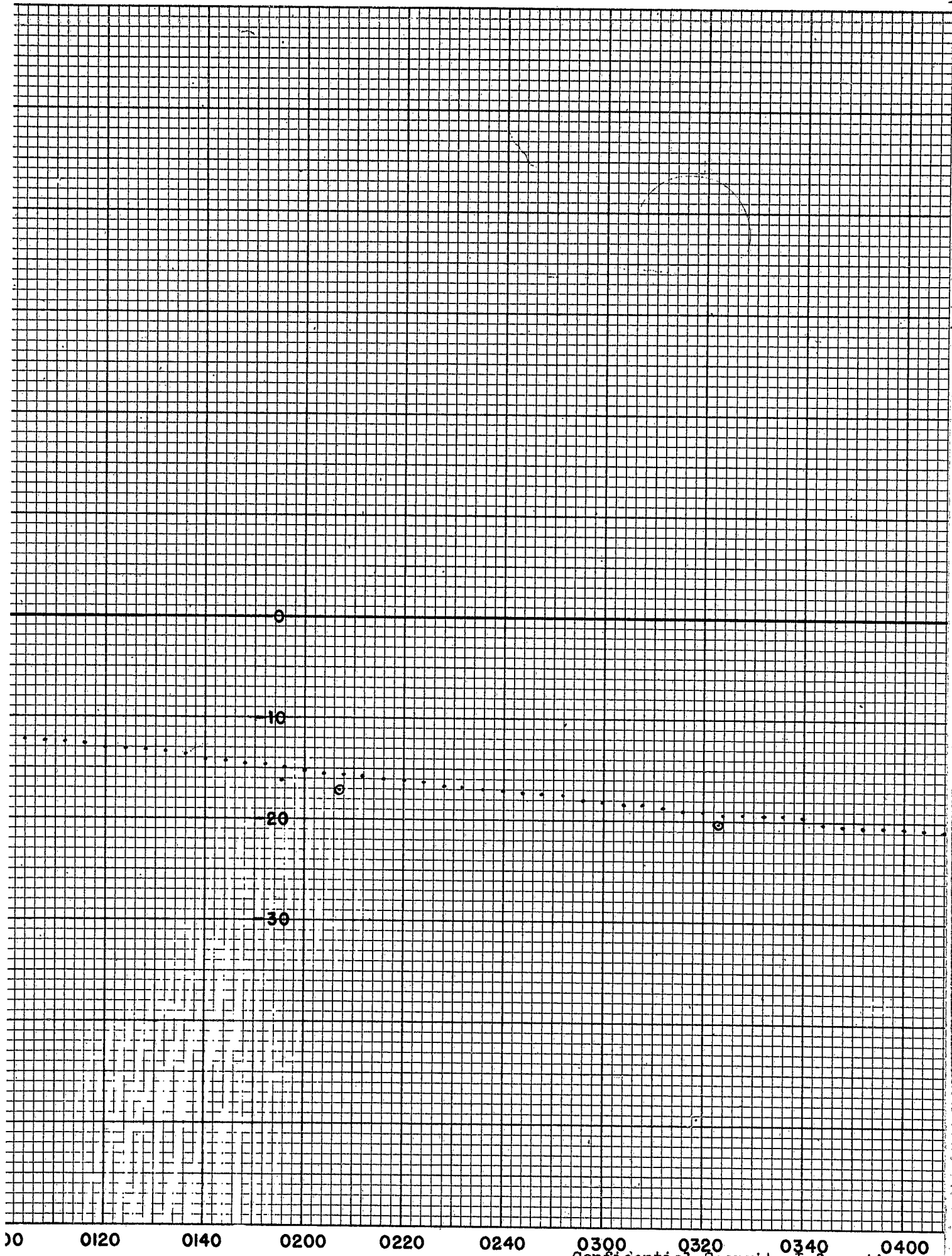
• • • FIRST READING

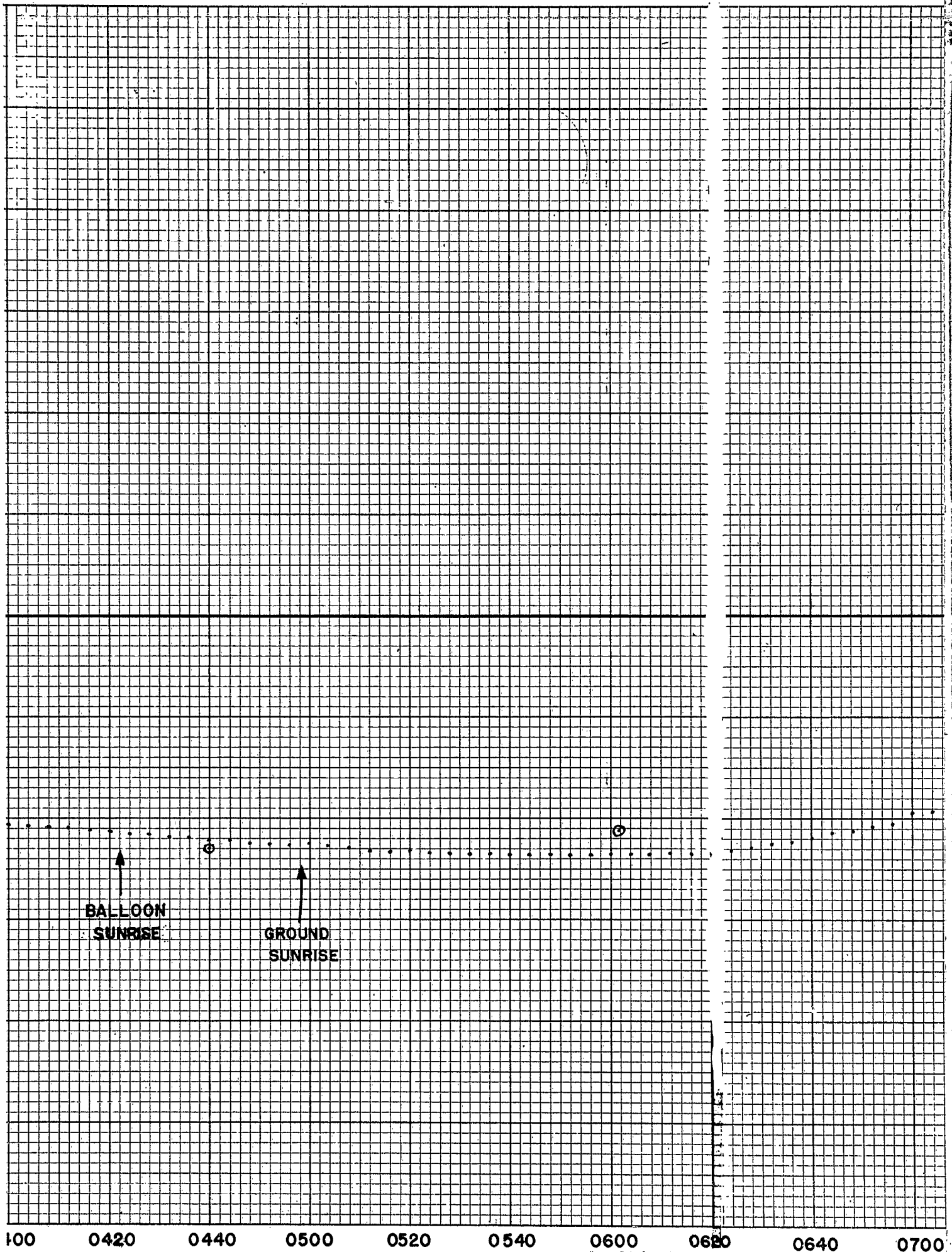
○ ○ RE CHECK

1620 1640 1700 1720 1740 1800 1820 1840 1900
CENTRAL STANDARD TIME Confidential Security Information

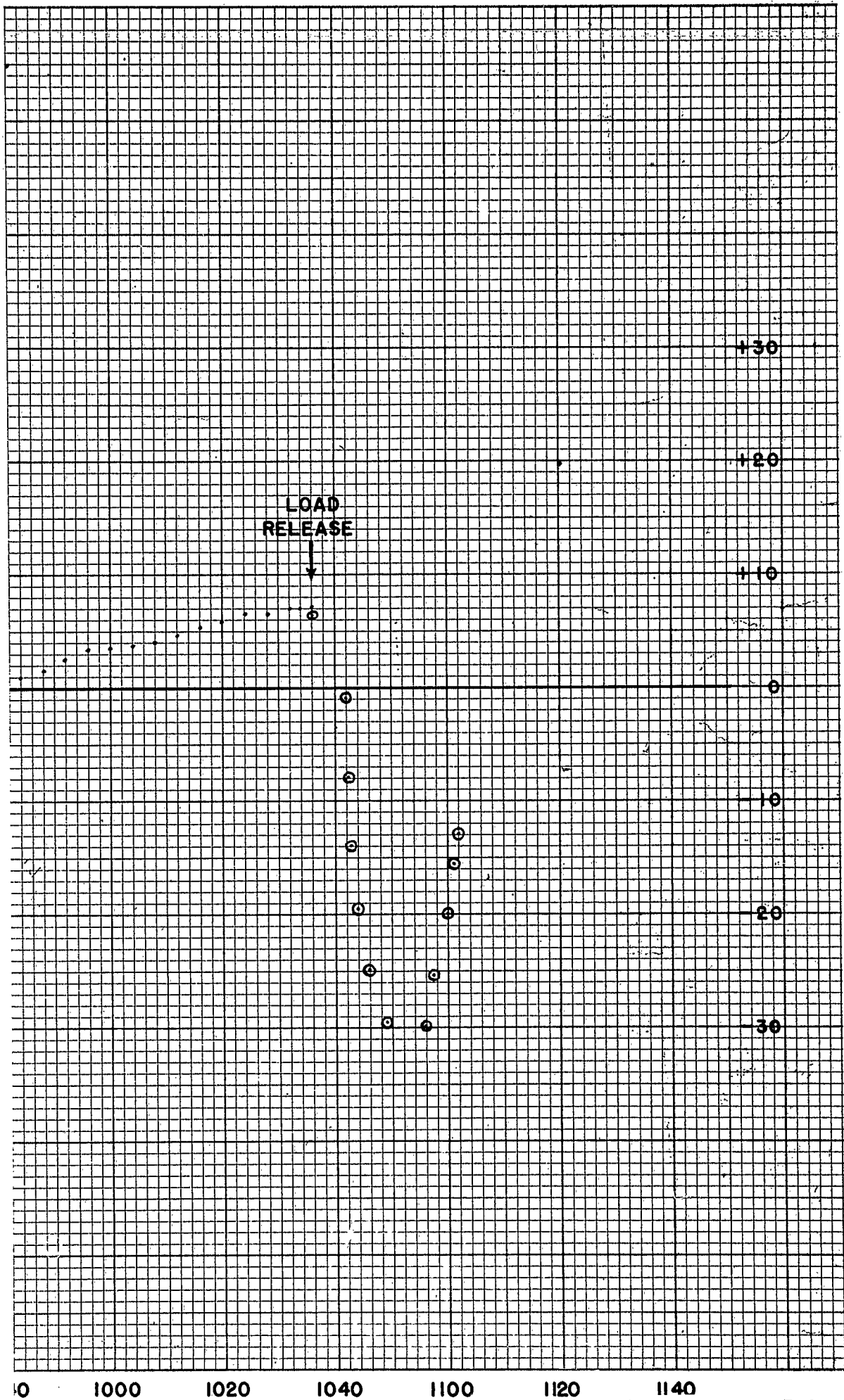


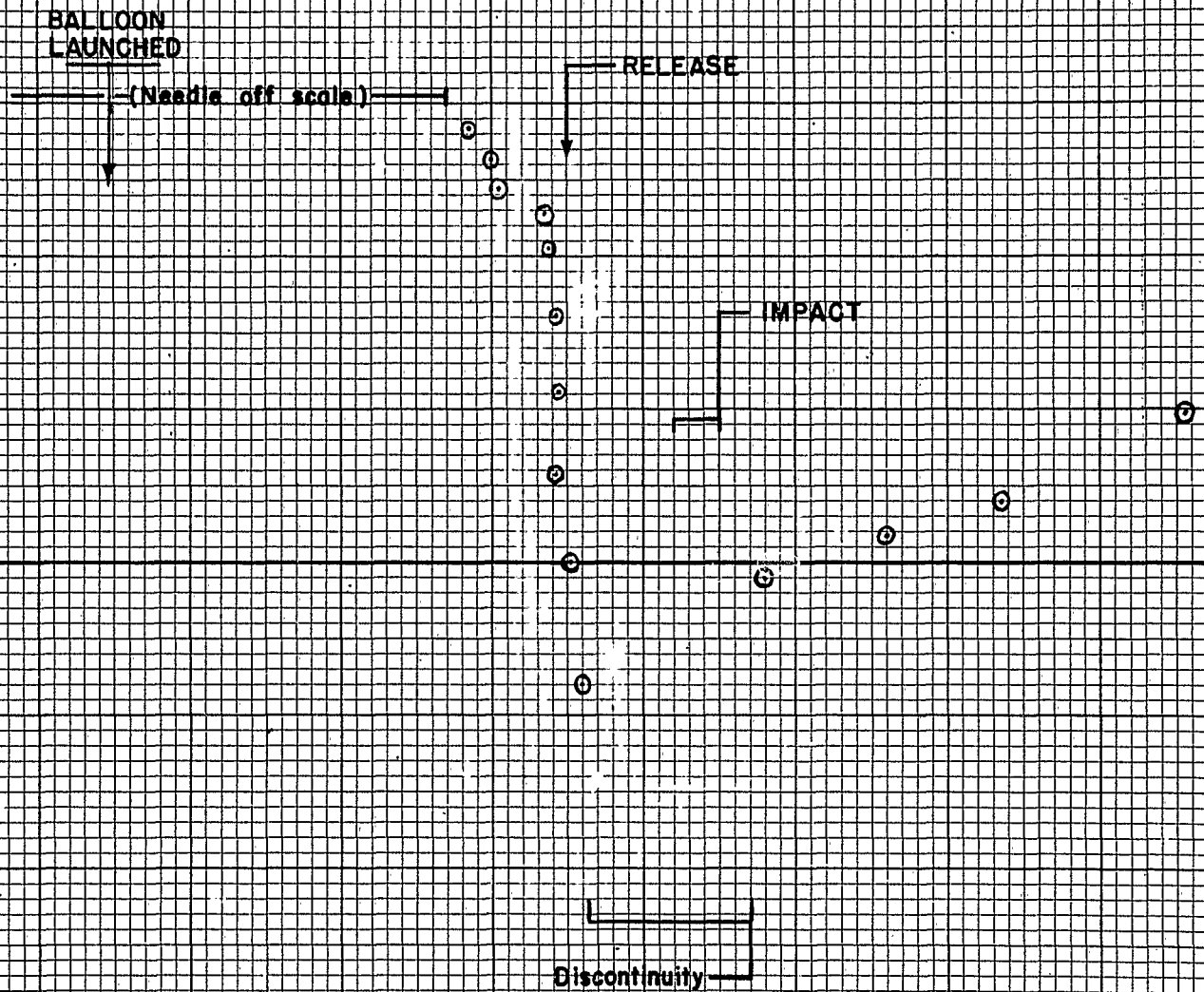












TIME — TEMPERATURE

FLIGHT NO. 26

21 JULY, 1952

DATA FROM THERMOGRAPH RECORD

BALLOON
LAUNCHED

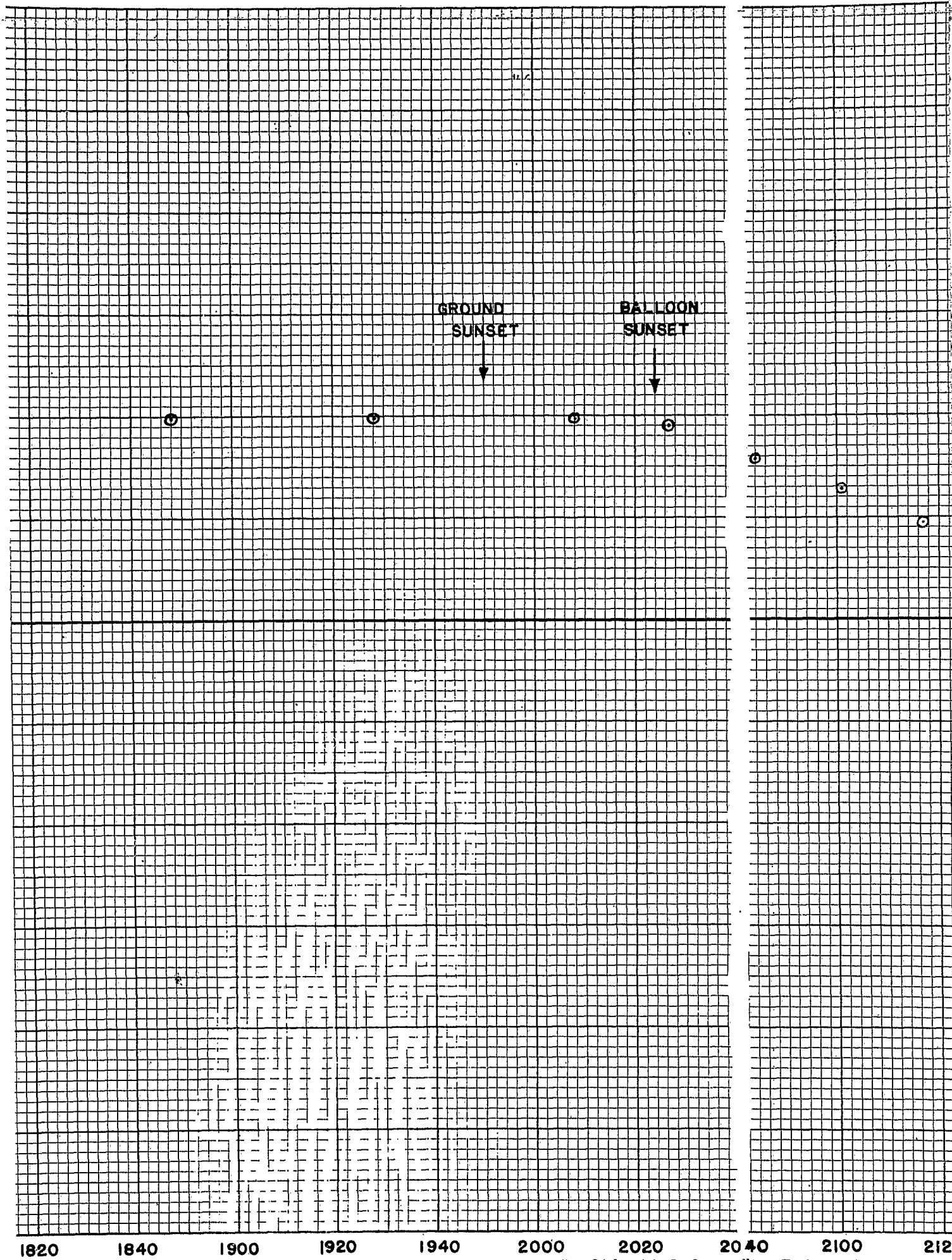
TIME — TEMPERATURE

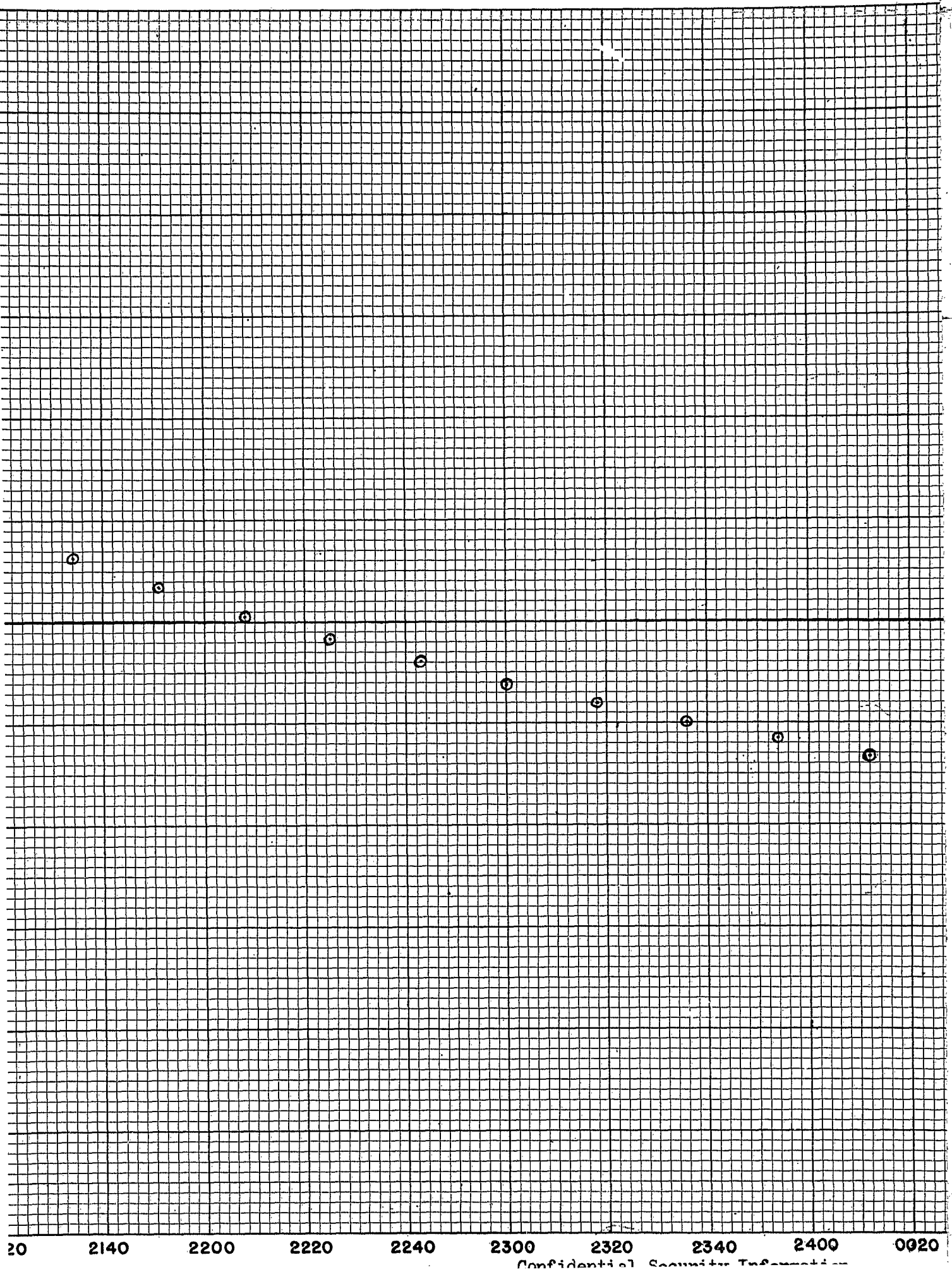
FLIGHT NO 27

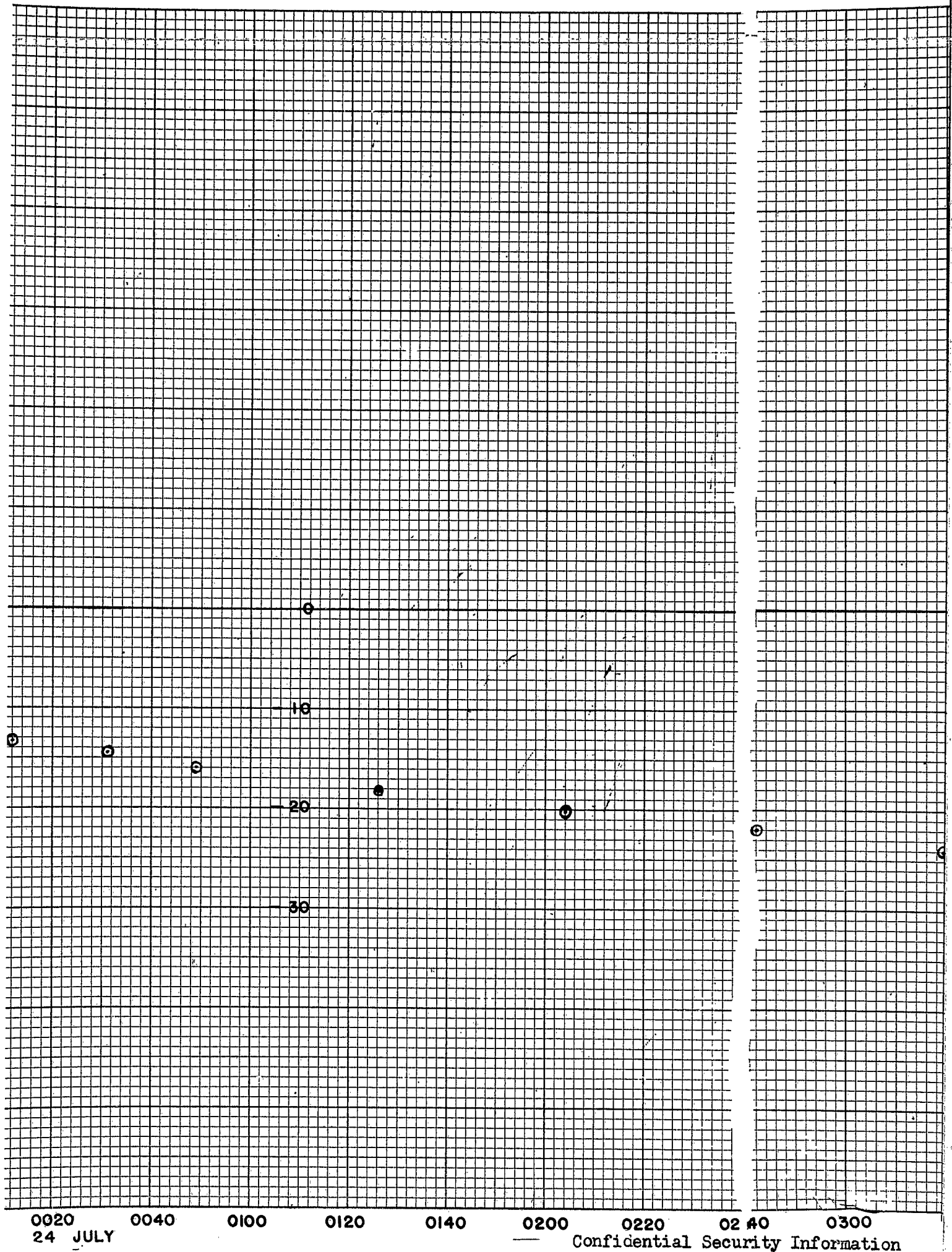
23 JULY, 1952

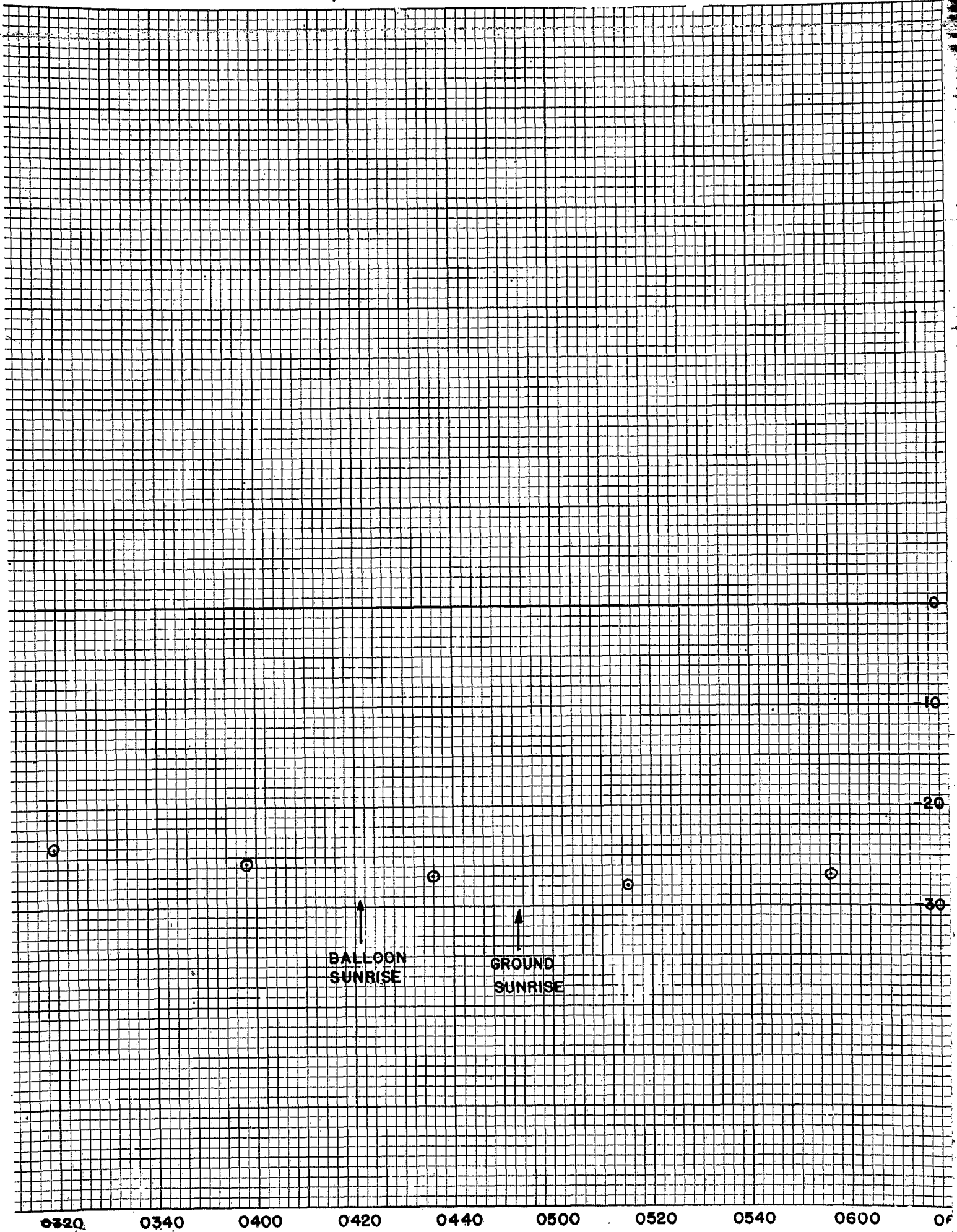
DATA OBTAINED FROM
THERMOGRAPH RECORD

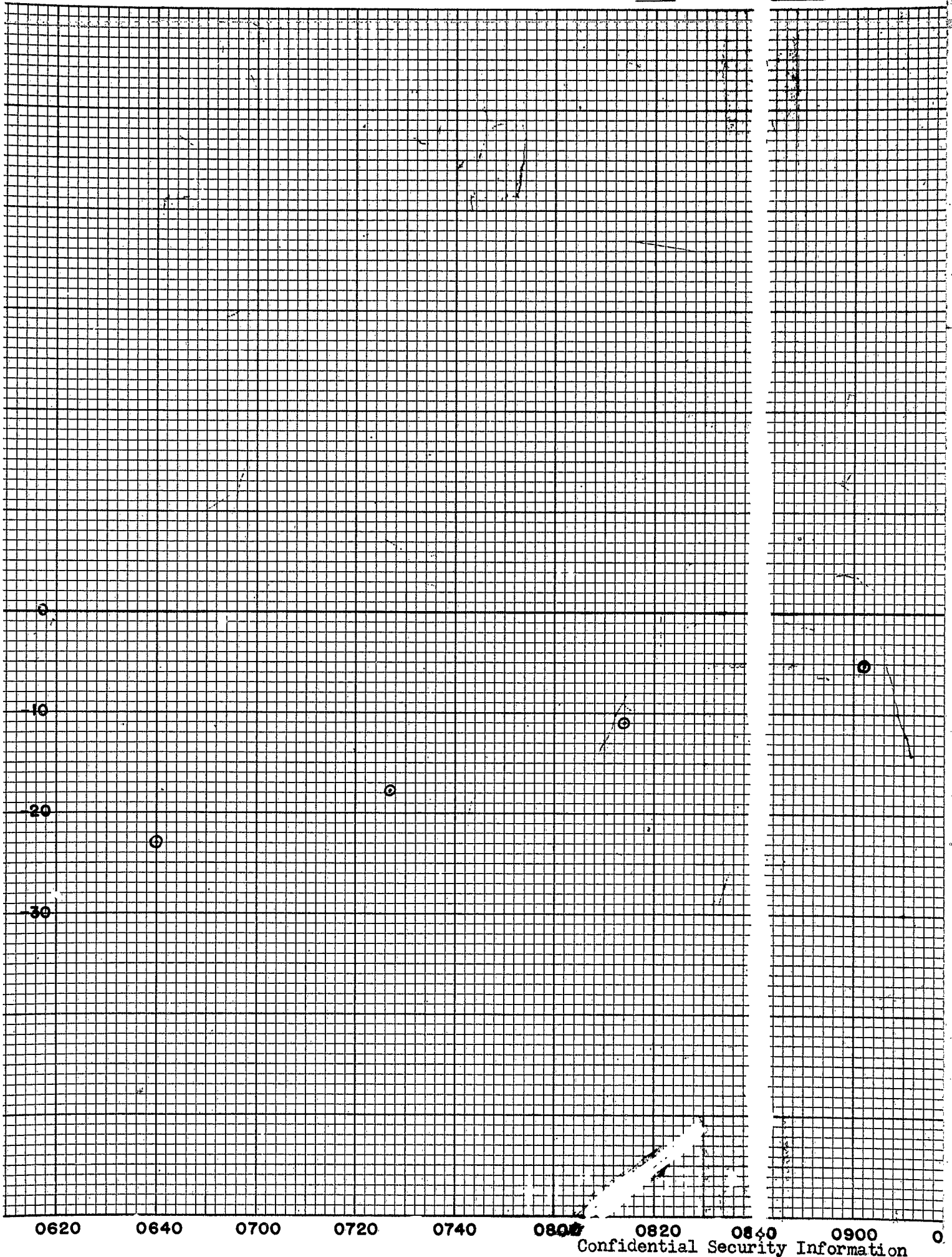
1520 1540 1600 1620 1640 1700 1720 1740 1800 1820

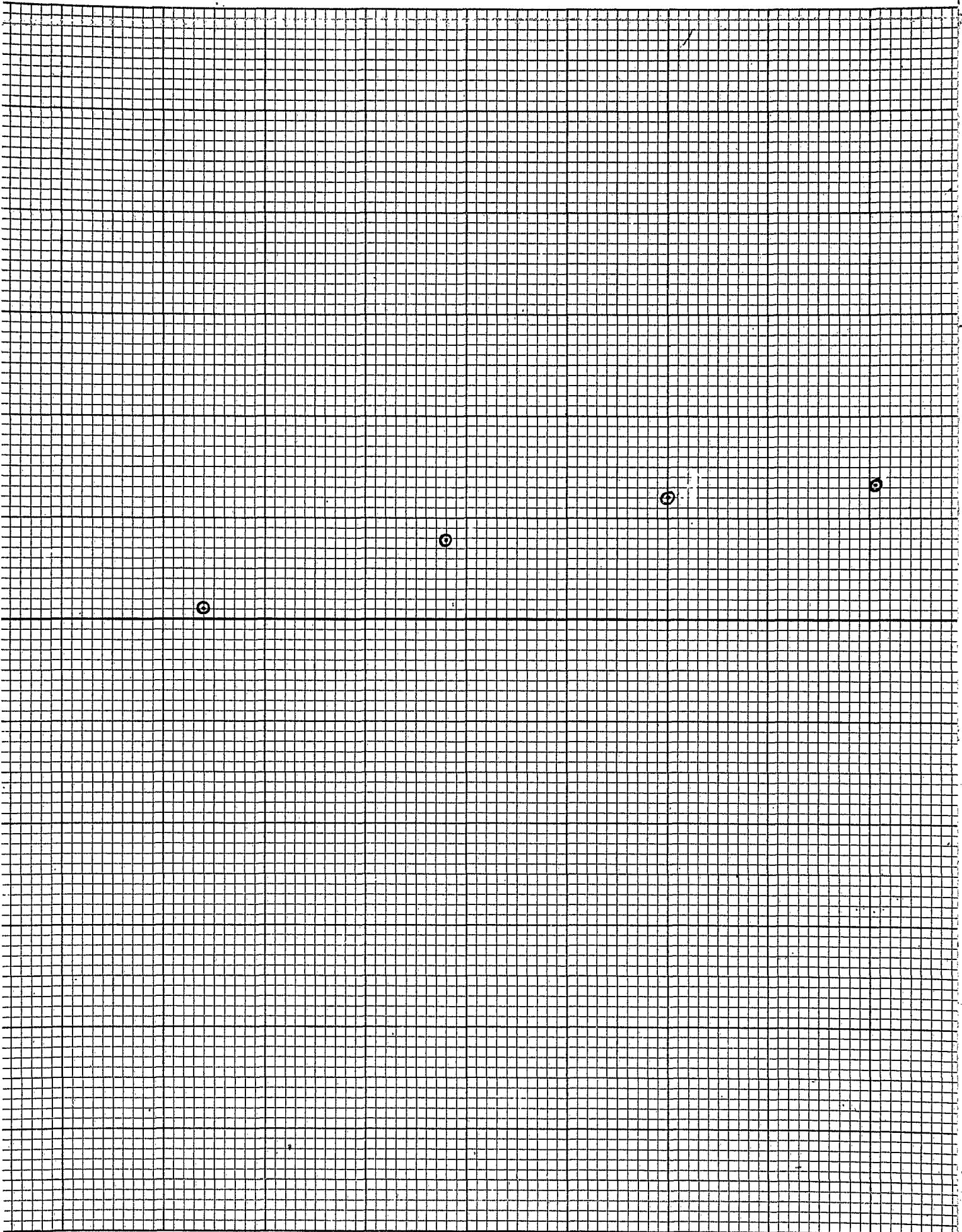


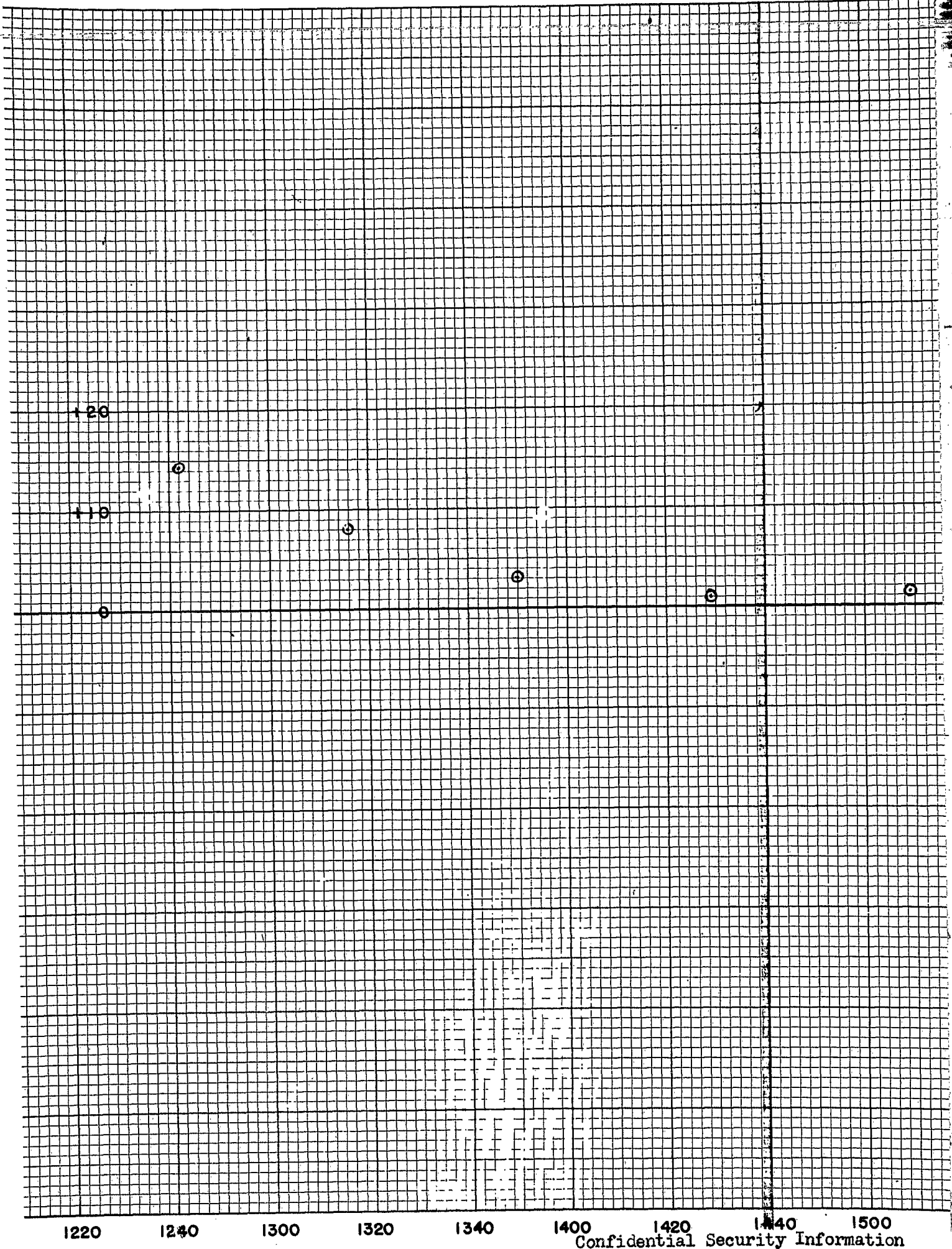


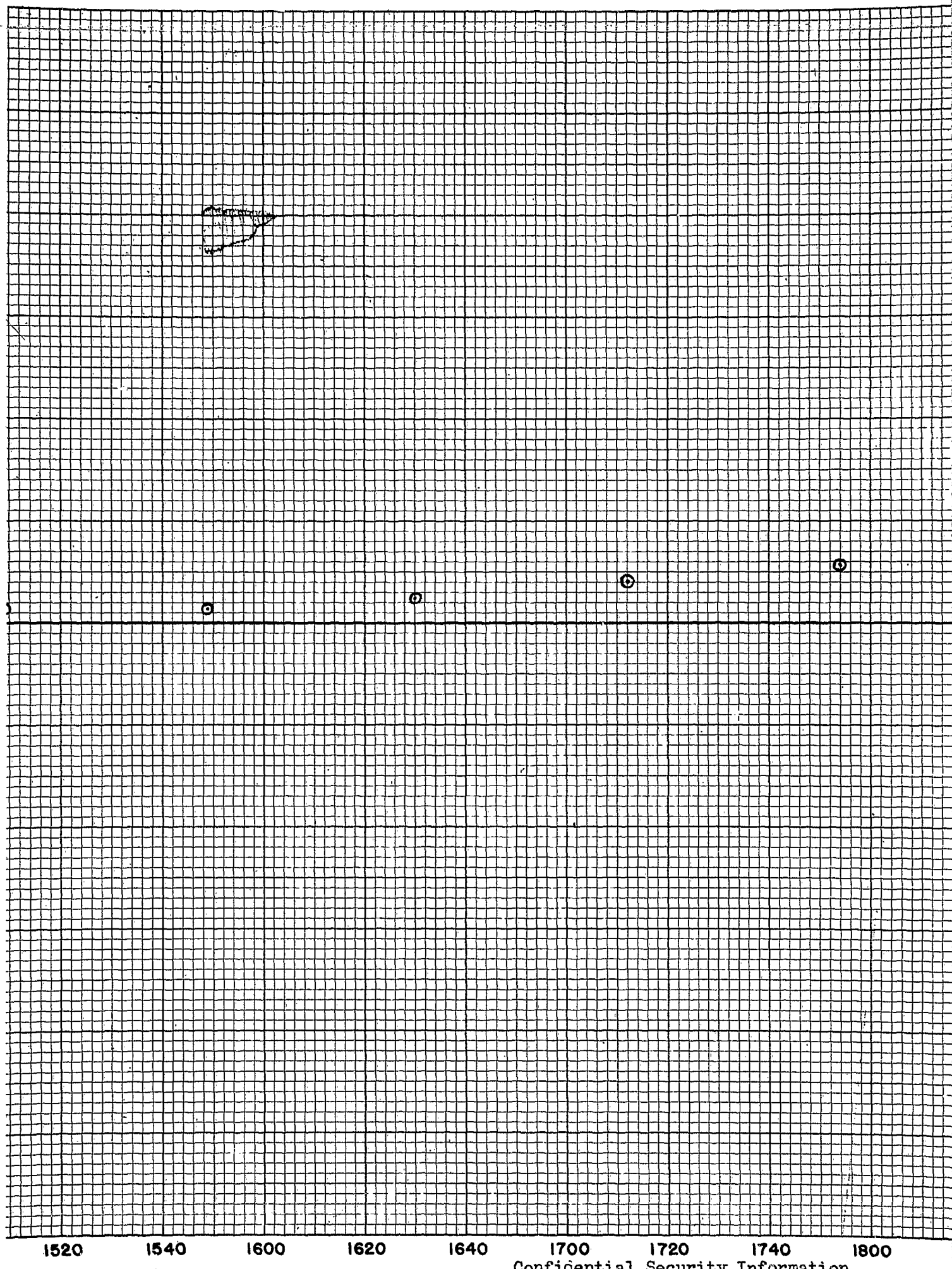


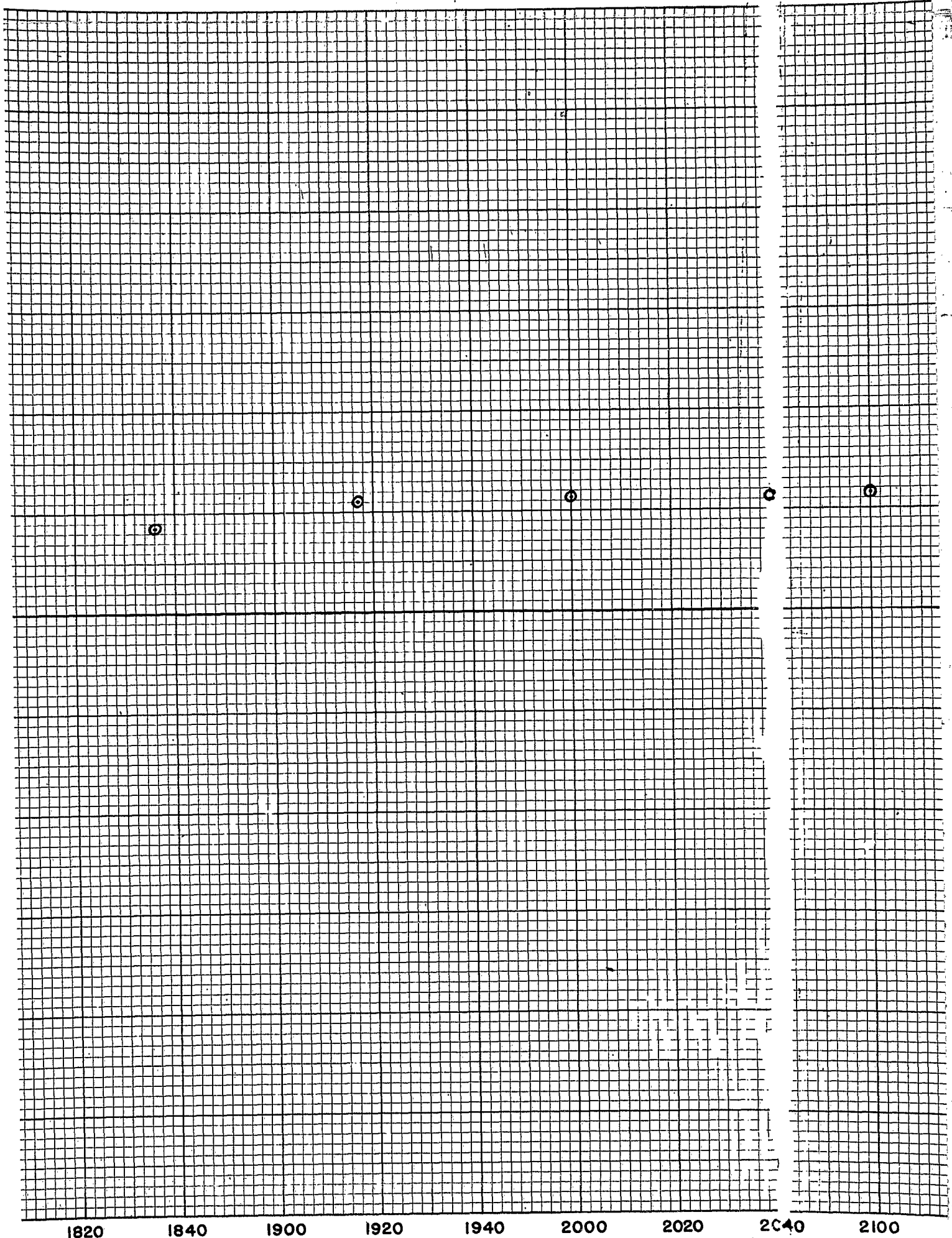


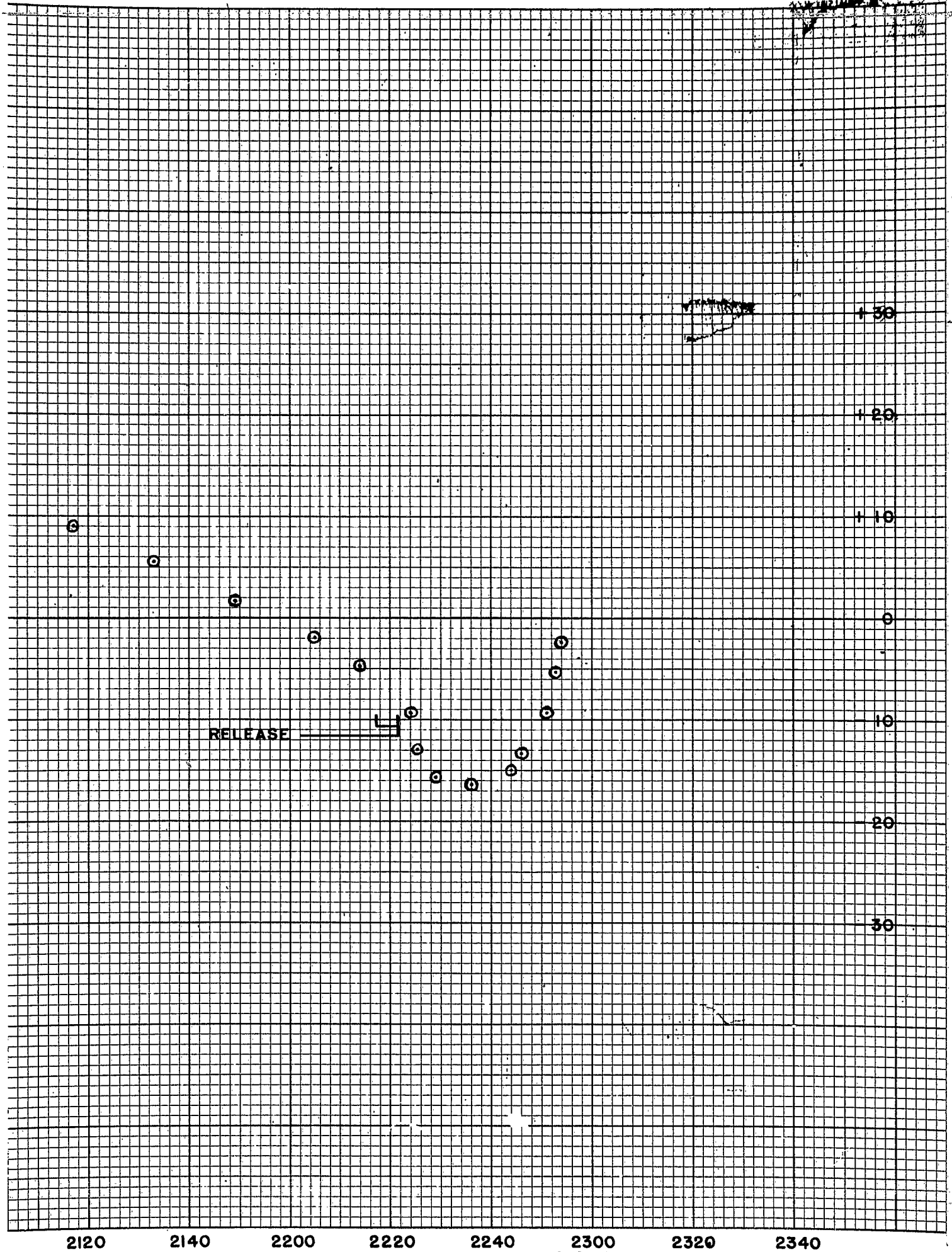




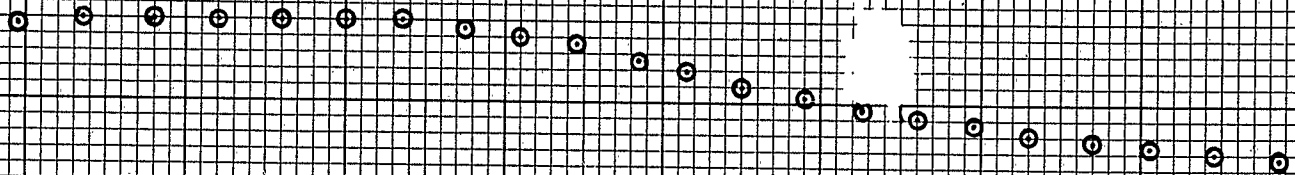


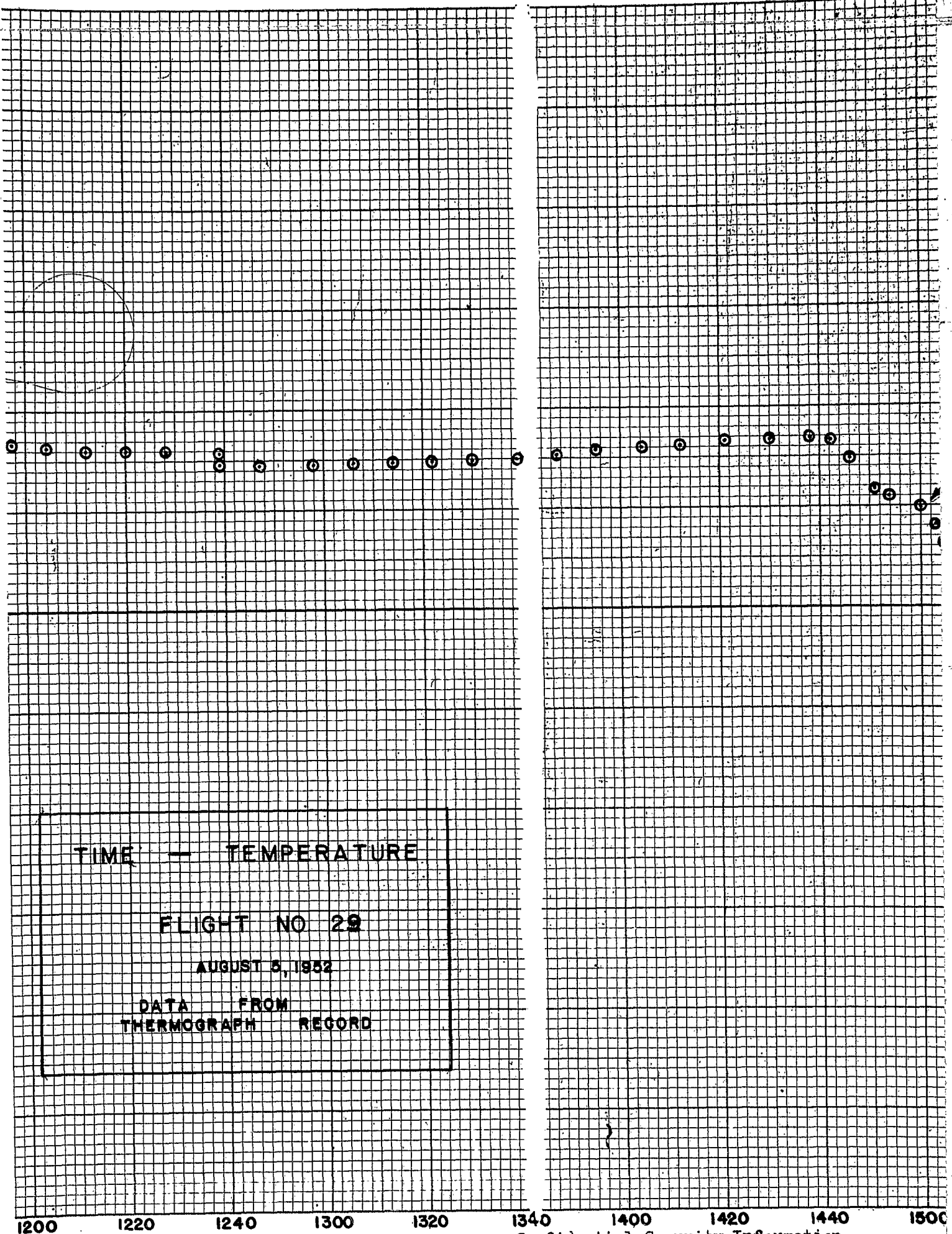


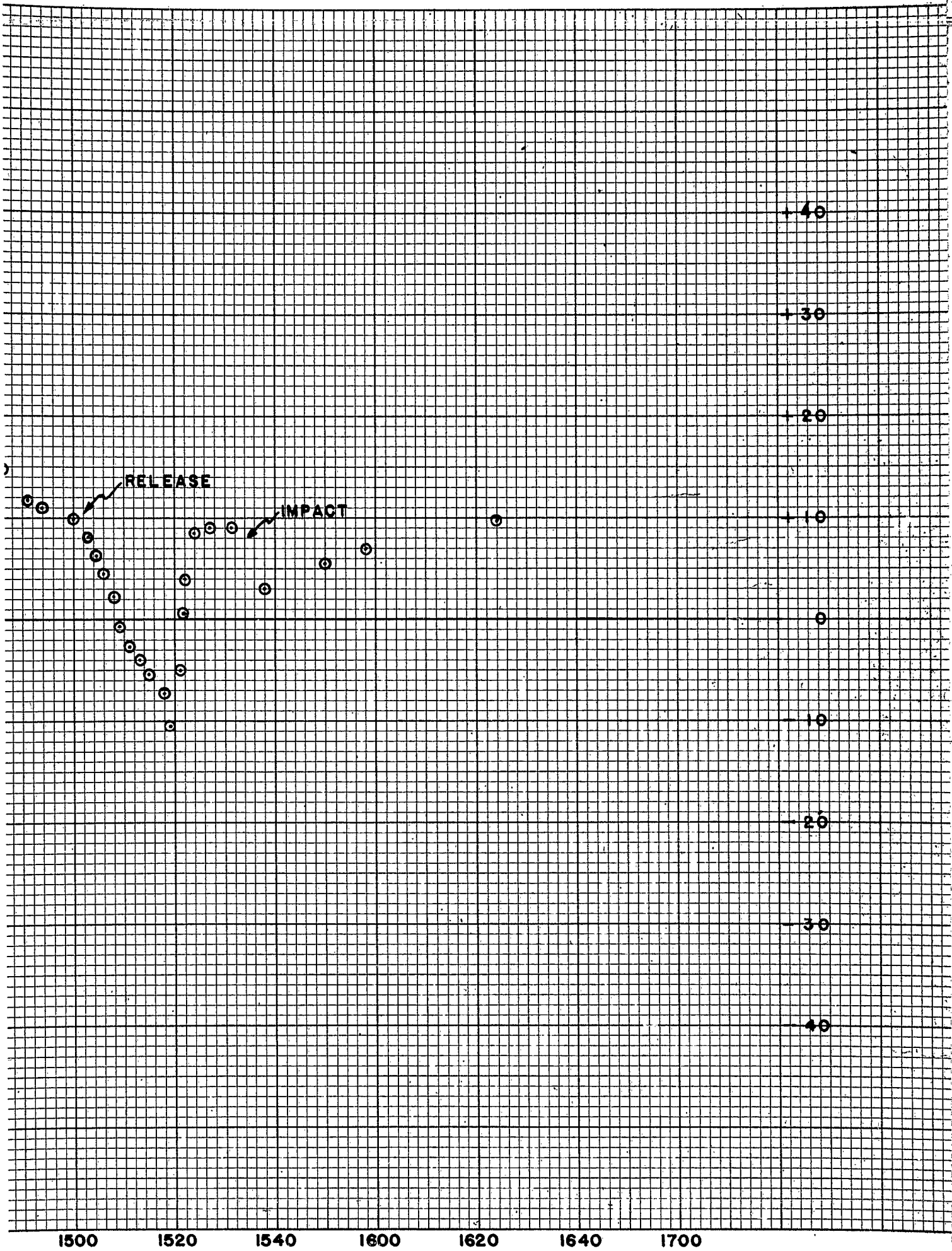


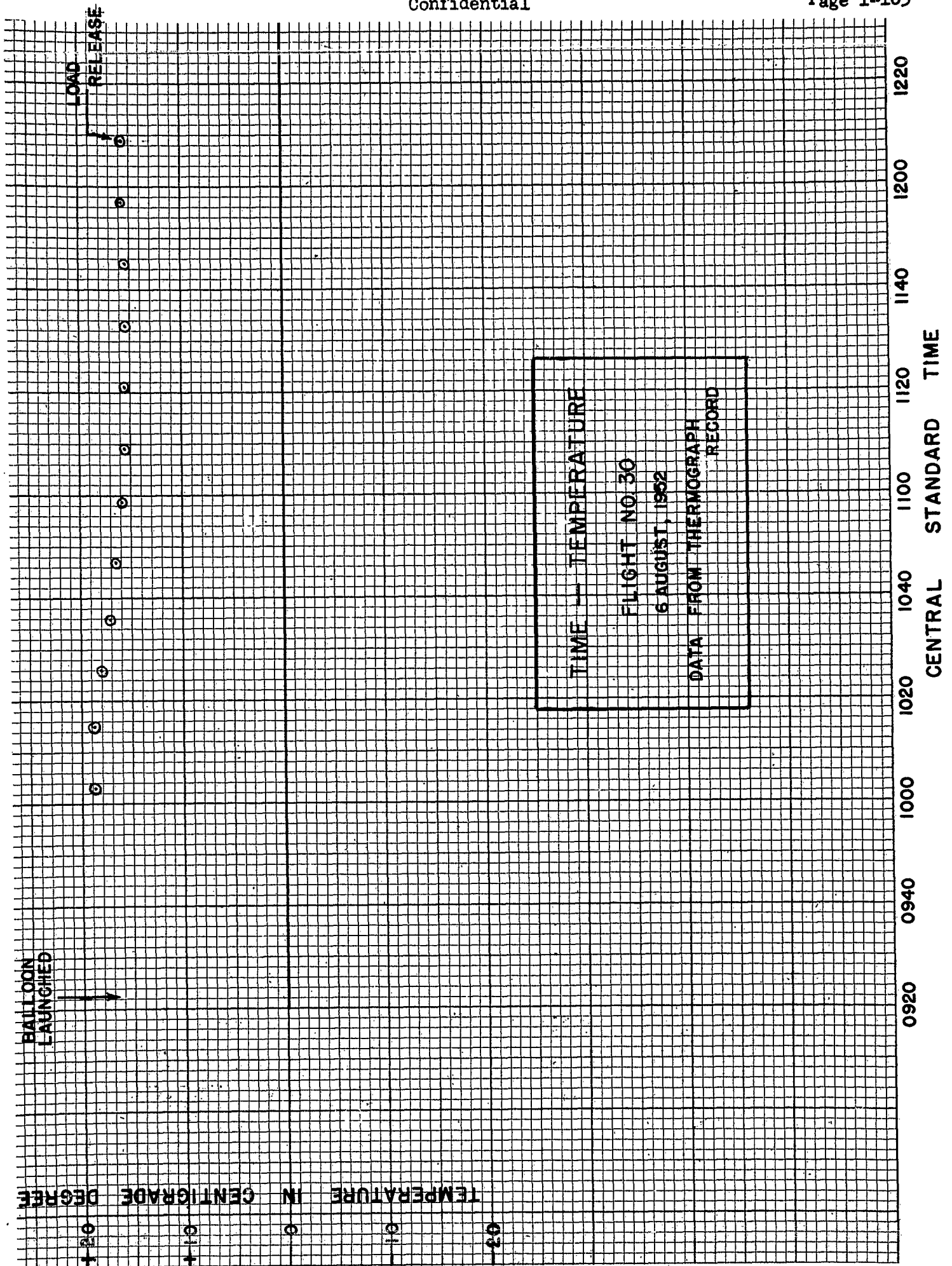


BALLOON
LAUNCHED









BALLOON LAUNCHED
AT 0751 19 AUGUST

THERE IS NO READABLE
THERMOGRAPH RECORD FOR
THE TIME PREVIOUS TO 1821

1600

1620

1640

1700

1720

1740

1800

1820

1840

Confidential Security Information

GROUND
SUNSET

BALLOON
SUNSET

OBSERVED

THEORETICAL

TIME — TEMPERATURE

FLIGHT NO. 32

19 AUGUST, 1952

DATA FROM THERMOGRAPH RECORD

1900

1920

1940

2000

2020

2040

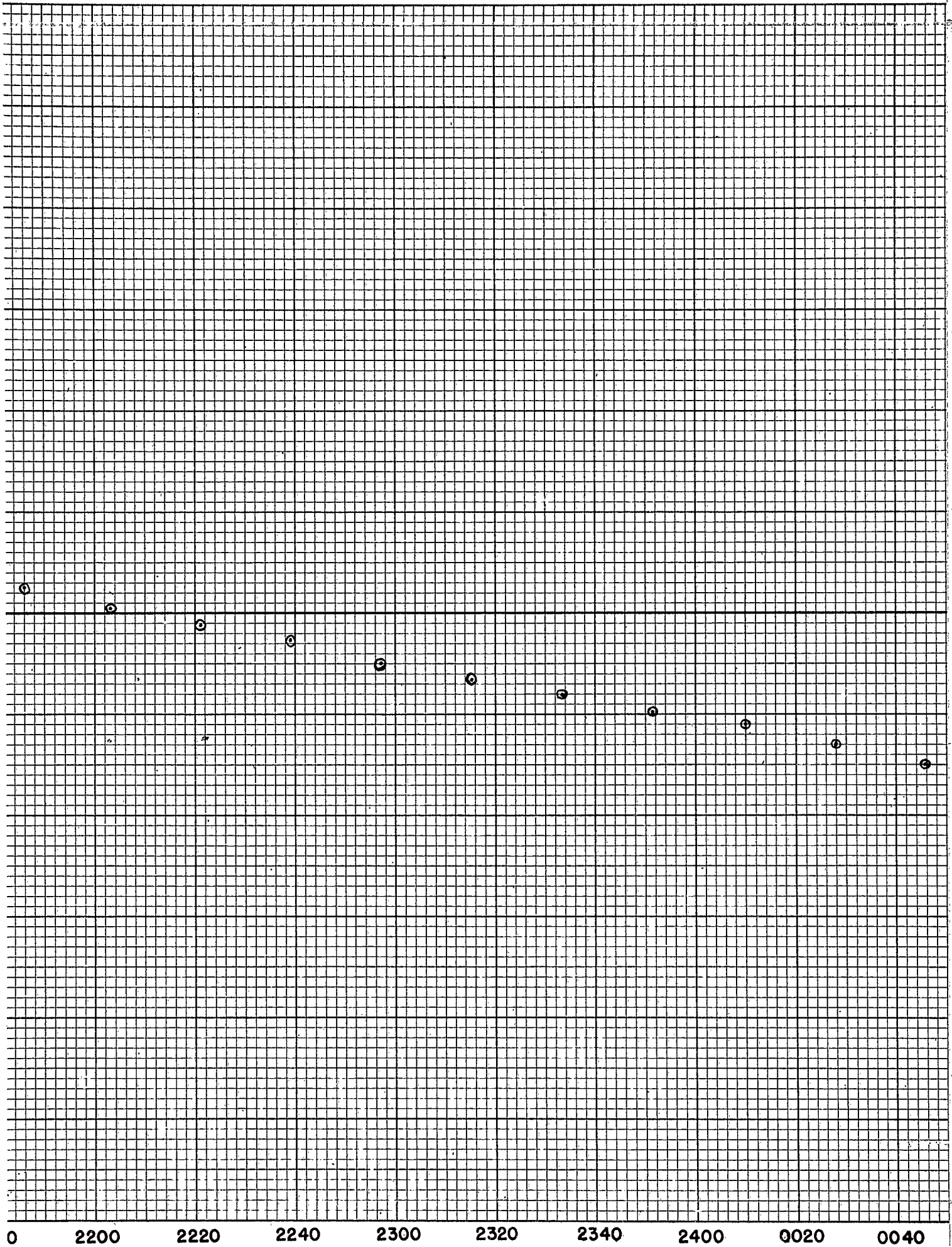
2100

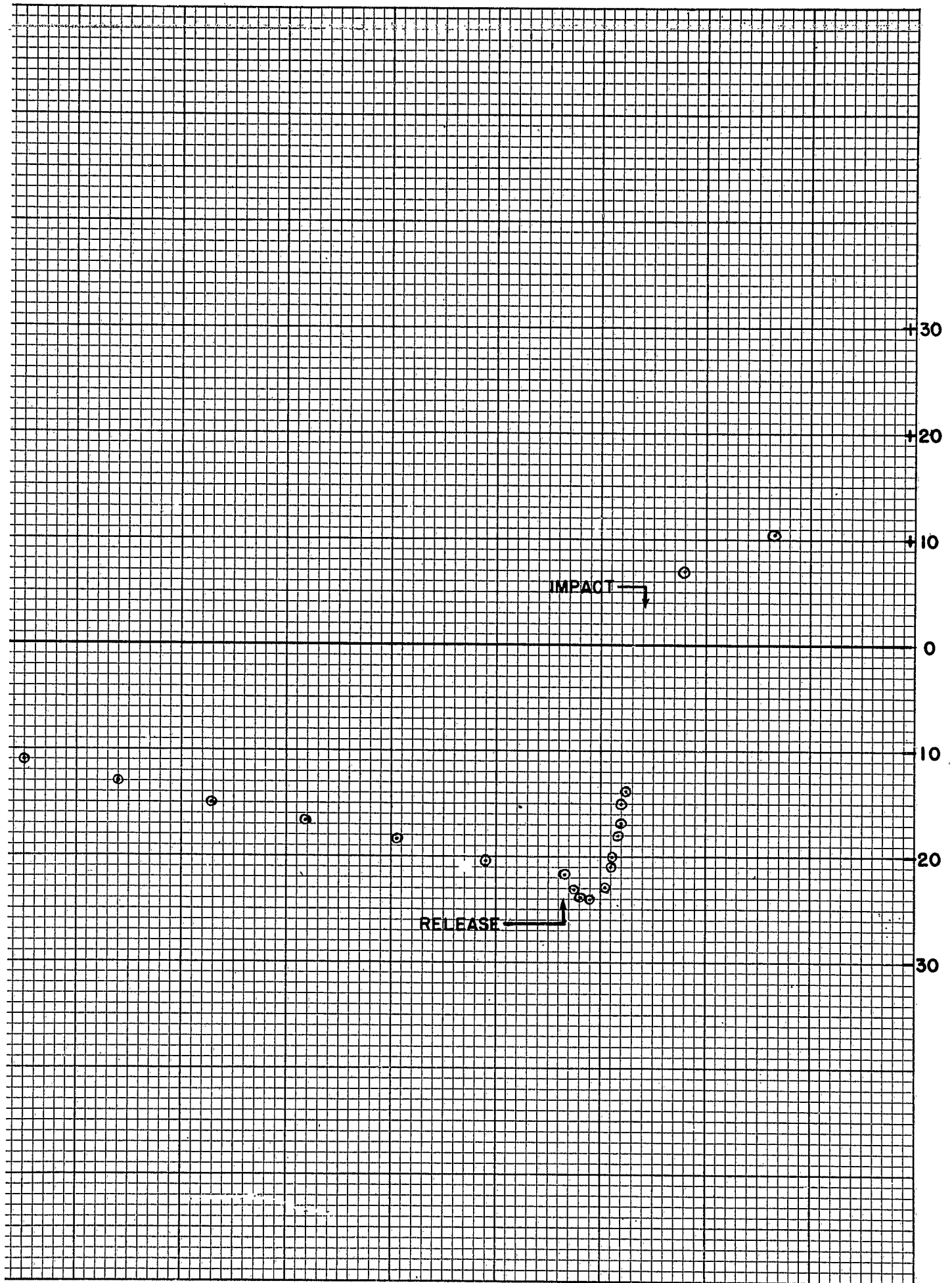
2120

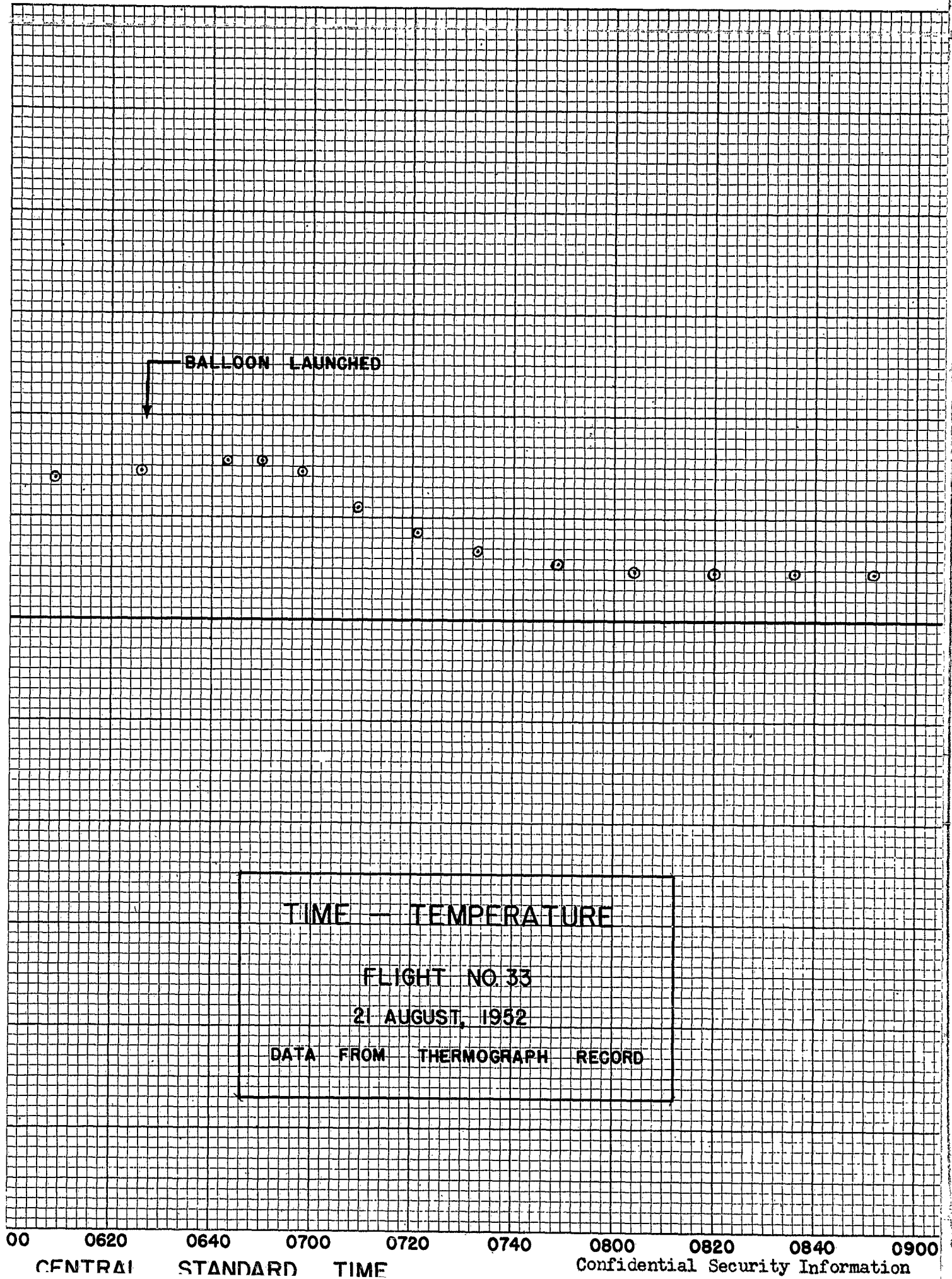
2140

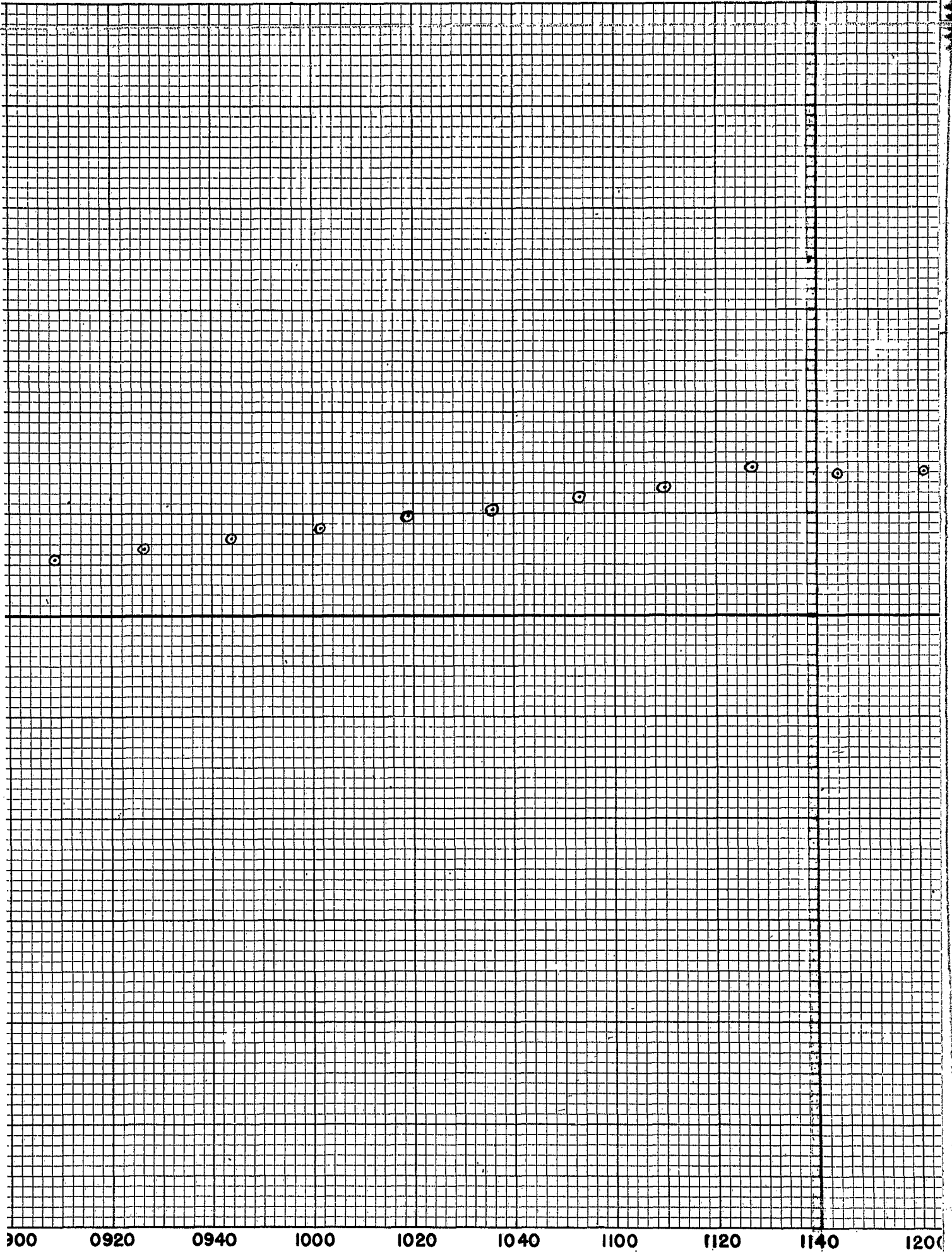
CENTRAL STANDARD TIME

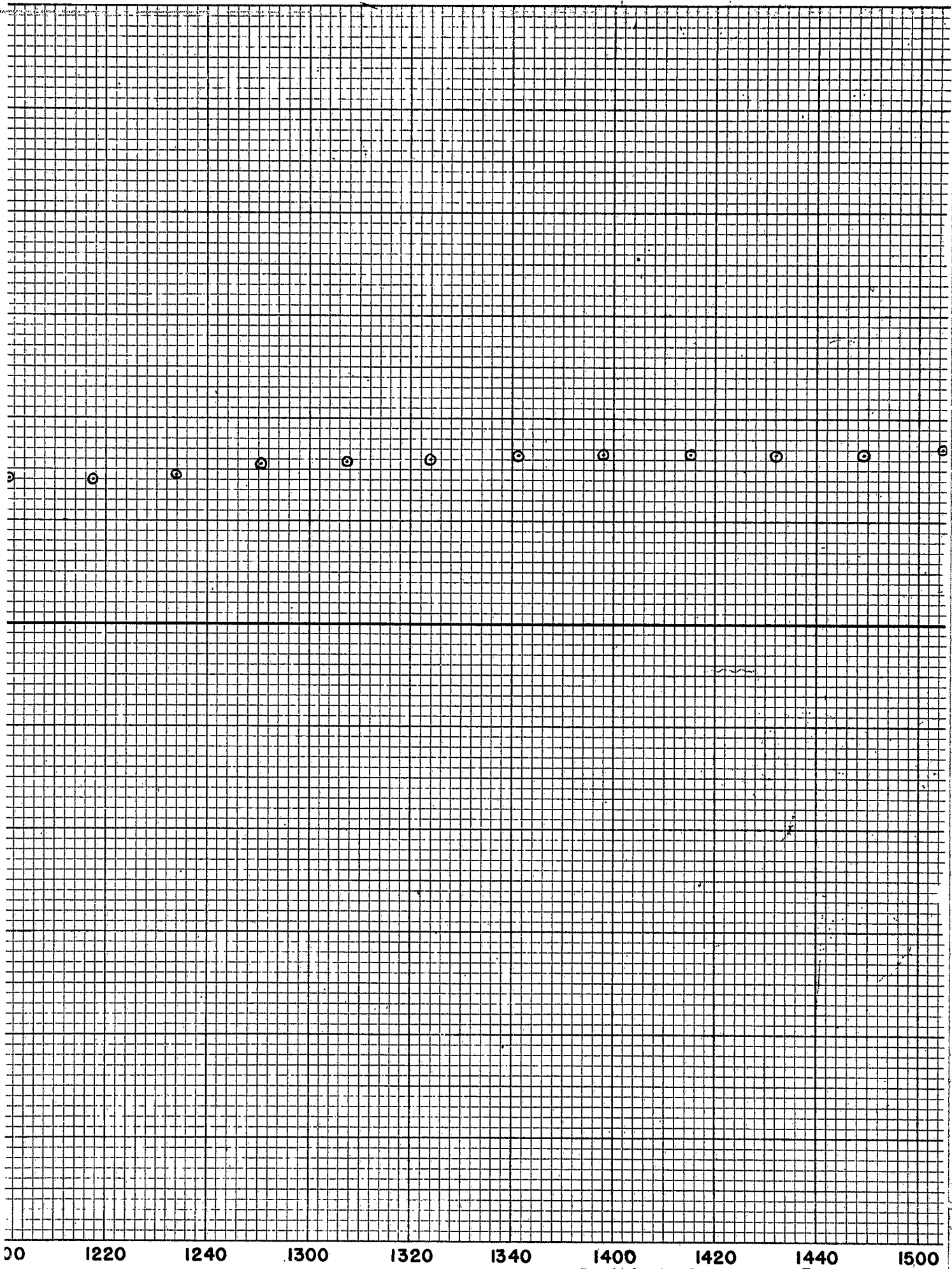
Confidential Security Information

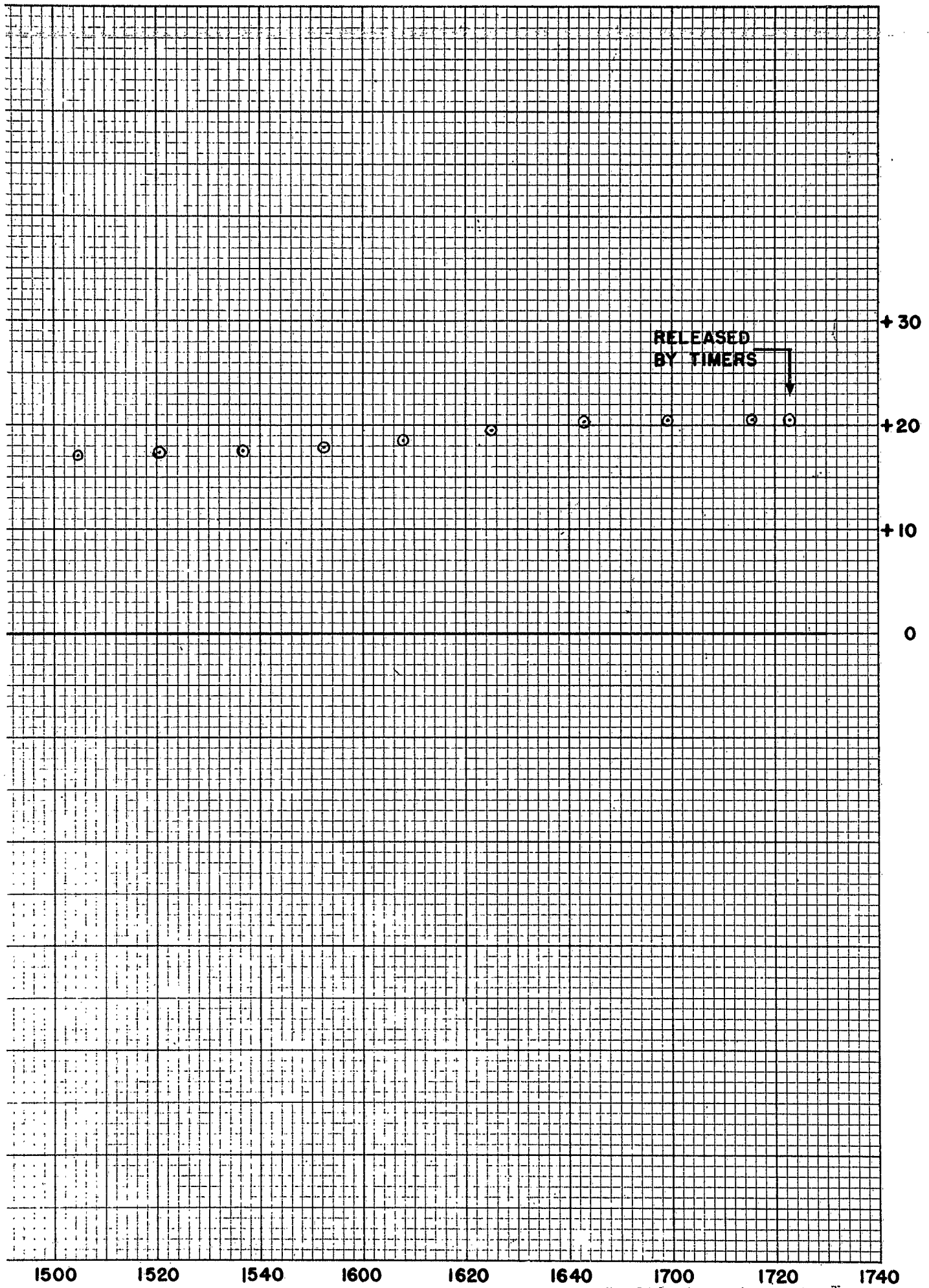


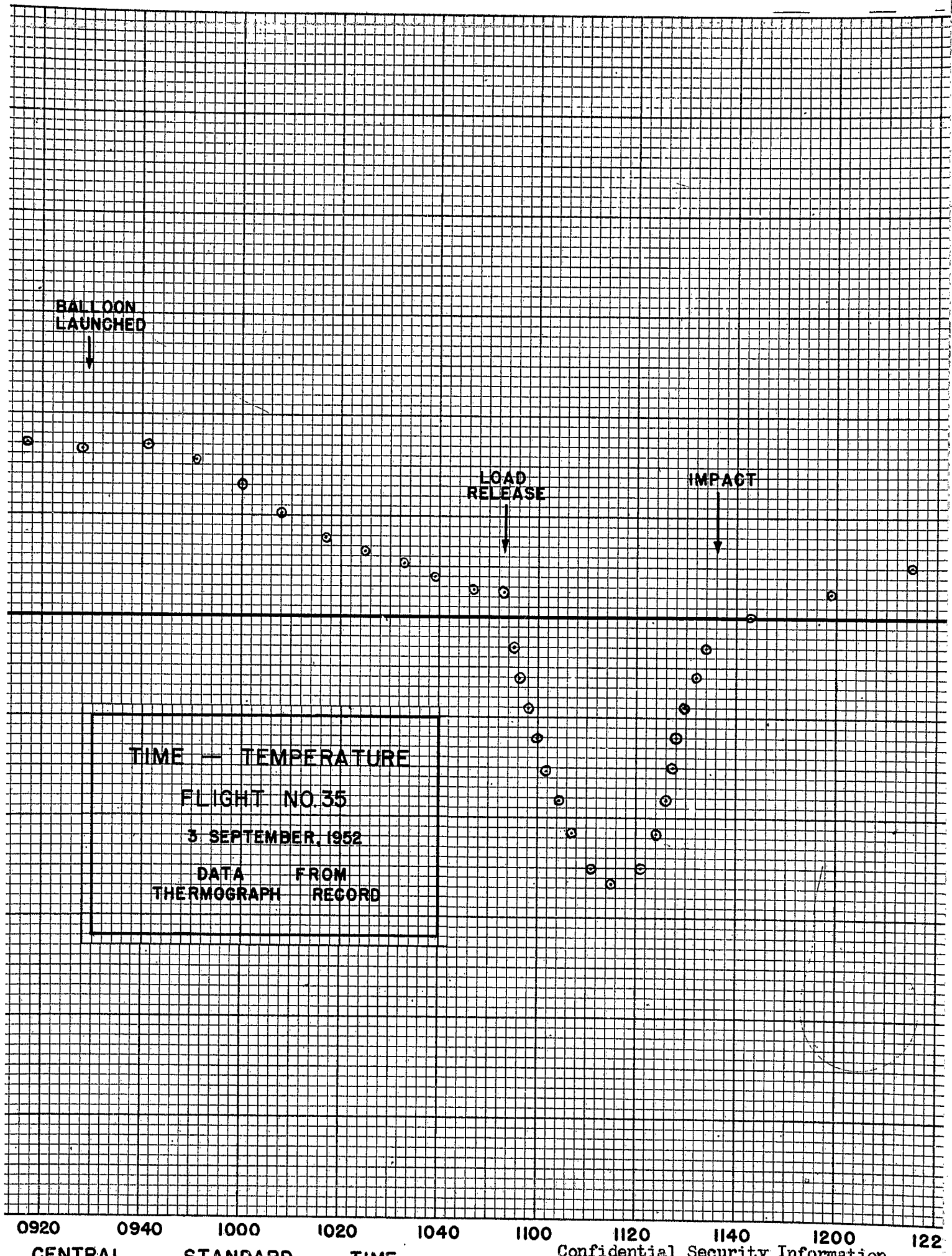


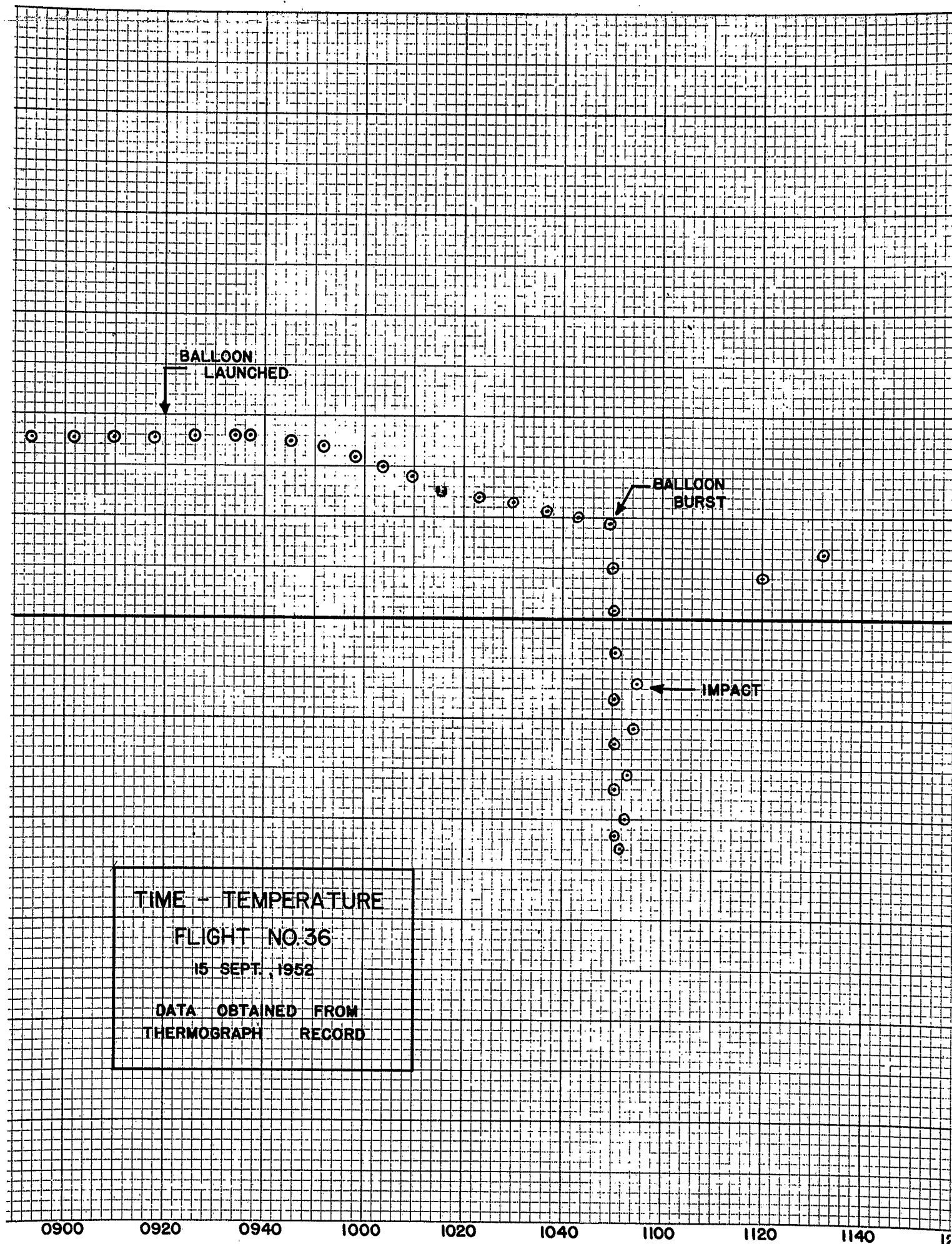


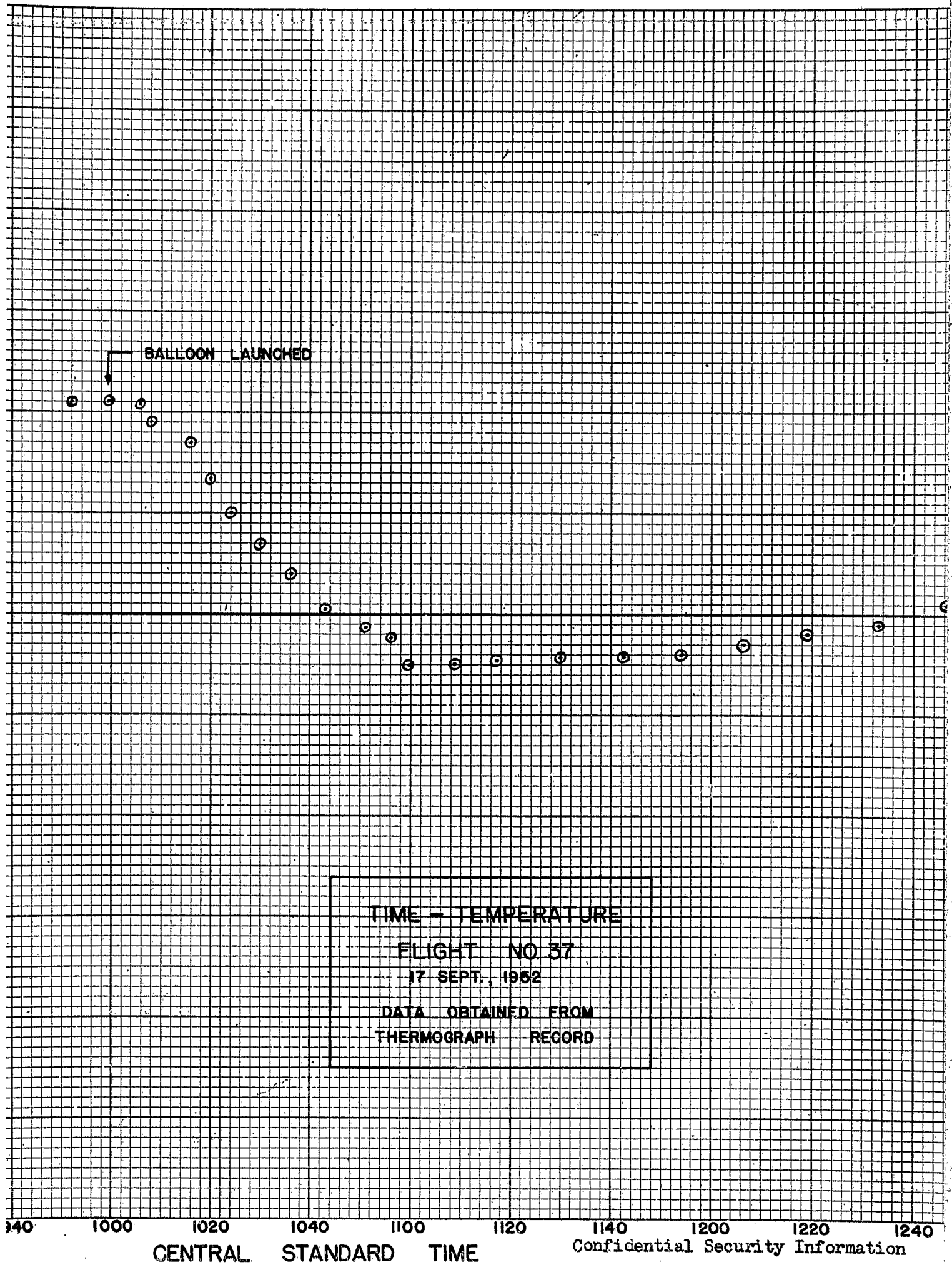


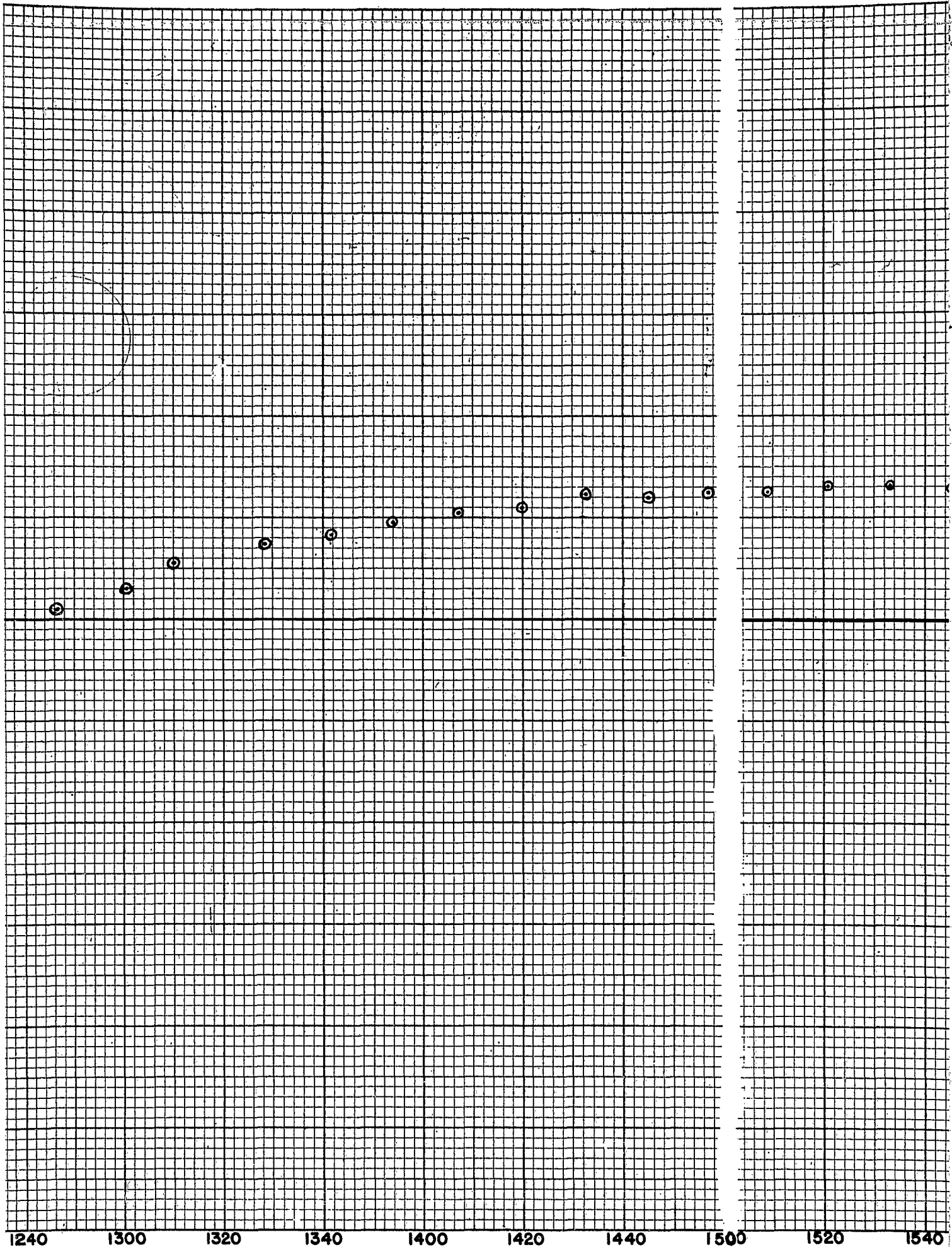


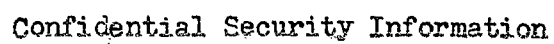


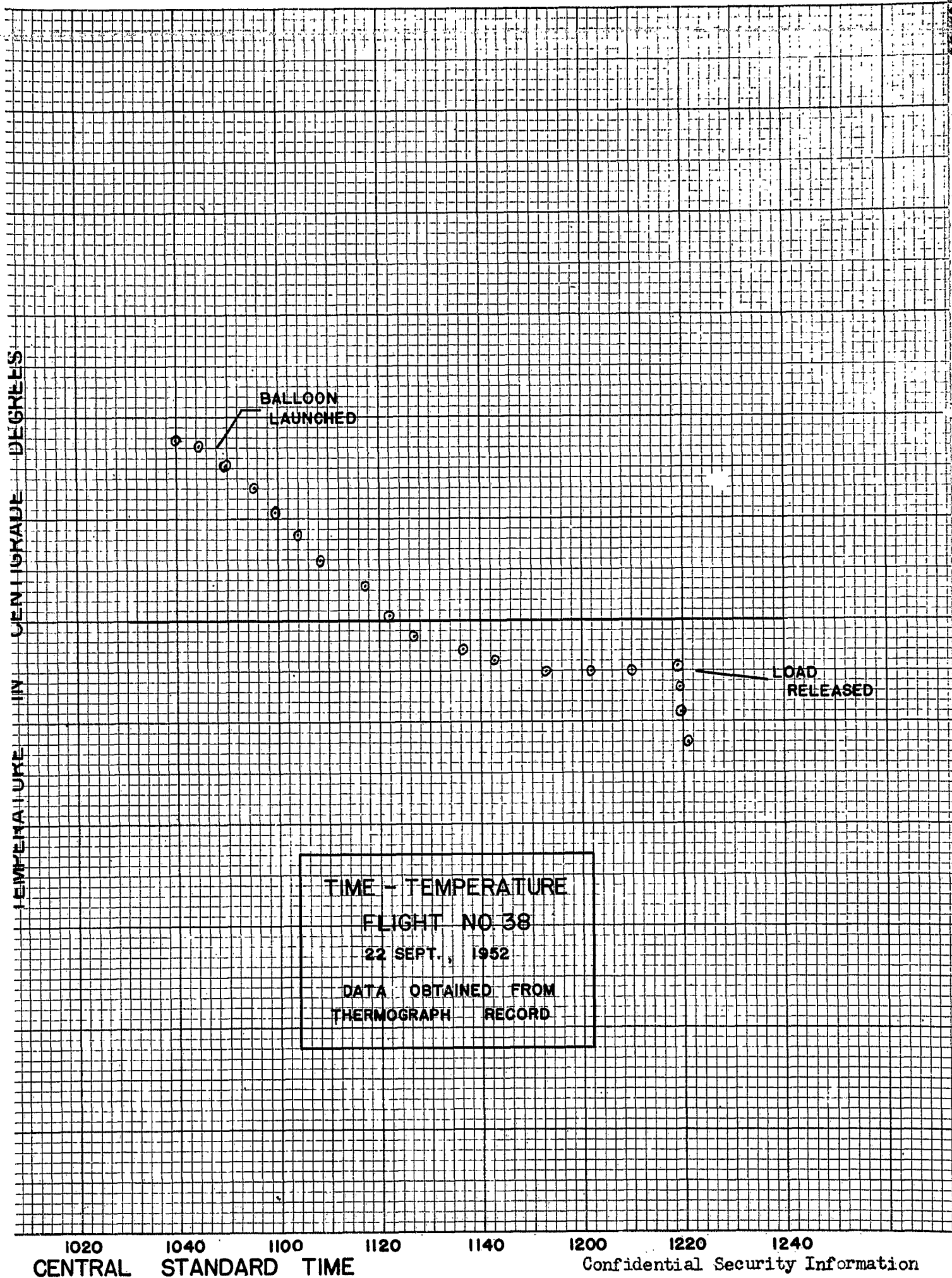












Balloon Launched

TIME - TEMPERATURE

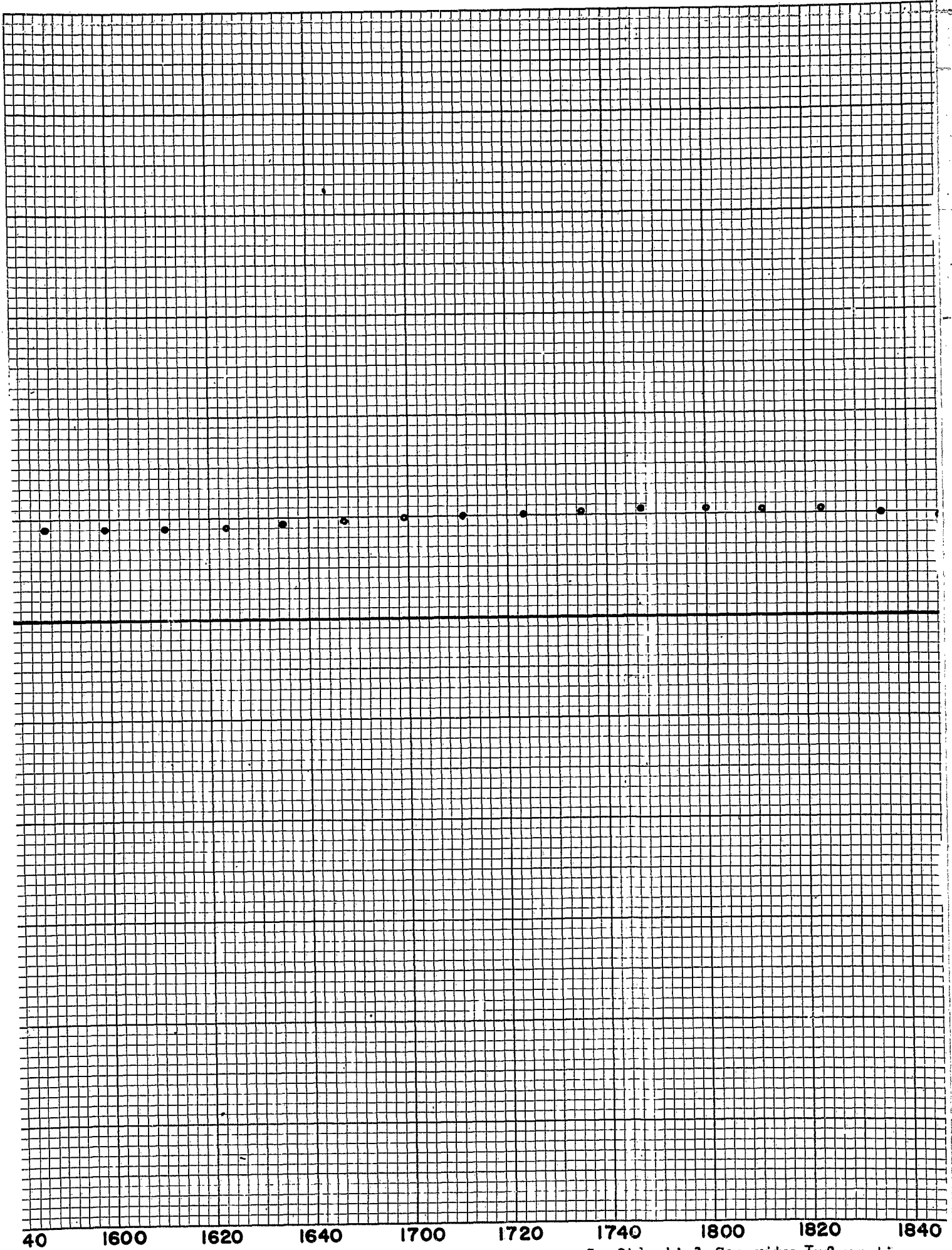
FLIGHT NO.40

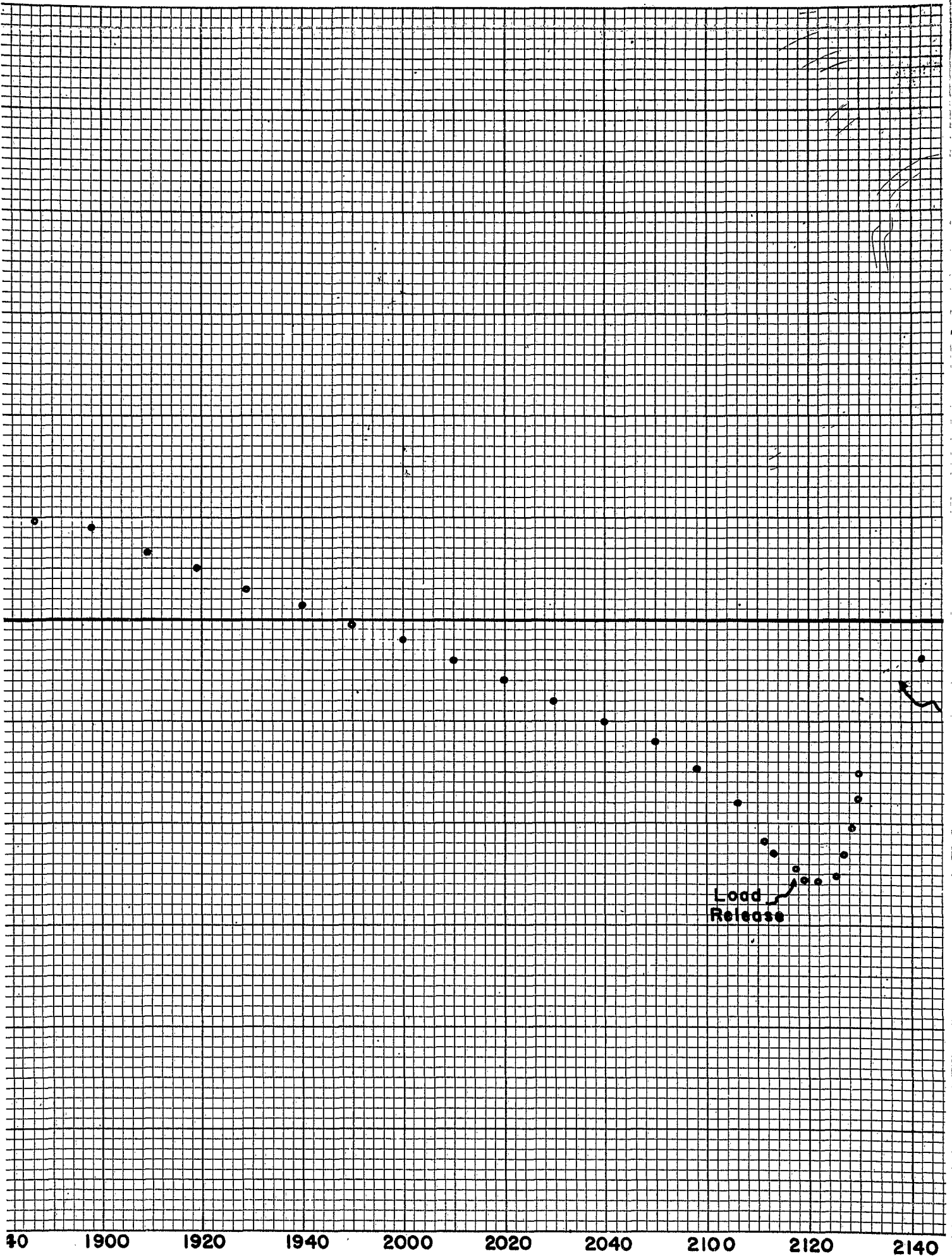
26 September 1952

DATA OBTAINED FROM
THERMOGRAPH RECORD.

0 1300 1320 1340 1400 1420 1440 1500 1520 1540
CENTRAL STANDARD TIME

Confidential Security Information





BALLOON LAUNCHED

TIME - TEMPERATURE

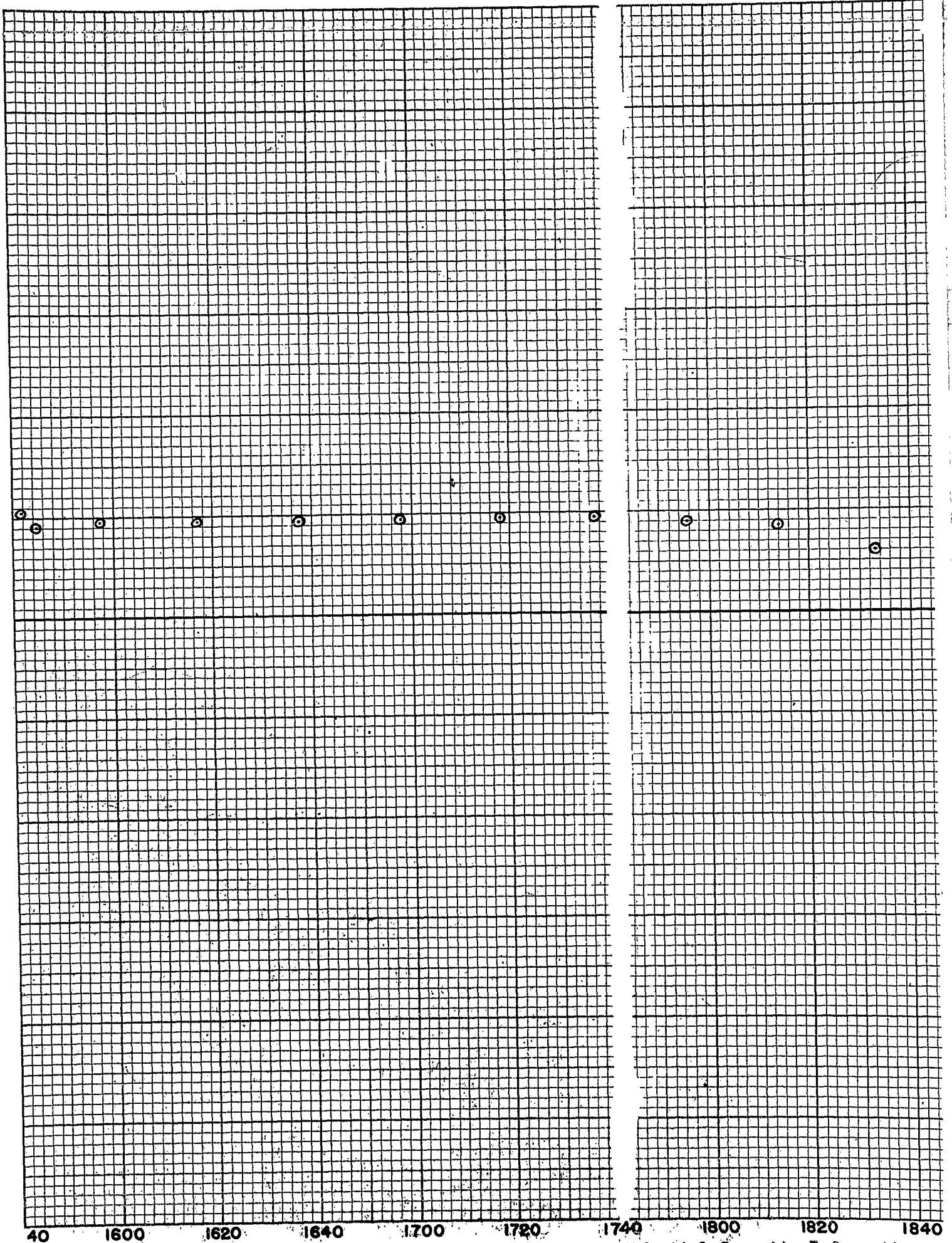
FLIGHT NO. 42

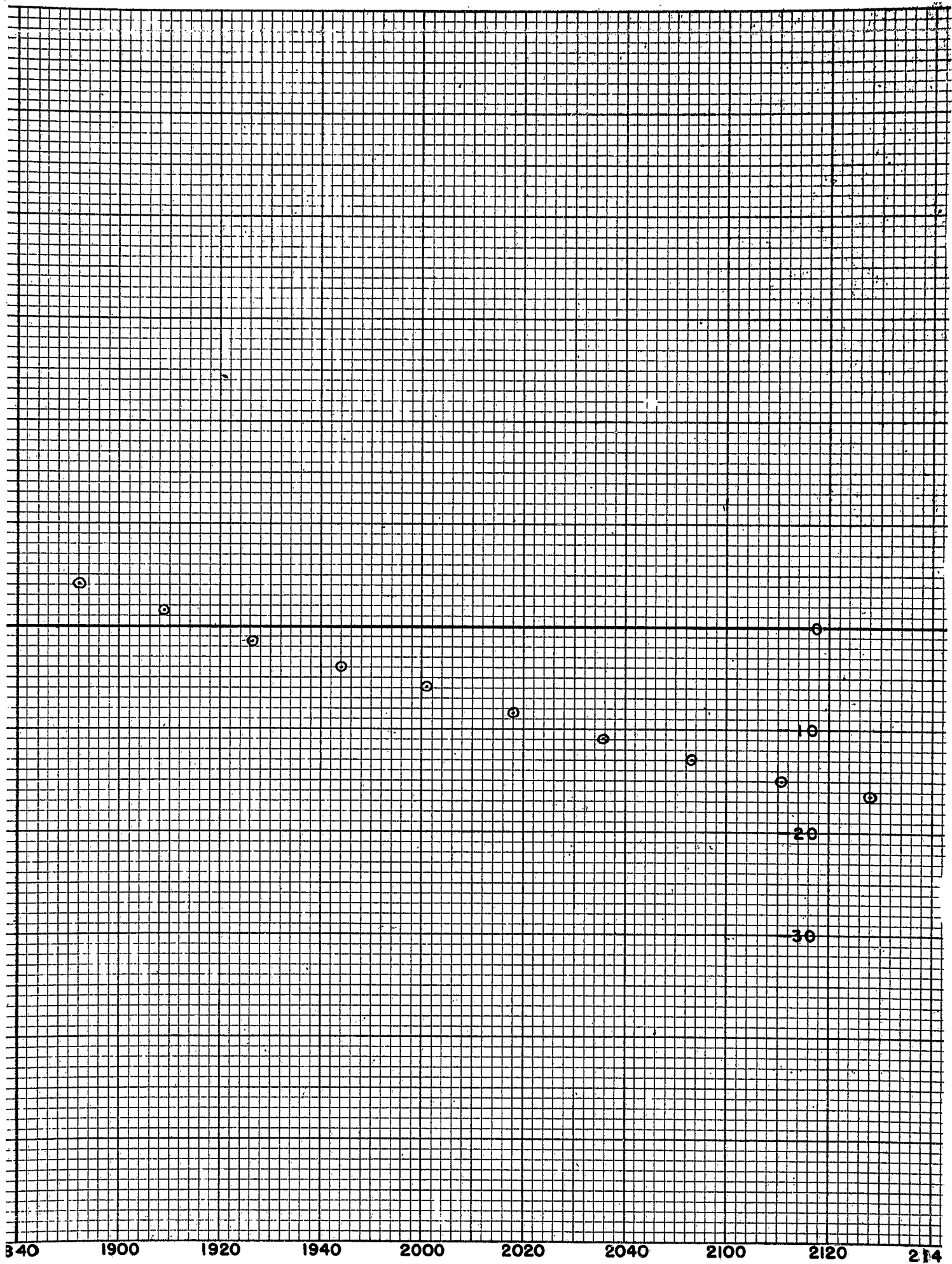
9 OCTOBER, 1952

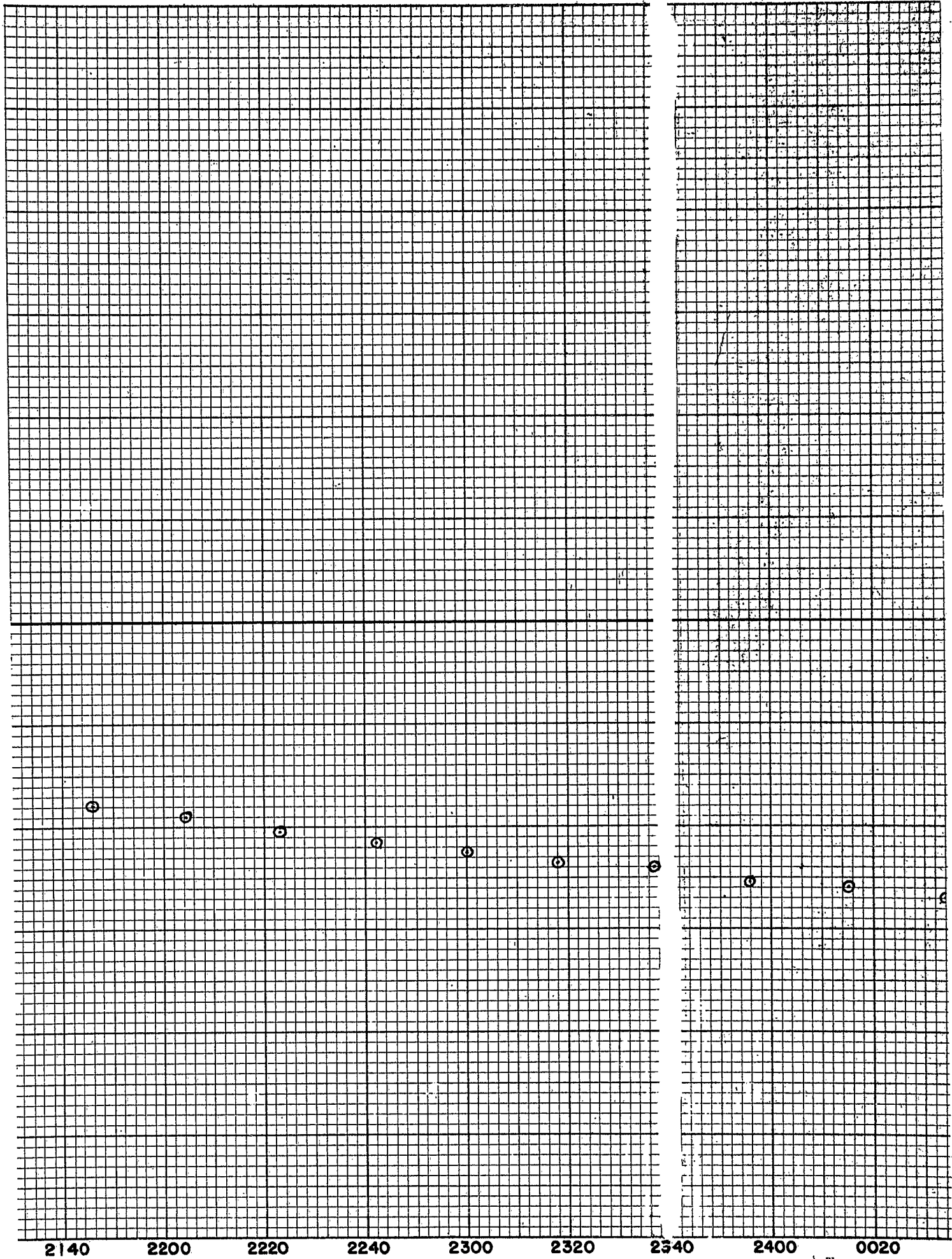
DATA FROM
THERMOGRAPH RECORD

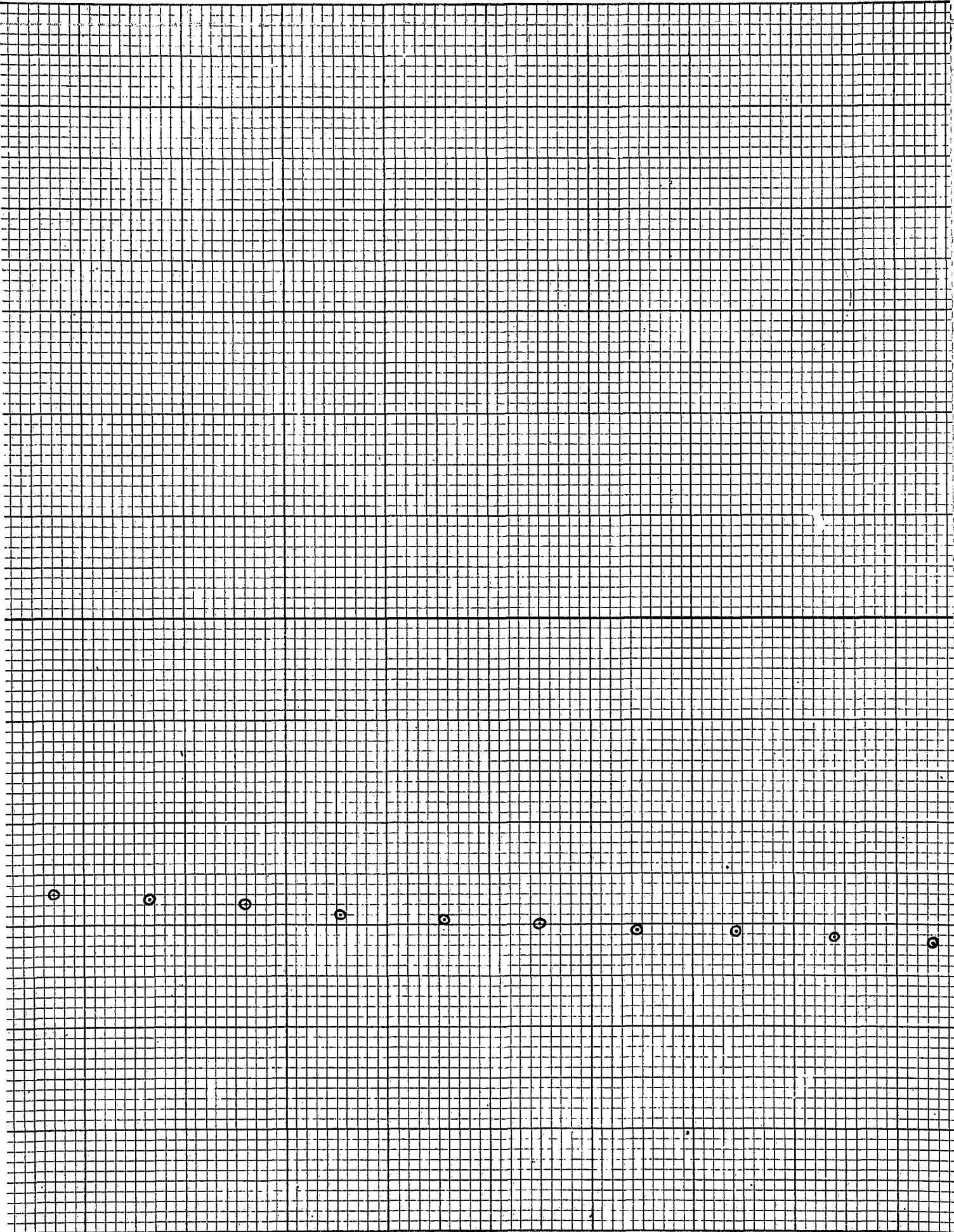
40 1300 1320 1340 1400 1420 1440 1500 1520 1540
CENTRAL STANDARD TIME

Confidential Security Information









0040

0100

0120

0140

0200

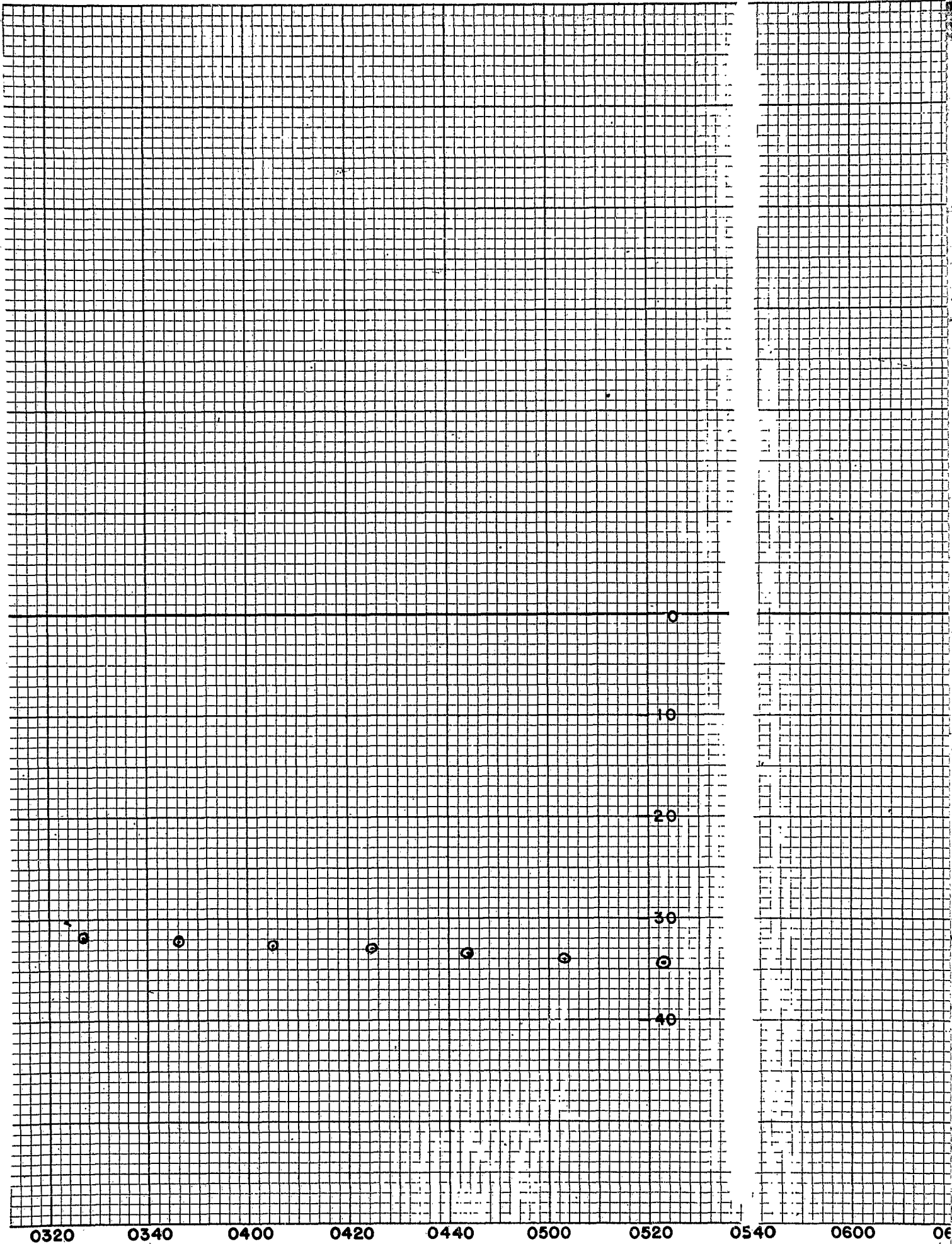
0220

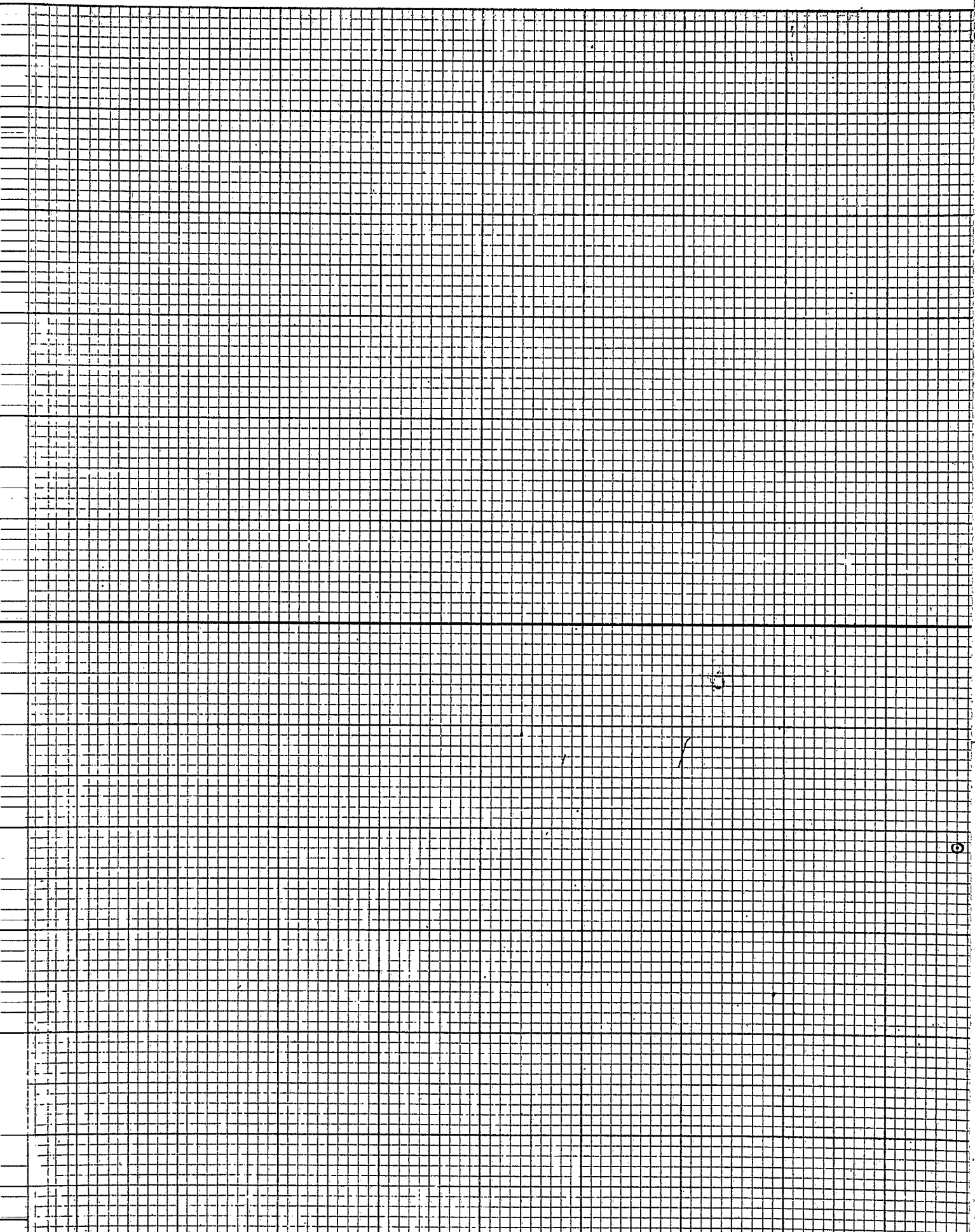
0240

0300

0320

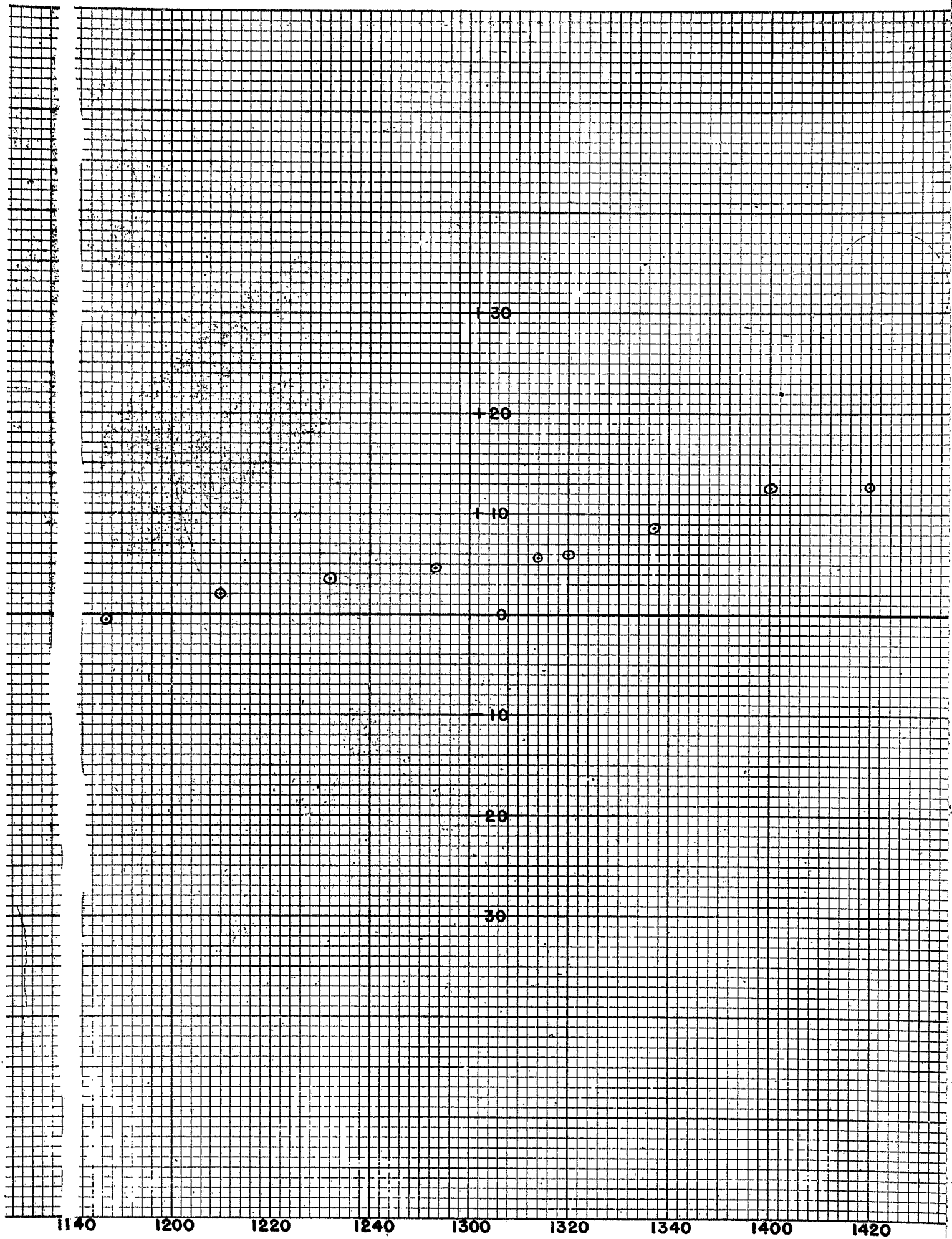
Confidential Security Information

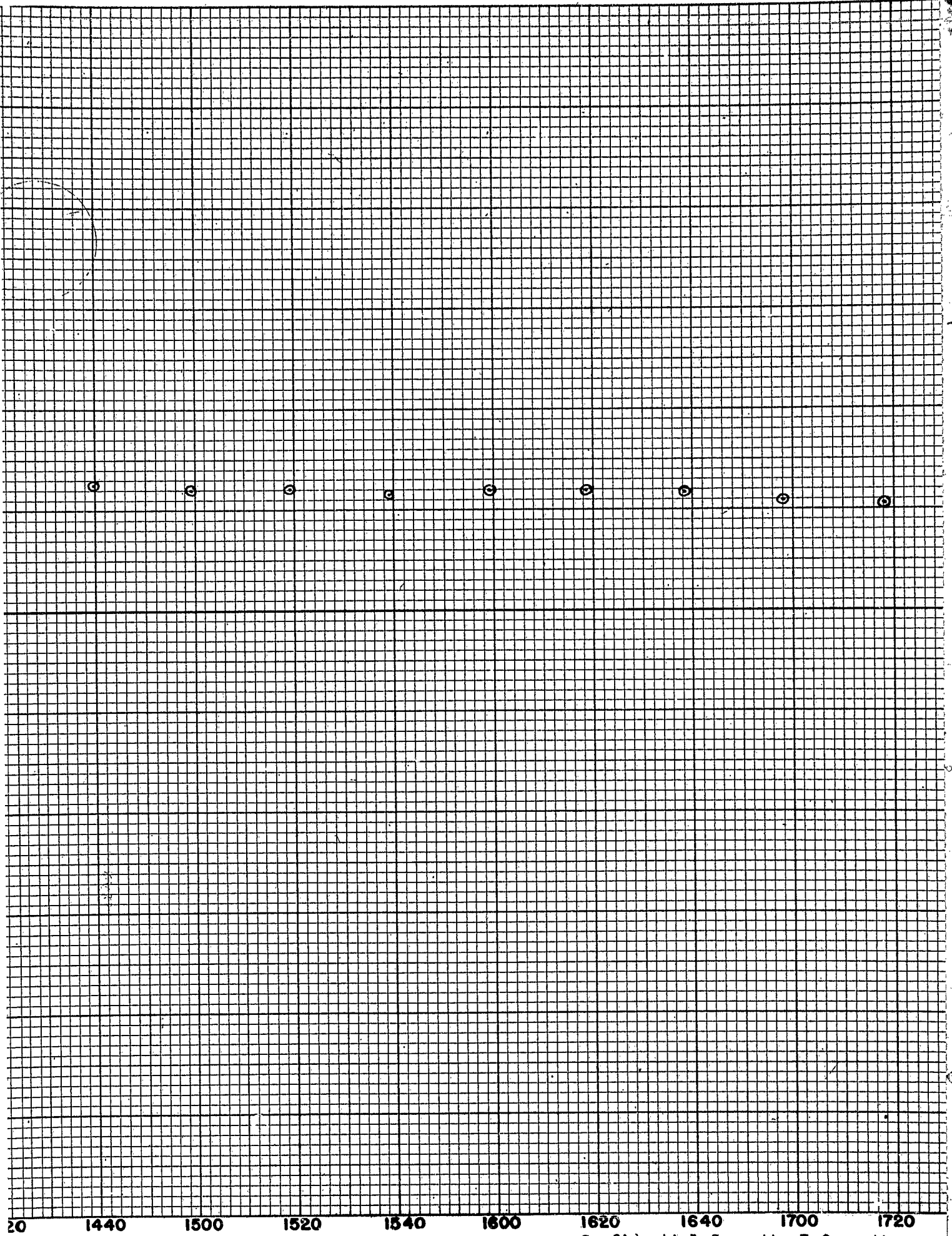


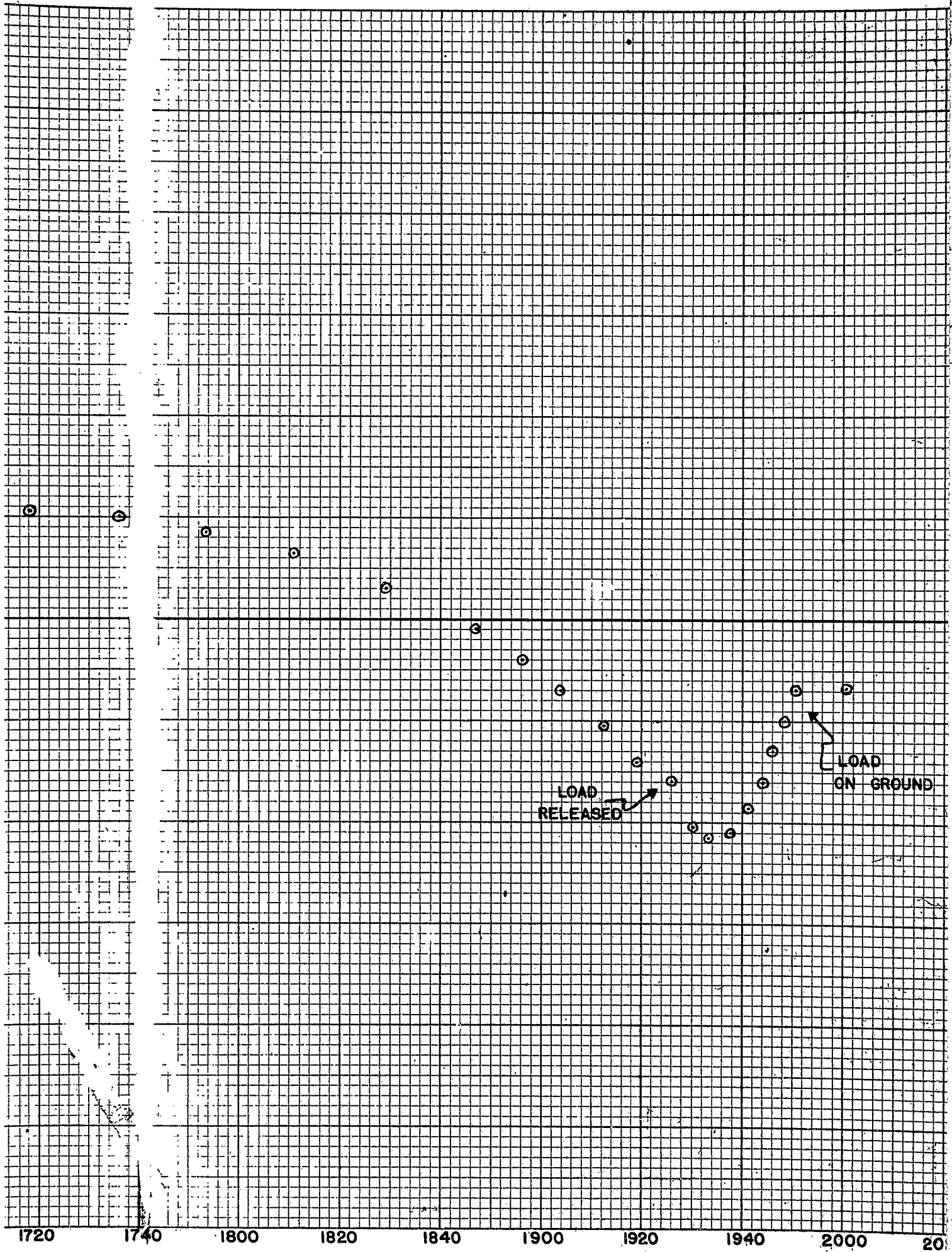


0600 0620 0640 0700 0720 0740 0800 0820 0840









TIME - TEMPERATURE

FLIGHT NO. 45

20 October, 1952

Data from thermograph record
inside the gondola.BALLOON
LAUNCHED1320 1340 1400 1420 1440 1500 1520 1540 1600
CENTRAL STANDARD TIME

Confidential Security Information

SECTION II - THEORETICAL METEOROLOGICAL ANALYSIS

A. CHARACTERISTICS OF STRATOSPHERIC FLOW

Contents

I. General considerations

1. Purpose
2. Review of previous work on tropospheric motion
3. Data

II. Method of analysis

4. Approach
5. Effect of small-scale motion on the computation of larger scale motion
6. Limitations introduced by the linear assumption for the large-scale motion and the interpretation of the observed velocity deviation
7. Effect of observation errors

III. Results of the analysis

8. Example of the analysis, flight #24
9. Results of all cases

IV. Conclusions

10. The scale of stratospheric motions
11. Forecasting implications

References

Figure II-1. Form of assumed velocity fluctuation

Figure II-2. The maximum error of the computed large-scale acceleration as a percentage of the small scale acceleration α , plotted as a fraction of the ratio of observation interval to wave period, τ/T

Figure II-3. Example of the trajectory obtained by a best fitting linear function of the velocity, if the observation interval is comparable to the wave period.

Figure II-4. Observed trajectory flight #24, broken line, and trajectory computed from a linear velocity trend, solid line. The sections of the trajectory selected for a second linear approximation are marked A and B.

Table I. Observational errors equivalent to a position error of 0.2 mile for a balloon at 80,000 feet, 80 miles away.

Table II. Maximum error in the computation of acceleration in units 10^{-2} cm sec⁻² for an error in position of 0.4 mile.

Table III. Analysis of the north-south component of flight #24.

Table IV. Analysis of east winds.

Table V. Analysis of west winds.

B. WINDS IN THE UPPER TROPOSPHERE AND LOWER STRATOSPHERE

I. Introduction

II. A summary of the winds in the lower stratosphere

III. Some features of the wind maximum at the tropopause

IV. Extension of the methods of analysis to the stratosphere

Figure II-5. Average wind velocities (m sec^{-1}) in the lower stratosphere observed for the balloon flights, April through November, 1952. The vertical lines give the vertical range of each observation. The circle denotes the level above which the flow becomes easterly.

Figure II-6. Hodograph for flight #35. The location of the nearby Radiosonde stations with respect to Minneapolis are also indicated.

Figure II-7. Radiosonde observation made at stations located along a line perpendicular to the shear vector of flight #35, see Figure 6. The highest temperatures in the lower stratosphere are observed to the right of the shear vector.

Table VI. Distribution of maximum wind speeds (m sec^{-1}) in the sixteen cases of high winds.

I. General Considerations

1. Purpose

The greatest portion of the flight of the plastic stratosphere balloons is usually spent floating on a constant pressure surface. The flight trajectories during this period describe the stratospheric flow in considerable detail but the number of flights, by meteorological standards constitute an extremely small sample. This description of the atmospheric flow is unusual for the conventional meteorological upper air reports consist of successive observations of the motion at fixed points while the balloon trajectory might be termed a quasi-Lagrangian¹ system, describing the motion of a particle in time. While Lagrangian systems are frequently employed in atmospheric hydrodynamical analysis, this type of observation is sufficiently new to warrant some discussion before comparing the present observations of the stratospheric flow with the better known characteristics of the flow in the troposphere.

It is the purpose of this study to gain an insight of the nature of the stratospheric flow by summarizing certain of its physical characteristics, the amplitudes and periods of the velocity fluctuations of the horizontal component of the flow. It is hoped that some of the limitations imposed by a restricted sample will not be so great for a summarization of physical characteristics as they may be for a climatological summary. The type of summary undertaken has some advantages also in providing a quantitative basis for comparison with the flow in the troposphere.

This investigation was also motivated by a direct requirement of the balloon program, that of the prediction of the future course of the balloon. Extrapolation will be a fundamental part of any system of prediction and the

¹In the sense that the flow is quasi-isobaric, if this extension of the terminology of Starr, Journal of Meteorology, 1945, is permissible.

"representativeness" for this purpose, of a velocity observation will obviously depend upon the length of the period of observation and the periods of the velocity fluctuations. It is also possible that information on the different scales of stratospheric motion may be useful in studies of diffusion.

2. Review of previous work on tropospheric motion

Actually more observations of trajectories of constant altitude balloons have been made in the stratosphere than in the troposphere so that an entirely equivalent description of the tropospheric flow is not available. Some of the value of the stratospheric data, therefore, cannot be realized because it is necessary to rely on different sources using more indirect observations to provide the tropospheric comparison.

The weather systems and associated motions with which the meteorologist is usually concerned, are frequently termed large-scale. In the upper air, for example, the pressure disturbances and streamline patterns are tracked without difficulty in a network of observations spaced at intervals of several hundreds of miles. While the trajectories do not in general coincide with the streamlines, the available tropospheric balloon trajectories² at least establish that similar amplitudes are quite common. It is also recognized that velocity fluctuations of smaller period and amplitude exist in the troposphere although this motion is not detectable from the present network of observations. A number of investigators have made special measurements of the smaller scale motions by tracing smoke puffs and constant altitude balloons (Durst, 1948; Durst and Gilbert, 1950) and by making a series of closely-spaced pilot balloon runs (Brooks, 1947; Rapp, 1952). The reported small-scale velocity fluctuations

² Trajectories of constant altitude balloons at 300 mb are given in Report 1072, General Mills Aeronautical Research Laboratories, 21 March 1952.

are as large as 2.5 m sec^{-1} with periods of at least one hour, and for periods of 5 to 15 minutes fluctuations of 2 m sec^{-1} have been observed. The accelerations implied by these values are considerably larger than the accelerations of the large-scale motion, and it is necessary to perform some sort of averaging or filtering process, in order to observe these fundamental quantities in the hydrodynamical equations for the large-scale motion.

The large-scale accelerations have been obtained by averaging the motion of constant altitude balloons over relatively long time intervals (Durst and Gilbert, 1950; Mantis, 1952). Besides the order of magnitude the most important fact that emerged from these measurements is that the component of the acceleration perpendicular to the trajectory is frequently greater than the component tangential to the flow³. Estimates of the magnitude of the tangential component of the accelerations are fairly consistent; from the rms value for the acceleration of $2.9 \times 10^{-2} \text{ cm sec}^{-2}$ (Mantis) the amplitude of a representative 24 hour velocity fluctuation will be at least 10 m sec^{-1} . The centrifugal acceleration has a very unusual distribution and a representative value is difficult to estimate. However, values of acceleration as large as $10 \times 10^{-2} \text{ cm sec}^{-2}$ are frequently observed.

The investigations of Durst and Rapp have provided a large portion of the data for the tropospheric comparison and some of the same methods of analysis are used in the present study.

3. Data

The data available for this analysis consisted of 12 flights made by the University of Minnesota and two by the General Mills Laboratories. The floating elevation and periods of observation are rather variable; the range of elevation of all flights was from 79 to 94 thousand feet and the time interval ranged

³This is implied by the proponents of the gradient wind relationships but observational evidence was lacking until recently, Neiburger, M. et.al, 1948; Godson, 1950.

from twenty five minutes to five hours. The majority of these flights were made in the summer season of easterly stratospheric winds. Some cases of westerly flow are also included but no soundings were available in mid-winter and the few cases of light variable winds of the transition season were not analyzed.

The balloon's trajectory was determined from theodolite observations at five minute intervals; the elevation above the surface has been determined from the measurement of pressure and the assumption of the standard atmosphere. In a few cases double theodolite observations were also made and in most university flights, trajectories were also determined by photographing the earth from the balloon. Except for the most recent flights, the timing of the photographs was inaccurate and the principal value of the double theodolite and camera track has been in verifying the single theodolite plot.

II. Method of Analysis

4. Approach

The different time-scales of stratospheric motion are to be separated by a statistical procedure. The observed trajectory consists of a set of position points at equal time intervals. Each "leg" of the trajectory, therefore, represents the mean velocity vector in the time interval between position fixes.

This set of vectors comprising the trajectory will be a function of time:

$\vec{V}_i = \vec{V}_i(t)$ where \vec{V}_i is the mean velocity vector in the i th leg.

Now it will be assumed that the east-west and north-south components of the \vec{V}_i can be adequately represented by linear functions of time; for each component there will be a function:

$$V_i = \bar{V} + at_i \quad (1)$$

$$i = 1, 2, \dots, n$$

where V_i = the component of the large scale motion in the i th leg

t_i = the time measured from the midpoint of the trajectory to the midpoint of the i th leg

n = the total number of legs being given by $n = \tau/\varepsilon$
 τ and ε = the observation and leg intervals respectively

The constants \bar{V} and Q are determined for a given observation interval by the method of least squares. We should like to ascribe the observed departures of the velocities from the linear function to the effects of motion of small-scale and possibly also to error.

The proposed method does not, of course, provide an absolute separation of different scales of motion. The capabilities and limitations of the method were briefly explored by analyzing simple model velocity waves or fluctuations. These tests were designed to provide information on several questions of interpretation of the analysis: (1) The error introduced by small-scale motion into the computation of the function for the large-scale motion; (2) The limitation on the linear assumption as a description of the large-scale flow, and the related question of the significance of the deviations from the linear function.

5. Effect of small-scale motion on the computation of larger-scale motion

The error produced by small-scale motion in the computation of the linear functions will be discussed by considering the effect upon the value of the large-scale acceleration, the quantity Q in equation (1). We shall naturally expect that the error will decrease as the observation interval, τ , becomes large with respect to the period of the fluctuation, T . The leg interval may also affect the computation but in no systematic fashion, it was found, so long as the leg interval is small compared to the period, $\varepsilon \ll T$. In any given computation the phase displacement of the wave with respect to the origin of the computation will be important since the computed acceleration may be zero for a symmetrical wave. Such a fortuitous cancelling of the effect of the small scale motion cannot be expected in practice so that the upper limit of the error, the maximum error for a given ratio τ/T was investigated. For this

purpose a simple velocity fluctuation of saw-tooth shape was chosen in which the velocity fluctuation consists of half periods of constant acceleration α with alternate sign:

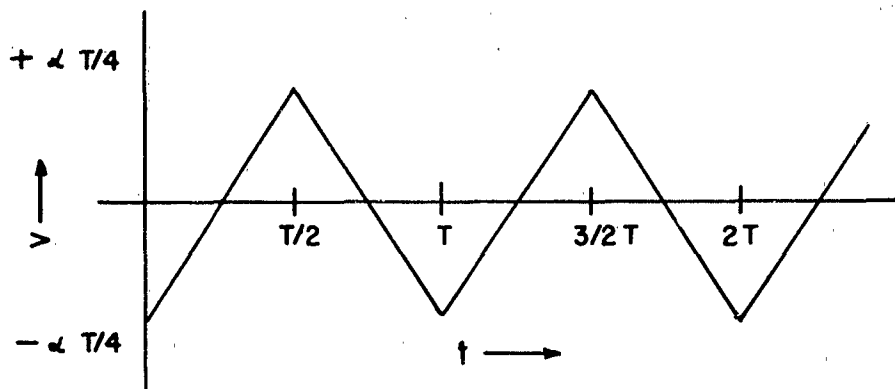


Fig. II-1. Form of assumed velocity fluctuation.

It will simplify the discussion if we assume the origin of the computation to be centered in the observation interval and the total number of legs to be even, $2k = \tau/\xi$. By definition, the large-scale acceleration in equation (1) will be given by the expression:

$$a = \frac{\sum_{i=1}^k v_i t_i + \sum_{i=-1}^{-k} v_i t_i}{2 \sum_{i=1}^k t_i^2} \quad (2)$$

Where t_i is the time measured from the origin to the center of the i th leg. It was then established for the limiting case where $\xi \rightarrow 0$, the contributions of like sign to the partial sum $\sum_{i=1}^n v_i t_i$, $n = \tau/2\xi$ over any time interval $\tau/2$ will be a maximum only if the entire half wave with constant sign of v_i is included. Hence, the total contribution of the two partial sums over a half period at either end of the trajectory (which will be the greatest since t_i is largest) must be equal or less than the case for the complete half wave at the end of the trajectory, i.e.:

$$\leq \alpha \frac{3}{8} \left(\frac{\tau}{4}\right)^3 \left(2\frac{\tau}{T} - 1\right)$$

The total acceleration must be smaller than this quantity since the next larger partial sum $\sum_{i=1}^{i+1} v_i t_i$ will be of opposite sign. The case where $\frac{\tau}{T}$ is an integer is readily computed:

$$|a| = \propto \frac{3}{8} \left(\frac{T}{\tau}\right)^3 \left| \sum_{n=1}^{\frac{\tau}{T}} (2n-1)(-1)^n \right| = \propto \frac{3}{8} \left(\frac{T}{\tau}\right)^2$$

The residual errors in the computed acceleration expressed as a fraction of the small-scale acceleration a/a are plotted against the ratio of observation interval to period in Figure 2.

6. Limitations introduced by the linear assumption for the large-scale motion and the interpretation of the observed velocity deviation

The acceleration computed by the linear assumption cannot yield representative values of the large-scale acceleration if the observation interval includes too large a fraction of the period of the fluctuation. Several tests were made with sinusoidal velocity fluctuations to study the extent of this limitation.

A velocity oscillation:

$$v_i = v_0 + v_a \sin \frac{2\pi}{T} i \varepsilon \quad (3)$$

was chosen in which the maximum acceleration will be $2\frac{\pi}{T} v_a$. An observation interval of $1/5$ the period of the wave was used in this computation, $\tau = T/5$. The quantity a in equation (1) was then computed for different phase angles. All values of the acceleration from zero to $2\frac{\pi}{T} v_a$ were found with the representative rms value of $0.71 \cdot 2\frac{\pi}{T} v_a$ for all cases. Hence it would seem that a linear function will yield representative accelerations, at least if:

$$\tau \leq T/5$$

The case of intermediate values of the ratio τ/T will be discussed by a further example. The same type of velocity fluctuation was used but with a longer observation interval $\tau = 1.8T$. The lag interval in this case was $\varepsilon = T/15$.

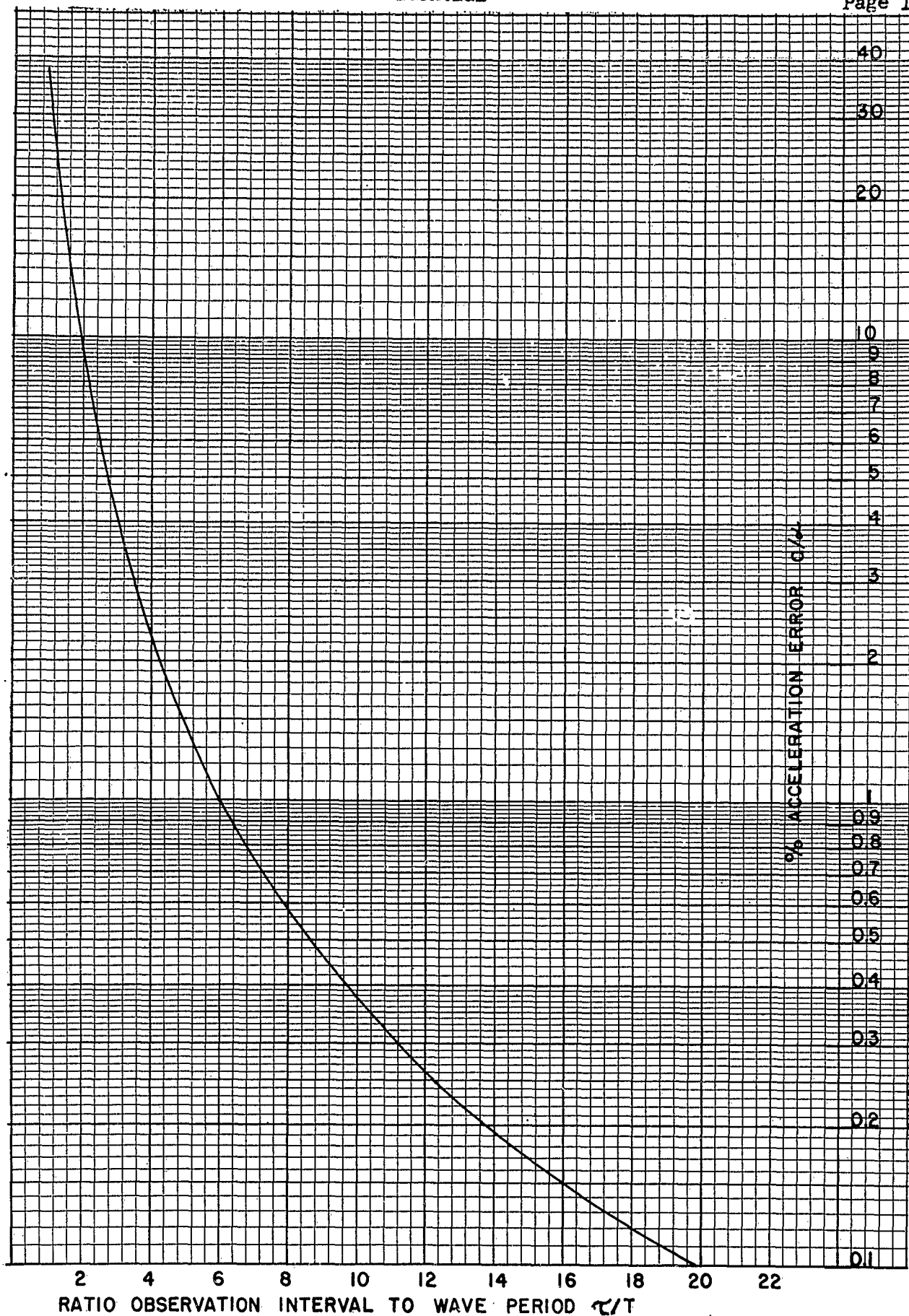


Fig. II-2. The maximum error of the computed large-scale acceleration as a percentage of the small scale acceleration α , plotted as a fraction of the ratio of observation interval to wave period, τ/T .

The wave and the computed linear trend are illustrated in Figure 3.

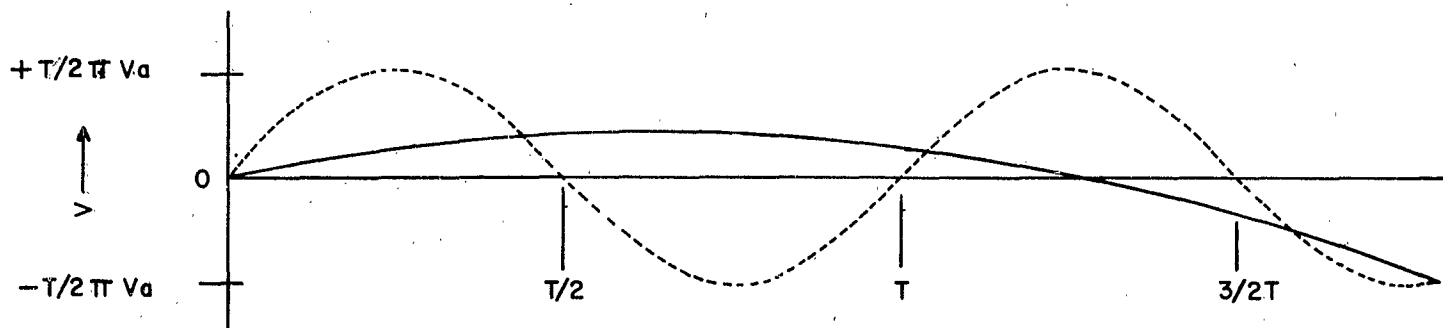


Fig. II-3. Example of the trajectory obtained by a best fitting linear function of the velocity, if the observation interval is comparable to the wave period; $T = 1.8T$ in this instance.

The large-scale acceleration was found to be 5% of the maximum acceleration, $= 0.05(2\pi \frac{V_a}{T})$, a reasonable residual value for the case where the observation spans almost two periods (See Figure 2).

The velocity wave appears principally as the deviations from the linear trend. The rms velocity deviation of the legs from the linear function was $0.67V_a$. The approximate half period of the fluctuation is shown by the sequence or runs of like sign of the deviations of the legs of the trajectory from the computed linear trend. The major runs average 7.7 legs and we compare this time to a half period:

$$\frac{T}{2} = \frac{15 \epsilon}{2} \sim 7.7 \epsilon$$

If these were actual observations there always remains the possibility that a given run of like sign might occur simply by chance. For the above example the probability of such a sequence as observed occurring by chance will be computed to be 0.02 (Hoel, 1947, Page 177-182).

Representative accelerations of the smaller scale motion can be obtained by fitting the run of deviations of like sign by a second linear regression. In the two longest runs the accelerations were computed to be $0.74 V_a \frac{2\pi}{T}$ and $-0.73 V_a \frac{2\pi}{T}$. The deviations of the velocity in the individual legs, however, must be ascribed to the limitation of the linear assumption for an interval as long as a half period. The rms velocity deviations of the legs were $0.17 V_a$ and $0.10 V_a$, roughly 15% of the amplitude of the half wave being fitted.

The effect of leg interval was not pronounced in any of the computations unless the leg interval spans a large fraction of the wave period. To illustrate some of the difficulties, the same wave was fitted using a leg interval four times larger, $\epsilon = \frac{4}{15} T$ and $\tau = 2.4 T$. The average number of runs of like sign is 2 and again this is very nearly a half period, $2\epsilon = \frac{8}{15} T \sim \frac{1}{2} T$. However, the probability of such an observed distribution of signs occurring by chance is very high, 0.29.

7. Effect of observation errors

In the analysis of observed trajectories a further restriction on the interpretation of the velocity fluctuations is determined by the accuracy of the observations. The various elements of an observation of position were reviewed in order to assess the order of magnitude of the error. The observations consist of measurement of time, of elevation and azimuth angles and an altitude determined by a pressure measurement. The computation of the distance away from the observation point for trajectory lengths encountered, requires a correction for atmospheric refraction and earth curvature. This correction is most conveniently made graphically and the error introduced at this point is quite large. The error in the distance computed from the graph is rather independent of distance out and the rms deviation from the mean of a set of independent readings of the graph was found to be of the order of 0.2 mile.

Some examples of observational errors which are equivalent to a position error of 0.2 mile for a balloon 80 miles away at an elevation of 80,000 feet

are given in Table I.

Table I

Observational errors equivalent to a position error of 0.2 mile for a balloon at 80,000 feet, 80 miles away.

Elevation angle	=	0.03°
Azimuth angle	=	0.15°
Altitude	=	200 feet

Since the relative altitude not the absolute altitude is important in the computation of velocity it would seem that only in measurement of the elevation angle could errors of comparable magnitude be introduced. The fact that the greatest error will be made in the computation of the distance out has some further importance in the analysis because the error will depend upon the orientation of the trajectory and the greatest error will be made in the direction along rather than across the line of sight.

The effect of the error upon the computation of the large-scale acceleration may be determined in very much the same way as the effect of small-scale motion. If, despite the above discussion, the error is independent of the trajectory a given observation fix must lie within a circle of radius r , the maximum error in position. Then as before, the maximum contribution to the computed acceleration will be made by the end legs of the trajectory and the maximum velocity deviation in each end leg will be $v = \frac{2r}{\epsilon}$. For the case that the number of legs is $2k+1 = \frac{\tau}{\epsilon}$, the maximum error in the computation of the acceleration, produced by a position error r , will be:

$$\begin{aligned} \Delta a &= \frac{2 v k \epsilon}{2 \sum_{i=1}^k (\epsilon)^2} = \frac{(2 \frac{r}{\epsilon}) k \epsilon}{\epsilon^2 \sum_{i=1}^k (1)^2} \\ &= \frac{12r(2k+1)}{\tau^2(k+1)} \sim \frac{24r}{\tau^2} \quad \text{where } k \text{ is large.} \end{aligned} \quad (4)$$

If we take the absolute maximum error = 0.4 miles (smaller values will be expected for distances out less than 30 miles) the maximum errors in the computation of the acceleration as a function of the observation interval

may be determined from equation (4).

Table II

Maximum error in the computation of acceleration in units $10^{-2}\text{cm sec}^{-2}$ for an error in position of 0.4 mile*.

Observation interval, minutes	5	10	20	40	80	160	240	320
Acceleration error, $\text{cm sec}^{-2} \times 10^{-2}$	16×10^2	420	104	26	3.2	1.6	0.72	0.40

*For comparison note that values of acceleration for 150 minute observation intervals are frequently larger than 10×10^{-2} while for 300 minutes, values of 3×10^{-2} are observed.

The probability of the occurrence of the maximum velocity deviation with opposite sign at each end leg is very small. On the assumption that the distribution of acceleration error is a multivariate normal function of uncorrelated position fix errors, the standard deviation of acceleration error is no more than one sixth the indicated maximum error.

III. Results of the Analysis

8. Example of the analysis, flight #24

As an aid in the interpretation of the results of the analysis of the flights reported in the following section, one trajectory analysis is presented here in detail. This flight, #24, which happens to be the longest observation in the group, was made from Minneapolis, 18 July 1952. The constant altitude portion of the flight began some 21 miles from the observation point and ended 320 minutes later at a distance 155 miles to the west. The pressure altitude during this interval varied by approximately ± 200 feet from the mean elevation of 83,000 feet. The computation was based on position fixes at ten minute observation intervals.

The large scale motion was determined by fitting the linear function to the velocity components as discussed above. The comparison between the observed trajectory and the linear function for the large scale motion is shown in Figure 4 and the data and the results of the computations for the north-south component

of the motion are listed in Table III. In column B are tabulated the values of t_i , the time measured from the mid-point of the observation interval to the mid-point of the leg interval. Column C lists the observed average north-south component of the velocity in each 10 minute leg, determined graphically from a plot of the trajectory. The large-scale velocity in each leg, computed from the linear relation, equation (1) is given in column D. The mean north-south velocity $\bar{V} = -1.82 \text{ m sec}^{-1}$ and the large scale acceleration $a = 2.51 \times 10^{-2} \text{ sec}^{-1}$.

The deviations of the observed velocity from the computed large-scale velocity are tabulated in Column E, labeled ΔV_i where $\Delta V_i = V_{oi} - V_i$. These deviations may be interpreted as motion of smaller scale, observation error, or simply the result of the limitation of a linear description for the motion. This latter possibility cannot be excluded immediately if only because the rms $\Delta V_i = 1.34 \text{ m sec}^{-1}$ is almost as large as the mean velocity.

The effect of observational error is difficult to estimate because of the wide range in balloon distance and hence in probable error. The circle of maximum error, following the discussion in section 7, varies in radius from 0.05 miles at the beginning to 0.65 miles at the end of the trajectory. The rms value of the radius of maximum error for this trajectory was 0.45 miles which corresponds to a maximum velocity error of 2.4 m sec^{-1} in a ten minute leg. It will be observed that a number of the values of ΔV_i , therefore are too large to be explained by error alone. Actually if the error is at all reasonably distributed the rms deviation due to error would perhaps be no greater than one-third of the maximum value. This estimate is based upon the assumptions that the maximum displacements of the end points of a velocity vector correspond to twice the standard deviation of the position fix error and that the distribution of the velocity error is a joint normal distribution function of the two uncorrelated end point errors.

Table III. Analysis of the north-south component of flight 24

Obs no. i	Obs time t_i 10^2 sec	Obs vel $V_{0,i}$ $m \cdot sec^{-1}$	Trend vel V_i $m \cdot sec^{-1}$	Dev from trend ΔV_i $m \cdot sec^{-1}$	Accum dev d_i $m \cdot sec^{-1}$	Int wave obs time t' 10^2 sec	Trend vel V' $m \cdot sec^{-1}$	Dev from trend $\Delta V'$ $m \cdot sec^{-1}$
A	B	C	D	E	F	G	H	I
1	-93	-3.9	-4.2	.3	.3			
2	-87	-4.4	-4.0	-.4	-.1			
3	-81	-4.4	-3.9	-.5	-.6			
4	-75	-3.9	-3.7	-.2	-.8			
5	-69	-3.6	-3.6	0	-.8			
6	-63	-4.1	-3.4	-.7	-1.5			
7	-57	-2.7	-3.3	.6	-.9			
8	-51	-4.1	-3.1	-1.0	-1.9			
9	-45	-4.2	-3.0	-1.2	-3.1			
10	-39	-2.9	-2.8	-.1	-3.2			
11	-33	-2.8	-2.7	-.1	-3.3			
12	-27	-2.4	-2.5	.1	-3.2			
13	-21	-2.9	-2.4	-.5	-3.7	-15	-1.0	.5
14	-15	-3.7	-2.2	-1.5	-5.2	-9	-.5	-1.0
15	-9	-1.8	-2.0	.2	-5.0	-3	.1	.1
16	-3	-1.1	-1.9	.8	-4.2	3	.6	.2
17	3	0	-1.7	1.7	-2.5	9	1.1	.6
18	9	-.4	-1.6	1.2	-1.3	15	1.6	-.4
19	15	1.4	-1.4	2.8	1.5	-18	3.7	-.9
20	21	.7	-1.3	2.0	3.5	-12	2.7	-.7
21	27	3.7	-1.1	4.8	8.3	-6	1.7	3.1
22	33	-1.0	-1.0	0	8.3	0	.7	-.7
23	39	-1.8	-.8	-1.0	7.3	6	-.4	-.6
24	45	-2.4	-.7	-1.7	5.6	12	-1.4	-.3
25	51	-2.8	-.5	-2.3	3.3	18	-2.4	.1
26	57	-.7	-.4	-.3	3.0			
27	63	-1.4	-.2	-1.2	1.8			
28	69	-.4	-.1	-.3	1.5			
29	75	.2	.1	-.1	1.6			
30	81	-2.4	.3	-2.7	-1.1			
31	87	.5	.4	.1	-1.0			
32	93	1.4	.6	.8				

A major cause of the observed velocity deviation is immediately suggested by the comparison of the trajectory for the large scale motion and the observed trajectory, Figure 4. The almost regular oscillation about the smooth curve makes it appear that these are velocity fluctuations of shorter period than the observation interval. This possibility is investigated quantitatively by determining the accumulated deviations, d_i listed in column F. (The displacement of an observation fix from the linear trend is given by the product $\sum d_i$). The rms $d_i = 3.51 \text{ m sec}^{-1}$ considerably larger than the rms ΔV_i , indicating runs of the deviations of like sign. Further confirmation is found by investigating the distribution of algebraic sign of the values in column F. The probability that this distribution would occur by chance is less than 0.025.

The intermediate waves will not necessarily appear as changes in sign of the d_i unless the amplitudes of the waves are uniform. The half-period of the intermediate waves are best selected by the cases of increasing and then decreasing sign of the d_i . From the total number of cases the average period is found to be 130 minutes and the half periods of greatest amplitude chosen for further analysis are indicated as A and B in Figure 4. The north-south accelerations in these segments were computed by fitting a second linear regression and the values obtained were 8.9×10^{-2} and $-17.0 \times 10^2 \text{ cm sec}^{-2}$. The corresponding quantities of the second regression computations are distinguished by using the prime symbol and the values are tabulated in columns G, H and I.

It is now possible to decide that the intermediate accelerations do not appreciably affect the computation of the large-scale acceleration. From Figure 2 it may be determined that the maximum contribution of a small-scale acceleration is 6% for this observation interval and wave period. The maximum contribution of the largest small-scale acceleration is therefore 1×10^{-2} which may be compared with the observed large-scale value of $2.5 \times 10^{-2} \text{ cm sec}^{-2}$.

Velocity fluctuations of even smaller scale should appear as deviations from the second linear regression. The rms of these deviations $\Delta V' = 0.92 \text{ m sec}^{-1}$,

Confidential Security Information

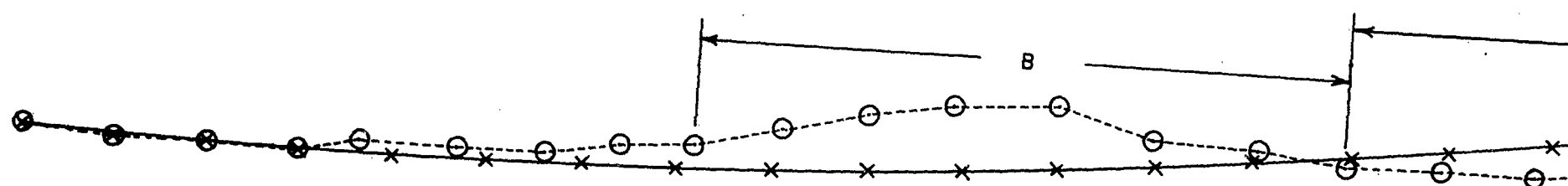
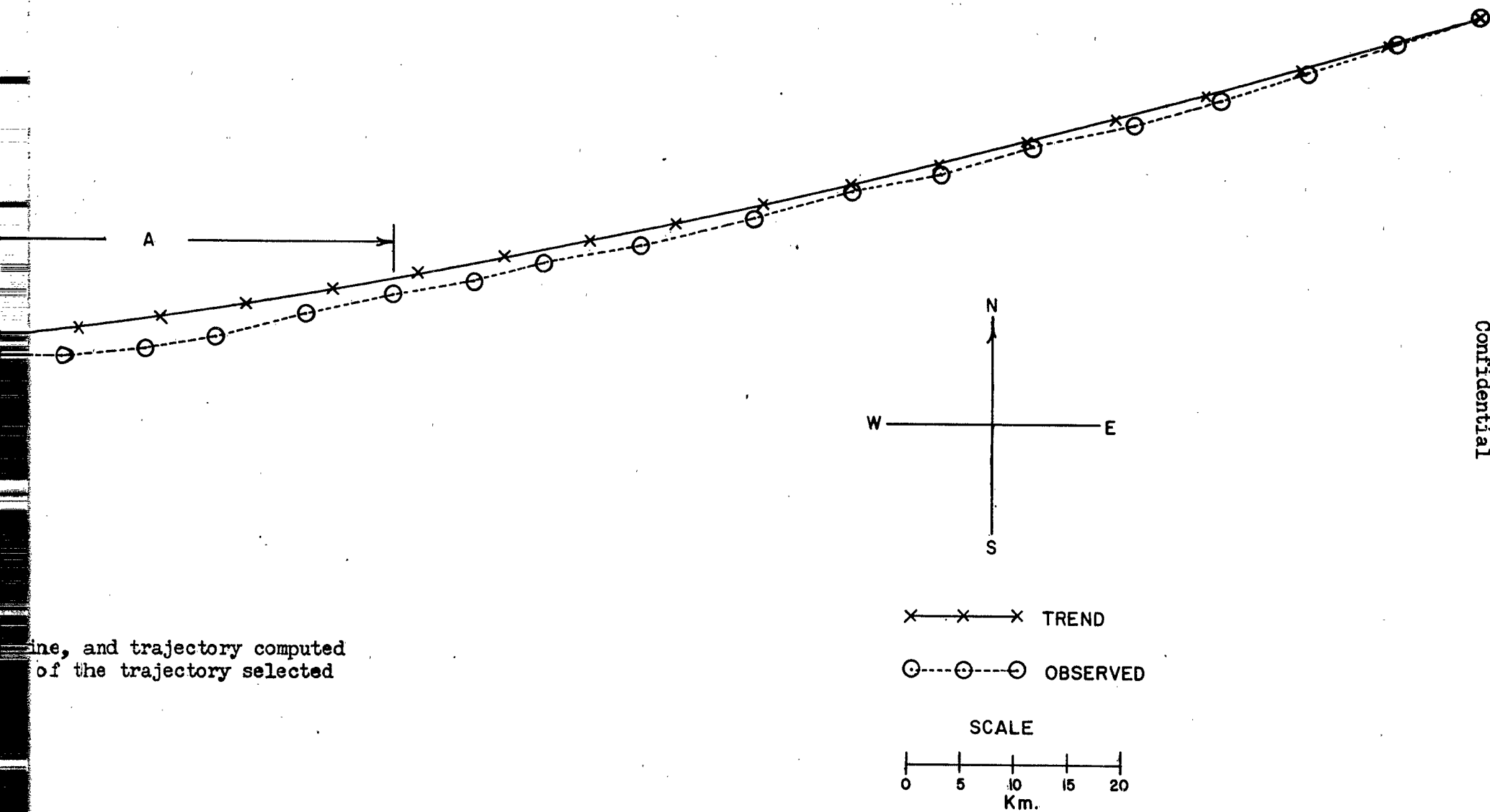


Fig. II-4. Observed trajectory flight 24, broken line, a from a linear velocity trend, solid line. The sections of th for a second linear approximation are marked A and B.



Confidential

which is smaller than our estimate of maximum error. Again some of the values of $\Delta V'$ are too large to be explained by error, but in general these fluctuations are so small as not to be distinguishable from the possible error.

In summary flight #24 exhibits three scales of atmospheric motion:

- (1) The acceleration measured for the large-scale component which apparently has a period greater than 10 hours is $2.5 \times 10^{-2} \text{ cm sec}^{-2}$.
- (2) An intermediate fluctuation of average period of about 2 hours with accelerations of as large as $17 \times 10^{-2} \text{ cm sec}^{-2}$, and
- (3) Some evidence for waves with a period shorter than one hour but with amplitudes smaller than 1 m sec^{-1} .

9. Results of all cases

The results of the analysis of the 14 observations are given in Table IV for the cases of easterly flow and in Table V for west winds. Most of the column headings are self explanatory with notation following conventions described in the body of the report. Where applicable, the north-south and east-west components of a measurement are indicated after the column number. Distance out, column 5, refers to the average horizontal distance between the balloon and the observation point. In order to estimate more representative values of the large-scale acceleration, the maximum effect of the intermediate acceleration was computed using the diagram in Figure 2, and this value subtracted from the large-scale accelerations. The residuals which represent a minimum value of the large-scale acceleration are listed in column 11. Columns 12, 14 and 19 give the error estimates based on the possible displacement of the position fix. The error in the acceleration or overall trend (column 12) are the estimated standard errors computed from the error in position fix and the observation interval; these values are to be compared with the quantities in column 8. The estimated standard error in velocity (column 14) is computed from the error in position fix and the leg interval and may be compared with the values in columns 13, 16 and 18. The

Table IV. Analysis of east winds

Fit	τ	ϵ	Alt	Dist	Mean vel	Overall	Interm	Interm	Interm	Adjusted	Overall	RMS vel	Stnd	RMS vel	RMS vel	RMS vel	RMS vel	Max	RMS dev	Prob. of
					mag dir	trend	trend	period	min	trend	trend	dev from	error vel	dev from	flux of	int wave	int wave	fix error	position	dist. of
					$m \cdot s^{-1}$	$10^{-2} cm \cdot s^{-2}$	$10^{-2} cm \cdot s^{-2}$	$10^{-2} cm \cdot s^{-2}$	$10^{-2} cm \cdot s^{-2}$	$10^{-2} cm \cdot s^{-2}$	$10^{-2} cm \cdot s^{-2}$	$m \cdot s^{-1}$	$m \cdot s^{-1}$	$m \cdot s^{-1}$	$m \cdot s^{-1}$	$m \cdot s^{-1}$	$m \cdot s^{-1}$	mi	mi	$d \cdot \epsilon$ signs
1	2	3	4	5	6	7	8-N	9-E	10-N	11-E	12	13-N	14	15-N	16-E	17-N	18-E	19	20-N	21-E
16	25	5	81	55	5	87	-3.4	-0.4	--	--	10	.78	2.77	1.3	.13	0	.77	2.77	.38	.43
20-1	60	5	86	30	11	59	10.4*	15.0	38	16	.15	2.16	2.56	.32	1.07	1.57	.81	1.86	.09	.28
20-2	75	5	78	38	6	100	13.5*	16.7	12	4	.32	2.67	2.34	.36	1.74	2.16	.71	1.42	.52	.10
24	320	10	83	90	13	82	2.5	0.9	13	10	.08	2.00	2.02	.80	1.50	.55	.92	1.32	1.35	.025
27-1	140	10	84	15	9	96	1.0	-3.6	13	--	.25	1.18	1.69	.50	.22	.88	.55	1.44	.28	.55
27-2	200	20	79	120	10	112	3.6	3.0	--	--	.20	1.72	2.09	.40	1.16	1.73	0	1.27	1.17	.30
33	60	5	84	30	7	96	-8.0*	0.3	--	25	.15	1.63	1.39	.36	.67	0	1.49	.69	.09	.25
491	105	5	83	20	6	104	0.9	5.2	10	4	.11	1.26	1.12	.25	.53	.89	1.14	1.09	.07	.24
462	160	10	79	50	4	116	2.1	1.4	13	5	.22	1.57	.77	.53	.59	.24	1.46	.73	1.23	.56

Table V. Analysis of west winds

1	2	3	4	5	6	7	8-N	9-E	10-N	11-E	12	13-N	14	15-N	16-E	17-N	18-E	19	20-N	21-E
8	110	10	82	100	7	251	-6.6	2.7	18	--	.10	1.87	1.59	.80	1.58	.66	.99	1.45	.94	0
9	140	10	87	28	3	280	-3.9	1.6	8	--	.08	1.39	.79	.15	.95	.38	1.01	.69	.85	0
10	100	10	94	40	10	296	2.9	-7.3	13	--	.18	1.53	1.59	.18	.52	1.25	1.44	.98	1.12	0
40	100	10	86	100	11	302	5.9	-3.7	--	--	.80	1.57	1.37	.80	1.01	.62	1.20	1.22	0	0
42	80	10	85	70	11	271	-11.4	.8	--	--	1.25	1.99	1.10	.80	1.57	.16	1.23	1.09	0	0

* These large values of the acceleration have been determined for an observation interval which is too short to eliminate waves of intermediate period.

** Col 15 is obtained: $(Col 15)^2 = (Col 13)^2 - (Col 16)^2$

*** Col 17 is obtained: $(Col 17)^2 = (Col 16)^2 - (Col 18)^2$

position fix errors are maximum estimates so that roughly half of these values should be comparable to the rms values of the observed trajectory displacement (column 20). Column 21 lists the results of the analysis of the sign sequences of position displacements. For example, a sign probability of 0.025 indicates that, assuming random error distribution about a long period wave, the probability that the observed sign sequence is due to error alone is less than 2.5%.

The results listed in the table indicate the existence of three general scales of motion. Long period waves are suggested by the overall trend and judging by the appearance of the trajectories the period in all cases is greater than twice the observation interval, i.e. greater than 5 hours for flights #8, #9, #24 and #27. The remaining overall trend values give evidence of either long period fluctuations or of waves of intermediate period - from 1 to 5 hours. The intermediate scale of motion is also indicated by the sign sequence analyses. The evidence of shorter waves, - 1 hour or less - is suggested by the part of the velocity deviations which cannot be accounted for as error in observation or as deviations inherent in the linear trend method.

The magnitudes of the accelerations obtained may be arranged according to the period of the fluctuation. The acceleration in the fluctuations of the largest scale range from 0 to $4 \times 10^{-2} \text{ cm sec}^{-2}$. In the fluctuations of intermediate period accelerations as large as $15 \times 10^{-2} \text{ cm. sec}^{-2}$ are observed; while for fluctuation with periods less than an hour the deviations are not entirely distinguishable from the error it seems likely that the values of $50 \times 10^{-2} \text{ cm sec}^{-2}$ must occur.

The amplitude of these velocity fluctuations in these three scales of motion may also be estimated. If we assume the velocity fluctuations in each scale to be independent and normally distributed the variance of the observed velocity deviations σ_0^2 will be equal to the sum of the variance due to each scale of motion and to error:

$$\sigma_0^2 = \sigma_1^2 + \sigma_2^2 + \sigma_3^2 + \sigma_e^2 \quad (5)$$

where the subscripts 1, 2, 3 and e denote the variance due to large-scale, intermediate scale, and small-scale motion and to error, respectively. For an observation of several hours the large-scale motion is determined by the linear function and the variance about this function σ_1^2 is assumed to be due to smaller scale motion and to error hence:

$$\sigma_1^2 = \sigma_2^2 + \sigma_3^2 + \sigma_e^2 \quad (6)$$

The variance due to the largest scale of motion will, therefore, be determined as the difference of the total variance (5), and the variance about the linear trend (6). The square root of the variance due to the largest scale motion is listed in column 15; the corresponding values for the total observed fluctuations and the deviations from the trend are in columns 13 and 16.

The operation can be repeated to determine the variance due to the motion of smaller scale although the error due to limitations of the method and assumptions will increase after successive differences. These figures for the amplitude of smaller scale motion listed in column 17 and the remaining deviations of column 18 must be viewed as rough estimates.

IV. Conclusions

10. The scale of stratospheric motions

It has been found that, subject to limitations due to the length and accuracy of the observations, it is possible to distinguish motion over a rather wide range of periods. As noted in the preceeding section, the method of analysis seems to distinguish three general groups of periods. The characteristics of the motion in each group are summarized in Table VI.

Table VI

Characteristics of stratospheric motions of different periods

Period, hours	5-15	1-3	$\frac{1}{2}$
Accelerations $\times 10^{-2} \text{ cm sec}^{-2}$	0-4	10-15	~ 50

Table VI (continued)

Characteristics of stratospheric motions of different periods

Amplitude of velocity fluctuation, m sec ⁻¹	1.5	1.0 - 1.5	~ 1.0
Amplitude of trajectory fluctuation miles	25*	1 - 2	~ 0.5

*Estimated to be consistent with the amplitude of the velocity fluctuation and the estimated period.

While the data is separated into three groups of motions according to the period it should not be assumed that it shows any discontinuities in the spectrum of the stratospheric motion. The rather surprising fact that the velocity amplitude is almost independent of period suggests that there is no different in the type of flow in the range of periods investigated.

These results may be compared with the motion observed in the troposphere. The motion termed large scale in the troposphere is of somewhat longer period than observed here and the velocity amplitude is much greater. In contrast with the above results for the stratosphere, the large scale tropospheric flow is quite distinct from the smaller scale motion. The intermediate and small-scale stratospheric motions are very nearly comparable to the troposphere, although again the velocity amplitudes of the smallest scale stratospheric motions seems to be smaller.

11. Forecasting implications

The problem of the extrapolation of the course of the balloon may now be considered in the light of the derived characteristics of the flow. The motion is seen to consist of velocity fluctuations with a wide range of periods but with similar amplitudes. As a first approximation it would seem obvious that the best or most representative wind measurement for extrapolation will be obtained by using an observation interval of a length comparable to the forecast interval.

For periods of a few hours it would be possible to extrapolate only the large scale motion of the flow with an expected accuracy of the trajectory amplitude of the intermediate small-scale flow (several miles). In forecasts for

a period of a day and with suitable observation length, the errors would be comparable to the amplitude of the large scale trajectory fluctuations (25 miles).

References

- Brooks, E.M., 1947: The accuracy and Representativeness of the 10,000 Foot Pibal Report, Bull. Am. Met. Soc., v. 28, no. 9, p. 405.
- Durst, C.S., 1948: The Fine Structure of the Wind in the Free Air. Quart. Jour. Roy. Meteor. Soc., v. 74, p. 349.
- _____, and G.H. Gilbert, 1950: Constant Height Balloons - Calculation of Geostrophic Departures, Quart. Journ. Roy. Meteor. Soc., v. 76, pp. 75-88.
- General Mills Aeronautical Research Laboratories, 1952: Project A170, General Mills Report #1072, (unpublished)
- Godson, W.L., 1950: A study of the Deviations of Wind Speeds and Directions from Geostrophic Values, QJRMS, v 76, pp. 3-15.
- Hoel, P.G., 1947: Introduction to Mathematical Statistics, John Wiley and Sons New York.
- Mantis, H.T., and F.R. Ohnsorg, 1952: Development of methods for forecasting balloon trajectories, Final Report, Trajectory Forecasting Project, Engineering Experiment Station, Institute of Technology, University of Minnesota.
- Neiburger, M., Sherman, L., W.W. Kellogg, and A.F. Gustafson, 1948: On the Computation of wind from pressure data, Journal of Meteorology, v. 5, pp. 87-92.
- Rapp, E.R., 1952: The effect of Variability and Instrumental Error on Measurements in the Free Atmosphere, Meteorological Papers, College of Engineering, New York University, New York.

Confidential

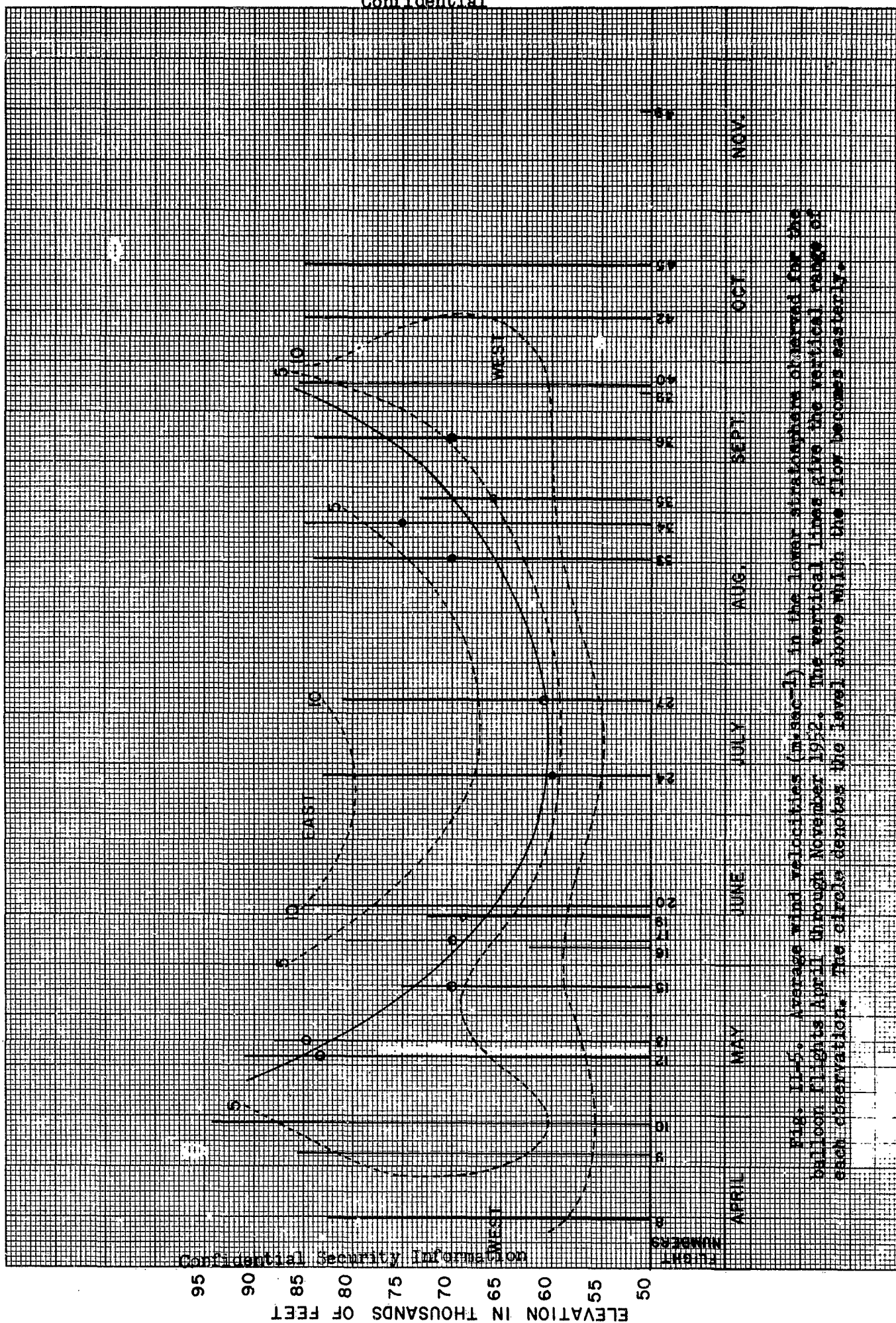


Fig. II-5. Average wind velocities (m/sec) in the lower stratosphere observed for the balloon flights April through November 1952. The vertical lines give the vertical range of each observation. The circle denotes the level above which the flow becomes easterly.

Confidential Security Information

FLIGHT NO. 35 9-3-52
TIME 0929 U.O.F.M.

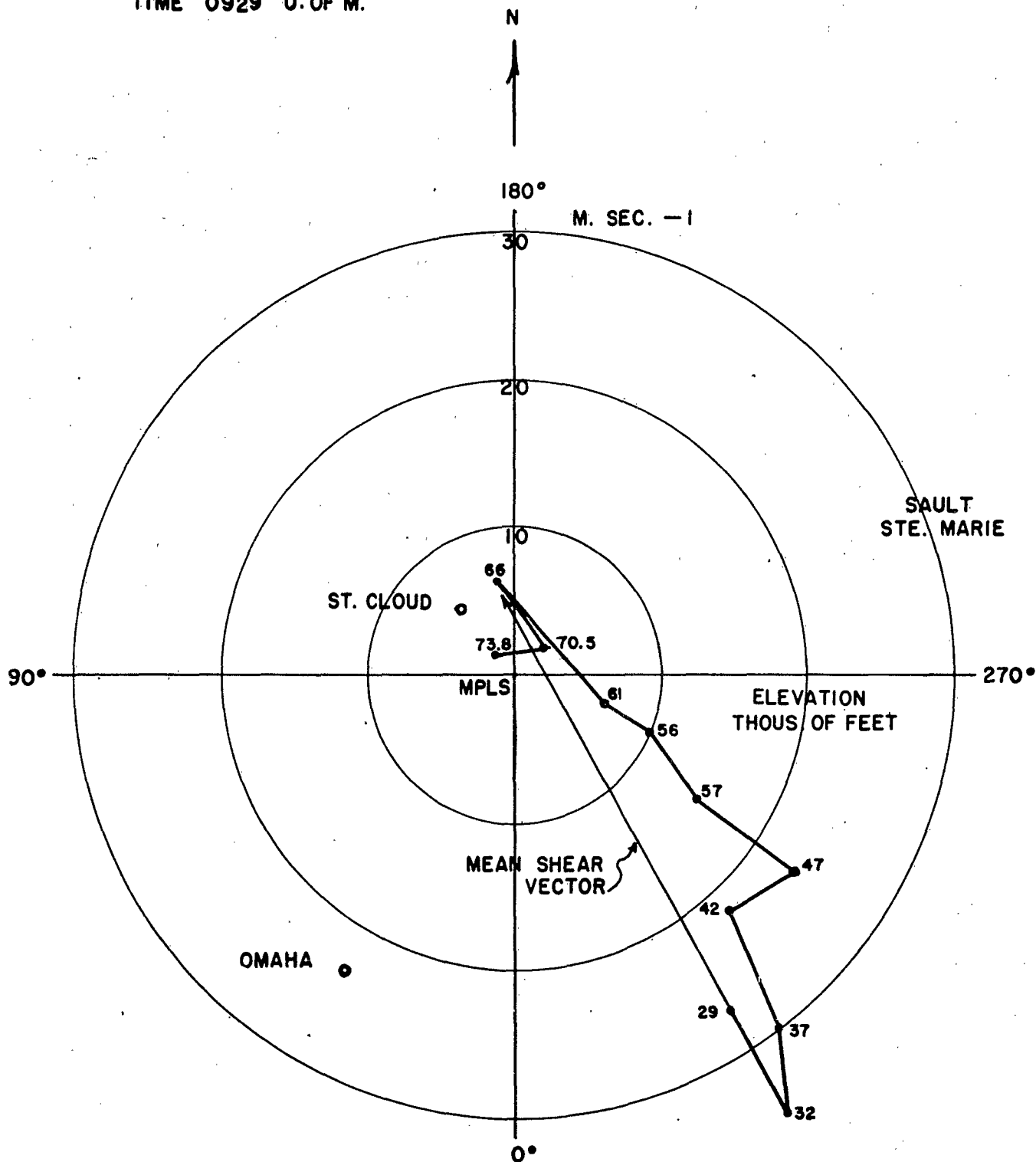


Fig. II-6. Hodograph for flight #35. The location of the nearby Radiosonde stations with respect to Minneapolis are also indicated.

some seasonal trend; the lowest elevation of reversal occurs in mid July in about the middle of the period of easterly flow. A slight tendency for the easterly flow to increase with elevation is also observed.

3. Some features of the wind maximum at the tropopause

The balloon ascents show several interesting details of the wind maximum which so frequently is found at the base of the stratosphere. In sixteen ascents winds in excess of 30 m sec^{-1} were observed. The distribution of the maximum observed wind speeds in these 16 flights is shown in Table VI.

Table VI

Maximum wind speeds m sec^{-1} observed in sixteen ascents during high winds.

Range of maximum wind speeds, m sec^{-1}						
	30-34.9	35-39.9	40-44.9	45-49.9	50-54.9	55-59.9
No. of cases	6	3	3	2	1	1

The elevation of the wind maximum is very closely related to the height of the tropopause. The average elevation of the wind maximum for these 16 cases was 37,600 feet, which is just 2000 feet below the average tropopause height. The standard deviation of both tropopause height and elevation of the wind maximum was 5400 feet. The correlation coefficient of the elevation of the wind maximum to the tropopause height in these 16 cases was 0.83. Because of fair weather bias almost all of these ascents were made in northwesterly flow and this relationship, if representative at all, may be limited to this type of weather situation.

Another characteristic of these wind profiles was the noticeably greater wind shear in the layer above the wind maximum than below. The average vertical wind shear just below the maximum was $2.89 \times 10^{-3} \text{ sec}^{-1}$ (2.0 mph per thousand feet) and above the maximum, the average shear was $-7.6 \times 10^{-3} \text{ sec}^{-1}$ (5.2 mph per thousand feet).

B. WINDS IN THE UPPER TROPOSPHERE AND LOWER STRATOSPHERE

1. Introduction

The wind measurements made during the ascent of the plastic balloons frequently provide information in the upper atmosphere unavailable by conventional radio wind measurement. Because of the size and rate of ascent of the balloon no observations were lost during ascent solely because of too great a range. The tracking methods, both camera and theodolite, are essentially fair weather systems and the data will therefore suffer this bias.

A total of twenty-three ascents with wind measurements were made from Minneapolis, Minnesota, or Pierre, South Dakota, in the period April through November, 1952. The information obtained from these wind measurements will be reviewed in this report. The data will be discussed under three headings in the following sections: (1) A Summary of the winds in the lower stratosphere; (2) Some features of the wind velocity maximum in the vicinity of the tropopause; and (3) The extension of meteorological analysis to the stratosphere.

2. A summary of the winds in the lower stratosphere

The broad features of the observed stratospheric winds are shown in Figure 1 which gives the variation of the vertical wind profile with season. The location and vertical extent of each observation is shown by the vertical lines. Isopleths of average velocity, which have been smoothed rather arbitrarily are given in $m\ sec^{-1}$. The location of the shift from westerly to easterly flow is noted by a circle for each observation and the smoothed average limit of easterly flow is given by the solid curve.

Perhaps the most important features of Figure 5 are the details of the period of easterly flow. Both the onset of easterly winds in the spring and the termination in the fall are very abrupt. The elevation of the boundary between easterly and westerly flow varies from day to day but does exhibit

4. Extension of the methods of analysis to the stratosphere

The observed winds were also reviewed with the thought of extending the methods of analysis to the lower stratosphere. The methods of extrapolating the wind and pressure field in regions of sparse data are essentially based upon the use of the thermal wind relationship in an effort to make the analysis of pressure, wind and temperature mutually consistent. The thermal wind vector or shear vector in the stratosphere was therefore investigated by plotting hodographs for all the ascents and in addition for all the available SKYHOOK ascents.

The hodographs in cases of strong tropospheric flow were quite similar, again possibly because these are all similar weather situations. A typical case is illustrated by the hodograph for flight #35, Figure 6. The flow is from the northwest just below the tropopause. From the shear vector it appears that the horizontal temperature distribution is quite constant in the layer from 32 to 66,000 feet, and that there is a slight cold air advection in this deep layer. The actual temperature distribution is substantially verified by the plot of the Radiosonde data observed along a line perpendicular to the shear vector, Figure 7.

A deep layer extending from the base of the stratosphere to as high as 75,000 feet, in which the orientation of the shear vector and sign of the advection is constant, is typical of a large number of the hodographs with strong flow. Above this layer a completely different horizontal temperature distribution is found which seems to be highly dependent upon season with no obvious relationship to the tropospheric weather system. The suggestion is rather strong therefore that the level 65,000 to 75,000 feet marks the upper extent of the tropospheric weather systems. In this respect the consistency of the sign of the advection is particularly significant because of the high correlation between advection and the sign of the vertical motion¹.

¹Fleagle, R.G., 1948, Journal of Meteorology, p. 290.

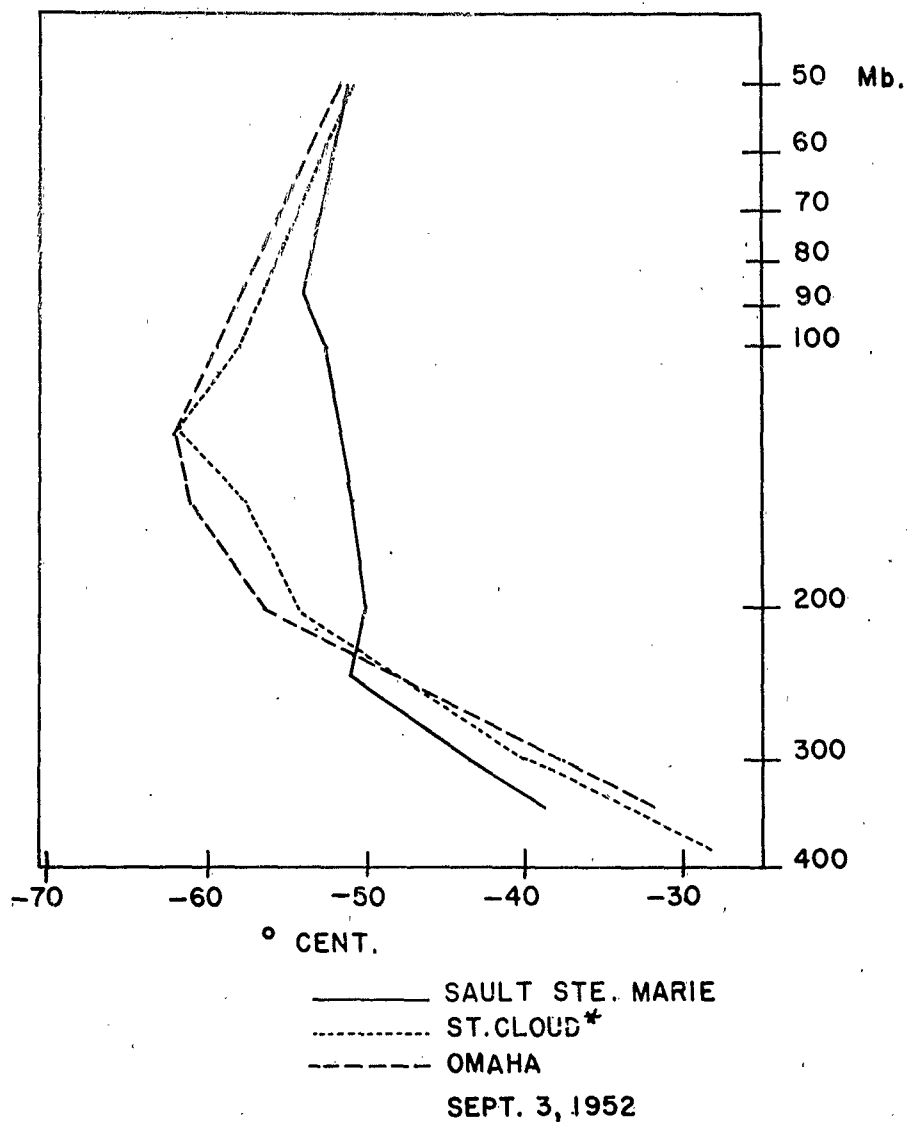


Fig. II-7. Radiosonde observation made at stations located along a line perpendicular to the shear vector of flight #35, see Figure 6. The highest temperatures in the lower stratosphere are observed to the right of the shear vector.

* St. Cloud sounding for 4 September 03 Z substituted for missing data.

Several of these observations are pertinent to the question of extrapolating the methods of analysis. The temperature and wind observations are consistent so that the usual methods for extending the analysis to upper levels should be valid to perhaps 65,000 feet. However, it also strongly suggests that flow patterns at this elevation will be as complicated as the isotherm pattern just above the tropopause. In this case it would seem that a rather dense network of upper air observations would be required to construct a weather map which would depict the flow at these elevations.

Armed Services Technical Information Agency

AD

20133

NOTICE: WHEN GOVERNMENT OR OTHER DRAWINGS, SPECIFICATIONS OR OTHER DATA ARE USED FOR ANY PURPOSE OTHER THAN IN CONNECTION WITH A DEFINITELY RELATE GOVERNMENT PROCUREMENT OPERATION, THE U. S. GOVERNMENT THEREBY INCURS NO RESPONSIBILITY, NOR ANY OBLIGATION WHATSOEVER; AND THE FACT THAT THE GOVERNMENT MAY HAVE FORMULATED, FURNISHED, OR IN ANY WAY SUPPLIED THE SAID DRAWINGS, SPECIFICATIONS, OR OTHER DATA IS NOT TO BE REGARDED BY IMPLICATION OR OTHERWISE AS IN ANY MANNER LICENSING THE HOLDER OR ANY OTHER PERSON OR CORPORATION, OR CONVEYING ANY RIGHTS OR PERMISSION TO MANUFACTURE OR SELL ANY PATENTED INVENTION THAT MAY IN ANY WAY BE RELATED THERETO.

Reproduced by
DOCUMENT SERVICE CENTER
KNOTT BUILDING, DAYTON, 2, OHIO

CONFIDENTIAL

**Best
Available
Copy**